# THE DEVELOPMENT OF A SIMPLE STEREOTACTIC DEVICE FOR NEUROSURGICAL APPLICATIONS

BY

BARBARA ANNE VAN GEEMS

M.SC. (ENGINEERING)

UNIVERSITY OF CAPE TOWN

Thesis presented for the Degree of

DOCTOR OF PHILOSOPHY

in the Department of Biomedical Engineering

UNIVERSITY OF CAPE TOWN

MAY 1997

## ABSTRACT

Stereotactic neurosurgery is used to accurately locate an intracranial point in relation to an external reference system attached to the patient's head, utilising imaging techniques, such as computed tomography (CT), to supply both images and 3D spatial information. In frame-based stereotactic systems, an external reference frame is bolted to the patient's head prior to the imaging procedure, and the resultant spatial data is utilised to set a mechanical instrument guidance system, attached to the frame, which will direct a surgical instrument to the intracranial point. With modern interactive image-guided stereotactic systems, the external markers may be attached directly to the patient's head and a 3D measuring system, operating interactively with the images, is used to guide the surgical instrument. These superb systems are too expensive for neurosurgeons in developing countries. To give these neurosurgeons access to stereotactics, a simple, cost-effective alternative - the Cape Pointer - has been developed, which avoids the necessity of bolting a frame to the patient's head, while maintaining the accuracy of its more sophisticated counterparts.

The Cape Pointer, an instrument guidance device, is only approximately a quarter of the size of present frame-based systems and only weighs 150 grams. The external reference system consists of three radio-opaque markers embedded in a small light-weight plastic halo, attached to the head with two sutures or small surgical screws. The halo also functions as a platform for the Cape Pointer. The system is software driven and can accommodate any type of 3D imaging coordinate system. The only software inputs are the 3D CT coordinates of the three external markers and the intracranial point. As the Cape Pointer is set with the aid of a phantom, the only software outputs are the three translations to set the phantom marker. The Cape Pointer is simply set by directing a long pointer through its instrument guide so that pointer tip rests on the phantom marker. The Cape Pointer can be set for any trajectory to any intracranial point within the mechanical range of the Cape Pointer and the phantom. To set the trajectory through a specific entry point, a simple mechanical entry point simulation device is utilised. Prior to its use in the clinical environment, the Cape Pointer was thoroughly tested using various phantom heads. It has an application accuracy of 1.9mm+/-0.6mm when used with 2mm CT slice thicknesses, which compares very well with application accuracies of other frame-based systems. To date, the Cape Pointer has been used successfully in forty patient procedures.

The initial Cape Pointer was designed to operate in conjunction with a stereo-photogrammetric (SPG) system, to allow patients freedom of movement during the CT procedure and nevertheless determine 3D coordinates of external markers and intracranial points from which all patient movement had mathematically been removed. The SPG system

achieves this objective by making the SPG and CT coordinate system coincident. Any movement made by the patient is quantified by the SPG system, and applied to the CT system, thus resulting in corrected CT coordinates. To assist with this objective a technique has been developed whereby CT surviews, normally only used for planning CT procedures, are used to determine 3D coordinates of external markers. The SPG system, in conjunction with the Cape Pointer, was tested using a phantom head with the lesion centre represented by a radio-opaque marker. The lesion marker coordinates were determined with a mean vector error of 1.4mm and the final setting of the Cape Pointer was approximately 2mm off target, verifying that the SPG system could achieve the necessary accuracy for stereotactic procedures. The SPG system is a valid system for correcting patient movement during a CT procedure, but is not part of the final Cape Pointer system as, in its present format, it is time consuming and unwieldy.

As the present format of the Cape Pointer is unsuited for use during an open craniotomy, an interactive image-guided neurosurgical aid (NSA) system has been developed to be used specifically with the CT scanner at Groote Schuur Hospital. The NSA system, in near real time, identifies the exact intracranial point at which the neurosurgeon is working and marks this point on the appropriate CT slice, thus guiding the neurosurgeon during the craniotomy. A stereophotogrammetric system, with two CCD cameras, is utilised to transform the theatre coordinate system into the CT coordinate system, utilising the external reference markers attached to the patient's head prior to CT scanning. As the tissues of the brain within the cranium are not visible to the cameras, a long pointer, with three markers attached in a known configuration, is utilised to coordinate intracranial points in the theatre system, and therefore also in the CT system. The intracranial point, in contact with the pointer tip, is identified with a flashing cursor on the relevant CT slice, which has been converted into a format appropriate for display on the additional NSA monitor. By continually fixing and displaying points on the relevant CT slice, the neurosurgeon is image-guided during the craniotomy. Testing the NSA system with a phantom head has resulted in a mean vector error of 1.9mm+/-0.7mm for determining intracranial points, which is on par with other interactive image-guided stereotactic systems. The NSA system still requires further adaptation prior to use in the clinical environment.

Of the three systems developed in this thesis, the stand alone Cape Pointer has proven itself in the clinical environment, and represents a simple, yet elegant solution to the complex stereotactic problem, and will hopefully become a viable tool for neurosurgeons seeking a cost-effective way of adding a stereotactic string to their surgical bow.

**DECLARATION**

I, Barbara Anne van Geems, hereby declare that the work on which this thesis is based is my original work (except where acknowledgements indicate otherwise), and that neither the whole work nor any part of it has been, is being, or is to be submitted for another degree in this or any other university.

I empower the University of Cape Town to reproduce for the purpose of research either the whole or any portion of the contents in any manner whatsoever.

Signed .....

Signature

15 May 1997 .....

Date

## ACKNOWLEDGEMENTS

My sincere thanks go to Professor L.P.Adams, my supervisor, for all his help and support over the years. Without him I would never have embarked into the field of medical photogrammetry, or have progressed this far. His interest and enthusiasm in the work has made the research work not only interesting, but also enjoyable.

I would like to thank the neurosurgeons Professor Jonathan Peters (Department Head), Dr. Graeme Fieggen and Dr. Alan Taylor, of the Department of Neurosurgery, University of Cape Town (UCT) and the two Government teaching hospitals, namely Groote Schuur Hospital (GSH) and Red Cross Children's Hospital. They played a vital role in the development of the Cape Pointer. Their enthusiasm for the project, their various ideas and their consideration for the patients has made the Cape Pointer what it is today. My thanks also go to the neurosurgical theatre staff, who were ready and willing to describe and clarify various aspects of the surgical procedures.

I would like to thank Ms Hanli Potgieter and Ms Jasmina Waggie, radiographers in the Department of Radiotherapy, GSH, for the hours spent explaining various aspects of the CT scanner and conducting all the CT scans for the research work. I thank Mr. Jan Hough, a medical physicist at GSH, for his help with understanding the intricacies of the CT scanner.

I would like to thank all the staff at the Department of Biomedical Engineering, UCT, for all their help and assistance, especially Dr. Wayne Capper and Mr. Mike Price. I appreciate Mike Price building the various versions of the Cape Pointer, and without his suggestions the final design of the Cape Pointer would not have been as elegant as it is today. I would like to thank Dr. Capper for all his assistance as co-supervisor, it was most appreciated.

I would like to thank Mr. A. Bub, a Master's student in the Electrical Engineering Department of UCT for his assistance with decoding the CT scanner images, and Mr. A. Weisman of Information Technology Services, UCT, for downloading the CT tapes when required.

I would like to thank the Medical Research Council of South Africa for their financial support, without which I could not have afforded to do any of the research work. I would like to thank Dr. S. Wynchank and Mr. P. Selby for all their friendly support and assistance over the years, it was most appreciated. I would also like to thank Dr. R. Stewart and Prof. A. Bunne.

I would especially like to thank my husband, Alan van Geems, for all his love, support, patience and help, especially during the write-up phase of the thesis.

**TABLE OF CONTENTS** **PAGE**

## LIST OF ILLUSTRATIONS

## LIST OF TABLES

## CHAPTER 1 INTRODUCTION

Imagine a children's game - a small chocolate button has been placed approximately in the centre of a transparent glass bowl filled with clear jelly - the aim of the game is to remove the button, without unduly disturbing the jelly. The child is given a straw, into which a knitting needle has been inserted, filling the straw, with the needle tip just protruding from the end of the straw. The straw is inserted into the jelly until the needle tip makes contact with the button. The needle is then withdrawn without disturbing the straw. By simply sucking some of the air out, the child draws the button into the tip of the straw until it is firmly wedged. The straw, and therefore the button, can now be removed, leaving the jelly relatively undisturbed.

The analogy above can be equated to a neurosurgical biopsy. The bowl represents the human skull (cranium), the jelly the tissues of the brain and the button the tissue sample that has to be removed from a lesion for pathological examination. The removal of the tissue sample is accomplished with a biopsy needle, representing the straw and the knitting needle. However, as the human brain consists of vital and very complex neural tissues, a neurosurgical biopsy is a far more complicated procedure than removing a chocolate button from a bowl of jelly, and the surgical procedure has to be conducted with minimal disturbance to the brain tissues.

The first step in the process of removing a tissue sample, is to obtain images of the brain, and the lesion, using such imaging techniques as computed tomography (CT) or magnetic resonance imaging (MRI). Although most lesions can be detected with CT and MRI, histological evaluations, from the images alone, are not possible, and therefore tissue samples are removed for examination (Horner et al, 1984). A small hole (burr hole), less than half a centimetre in diameter, is drilled in the cranium at an optimal site near the lesion. The brain, almost entirely enclosed by the cranium, is not visible to the neurosurgeon. He utilises scanned images of the patient's brain, and relies on his ability to visualise the brain and its anatomical detail in three dimensional (3D) space, to guide the biopsy needle through the burr hole and towards the lesion. This is termed "a free-hand approach" and, despite the fact that the neurosurgeon can not see "the button which he is trying to extract", has quite a good success rate.

There is however a better approach, known as stereotactic surgery, used mainly in the field of neurosurgery. Its predominant use in neurosurgery is due to the fact that the brain, a solid organ, is almost entirely encompassed by bone and hardly any movement occurs between the brain and the skull. Any external point, forming part of an external reference system attached to outer surface of the patient's head, can thus be related to points within the brain.

Imaging technologies, such as CT, not only produce images of the various tissues of the brain, but provide accurate 3D spatial information for both the external radio-opaque reference points, and any intracranial point, displayed on the images. Even though an intracranial point is not visible to the neurosurgeon, its position, in relation to the external reference points, is exactly defined, and, using various approaches, the surgical instrument can be set on course to reach the intracranial point. Stereotactic neurosurgery thus assists the neurosurgeon in placing the tip of a surgical instrument, such as a biopsy needle, with great accuracy and repeatability, on a specific point within the brain and thus eliminating all of the uncertainties of the free-hand approach. Stereotactic neurosurgery is a powerful tool for the neurosurgeon, and beside being used for biopsies, is also employed in the evacuation of fluid from cysts, abscesses and hematomas in the brain, locating lesions prior to their removal and a host of other neurosurgical applications.

Prior to the 1990's, external reference systems have consisted mainly of stereotactic frames and this technique, which is still widely used, is usually referred to as frame-based stereotactic neurosurgery. The frame, which surrounds the patient's head, is literally bolted to the patient's skull with self-tapping screws or pins, thus maintaining a rigid relationship between the frame and the patient's skull. The frame is attached prior to imaging, and is not removed until the surgical procedure has been completed. During the imaging procedure, the stereotactic frame is bolted to the imaging table/bed. This prevents the patient from making any movement which would destroy the geometrical relationship between the various scanned images, and between the external reference points and any intracranial points appearing on the scanned images. The external reference points and intracranial points are measured on the scanned images. After various calculations, certain mechanical translations and rotations are applied to an instrument guidance system attached to the stereotactic frame, thus setting the correct trajectory for the surgical instrument to reach a specific intracranial point. In theatre, once the burr hole has been made, the surgical instrument is inserted through the instrument guide into the brain to a depth determined by the calculations. The tip of the surgical instrument is now coincident with the intracranial point, and a tissue sample can be removed.

Since the start of the 1990's, more sophisticated stereotactic techniques have been developed, which make use of sophisticated computer hardware, electronics and image processing techniques. An external reference system, consisting of either radio-opaque markers attached directly to the patient's head or a stereotactic frame bolted to the patient's head, is utilised. Using a 3D measuring system, for example a 3D digitiser, the position of the surgical instrument is determined in relation to the external reference system, and therefore also in relation to a specific intracranial point. This procedure is continually

repeated during surgery to ensure that the surgical instrument is guided to the intracranial point via an optimal route which causes as little disturbance to the tissues of the brain as possible. This is somewhat analogous to the old sailors guiding their ships to a specific destination using the stars as an "external reference system", or modern sailors using satellites and global positioning systems to keep the ships on course. A major benefit of this technique is that, as the external reference points are measured on the images, the relationship between the images and external reference system can be established. The position of the surgical instrument can therefore continually be related to specific points on the images. The neurosurgeon can thus "see" exactly where the surgical instrument is in relation to the tissues of the brain displayed on the images. This procedure is often referred to as interactive image-guided stereotactic neurosurgery.

Both the frame-based and image guidance techniques yield good results and have stood up to vigorous testing and years of use. However the neurosurgeons in South African government hospitals felt that neither of these stereotactic systems were really appropriate for an African/Third World situation. The commercially available interactive image-guided stereotactic systems are well beyond the price range of the Government Health Services. Although the cost of frame-based stereotactic systems is well below the cost of the image-guided systems, they are still expensive in South African monetary terms. Other drawbacks of frame-based stereotactic systems are that they are extremely cumbersome and patient unfriendly, as they have to be bolted to the skull, and as they require a fair amount of expertise and knowledge to operate, are mainly used by neurosurgeons specialising in stereotactics.

To give neurosurgeons in developing countries the ability to perform various stereotactic applications, it was decided to develop a simple stereotactic device, which would be accurate, cost-effective, easy to use and patient friendly. As the development of the new device has taken place in Cape Town, South Africa, and its main objective is to "point" the neurosurgeon in the right direction, the new device has been dubbed the Cape Pointer.

The concept of the Cape Pointer has its roots in a paper written by Adams (1981), where a stereotactic technique using conventional X-rays is described. Over ten years later the concepts in this paper, together with an idea put forward by Professor G.G.Jaros (at the time Head of the Department of Biomedical Engineering at the University of Cape Town Medical School), have been combined to spark the development of the Cape Pointer, utilising CT as the imaging medium. Although MRI has been considered as an imaging medium, and would be suitable for use with the Cape Pointer, no research utilising MRI has been conducted, as none of the government hospitals in Cape Town have any MRI facilities.

From the initial concept of the Cape Pointer, neurosurgeons have been involved in its design and development. (The neurosurgeons referred to throughout this thesis are all from the Department of Neurosurgery, a joint department of the University of Cape Town Medical School and the two Government teaching hospitals in Cape Town, namely Groote Schuur Hospital (GSH) and the Red Cross Children's Hospital.) The neurosurgeons set the guidelines for the development of the Cape Pointer, and these included that the new device should be simple to use and avoid having to bolt a stereotactic frame to the patient's head, and that the patient should not be constrained unduly during the CT imaging procedure. The guidelines were drawn up with consideration for very young patients, as a very young child has no understanding of why it is necessary to bolt a large metal frame to his/her head.

The development of the Cape Pointer is dependent on the CT scanner. The scanner and its measuring abilities are described, along with a new technique which utilises CT surviews - normally only used for planning a CT procedure - to determine 3D coordinates of external reference points (chapter 3). This technique is required in the development of a system to cater for patient movement during a CT procedure (chapter 4). The system is combined with the Cape Pointer (chapter 5) to fulfil the neurosurgeons' request that the patient should not be unduly restrained during the CT procedure. A trial (chapter 6) is undertaken to ascertain the accuracy of the combined system. The Cape Pointer is also developed as a stand alone stereotactic device (chapter 7).

At the request of the neurosurgeons, an additional system - an interactive image-guided neurosurgical aid (chapter 9) has been developed, in conjunction with the GSH CT scanner, to assist in the removal of the whole lesion during open brain surgery. This neurosurgical aid can be considered the "little brother" to the sophisticated image-guided stereotactic systems, and can also be used in conjunction with the Cape Pointer.

## CHAPTER 2 STEREOTACTIC NEUROSURGERY AND ITS HISTORY

### 2.1 EARLY STEREOTACTIC HISTORY - PRIOR TO COMPUTED TOMOGRAPHY

The era of stereotactic neurosurgery, as we know it today, began in 1908 when Horsley and Clarke presented their paper describing their apparatus to study the cerebellar function in the monkey. Robert Clarke said of his stereotactic frame "from its application to animals .... to its adaptation to human surgery is a long step... For my own part, I have no doubt that its application to various purposes in human surgery will only be a question of time..." (Guthrie et al, 1992). In fact, the equatorial frame built by Robert Clarke in 1920, shown in figure 2.1, bears a remarkable similarity to some of the modern stereotactic frames built today (Guthrie et al, 1992).

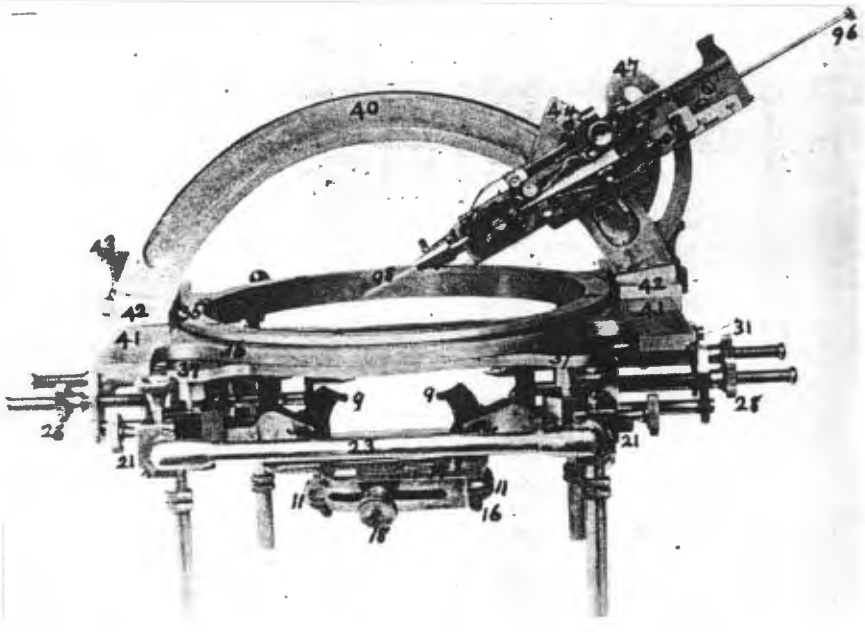

Figure 2.1: Clarke's stereotactic frame for animal use
(from Guthrie et al, 1992)

It was Robert Clarke who in 1912 coined the phrase "stereotaxic" approach, which described a variety of mechanically or radiographically guided cranial procedures (Guthrie et al, 1992). At the Sixth International Symposium on Stereoencephalotomy in Tokyo in 1973, there was considerable discussion on whether the acceptable spelling should be "stereotactic" or "stereotaxic". The majority voted on combining "stereo", from the Greek root meaning "three-dimensional", with "tactic", from the Latin root meaning "to touch", instead of "taxis", from the Greek root for an "arrangement", since surgery involves placing the probe at a certain point / target rather than defining the relationship. The International Society for Research in Stereoencephalotomy (encephalotomy: incision into the brain - Stedman (1982) ), who

organised the symposiums on stereoencephalotomy also agreed at the symposium in 1973 to change the Society name to the World Society for Stereotactic and Functional Neurosurgery, and now publish the Journal of Stereotactic and Functional Neurosurgery.

In all correctness, when looking back over the history of stereotactic neurosurgery, both Ditmar and Zernov have to be included in the early history, although stereotactic purists would say that their devices were, strictly speaking, not stereotactic instruments, but skull-mounted surgical guides. Ditmar in 1873 developed and reported the use of a mechanical guiding device for the placement of probes into the medulla oblongata of animals. The device provided three orthogonal degrees of precision (Ditmar, 1873). Zernov, a Russian anatomist, developed an arc-based guidance device based on polar co-ordinates. It was designed for both anatomical mapping and operations of the human brain. The device was used by Minor and Altuchov in 1887 on several patients to localise and remove cortical surface lesions. The device proved adequate for finding gross intracranial pathologies, but the patients died due to inadequate surgical and medical technology (Kandel et al, 1972). When looking at the work of Ditmar and Zernov, it must be remembered that these developments occurred prior to the invention of X-rays, which were only discovered by Wilhelm Röentgen in 1895.

Horsley and Clarke developed a stereotactic atlas of the brain, using a coordinate system based on various landmarks on the skull. From these landmarks the location of anatomical structures within the brain of a small animal could be reproduced with reasonable accuracy. In humans however, spatial variability of cerebral structures in relation to skull landmarks was much larger. This was due to different skull types and the variation of shape and size within each skull type. Only where cerebral structures lay close to the skull landmarks was there a reasonable certainty of the position of such a structure in relation to the landmark. The spatial variability of cerebral structures made human stereotactic neurosurgery impractical. It was only with the advent of ventriculography, developed by Walter Dandy in 1920, that intracerebral reference points could be visualised. More than 25 years later, Spiegel and Wycis considered using positive contrast ventriculography and the pineal body to localise intracranial targets (Kelly, 1991).

In 1946 Spiegel and Wycis developed the first stereotactic instrument to be used in human subcortical surgery. The stereotactic instrument was similar to that developed by Horsley-Clarke, and it is interesting to note that before Clarke's death in 1926, Spiegel had tried to have a Horsley-Clarke apparatus made by a London instrument maker, but decided against it, due to the high cost of about £300 (Kelly, 1991). For each individual patient, a plaster cap was made to which a head ring was attached (see figure 2.2). An electrode carrier was

mounted to this ring in a very similar design to that of Horsley-Clarke. The carrier could be moved laterally, vertically and horizontally, i.e. a translational system. Their unique contribution to medical history was relating anatomical landmarks to landmarks within the brain tissues, thus developing the first human stereotactic atlas based on ventricular system landmarks. In total Spiegel and Wycis developed six different models, of which later models included precision lockable hinges to adjust the angle of the electrode carrier in the anterior-posterior and lateral planes (Heilbrun, 1988).

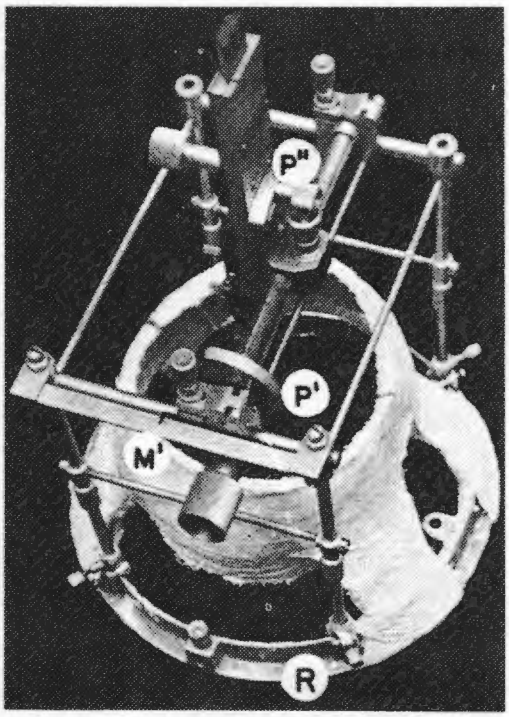


Figure 2.2: Spiegel and Wycis human stereotactic apparatus
(from Heilbrun, 1988, who extracted it from Spiegel et al (1947))

Who developed the second human stereotactic apparatus has never been resolved. Even while Spiegel and Wycis were working on their design, other stereotactic frames were being developed. Among the frames that were developed prior to computed tomography (CT), the most well known were:

| | |
|---|---|
| 1. Leksell frame | 1949 |
| 2. Talairach system | 1949 |
| 3. Riechert apparatus | 1951 |
| Riechert-Mundinger - a later modification | 1955 |
| 4. Todd-Wells system | 1967 |

These and other stereotactic systems fell into one of three categories (or combinations of the categories): systems using Cartesian coordinates, systems using polar coordinates and burr hole mounted systems (shown in figure 2.3).

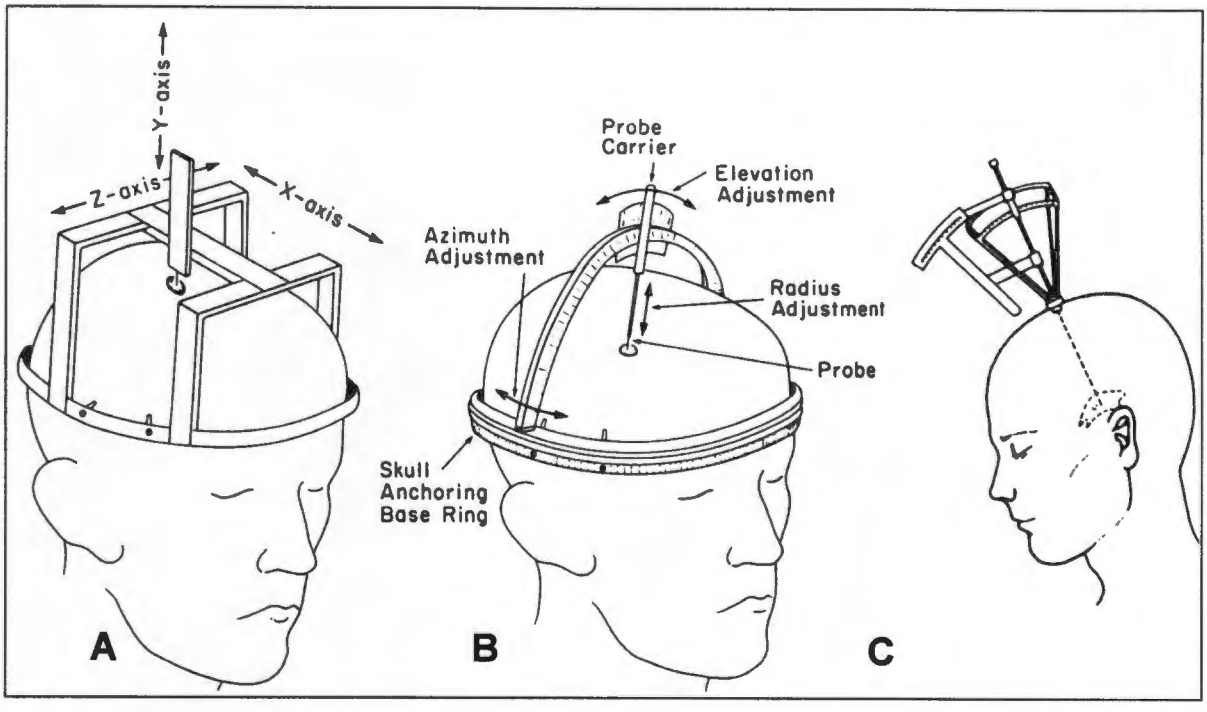


Figure 2.3: The three categories for stereotactic instruments:
A - Cartesian coordinate system, B - Polar coordinate system and
C - Burr hole mounted system
(A & B from Horner et al, 1984, C from Heilbrun, 1988)

The burr hole systems are very seldom used, as they are inherently less accurate than the other two types of stereotactic systems. Prior to the development of CT, they were mainly used by neurosurgeons, who only had limited knowledge of stereotaxis, for performing thalamotomies for Parkinson's disease. ("Thalamotomy is the destruction of a selected portion of the thalamus - a part of the brain - by stereotaxy for the relief of pain, involuntary movements, epilepsy, and rarely emotional disturbances; it produces few, if any neurological deficits or unpleasant personality changes" - Stedman, (1982).) Burr hole-mounted systems (see figure 2.3c) were made up of a fulcrum (a pivot about which a lever turns) to which an electrode carrier had been attached. The fulcrum was attached to the burr hole in the skull and the angle of the electrode was adjusted so that it pointed at the target.

The stereotactic system, when used prior to CT, made use of ventriculography and X-ray imaging to set the various stereotactic devices. This was time consuming, and required a good deal of expertise to set the stereotactic devices. It was also less accurate than the stereotactic work that is done today, as the positions of the intracerebral structures, not visible on the images produced, had to be determined from the various skull and anatomical landmarks using stereotactic atlases of the brain. Several human stereotactic atlases were developed over the years by Spiegel and Wycis, Talairach etc.. The problem with stereotactic atlases and therefore stereotactic neurosurgery was that measurements taken from these atlases did not always yield satisfactory results, due to variations in the human patient population. However it was still much more accurate than any free hand approach, and stereotactic procedures continued to increase rapidly from the 1940's to the 1960's. The most common disorders to be treated were movement disorders, such as Parkinson's disease, and chronic pain (Kelly, 1991). The advent of the drug L-dopa in the treatment of Parkinson's disorder so drastically curtailed stereotactic procedures, that in the early 1970's most American neurosurgical training programs did not provide experience in stereotactic neurosurgery (Kelly, 1991).

The advent of computed tomography (CT), described by Hounsfield in 1973 (Hounsfield, 1973), brought about a revival of stereotactic neurosurgery. The well designed stereotactic devices, that had been developed prior to CT, stood the test of time and the change of imaging modalities. With some modifications for the CT technology, these stereotactic devices once again gained popularity

## 2.2 STEREOTACTIC NEUROSURGERY WITH THE ADVENT OF CT

There are two factors that caused CT to have such an influence on stereotactic procedures. The previously invisible intracerebral structures were now visible on CT images, and no longer had to be inferred from various landmarks with the aid of stereotactic atlases. On CT slices - CT images of thin transverse sections through the brain - both bone and soft tissue structures are imaged. It is possible to distinguish between white and grey matter, identify the cerebral ventricles and the CSF pathways (CSF - cerebro-spinal fluid) and lesions/tumours are visible. Tumour localisation only really became a reality with the advent of CT, and so the powerful imaging capabilities of CT widened the scope of stereotactic applications tremendously.

The second factor is that both CT scanners and stereotactic systems use a measuring system that is based on a Cartesian coordinate system (Heilbrun, 1988). CT slices are anatomically accurate configurations and therefore any point on the CT slice can be precisely measured in the three dimensional Cartesian coordinate system of the CT scanner. When the relationship between the CT slices and the stereotactic coordinate system is established, an intracranial point measured in the CT coordinate system can be related to stereotactic coordinates. In early CT stereotactic procedures this was more labour intensive than it is today, as earlier CT scanners lacked the soft- and hardware to measure Cartesian coordinates. By "transferring" the CT slice, on which the lesion could be clearly seen, onto stereo x-rays, taken of the patient's head within the stereotactic frame, the relationship between the frame and the lesion could be determined (Kelly, 1991). Modern CT scanners, with much improved soft and hardware, make it a simple matter to obtain three dimensional Cartesian coordinates, and laborious image transfer procedures are no longer necessary. To be able to determine the relationship between the coordinate systems of the stereotactic frame and the CT scanner, a fiducial reference system is integrated into the stereotactic frame, so that the reference marks image on each CT slice.

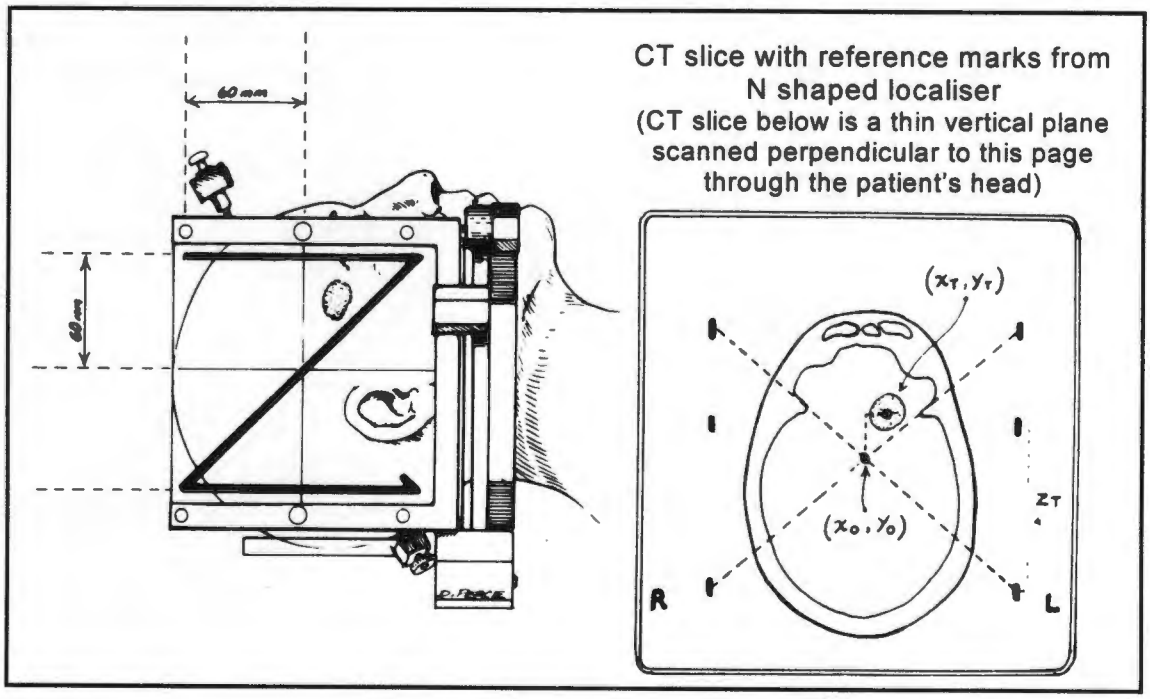


Figure 2.4: The N shaped localiser system used in many stereotactic systems (from Heilbrun, 1988)

The most popular fiducial reference system to be employed in stereotactic frames is the N shaped localisation system (see figure 2.4 - as the patient is lying down the N appears as a bold Z). N shaped radio-opaque elements/plates are attached to the stereotactic frame.

Each N element creates three reference marks on each CT slice. Normally two or three N elements are utilised in a stereotactic frame, creating six to nine reference marks, from which the height and inclination of each CT slice can be determined above a known base plane (Kelly, 1991). From this information, stereotactic coordinates can be calculated for intracranial points on the CT slice.

Using the stereotactic coordinates of the intracranial point, the stereotactic device is set so that the tip of a surgical instrument, when inserted into the patient's brain, comes to rest on that intracranial point. The type of surgical instrument used, for example probe, electrode, biopsy cannula etc., is dependent on the surgical procedure to be performed.

The various stereotactic applications can be divided into three broad categories:

a) Treatment of lesions:

Biopsy of intracranial lesions - this involves the removal of a small living tissue sample (1-2mm$^3$) from the lesion, through a small hole made in the skull, using a biopsy cannula. The tissue sample is removed for diagnostic examination, for example to determine whether the lesion is benign or malignant.

Evacuation of fluids from cysts, abscesses and hematomas etc.

b) Localisation

Localisation of a lesion prior to its conventional surgical removal. The removal of the lesion through conventional methods is referred to as an open craniotomy or simply a craniotomy.

c) Functional stereotactic procedures

Treatment of movement disorders, such as Parkinson's disease

Intractable pain

Epilepsy

Psychiatric disease

In functional stereotactic procedures lesions are created by inserting an electrode into the brain and destroying the brain tissue directly surrounding the electrode tip. For example, by creating lesions in specific areas of the brain, the tremors caused by Parkinson's disease, and other diseases, can be greatly reduced.

The most common of the above applications is the biopsy of intracranial lesions (Kelly, 1991), and is of growing importance with the increasing number of AIDS patients presenting with a wide variety of different lesions (Heilbrun, 1988).

The most well known stereotactic systems, that survived the transfer to the CT era of stereotactics, were the Leksell system, the Riechert-Mundinger system, and the Todd-Wells system. For the Talairach stereotactic system, adaptations to CT have been proposed by Kelly (Kelly, 1991), however the important contribution made by Talairach and Szikla was stereotactic angiography in 1977, i.e. after the advent of CT (Kelly, 1991).

Many other new CT compatible stereotactic systems have been developed after the advent of CT. The well known stereotactic systems include the Brown-Roberts-Wells (BRW) stereotactic system, the Cosman-Roberts-Wells (CRW) system (a modification of the BRW system), and the Kelly-Goerss system, which soon thereafter was replaced by the COMPASS system.

Each of these systems will be briefly described, as they are the best known frame-based stereotactic systems and encompass nearly every aspect of frame-based stereotactic neurosurgery. Even with the advent of frameless/image guided stereotactic neurosurgery, the Leksell, CRW and COMPASS stereotactic systems, for example, are still widely sold and used today.

### 2.2.1 The Leksell Stereotactic System

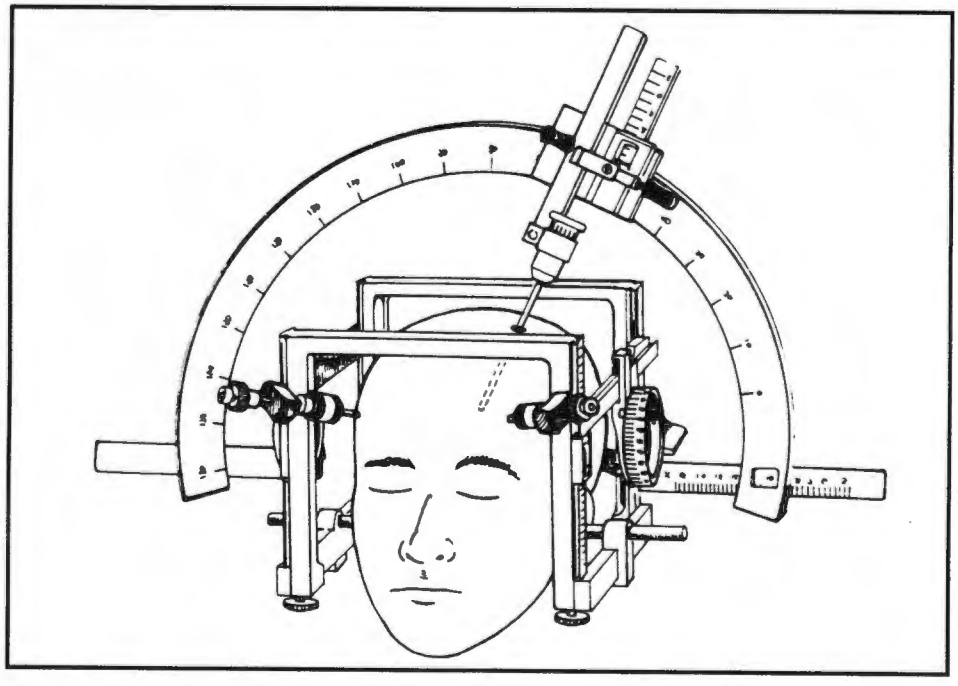

Figure 2.5: The Leksell stereotactic system
(from Heilbrun, 1988)

The Leksell stereotactic system (see figure 2.5) was first developed by Lars Leksell in Stockholm in 1949. It is remarkable that this stereotactic system, that was first developed nearly 50 years ago, is still one of the most popular stereotactic systems today.

The Leksell system consists of a cuboidal frame, a three dimensional coordinate system with x, y and z scales inscribed on the horizontal and vertical bars. As with most of the frame-based stereotactic systems, the cuboidal frame is attached to the skull by 4 pins, which are inserted into holes drilled into the outer layer of the skull. Prior to the CT scan, the N shaped localiser plates are attached to the vertical supports of the cuboidal frame (see figure 2.4), so that the relationship between the stereotactic frame and CT coordinate system can be established. During the CT scan, the cuboidal frame is bolted to the CT table and thus the patient is immobilised throughout the scan. The procedure of indirectly bolting the patient to the CT table, via the frame, is utilised in most frame-based stereotactic systems. Once the CT procedure has been completed, the N shaped localiser plates are removed. Once all the calculations have been completed, the moveable arc-quadrant, a concept developed by Leksell, is attached to the cuboidal frame using the settings obtained from the calculations (see figure 2.5). The probe is set, so that it is equal in length to the radius of the arc. The probe tip, regardless of the arc rotation around the supporting gimbals (arc moving perpendicular to the plane of the page in figure 2.5) or the movement of the probe carrier along the circumference of the arc (probe carrier moving in the plane of the page in figure 2.5), remains at the centre of the arc. As the side bars and arc supports are adjustable in three dimensions, the arc centre is made coincident with the target point. Thus, once the stereotactic system is set, the probe can be inserted from any horizontal and vertical approach angle on the arc-quadrant and the probe tip will come to rest on the intracranial target point.

The Leksell frame makes use of both CT and MRI (magnetic resonance imaging) compatible N shaped localiser plates, so that it can be used with both imaging modalities. MRI produces far superior images of brain tissues, but its three dimensional measuring abilities, even though they have improved tremendously, still leave something to be desired. Thus most stereotactic systems making use of MRI, will do so in conjunction with CT.

Theoretically, the Leksell frame can be used for multiple procedures, with the frame being removed between procedures. This is done by marking the depth to which the pins have been inserted into the skull on the actual pins. By relocating the holes, and inserting the pins to their marked depth, the cuboidal frame should resume the same relationship to the skull, as it did prior to its removal.

The Leksell system is an excellent stereotactic system for accurately reaching an intracranial target. It is used for functional procedures, lesion biopsies and evacuations of cysts etc., and for implanting radionuclide sources for interstitial irradiation. A disadvantage. however, is that the cuboidal frame limits the classic Leksell system for use in stereotactic craniotomies, as it "simply gets in the way" when the scalp is incised and a portion of the skull is removed (Kelly, 1991).

### 2.2.2 The Talairach Stereotactic System

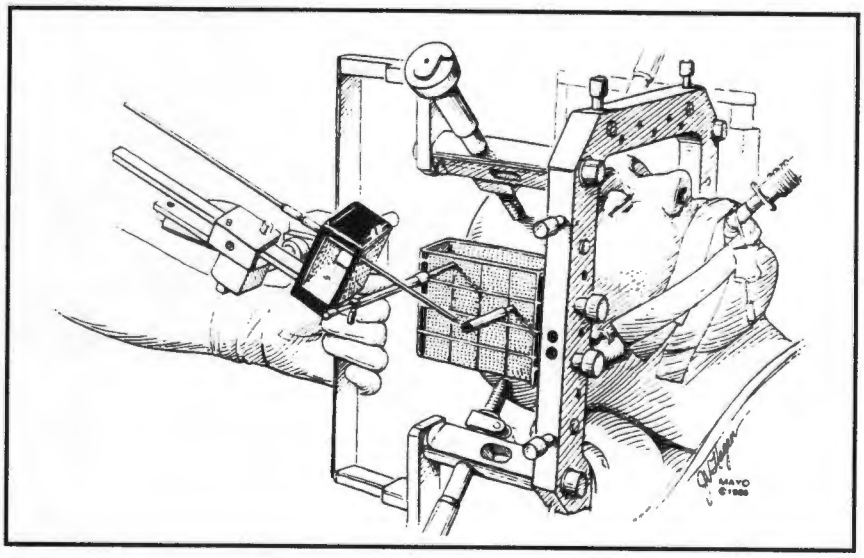

Figure 2.6: The Talairach stereotactic system
(from Kelly, 1991)

The Talairach system (see figure 2.6) was developed in 1949, in the same year as the Leksell system, by Jean Talairach in Paris. The Talairach system consists of a base unit with four vertical supports, through which fixation devices are inserted into the patient's skull. A double grid is attached to the base plate. Using teleradiography and ventriculography, lateral and anterior-posterior images of the double grid superimposed on the skull and ventricles of the brain are obtained. (Teleradiography is a concept developed by Talairach in which tightly collimated x-ray beams and a long tube-to-patient distance is utilised to reduce magnification distortions of the x-ray images. The terms of lateral and anterior-posterior (AP) are some of the medical terms used to describe the human "coordinate system", and are defined in Appendix A - an extract from Gray's Atlas of Anatomy (Williams et al, 1980) ).

The neurosurgeon selects the hole in the double grid that directly overlies the intracranial target. By adjusting a depth stop on the probe and directing it orthogonally through the holes in the double grid, the tip of the probe comes to rest on the intracranial point. Due to the double grid system, the Talairach system is ideal for introducing multiple electrodes to study seizure foci in the temporal lobes of the brain. The Talairach system can also be used for oblique probe vectors, although this is a more complicated procedure than using orthogonal probe vectors (Kelly, 1991).

Talairach, together with Szikla - a member of the Talairach group, made an important contribution to stereotactics by introducing stereotactic angiography in the late 1970's. The vascular structures (blood vessels) are superimposed on the teleradiographs and ventriculograms, making it possible to avoid them during surgical procedures (Kelly, 1991).

The disadvantage with the Talairach system at present, is that the base unit and four vertical supports are entirely made of metal. It is therefore not CT compatible, as metal in too great a quantity causes artefacts in the images. Kelly felt that only some minor modifications were required to make the Talairach system CT compatible (Kelly, 1991).

### 2.2.3 The Riechert-Mundinger Stereotactic System

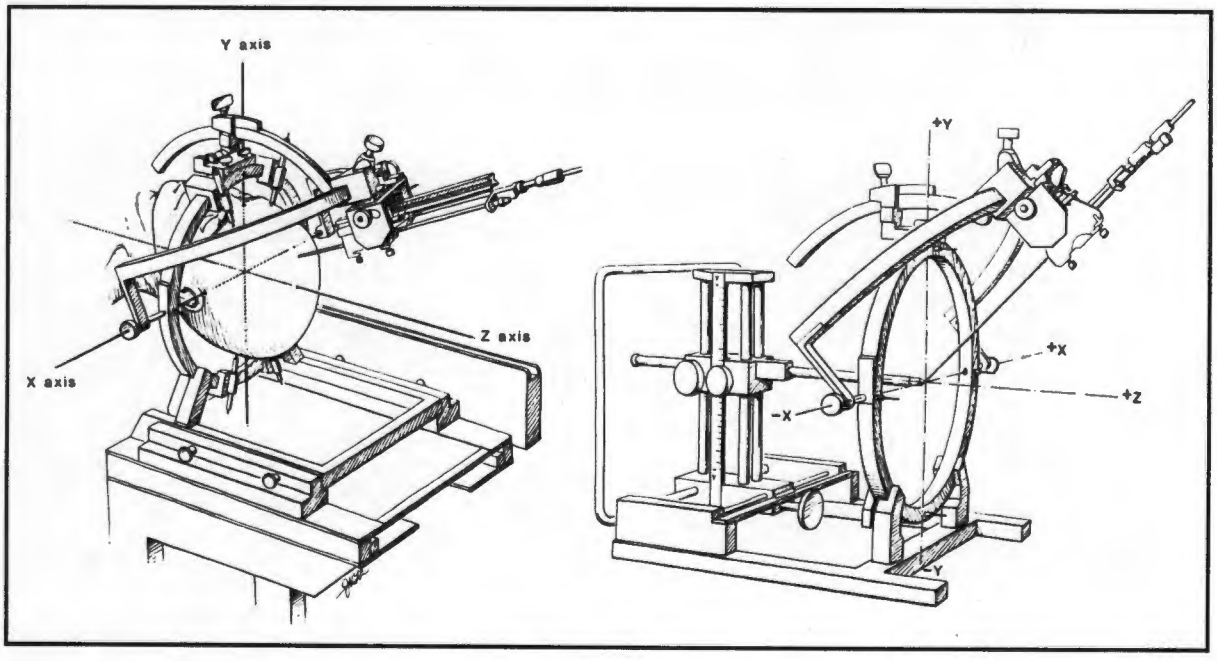


Figure 2.7. :The Riechert-Mundinger system (left) and the target point simulator (right) (from Kelly, 1991)

The stereotactic system developed by Riechert in Germany, and its later modifications with Mundinger, became known as the Riechert-Mundinger stereotactic system (figure 2.7 - left). It is similar to the Leksell system, in that the probe carrier is mounted on a semicircular arc. The probe carrier in turn is mounted on a head ring, which surrounds the lower part of the patient's head and is bolted to the patient's skull with 4 pins. The difference between the Riechert-Mundinger system and the Leksell system is that in the former system the intracranial target is offset from the centre of the arc. Therefore it is desirable to set the system with a target point simulator (see figure 2.7 - right), or use a PC to calculate the settings on the stereotactic device (Heilbrun, 1988).

As with the Leksell system, the Riechert-Mundinger system also makes use of the N shaped localisation system to establish the relationship between the stereotactic and CT coordinate systems. By setting the stereotactic coordinates of the intracranial target on the target point simulator, the probe guide can be set on the semicircular arc, which had been transferred to the simulator (see figure 2.7 - right ). Once the probe guide has been set, the arc is reattached to the head ring, which is attached to the patient's head, and the stereotactic procedure can be completed.

### 2.2.4 The Todd-Wells Stereotactic System

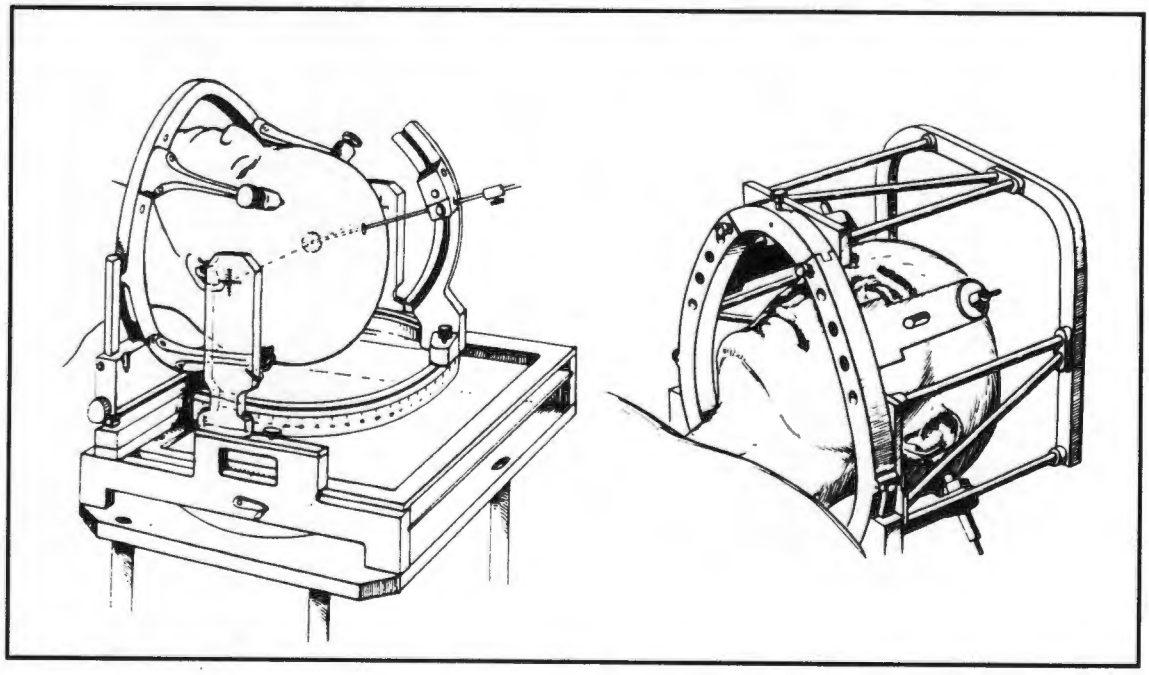

Figure 2.8 : The Todd-Wells stereotactic system (left, from Heilbrun, 1988) and the N shaped localiser attached to the base frame (right, from Kelly, 1991)

The Todd-Wells system (figure 2.8) is a fixed arc-quadrant system. Instead of moving the arc to place the intracranial target at the centre of the semicircular arc as in the Leksell system, the patient's head is moved in a controlled manner to align the intracranial point with the centre of the sphere defined by the arc-quadrant (Heilbrun, 1988).

An oval shaped frame is attached to the patient's head via four vertical supports, which are bolted to the patient's skull with 4 pins. As with several other removable stereotactic frames, the pins have micrometers attached to them, so that the depth to which the pins have been inserted can be determined. In this way the frame can accurately be replaced by reinserting the pins in the skull to the depth previously recorded on the micrometers. At the time of surgery, the frame is attached to a base unit, which is either bolted to the floor or attached the operating table (see figure 2.8 left). Six mechanical adjustments are required to set the device, three orthogonal adjustments in x, y, and z, two angular adjustments (on the horizontal and vertical arcs in figure 2.8 left) and a probe depth adjustment.

Originally the Todd-Wells system was designed to be used with lateral and AP x-rays. However Kelly (Kelly, 1991) described the adjustments his team made to their Todd-Wells system to make it CT compatible. The oval frame was replaced with a circular frame to allow for the patient being placed in prone or lateral positions on the CT table. As with the Leksell system, Kelly made use of an N shaped localisation system, mounted on the frame attached to the patient's head, to establish the relationship between the Todd-Wells system and the CT scanner (see figure 2.8 right). As the vertical supports of the Todd-Wells system were made of metal, and therefore not CT compatible, Kelly had vertical supports made of molybdenum disulphide, a material that does not cause any artefacts in the CT image.

The Todd-Wells system, modified for use with the CT scanner, proved ideal for functional procedures, stereotactic biopsies and certain stereotactic craniotomies. However Kelly found that when more that one intracranial target was required, the manual resetting of the Todd-Wells system was cumbersome, and that access to lateral targets was limited, due to the mechanical design of the arc-quadrant (Kelly, 1991).

For this reason Kelly designed an intermediate system that used portions of the Todd-Wells system, and this system was named the Kelly-Goerss system. The reader of this literature review may question why Kelly described the modifications to the Todd-Wells system, which he later abandoned. Kelly felt that as over 700 Todd-Wells stereotactic systems had been sold world wide, the owners of such systems would be interested in how their Todd-Wells system could be modified for CT.

### 2.2.5 The Kelly-Goerss - and its later adaptation into the COMPASS System

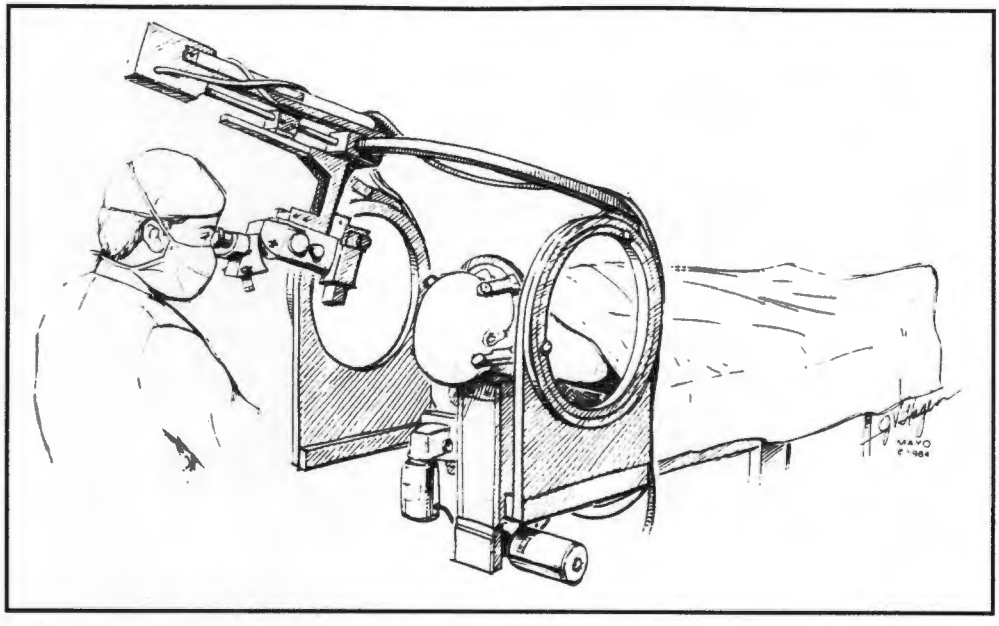

Figure 2.9: The Kelly-Goerss stereotactic system
(from Kelly, 1991)

The Kelly-Goerss stereotactic system (figure 2.9), the forerunner of the COMPASS system, made use of many of the aspects of the Todd-Wells system. Kelly used his own modifications for the frame, vertical supports and N shaped localiser system. The base unit, attached to the operating table, contained three optical encoder controlled servo-motors, which made it possible to perform three orthogonal adjustments from a control panel. At the time of the operation, the frame (and the patient's head) were fixed to the base unit. The original 135mm radius arc-quadrant of the Todd-Wells system could be removed and replaced by a 160mm radius arc-quadrant or by a 400mm arc-quadrant on which an operating microscope or laser could be mounted. In figure 2.9, the operating microscope is attached to the 400mm arc-quadrant, allowing the neurosurgeon a microscopic view of the brain. To position the intracranial point at the centre of sphere defined by the arc-quadrant, the various adjustments were controlled via the servo-motors and optical encoders.

After 500 procedures, the Kelly-Goerss system was abandoned, as the circular frame proved to be too small for large heads, it was cumbersome to change the viewing angle of the microscope on the 400mm arc-quadrant during an operation, and the large arc-quadrant was very difficult to drape. With the experience gained with the Todd-Wells and Kelly-Goerss system, it was possible to design the COMPASS system incorporating all of the advantages of the two systems. The COMPASS system was mainly designed for tumour stereotactics.

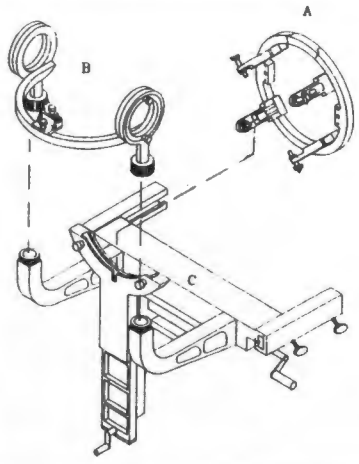


A - CT/MRI compatible circular frame to hold patient's head

B - 160 mm radius arc-qudrant that attaches to C

C - Base unit with three orthogonal adjustments. Movements in the x, y and z are controlled by hand cranks, and in later versions by stepper motors and optical encoders

Figure 2.10: The COMPASS system
(from Kelly, 1991)

The COMPASS system (figure 2.10) utilises the fixed arc-quadrant and base unit concept of the Todd-Wells and Kelly-Goerss systems. The frame, that is bolted to the patient's head, has a diameter of 10.5 inches to accommodate even the largest head and is attached to the skull via the four vertical supports with carbon fibre pins. The carbon fibre fixation system is constructed in such a manner that the frame can easily be replaced for multiple procedures. Also included in the COMPASS system are the localisation systems for CT, MRI and DSA (digital subtraction angiography). An optional addition is the computer hardware and software to run the COMPASS system.

The 160mm radius arc-quadrant (see B of figure 2.10) has two angular degrees of freedom, the movement of the probe holder along the horizontal arc and the rotation of the arc about the lateral rings holding the arc. The two degrees of freedom allow various approach trajectories to the intracranial target. Once the frame, and therefore the patient, has been fixed to the base unit, the three orthogonal adjustments are made to bring the intracranial target to the centre of the sphere defined by the arc. These adjustments are made by computer-controlled stepper motors, once the computer has converted the stereotactic coordinates of the intracranial target into mechanical adjustments (Kelly, 1991). The COMPASS system thus falls between the frame-based stereotactic systems and a robotic system.

### 2.2.6 The BRW Stereotactic System

The BRW (Brown-Roberts-Wells) stereotactic system, unlike the other systems, was developed specifically for CT stereotactic surgery.

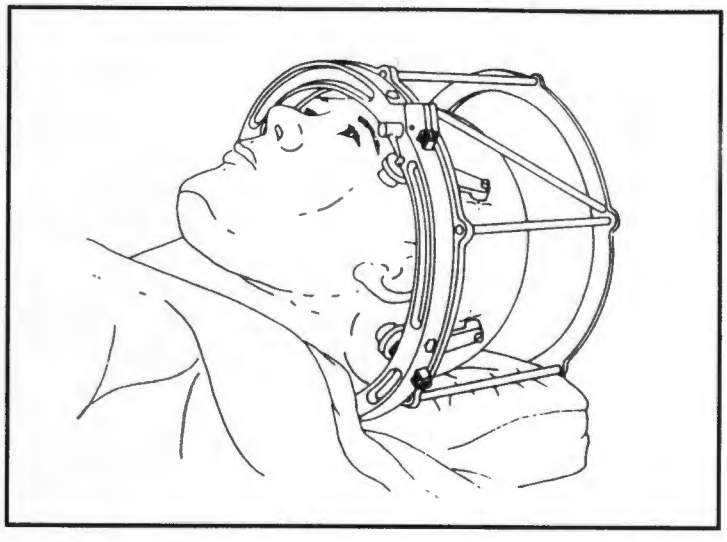

Figure 2.11: The N shaped localiser attached to the head ring
(from Heilbrun et al, 1983)

The head ring of the BRW system is attached to the patient's skull with four penetrating pins. Prior to the CT scan, an N shaped localiser system is attached to the head ring (see figure 2.11). The resulting fiducial marks, imaging on every CT slice, indicate the spatial relationship between that slice and the head ring (Heilbrun, 1988).

Once the CT procedure has been completed, the N shaped localiser system is removed and later replaced with an arc guidance system, which consists of interlocking arcs. Due to the complexity of setting the individual arcs to obtain the desired trajectory to reach a specific intracranial target, the BRW system also includes software run on a hand-held programmable calculator or PC. The software is also used to determine the x, y and z coordinates of the intracranial target in the BRW stereotactic coordinate system, from the measurements of the fiducial marks and intracranial target in the CT scanner system (Heilbrun, 1988).

The intracranial target, accessed via various approaches, can be simulated on a phantom. The phantom apparatus consists of a base ring, identical to the head ring, and a moveable pointed tip to simulate the intracranial target. The simulated target can be set at any x, y and z coordinates within the range of the phantom. The arc-guidance system, prior to its

attachment to the head ring, is attached to the base ring of the phantom apparatus. The simulated target is set at the x, y and z coordinates, calculated by the software for the intracranial target, and the four arc settings, also calculated by the software, are set on the interlocking arcs. In this way the neurosurgeon can check the accuracy of the setting and check the trajectory to the simulated target (see figure 2.12 left) (Heilbrun et al, 1983). The phantom apparatus can also be used to mechanically determine the entry point coordinates, and determine the depth to the intracranial target (Heilbrun, 1988), instead of using software to calculate them.

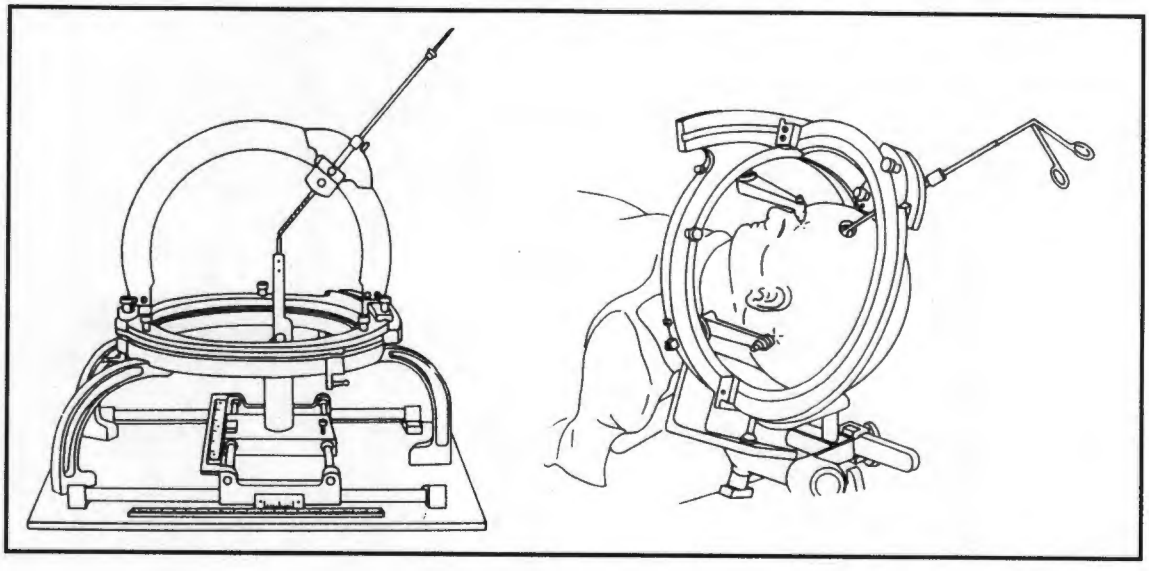

Figure 2.12: The BRW phantom apparatus (left) and the BRW system in use in theatre (right) (from Heilbrun et al, 1983)

Once the neurosurgeon is satisfied with the settings, the arc-guidance system is transferred to the head ring and the stereotactic procedure can be undertaken (see figure 2.12 (right) (Heilbrun et al, 1983).

### 2.2.7 The CRW Stereotactic System

The CRW (Cosman-Roberts-Wells) stereotactic system (see figure 2.13) is a modification of the BRW system. The changes in the design have been made to improve the procedures for stereotactic biopsies and craniotomies (Pell et al, 1991).

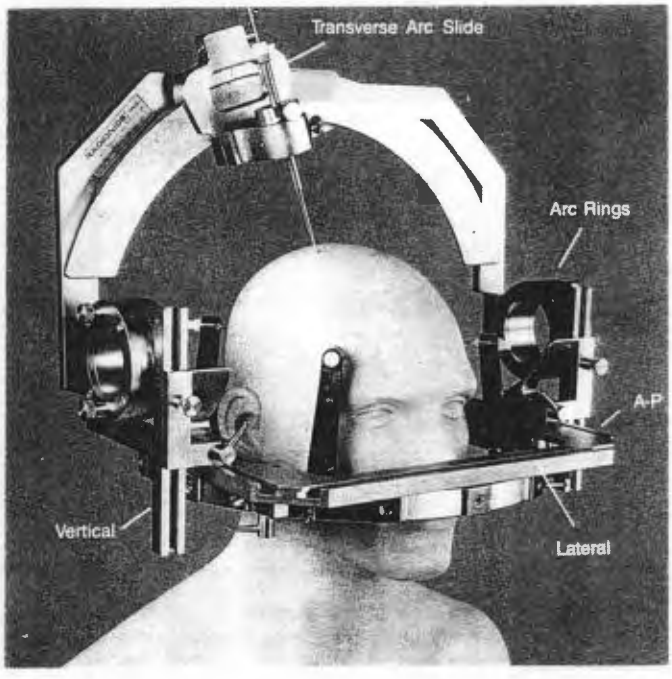


Figure 2.13: The CRW stereotactic system
(from Pell et al, 1991)

The CRW system utilises the BRW head ring, the BRW N shaped localiser system, and the BRW phantom apparatus to check the settings on the CRW arc. Where the BRW system made use of an arc-radius design, the CRW system makes use of a target-centred arc design.

The CRW system is in fact very similar in design to the Leksell stereotactic system. The target-centred arc design is based on three orthogonal movements (anterior-posterior=A-P, lateral and vertical - see figure 2.13), as is the Leksell system with its cuboidal frame and x, y and z axes. In both the CRW and Leksell systems, the centre of the arc is made to coincide with the intracranial target. The CRW has a fixed radius of 160mm and this is the fixed distance between the top of the probe guide and intracranial target. Once the orthogonal movements, calculated by the software, have been made to place the intracranial target at the centre of the arc, any rotation angles of the arc rings and transverse arc slide (see figure 2.13) will set a trajectory that will guide the probe to the intracranial target.

The target-centred arc design in the CRW system allows the neurosurgeon to approach the intracranial target through an infinite number of entry points. The neurosurgeon can also approach multiple intracranial target sites through the same entry point, for example in a stereotactic biopsy, where both the centre of the lesion as well as its periphery are of interest. A further advantage of the arc design is that the arc can be swung down leaving the upper area of the head free, thus giving the neurosurgeon the necessary room to perform an open craniotomy. In this way the CRW system has the advantage over the Leksell system, as the Leksell cuboidal frame surrounds the head, making it difficult to perform an open craniotomy. Due to the way in which the head ring is draped, the orthogonal settings can be altered during a surgical procedure without compromising the sterile conditions, and thus different intracranial targets can be approached during the surgical procedure without too many problems.

## 2.3 THE FRAME-BASED STEREOTACTIC SYSTEMS

Of the systems listed above, the BRW, CRW, COMPASS and Leksell frame-based stereotactic systems are widely used at present. Their manufacturers are listed below:

- the BRW and CRW stereotactic systems are made by Radionics, Inc (Galloway et al, 1991).
- the COMPASS stereotactic system is made by Stereotactic Medical Systems Inc., America (Kelly, 1991)
- the Leksell stereotactic system is made by Electa Corp., Sweden (Galloway et al, 1991).

Various modifications of the basic principles employed in these different stereotactic systems have led to a whole host of other frame-based stereotactic systems, which are usually only used by a small number of stereotacticians or by the people who developed them.

Some other stereotactic systems have been developed primarily for specific aspects of tumour stereotactics, and since they are commercially available today, these are listed here. They include the Patil system (Patil, 1984) and the Gouda frame (Gouda et al, 1983). These stereotactic systems have not been described here as both the Gouda and Patil systems are arc based systems, the Gouda system being very similar to the CRW system.

Of the frame-based stereotactic systems described so far, all have the head frames/rings bolted to the patient's skull, to maintain a rigid relationship between the stereotactic device and the patient's head. There are however a few stereotactic systems that were designed with non-invasive stereotactic frames. These systems make use of various devices to ensure

that the frame, at the time of the CT procedure and the surgical procedure, always maintains the same relationship to the patient's skull. This is usually done using a custom made bite plate for the upper dentition (other fixation devices that have also been tried/employed include ear plugs, nasion rests, occipital rests, and plastic helmets (Horner et al, 1984) ). The patient's custom made bite plate is attached to the head frame, and by the patient biting on his/her custom made bite block, the frame can be relocated at any stage with very good accuracy. An example of such a system is an adaptation of the Gill-Thomas stereotactic frame, a modification of the BRW system, (Graham et al, 1983). These types of systems have not proved to be very popular. This may be due to the fact that for every patient a custom made bite plate must be made, which is time consuming, and a dental technician must be on hand to do the work. Also it may be difficult to ensure that the patient's upper dentition is properly "seated' in the bite plate, when the patient is under general anaesthetic.

## 2.4 ACCURACY OF FRAME-BASED STEREOTACTIC SYSTEMS

The accuracy of frame-based stereotactic systems is often claimed to be approximately 1mm by various manufacturers, which can be very misleading to the user of the system as this accuracy is not often achieved. In the manufactures terms of reference this is not an incorrect statement, as it is based on the design specifications of the particular stereotactic instrument and not on the application accuracy of that stereotactic system.

The reason why the manufacturers only quote design specification accuracies, is that they have no knowledge of what imaging modality the stereotactic instrument is to be used with, with what accuracy that imaging modality can determine 3D coordinates, and what other inaccuracies will arise from actually setting the instrument. All these different aspects are encompassed in the application accuracy, and will give the neurosurgeon a much better idea of the accuracy he/she can expect from their stereotactic system, when it is actually used in the clinical environment.

Various papers have been published to try and establish the application accuracy of frame-based stereotactic system. The most quoted paper on this subject is written by Galloway et al (1991). Galloway and his team examined four well known frame-based stereotactic systems, the BRW, CRW, Kelly-Goerss and Leksell systems. Various CT slice thicknesses were used, as this has an effect on the application accuracy. Most CT scanners have digitisers that are accurate to the nearest millimetre, i.e. in the two axes of the imaging plane, with the accuracy of the third axis determined by the slice thickness of that image. In total Galloway and his team made 7681 independent measurements, with slice thicknesses

of 1mm, 4mm and 8mm being used. The results for the 1mm slice thicknesses are listed in table 2.1 below. The measured vector error in table 2.1 is the distance between the actual target and the target pointed at by the stereotactic system.

| | BRW (mm) | CRW (mm) | Kelly-Goerss (mm) | Leksell (mm) |
|---|---|---|---|---|
| Mean vector error | 1.9 | 1.8 | 1.0 | 1.7 |
| Std. Deviation | 1.0 | 1.1 | 0.6 | 1.0 |
| Maximum value | 5.0 | 4.9 | 3.1 | 4.5 |

Table 2.1: Application accuracies for four well known frame-based stereotactic systems using 1mm slice thicknesses (from Galloway et al, 1991)

From the data listed in table 2.1 above, it can be clearly seen that the design specification accuracy of 1mm is rather optimistic, and that the application accuracies can range from 1mm in a best case scenario to 5mm in a worst case scenario, when 1mm slice thicknesses are employed.

## 2.5 FRAMELESS STEREOTACTIC NEUROSURGERY

There are various types of frameless stereotactic systems, that have been developed since the end of the 1980's and the beginning of this decade. These systems were designed to improve on the frame-based stereotactic systems, taking advantage of the ever improving computing systems and imaging modalities. The modern imaging systems are capable of providing the neurosurgeon with the necessary three dimensional spatial data for locating intracranial targets, that are clearly visible on the images produced, without the necessity of fiducial localisers, such as the N shaped localiser.

In frameless stereotactic systems an external reference system, consisting of a minimum of three external reference points, is used to establish the relationship between the imaging modality, be it CT, MRI or DSA, and the stereotactic system. These external reference points can consist of either external markers, that are attached to the patient's head in some manner, or of certain cranial landmarks, such as the external auditory meatus, bridge of the nasal bone, or the junction of coronal and squamosal sutures (Kelly, 1991). Cranial landmarks are not used very often, as they are not as well defined on the resulting images as the external reference markers and are more difficult to use.

Most of the frameless stereotactic systems make use of a three dimensional (3D) measuring system in theatre to re-establish the relationship between the imaging modality and the patient's head. The 3D measuring systems consist of either robotic arms, such as the ISG viewing wand (Drake et al, 1993), 3D digitisers - optical or sonic systems, or 3D photogrammetric systems. The 3D measuring system is utilised to determine the 3D coordinates of any external reference markers and intracranial points in the coordinate system of the 3D measuring system. As the 3D coordinates of the external markers have now been determined in the coordinate system of the imaging modality and the coordinate system of the 3D measuring system in theatre, a three dimensional transformation algorithm can be utilised to establish the geometrical relationship between the two coordinate systems. By attaching reference markers to a surgical instrument, the position of the surgical instrument can thus be determined in the coordinate systems of the 3D measuring system and the imaging modality. The position of the surgical instrument can therefore also be related to the images and the intracranial structures appearing on the images. As this procedure occurs interactively at the time of the surgery, the neurosurgeon can therefore be guided through the intracranial structures on the images and therefore also through the physical intracranial structures of the brain. This interactive surgical procedure aids the neurosurgeon in reaching a specific structure, such as a cancerous lesion, and also assists the neurosurgeon in removing all of that lesion. These systems are referred to as interactive

image guided neurosurgical systems, and are designed to achieve accuracies that are consistent with those achieved by the frame-based stereotactic systems. This is verified in chapter 8, where the frameless stereotactic systems are described in more detail. These frameless stereotactic systems are not only beginning to supersede the frame-based stereotactic systems, but are also widening the scope of stereotactic neurosurgery (Kitchen et al, 1993).

There are however a few frameless stereotactic systems that have been developed using modern imaging modalities, where the relationship between the imaging modality and some type of stereotactic apparatus is established either by utilising an external reference system or by some mechanical means. The Pelorus system (Carol, 1985; Carol, 1986), one of the stereotactic systems that is commercially available, utilises mechanical means to establish a relationship between the patient's head, the imaging modality, and the stereotactic apparatus. The Pelorus system has been utilised in a range of applications from biopsies to interstitial radiation implant procedures, and can be used with imaging modalities such as CT, MRI, DSA and conventional X-ray (Carol, 1985).

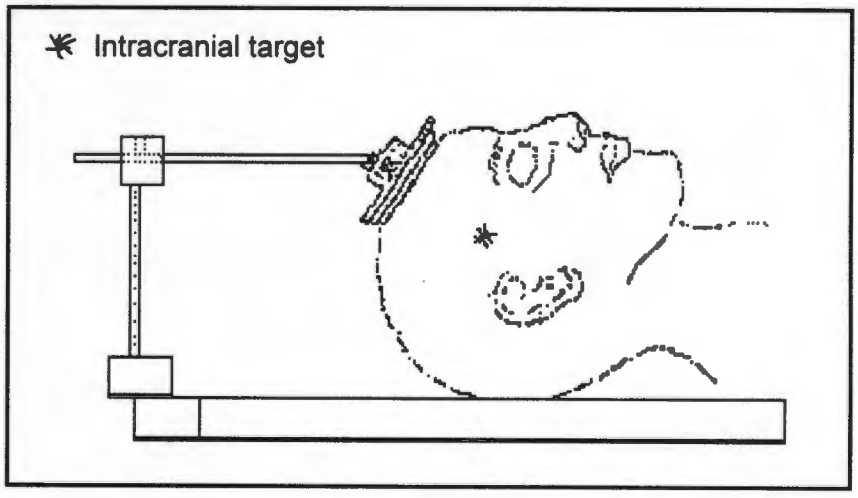


Figure 2.14: Utilising mechanical means to establish a relationship between the patient's head, the imaging modality, and the stereotactic apparatus (from Carol, 1986)

A series of interlocking discs, with a ball and socket joint forming the centre of the discs, is secured to the patient's skull with self-tapping screws, and forms part of the positioning fixture shown in figure 2.14. The positioning fixture is utilised to mechanically establish the geometrical relationship between the imaging modality and the patient's skull, by locking the various clamps on the fixture, when the patient has been correctly placed on the imaging table.

Once the imaging procedure has been completed, part of the position fixture is removed without disturbing the clamped settings, with only the outer disc remaining attached to the patient's skull via the self-tapping screws. The removed part of the positioning fixture is transferred to a phantom fixture (figure 2.15), thus transferring the geometrical relationship, set up in the imaging modality, to the phantom fixture. One criteria for the positioning fixture, is that the horizontal rod (figure 2.14), which is attached to the central ball of the positioning fixture, is parallel to both the longitudinal axis of the imaging table (axis running from head to foot of the table), and parallel to the vertical axis of the phantom fixture. Another is that during the scanning procedure, beside scanning an image through the intracranial target, an additional image is scanned through the central ball (made of translucent material), and therefore through the radio-opaque marker embedded at the centre of the ball. The differences in the x, y and z coordinates, between the radio-opaque marker and the intracranial marker in the imaging modality coordinate system, are duplicated in the phantom fixture, between the phantom target and the radio-opaque marker, transferred to the phantom fixture as part of the positioning fixture.

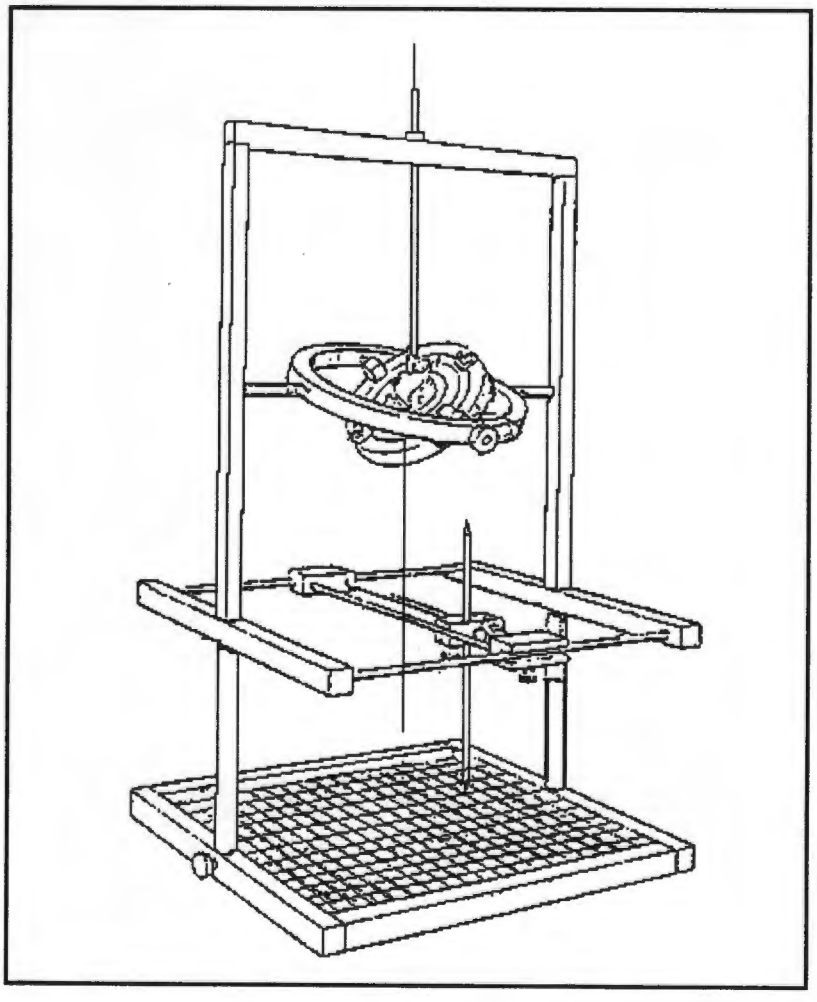

Figure 2.15: The phantom fixture used to set the Pelorus system (from Carol, 1986)

Once the geometrical relationship of the positioning fixture to the imaging modality has been duplicated in the phantom fixture, and the phantom target has been set, the central ball and horizontal rod (figure 2.14, vertical rod in figure 2.15) are removed. A surgical instrument is inserted through a trajectory ball, which has replaced the central ball in the positioning fixture, until the tip of the surgical instrument is coincident with the phantom target. The trajectory ball is clamped, thus setting the trajectory to the phantom target, and the surgical instrument removed. In theatre, once the burr hole has been made, the positioning fixture is replaced in the outer disc attached to the patient's head. The surgical instrument is inserted through the trajectory ball so that its tip comes to rest on the intracranial target (see figure 2.16).

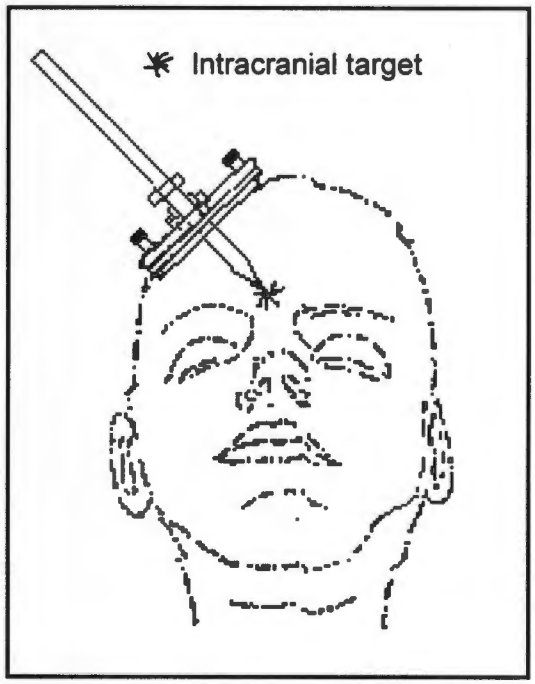


Figure 2.16: A surgical instrument tip placed at the intracranial target using the positioning fixture (from Carol, 1986)

The Cape Pointer is a stereotactic system, where the relationship between the modern imaging modality and the stereotactic device is established using an external coordinate system. The Cape Pointer is based on a much earlier concept developed by Adams in 1981 (Adams, 1981), which utilised conventional X-rays to set the device. Even though the concept was never taken further than the initial research phase, it will briefly described here, as it forms the basis on which the Cape Pointer was developed.

The principle of the device is that any three points (not in a straight line) define a plane, and that it is a simple mathematical problem to determine an orthogonal trajectory to the plane,

such that this trajectory intersects a target lying below the plane, if the three dimensional coordinates of the three points on the plane and the target are known. In figure 2.17 the three points defining the plane are labelled A, B, and C, and the target is labelled X, with all the points being marked on/in the phantom head by radio-opaque markers. By using X-ray stereophotogrammetric techniques, the 3D coordinates of all the radio-opaque markers are determined. The point, where the orthogonal trajectory to the target X intersects the plane defined by A, B and C, is calculated, and will hereafter be referred to as point D.

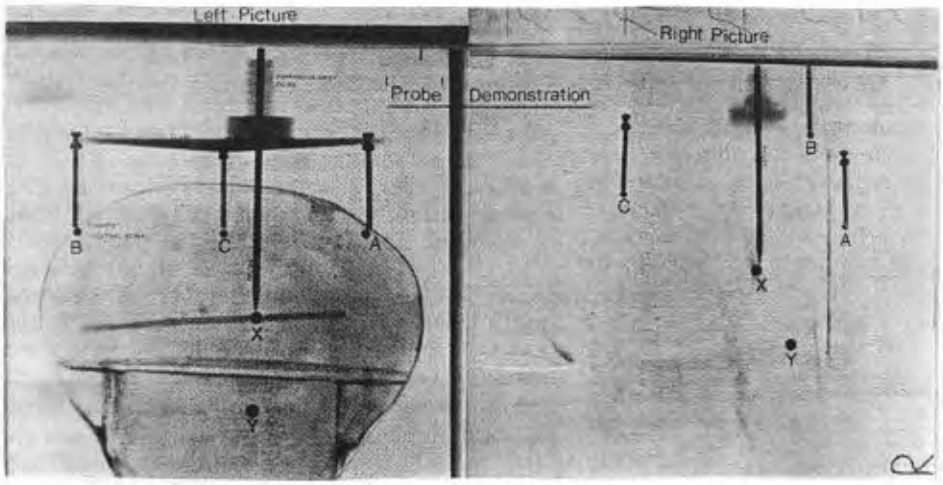


Figure 2.17: X-rays showing a three legged device and a vertical pointer, whose tip is in contact with target X (from Adams, 1981)

The orthogonal pointer, which can be moved to various positions within the three legged table like device shown in figure 2.17, has to be moved to point D using simple geometry. The distances between point D and the planar points A, B, and C (distances d1, d2, and d3 respectively in figure 2.18) are calculated, and using intersecting arcs the position of point D is determined, as shown in figure 2.18.

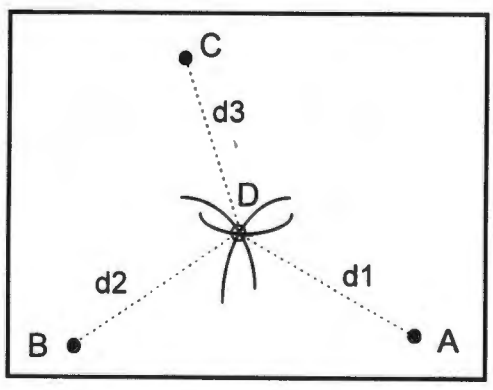


Figure 2.18: Intersecting arcs to determine where orthogonal trajectory intersects the plane

Once the orthogonal pointer has been set at point D, i.e. on the orthogonal trajectory to the target X, only the orthogonal distance from the surface of the three legged table to the target X has to be calculated - as all three legs have the same length, the length of the leg is simply added to the distance of the orthogonal trajectory from point D to target X. Thus the tip of the orthogonal pointer can be placed at target X.

X-ray stereophotogrammetry does yield accurate results, Adams (1981) obtaining vector displacement errors of less than 1mm between calculated and actual control coordinates (Appendix C briefly describes the stereophotogrammetric techniques). No error analysis was done on how accurately the orthogonal pointer could pinpoint the target X, although the X-rays in figure 2.17 - taken after the device was set, show that the orthogonal pointer is in contact with the target X. However X-ray stereophotogrammetric techniques are highly time consuming and labour intensive, and therefore not suited to the clinical hospital environment. It was not until CT was a common tool/imaging modality in South African government hospitals, that the techniques developed by Adams (1981) were revitalised, and the Cape Pointer developed.

# CHAPTER 3 COMPUTED TOMOGRAPHY

## 3.1 INTRODUCTION

Computed tomography (CT), also known as computerised axial tomography (CAT), combines X-ray imaging with computer techniques, thus permitting the visualisation of internal organs and body structures with much greater definition and clarity than could be attained with conventional X-ray methods. Because of it's non-invasive nature, it's use as an outpatient facility, and it's ability to image the brain directly, CT is now one of the primary investigative methods in many neurological disorders (Weatherall et al, 1985).

CT, first described by Hounsfield and Ambrose in 1973 (Ambrose, 1973; Hounsfield, 1973), has made a remarkable difference to many medical procedures. Positions of intracranial lesions, that previously had to be inferred from shifts of the ventricular system of blood vessels, can now be visualised and measured in relation to other intracranial structures and cranial landmarks. As the measuring system of modern CT scanners is based on Cartesian coordinate space, any point visualised by the CT system can be defined in three dimensions, i.e. assigned a X, Y, and Z coordinate, thus defining it's position in 3D space.

The ability to use the CT scanner as an accurate 3D measuring device has been utilised in various medical techniques. The CT scanner, at the Department of Radiotherapy, Groote Schuur Hospital, Cape Town, South Africa, where most of the research work for this thesis has been carried out, has been used to provide 3D information for subsequent proton beam radiotherapy to irradiate intracerebral lesions. It's role in this treatment is to determine the position of the lesion in relation to external reference markers attached to the patient's head (Levin et al, 1993). (The CT scanner at the Groote Schuur Hospital, hereafter referred to as the GSH scanner, is a Picker scanner Model No.174203).

Traditionally when the CT scanner has been used as a measuring device, 3D coordinates of reference markers and intracranial points have been determined using CT slices (figure 3.1). CT pilot or surviews (figure 3.1) were only utilised for slice planning purposes. CT surviews can however be utilised to determine three dimensional CT slice coordinates using a two dimensional projective transformation algorithm. The development of such an algorithm and it's application are described later in this chapter.

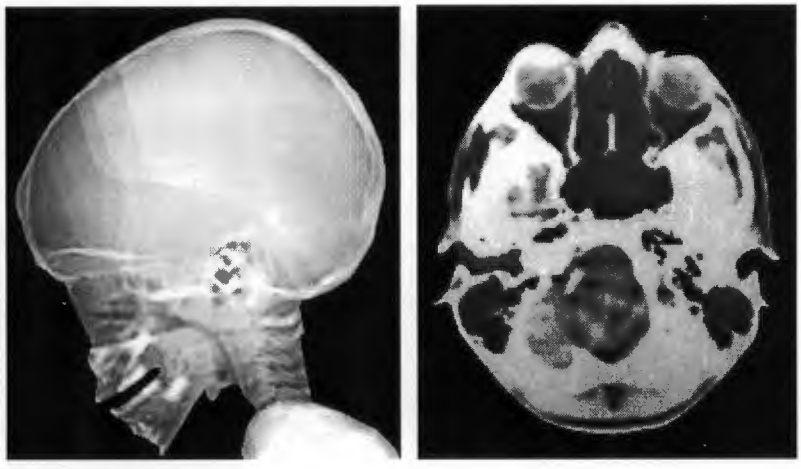

Figure 3.1: A surview and slice of the cranium

Although the CT's imaging capabilities are its primary function, it is the CT's measuring abilities that are under investigation in this chapter. Therefore the focus of this chapter is on the geometry and the measuring principles of the CT system, and only a brief overview concerning the actual CT image production is given.

## 3.2 A BRIEF OVERVIEW OF CT IMAGE PRODUCTION

Conventional X-ray images and CT images both utilise X-rays to visualise internal body structures. However the wealth of information reflected in a CT images, can never be duplicated using conventional X-ray techniques. The difference between CT images and conventional X-ray images lies in the manner in which they are produced.

A conventional X-ray image is literally a shadow of all the organs and structures in the path of the X-ray beam, with the most dense structures, such as bone, imaging much more clearly than soft tissue structures. The X-ray beam is directed through the entire body segment to be examined, and recorded on X-ray film (figure 3.2). The resultant X-ray, similar to the CT surviews (figure 3.1), gives an overview of that body segment.

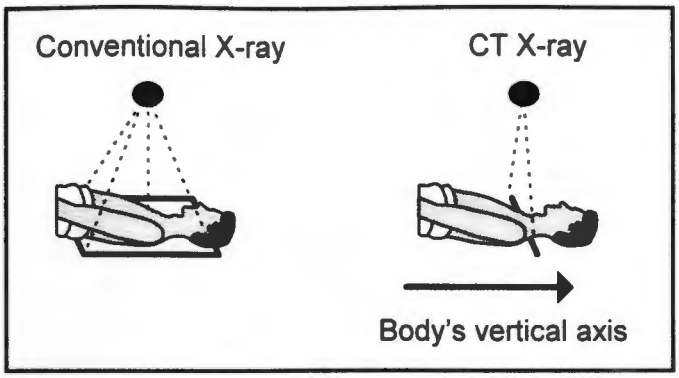


Figure 3.2: Conventional X-ray imaging and CT imaging

With CT slice imaging, a very narrow fan-like X-ray beam is directed at a narrow slice of tissue orthogonal to the body's vertical axis, i.e. in the body's horizontal/transverse plane, as shown in figure 3.2 above. (Cromwell et al , 1973). The resultant CT image/slice is a map of that transverse plane. (In descriptive anatomy, the body's reference system is defined for a person standing upright, the vertical axis runs from head to foot and the transverse/horizontal plane is perpendicular to the vertical axis. This reference system remains unaltered, no matter what the orientation of the body. That is, if the patient is lying down on the CT bed, the body's vertical axis still runs from head to foot, and the plane of the CT X-ray beam is parallel to the body's transverse plane. See Appendix A on the human anatomical "coordinate system".)

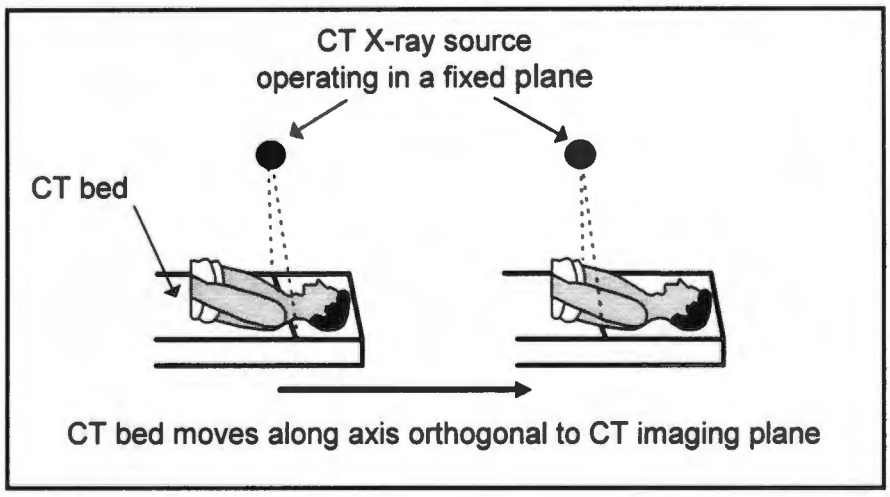


Figure 3.3: CT X-ray source and moving CT bed

The X-ray source in the CT system only operates in one fixed vertical plane (figure 3.3) - the CT imaging plane. To scan a slice through a particular transverse plane of the patient's body, the CT bed, on which the patient is lying, is moved along an axis orthogonal to the CT

imaging plane, until that transverse body plane is coincident with the CT imaging plane. The X-ray source is activated and the slice is scanned.

A CT slice is not exposed on film, as conventional X-ray images are. The intensity of the X-rays, after penetrating the body, are measured by detector elements in the detector system (D in figure 3.4, left). The detector elements can be made of various substances, such as sodium iodide, xenon or calcium chloride crystals. The detector system moves synchronously with the collimated X-ray tube/beam (C in figure 3.4, left), and is cycled around the patient in a cycle of 360 degrees (see figure 3.4, right) (Cromwell et al, 1973).

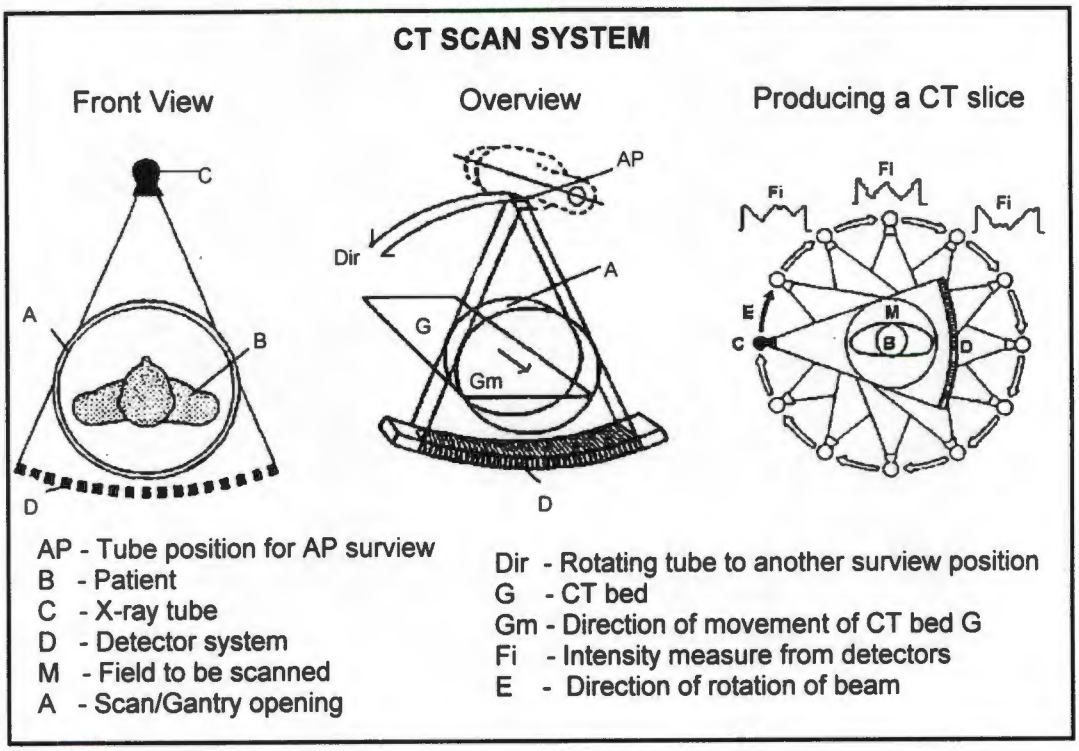


Figure 3.4: The workings of a CT scanner

The data, collected from the detector system as it is cycled around the patient, is used to reconstruct the anatomical density for that slice. The slice is divided into a matrix of tiny picture elements, called pixels, with the GSH scanner slice normally consisting of a 512 x 512 matrix. For each pixel a value is calculated, which is proportional to the X-ray density of that element (Cromwell et al, 1973). The numerical values can typically vary from -1000 representing air to +1000 representing bone (Weatherall et al, 1985). The GSH scanner has a range of -1024 to 3072, with air at -1024.

To reduce scanning time, modern CT scanners use a X-ray fan beam and multiple detector elements in the detector system, as shown in figure 3.4, to simultaneously measure the

density across a portion of the slice. A typical scan takes approximately 2 seconds. The most modern CT scanners, CT spiral scanners, are reported to scan a slice in approximately 100 milli-seconds and complete a full patient scan in the time it takes the conventional CT scanner to scan a single slice.

A typical slice thickness, i.e. the thickness of the transverse body plane to be scanned, can vary from approximately 1mm to 13mm and a pixel area is less than 1 square mm. The GSH radiotherapy scanner has a minimum slice thickness of 2mm and a minimum measuring resolution of 1mm on the CT slice itself.

By scanning CT slices at intervals along part of the body's vertical axis, for example of the patient's head, a comprehensive "three-dimensional picture" of the patient's brain can be achieved by "combining" the two dimensional CT slices.

Even though CT images are an immense improvement over conventional X-rays, precise tissue characterisation is not possible, as each pixel on the slice only reflects it's X-ray density. On CT slices of the brain it is possible to distinguish between white and grey matter, cerebral ventricles, and CSF pathways (CSF - cerebro spinal fluid). In the orbit (bony structure containing the eye) the optic nerve, orbital muscles and other retrobulbar structures are identifiable, due to surrounding low density fat. CT imaging capabilities can be enhanced by administering an intravenous injection of an iodine-containing contrast medium to the patient just prior to the CT scan. Retention of high density iodine occurs in areas of increased vascularity (increased volumes of blood) or where there are defects in the blood brain barrier. Contrast enhancement, when investigating brain disorders, significantly improves diagnostic accuracy of CT: 99 per cent of supratentorial mass lesions are detectable (Weatherall et al, 1985). Such lesions lie above the tentorium cerebelli (see figure 3.5), a dural sheet, roofing the posterior cranial fossa.

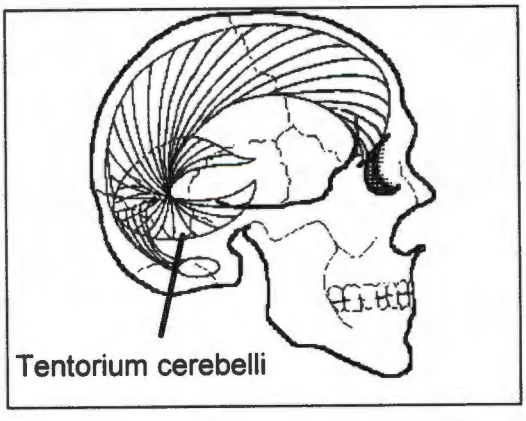


Figure 3.5: The tentorium cerebelli and its position in the cranium

## 3.3 OBTAINING ACCURATE 3D COORDINATES FROM CT SLICES

The CT scanner has been designed on exacting geometrical and mechanical principles. A CT slice therefore is a true map of the internal organs and body structures present in the thin slice of tissue scanned. The CT scanner can therefore be used as an accurate 3D measuring device.

Although CT scanners are designed on similar principles, certain aspects may vary from scanner to scanner. There is no uniform 3D coordinate system adopted for all CT scanners, for example in one CT scanner the vertical axis may be labelled as the Z axis, in another as the Y axis. As most of the work for this thesis has been carried out on the GSH scanner, the information in this thesis is pertinent to the GSH scanner.

When using the GSH scanner to coordinate external reference markers in relation to intracranial structures for stereotactic applications, the patient is usually placed in the supine position (i.e. on his back) on the CT couch/bed. As shown in the figure 3.6, the CT slice coordinate system, in relation to the patient is as follows: the Z axis runs from superior to inferior (i.e. from head to foot), the Y axis (vertical axis) from posterior to anterior (i.e. from back to front) and the X axis from the patient's right to left. The CT imaging plane, and therefore the CT slice, is parallel to the XY plane and the movement of the CT bed is parallel to the Z axis.

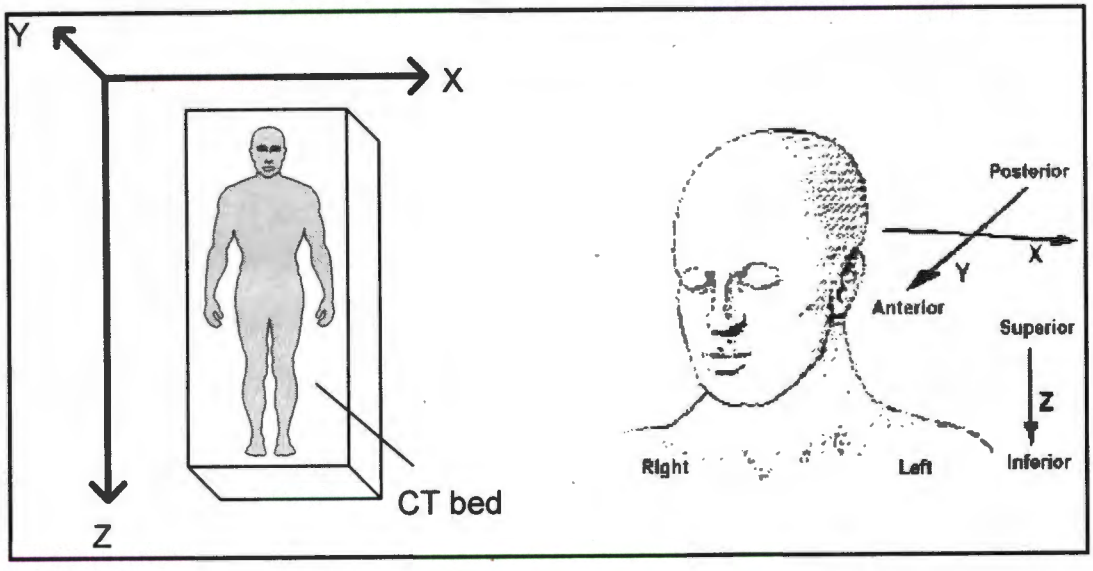


Figure 3.6: The CT slice coordinate system

To measure discrete points on an image, the CT slice is recalled onto the CT screen and a screen cursor activated. The screen cursor's position is displayed to the nearest millimetre.

By moving the cursor onto the discrete point, the X and Y coordinates of that point are displayed. The Z coordinate, determined by the bed position at which that particular slice was scanned, is also displayed. As the minimum slice thickness is 2mm and the measuring resolution in the XY plane is 1mm, the overall expected accuracy for target fixation is approximately 1.5mm.


Figure 3.7: The 2D control and phantom on the CT bed within the CT gantry

To test various aspects of the CT scanner geometry, a two dimensional control and a phantom head (see figure 3.7) were constructed. The control is made of thick glass to ensure that all control markers lie in a single plane, and can be imaged on a single slice. As glass is very radio-opaque, radio-opaque ball-bearings which serve as control markers, are mounted on radio-translucent perspex discs (see figure 3.8). The phantom head, a plastic face mask, was constructed with four external reference markers and one internal reference marker, to act as an intracranial target. (Only these 5 reference markers were used to simulate the Cape Pointer stereotactic application). Each marker consists of a 2mm round ball-bearing.

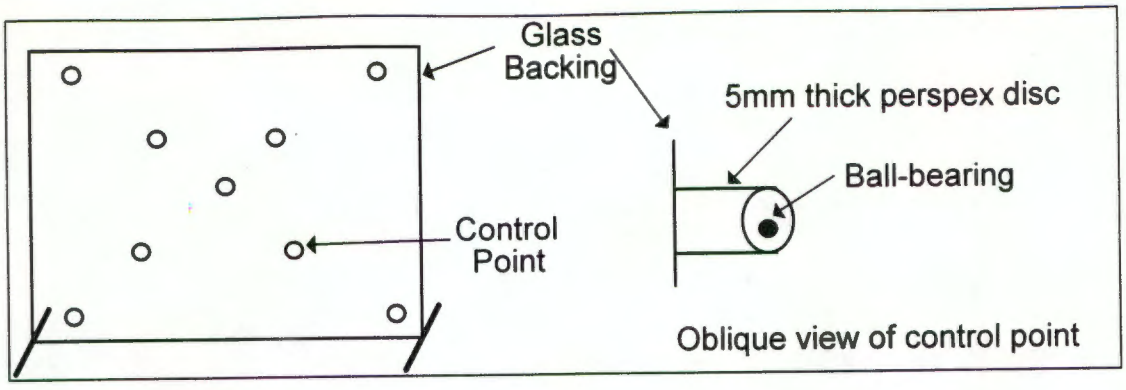


Figure 3.8: The CT control with nine coplanar control markers

The markers on both the control and phantom were measured in a reflex metrograph (Scott, 1981), which has a measuring resolution of 0.1mm. The resultant 3D coordinates were compared to the 3D coordinates measured in the CT slice coordinate system, using Rodrigues transformation (Appendix E, Thompson, 1969). The results are listed in the tables 3.1 and 3.2, and the standard deviations verify the measuring resolution of the CT slice system of 1.5mm. (Only standard deviations are given, as the mean dX, dY and dZ values resulting from the Rodriques transformation are always zero).

| CT control | dX | dY | dZ |
|---|---|---|---|
| Std. Dev. (mm) | 0.6 | 0.6 | 0.2 |

Table 3.1: Comparing 3D coordinates of the 9 control markers obtained by the reflex metrograph and the CT scan slice system (d of dX denoting the difference in the X coordinates etc.)

| Phantom Head | dX | dY | dZ |
|---|---|---|---|
| Std. Dev. (mm) | 0.2 | 0.7 | 0.7 |

Table 3.2: Comparing 3D coordinates of the 5 phantom markers obtained by the reflex metrograph and the CT scan slice system

## 3.4 OBTAINING ACCURATE 3D COORDINATES USING CT SURVIEWS

The positioning of CT slices is planned with the aid of CT surviews (also referred to as pilot views), as the CT surview gives an overall view of the body segment under investigation. On the surview the radiographer can plan where and at what intervals slices are to be scanned. In figure 3.9 the planned slice positions on the surview are indicated with numbered white lines, with the numbers corresponding to the CT slice numbers.

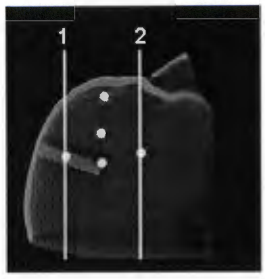


Figure 3.9: A surview showing the positions of CT slices to be scanned

The CT surview is somewhat analogous to a conventional X-ray. The geometric property of conventional X-rays - the central projection in which all rays pass from a perspective centre, i.e. the X-ray source, and radiate outward in 3D space - only partly applies to CT surviews. When scanning a surview, the CT scan beam projects outward from it's focus in a single fixed plane, the XY plane, i.e. in 2D space (see figure 3.10).

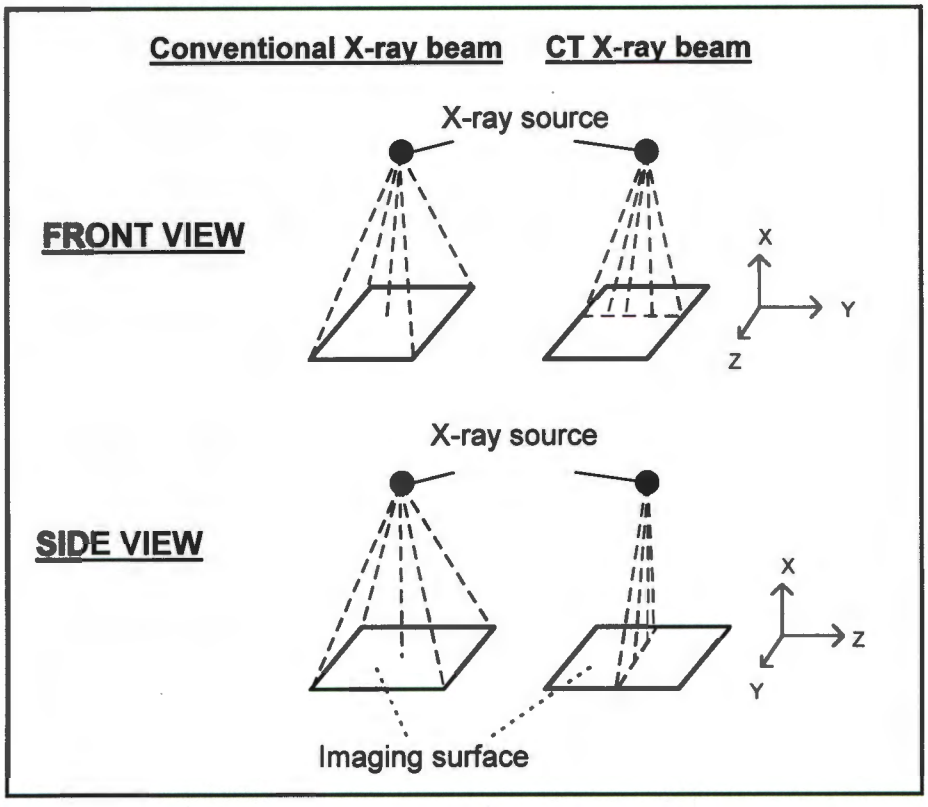


Figure 3.10: The Geometry of the X-ray beam in Conventional and CT surview imaging

The X-ray tube, and therefore the detector system, remain stationary during a surview scan. The fan-like X-ray beam is, for example, only projected from above the patient and recorded only once on the detector elements below the patient and results in one image line. (When scanning a CT slice, the X-ray beam and the detector system are cycled around the patient

and the stream of information continuously picked up by the detector elements is used to construct the CT slice (refer back to figure 3.5: The workings of a CT scanner)).

By moving the CT bed along the Z axis, through the CT's fixed scanning plane, a whole series of image lines are scanned and the surview image is built up. As the X-ray beam only operates in 2D space, i.e. in the XY plane, central projection geometry only applies to the one axis of the surview image (the APx axis and LATx axis of the AP and LAT surviews respectively in figure 3.11), whereas the axis that is parallel to the body's vertical axis is linearly mapped (Z axis in figure 3.11).

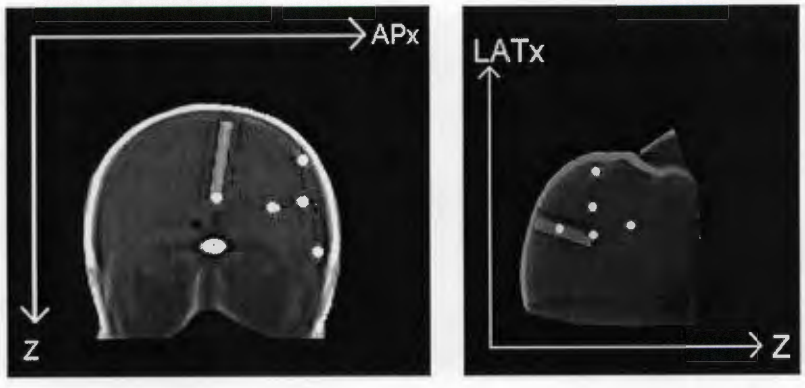


Figure 3.11: The axes of an AP and LAT surview

Surviews usually utilised for planning purposes are the anterior-posterior (AP) and lateral (LAT) surviews. If one visualises the gantry circle as a compass, the X-ray beam for the AP surview is set at 90 degrees on the compass, the lowest point on the gantry circle. (This holds true for the GSH scanner, but some scanners will scan the AP surview from the highest point on the gantry.) The LAT surview is scanned from right to left at a 0/360 degree setting. Most modern CT scanners are not restricted to only scanning the two conventional types of surviews, but can scan oblique surviews from any position on the 360 degree gantry circle.

As the external reference markers for the stereotactic applications normally image on both the AP and LAT surview, these surviews were investigated to determine whether the 3D reference marker coordinates could be determined from them, thus reducing the overall scan time and the number of slices to be scanned. X-ray beams travel outward form their source in straight lines and usually the position of the X-ray source is known (perspective centres in figure 3.12), i.e. the X-ray sources of the AP and LAT surviews are normally at right angles to one another and the distance (principal distance in figure 3.12) from the source to the surview plane is known. It therefore should be possible to reconstruct 3D

coordinates for those reference markers appearing on both the AP and LAT surviews. The CT Z coordinate can be measured directly from the CT surviews, as the Z axis is linearly mapped, and the CT X and Y coordinates can be calculated using simple intersection geometry (see figure 3.12). Figure 3.12 shows the X-ray beams intersecting at the external marker P in the CT's XY plane, i.e. the CT's imaging plane. By knowing the position of the X-ray sources, the distances from the sources to the surview planes, and measuring the APx and LATx coordinates, the CT X and Y coordinates can be calculated.

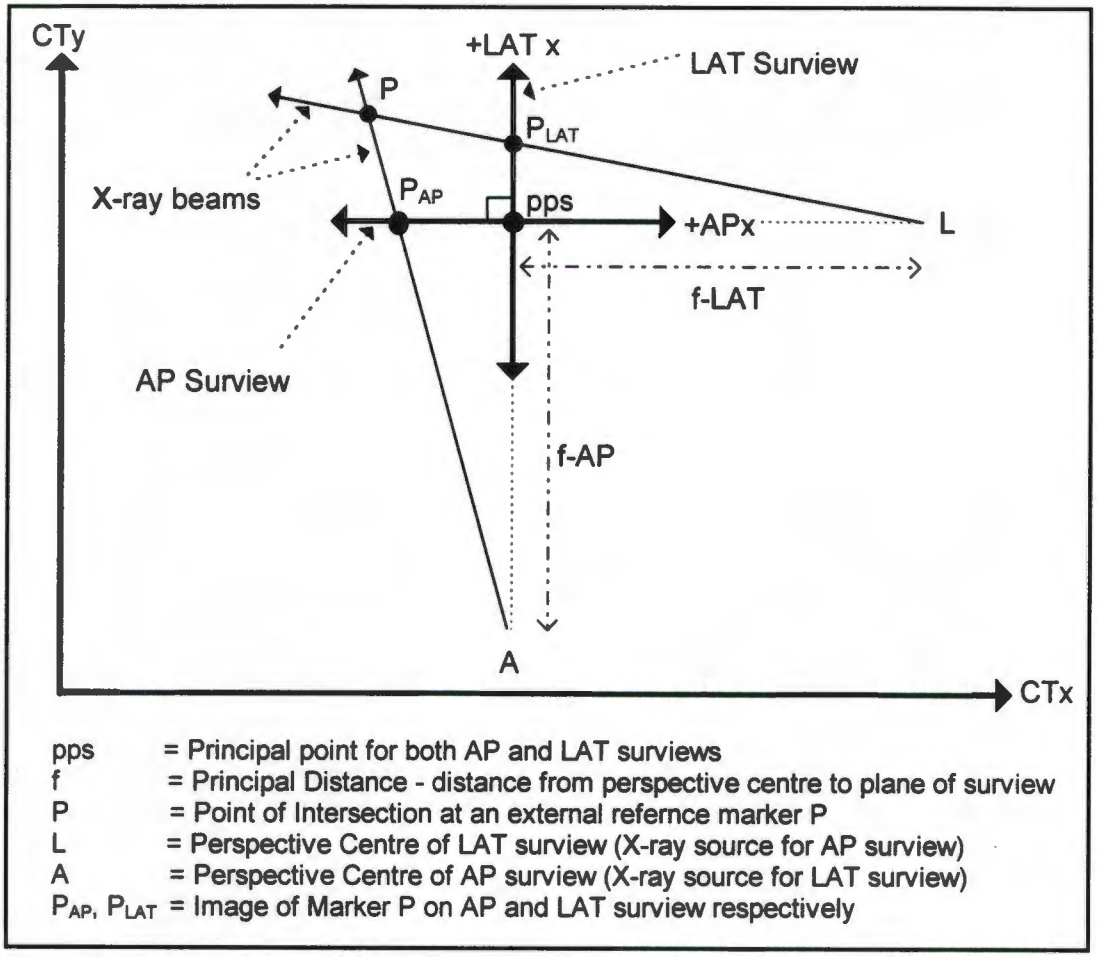


Figure 3.12: Showing the geometry of intersecting X-ray beams in the XY plane

This however did not prove to be the case, and errors as large as 12mm were not uncommon. Further investigation showed that the AP and LAT surview sources were not at right angles to one another and that the distance from the X-ray source to the surview plane was unknown. Therefore simple intersection geometry could not be utilised to determine 3D coordinates and new formula had to be developed, designed on similar lines to those used in determining 3D coordinates from stereo X-rays.

A stereo pair of X-rays, that is two X-rays of the same object taken from different perspectives, can be utilised to determine 3D coordinates of discrete points on that object, so long as the point to be coordinated is imaged on both X-rays (Adams, 1981). The equations for 3D coordinate determination are based on three dimensional projective transformation geometry (also known as the DLT - Direct Linear Transformation - Abdel-Aziz et al, 1971). The criteria for using this method is based on central projection geometry, i.e. on a conventional X-ray beam projecting in 3D space (Adams, 1981). As the CT X-ray beam only operates in 2D space, the surview equation was developed with the aid of a two dimensional projective transformation.

## 3.5 A TWO DIMENSIONAL PROJECTIVE TRANSFORMATION APPROACH TO SOLVE FOR 3D COORDINATES FROM CT SURVIEWS

To develop the algorithms and to test the accuracies obtained, the two dimensional control, with the nine control markers, and the phantom, with the four external and one internal reference marker, was used. The algorithms were tested initially using the AP and LAT surviews.

The surview equation, developed with the aid of 2D projective transformation algorithms, has been developed along similar lines to those used by Adams (Adams, 1981) to determine 3D coordinates of object points from stereo X-rays, utilising 3D projective transformation algorithms. The derivation of the surview equation to deal with CT surviews is shown in Appendix B. The surview equation for a point i on CT surview k is:

$$x_i = (h_{k,11} - x_i * h_{k,21})X_i + (h_{k,12} - x_i * h_{k,22})Y_i + h_{k,13} \qquad 3.1$$

- where the point i has a surview coordinate $x_i$ and slice coordinates $X_i$ and $Y_i$
- where the five h parameters ($h_{k,11}$, $h_{k,12}$, $h_{k,13}$, $h_{k,21}$, $h_{k,22}$) pertain to the surview k.

## 3. 6 USING THE SURVIEW EQUATION TO SOLVE FOR THE 3D SLICE COORDINATES USING THE AP AND LAT SURVIEWS

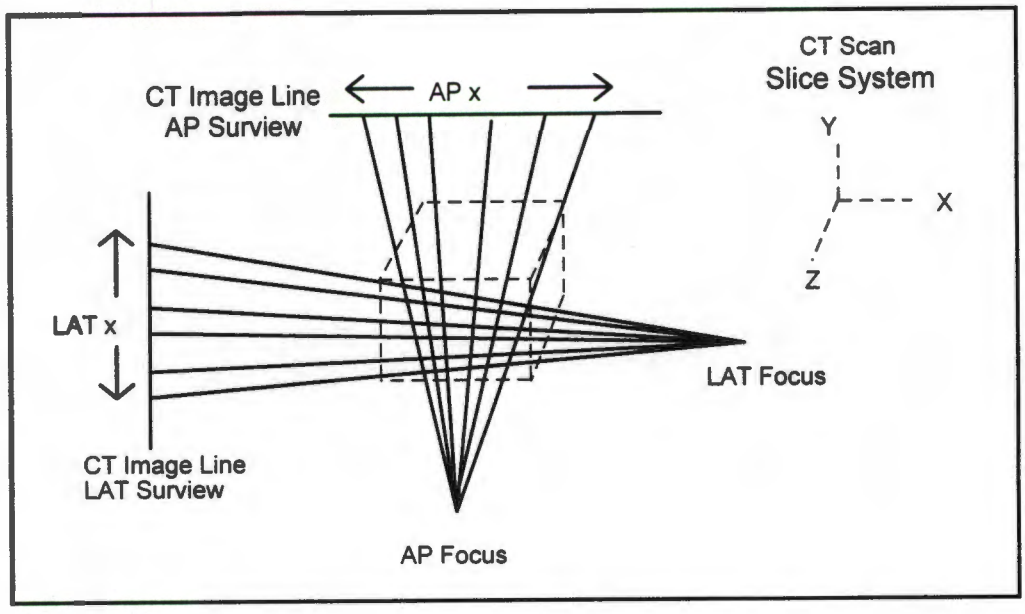


Figure 3.13: The two dimensional central projections of the AP and LAT surviews

The first requirement, in determining the 3D coordinates from surviews, is that two or more surviews of the patient are scanned from different positions on the 360 degree gantry circle, and that the points, that are to be coordinated, are visible on those surviews. The second requirement is that, before solving for the 3D coordinates of any markers, a minimum of five, non-collinear, control markers are required to solve for the five h parameters for each surview used.

The necessary control markers are supplied by the flat glass control, which is set up in such a way that all control markers fall within one XY plane. Thus only one CT slice is required to obtain the 3D slice coordinates for all the control markers. AP and LAT surviews of the glass control are also scanned. Once the glass control has been scanned, it can be removed. (Another option is to place the glass control further along the bed "above" the patient's head. Thus it is possible to scan the head and glass control simultaneously.)

For the nine control markers, slice coordinates $X_i$ and $Y_i$ , surview coordinate AP $x_i$ and surview coordinate LAT $x_i$ are measured/digitised (i denotes the control marker no., i.e. from 1 to 9). For the AP surview, by substituting $X_i$ , $Y_i$ and AP $x_i$ into the surview equation (equation 3.1), only five unknowns, the five h parameters for the AP surview remain, thus requiring five non-collinear markers for a unique solution. When more than five control markers are used to solve for the h parameters of the AP surview, there is an overdetermined solution and it is possible to use a least squares solution to solve for the unknown h parameters.

Rewriting equation 3.1,

$$x_i = h_{AP,11} * X_i + h_{AP,12} * Y_i + h_{AP,13} - h_{AP,21} * x_i * X_i - h_{AP,22} * x_i * Y_i \qquad 3.2$$

and writing equation 3.2 in matrix form for control markers 1 to n,

$$Aw = L \qquad 3.3$$

where

$$A = \begin{bmatrix} X_1 & Y_1 & 1 & -x_1X_1 & -x_1Y_1 \\ X_2 & Y_2 & 1 & -x_2X_2 & -x_2Y_2 \\ . & . & . & . & . \\ . & . & . & . & . \\ X_n & Y_n & 1 & -x_nX_n & -x_nY_n \end{bmatrix} \quad w = \begin{bmatrix} h_{AP,11} \\ h_{AP,12} \\ h_{AP,13} \\ h_{AP,21} \\ h_{AP,22} \end{bmatrix} \quad L = \begin{bmatrix} x_1 \\ x_2 \\ . \\ . \\ x_n \end{bmatrix} \qquad 3.4$$

the h parameters can be solved for using the least squares solution:

$$w = (A^T A)^{-1} * A^T L \qquad 3.5$$

The h parameters are determined for both surviews, i.e. the above process is repeated to obtain the h parameters for the LAT surview.

(From the various scans that were done on the GSH scanner, it was remarkable to see how constant the h parameters for the various surviews remained. Parameters that had been determined from scans a year earlier, still gave satisfactory results a year later. This may not be so for all scanners. Even with the GSH scanner, it would be dangerous to assume that because the system remained stable over long periods, it will always remain so. It may be advisable to calibrate, i.e. scan the glass control and calculate the h parameters, after each service, and have one or two markers that act as reference/check markers. By scanning the necessary surviews of these reference markers and using the h parameters determined from the last calibration, their 3D coordinates can be calculated and compared with their known 3D values. Any discrepancies in the coordinates would indicate that the CT system has undergone some changes since it's last calibration.)

The $X_i$ , $Y_i$ slice coordinates of a marker i can now be determined by backsubstitution into the surview equation (equation 3.1) as follows:

$$AP\ x_i = \frac{h_{AP,11}X_i + h_{AP,12}Y_i + h_{AP,13}}{h_{AP,21}X_i + h_{AP,22}Y_i + 1}$$

$$LAT\ x_i = \frac{h_{LAT,11}X_i + h_{LAT,12}Y_i + h_{LAT,13}}{h_{LAT,21}X_i + h_{LAT,22}Y_i + 1} \qquad 3.6$$

As their are two unknowns, $X_i$ and $Y_i$, to be solved for, a minimum of two equations is required to obtain a unique solution. It is for this reason that the marker to be coordinated has to appear on both the AP and LAT surviews. As the Z axis is linearly mapped, the slice Z coordinate is "equal" to the surview Z coordinate. Depending on the CT scan system, a constant may have to be added to the surview Z coordinates to make the surview Z axis and the slice Z axis truly coincident.

The glass control and phantom head were used to determine the accuracy that could be obtained using the AP and LAT surviews. The h parameters for both the AP and LAT surviews were calculated using the measured surview coordinates $x_i$ and the slice coordinates $X_i$, $Y_i$ of the nine control markers. (The precision that can be obtained is determined by using the calculated h parameters and the AP and LAT surview coordinates to calculate the slice coordinates for all the control markers and comparing the calculated slice coordinates to the measured slice coordinates.) A precision of 0.5mm was obtained for both the X and Y slice coordinates of the control markers. (The Z axis, as it is linearly mapped between the surview and slice system, does not play a role in determining the h parameters.)

Slice coordinates of the five phantom markers were determined from the h parameters and the phantom markers' surview coordinates, and compared to the measured slice coordinates (see table 3.3).

| | dX | dY | dZ |
|---|---|---|---|
| Mean Error (mm) | -0.9 | 0.3 | 1.4 |
| Std. Dev. (mm) | 0.5 | 0.5 | 0.6 |

Table 3.3: Comparing slice coordinates of the 5 phantom markers measured from actual slices and those calculated from the AP and LAT surviews

Both the X and Y coordinates are within the expected measuring accuracy of the CT scanner. The Z coordinates of the five phantom markers were calculated using a standard scale shift determined for the CT scanner. Although the standard deviation is good, the mean error is slightly larger than the expected accuracy of 1.5mm. This error can be corrected, by calculating a mean correction shift and applying it to the Z coordinates.

## 3.7 USING THE SURVIEW EQUATION TO SOLVE FOR THE 3D SLICE COORDINATES USING MULTIPLE SURVIEWS

Most modern CT scanners, beside scanning the conventional AP and LAT surviews, can scan oblique surviews from any position on the 360 degree gantry circle. There are two distinct advantages of using multiple surviews to determine 3D coordinates of external markers.

Firstly bone is a very dense material and markers may not always image on a particular surview. By using more than the minimum of two surviews for 3D coordination, it is no longer critical that the external marker appear on every surview. As long as the marker is imaged on a minimum of two surviews, and the two surviews have been taken sufficiently far apart on the gantry, 3D coordinates can be calculated. The closer the two surviews are together, the more the intersecting X-ray beams from the two surviews tend towards a single line, and the more the precision, with which the marker coordinates can be determined, decreases (see figure 3.14).

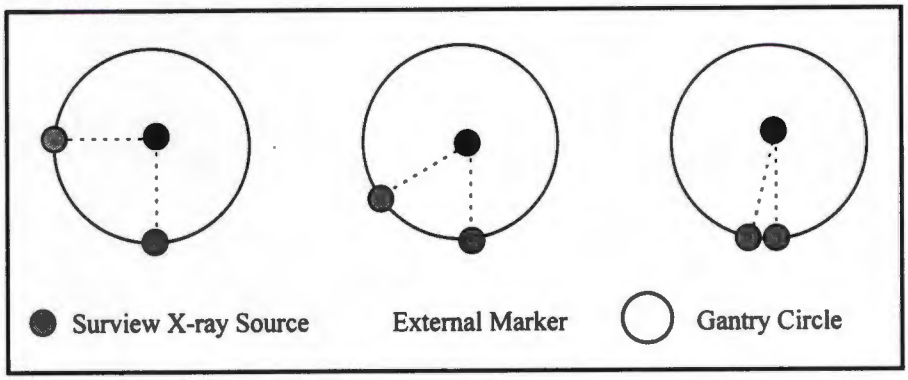


Figure 3.14: Showing the variation in intersecting angles from different surview positions

If the external marker is imaged on more than two surviews, the additional surviews can be used to obtain an overdetermined solution. Any incorrect identification of the marker or incorrect recording of the surview coordinates can be detected and corrected.

An AP and LAT surview (at 90 and 0/360 degrees respectively), as well as three oblique surviews at 340, 30 and 50 degrees on the gantry circle were scanned (see figure 3.15) of the glass control and the phantom head. Four external markers and one internal marker, to represent the lesion centre, were attached to the phantom head to simulate the Cape Pointer stereotactic application.

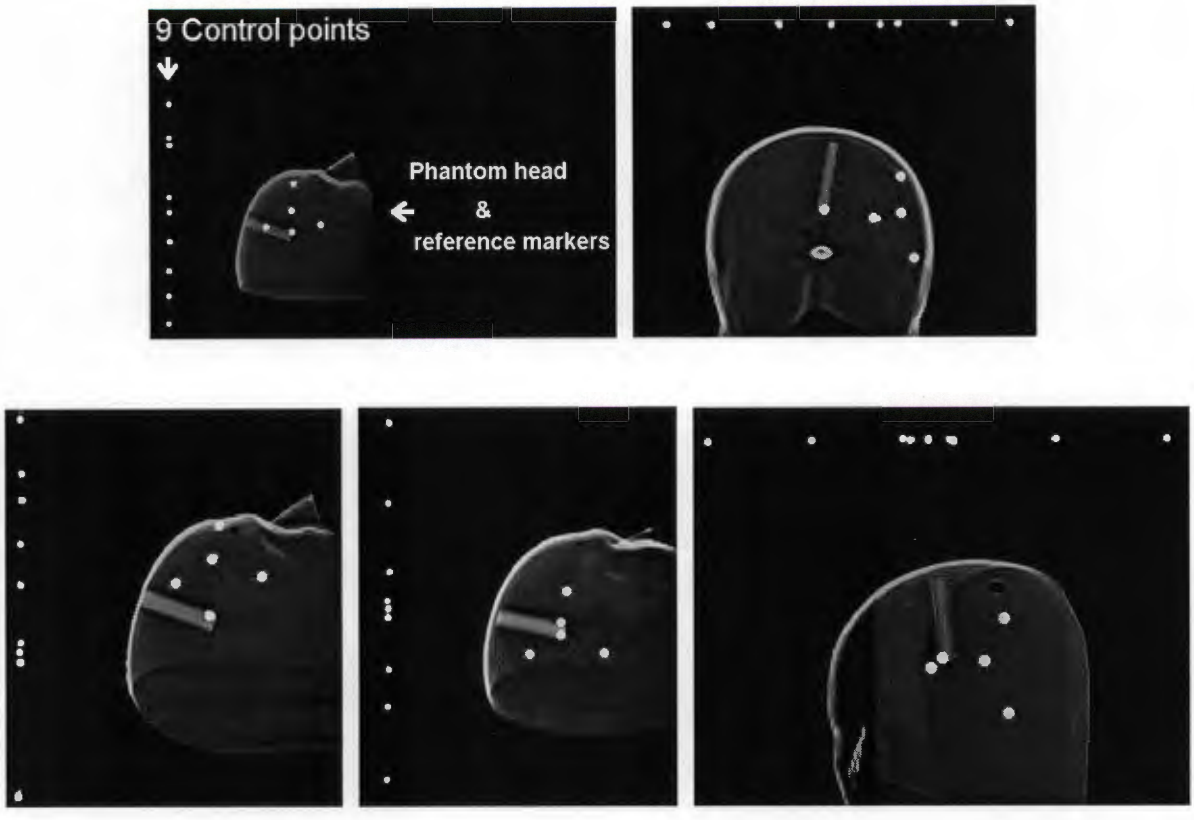


Figure 3.15: The five surviews scanned of the glass control and phantom head.
In order from left to right, LAT and AP surviews,
and three oblique surviews at 340, 30 and 50 degrees.
(These images have been enhanced for presentation purposes)

Six slices were also scanned, one in the XY plane containing the nine control points, and five in the XY planes, each containing a phantom marker. All the control and phantom markers were measured on the surviews and slices. h parameters for the five surviews were calculated and the accuracy of the h parameter determination assessed using all nine control points, with a standard deviation of 0.6mm and 0.4mm obtained in X and Y respectively.

3D CT coordinates for the phantom markers were calculated and compared to the measured CT slice coordinates, using the Rodrigues transformation (Appendix E), with the results listed in table 3.4.

| 5 Phantom Markers | dX | dY | dZ |
|---|---|---|---|
| Std.Dev. (mm) | 0.4 | 0.2 | 0.5 |

Table 3.4: Comparing calculated CT slice coordinates, obtained from the
five surviews, with the measured CT slice coordinates of the five phantom markers.

All five phantom markers were measured in the reflex metrograph (Scott, 1981), which has a measuring resolution of 0.1mm. The markers were measured four times and the mean adopted as "error free". Standard deviations of residual errors, obtained from comparing various data sets using the Rodrigues transformation, are listed in table 3.5.

| Std. Dev. (mm) from comparing: | dX | dY | dZ |
|---|---|---|---|
| Metrograph & calculated slice coordinates | 0.6 | 0.7 | 0.2 |
| Metrograph & measured CT slice coordinates | 0.8 | 0.8 | 0.6 |

Table 3.5: Std. deviations from comparing the 3D coordinates of the five phantom markers obtained in the metrograph to the measured and calculated CT slice coordinates.

These results verified that multiple surviews can be used to calculate 3D slice coordinates from surviews and still maintain the accuracy achieved by the conventional method of obtaining 3D CT coordinates.

The above procedure was repeated with an actual cranium to better simulate the patient situation. Both bone and the metal ball-bearings, used as external markers, yield very high Hounsfield numbers and therefore show up white on the CT images. By using a cranium, the effect of the bone on the visibility of the external markers could be tested. Six surviews of the glass control and cranium, to which four external markers were attached, were scanned. The six surviews included an AP and LAT surview and four oblique surviews scanned at 340, 30, 60 and 120 degrees on the gantry circle. Five slices to image the control and external markers were scanned. The oblique surviews at 30 and 60 are illustrated in figure 3.16.

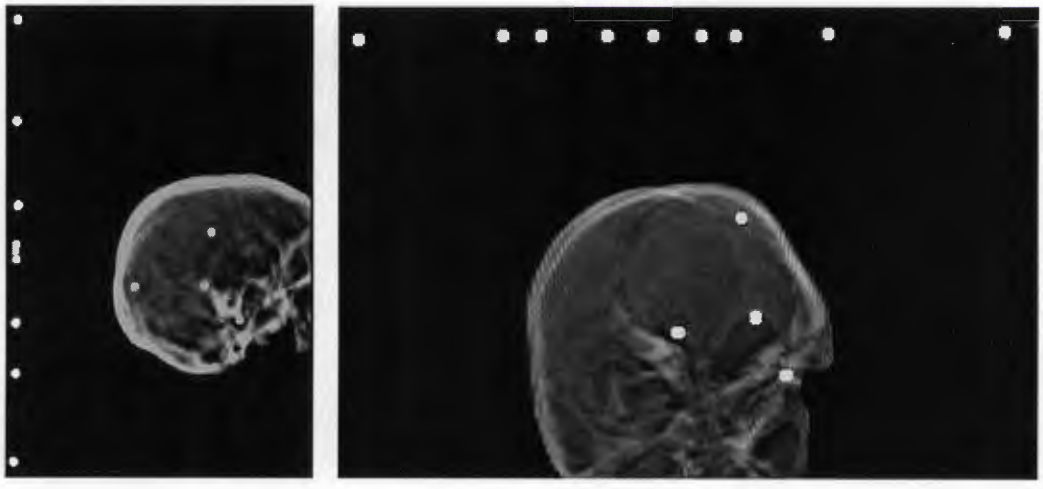

Figure 3.16: Oblique surviews, at 30 & 60 degree gantry settings, of the glass control & cranium (These images have been enhanced for presentation purposes)

The standard deviations of the residual errors, resulting from the determination of the h parameters, were 0.8mm and 0.3mm in X and Y respectively. The standard deviations of the residual errors, resulting from the calculated and measured slice coordinates of the cranium markers are listed in table 3.6.

| 4 Cranial Markers | dX | dY | dZ |
|---|---|---|---|
| Std. Dev. (mm) | 0.4 | 0.7 | 0.4 |

Table 3.6: Comparing calculated slice coordinates, obtained from the six surviews, and the measured CT slice coordinates of the cranial markers.

The cranial markers were measured four times in the reflex metrograph (Scott, 1981) and the mean adopted as "error free". Standard deviations of residual errors, obtained from comparing the various data sets using the Rodrigues transformation, are listed in table 3.7.

| Std. Dev. (mm) from comparing: | dX | dY | dZ |
|---|---|---|---|
| Metrograph & calculated CT slice coordinates | 0.4 | 1.0 | 0.2 |
| Metrograph & measured CT slice coordinates | 0.2 | 1.0 | 0.2 |

Table 3.7: Std. deviations from comparing the coordinates of the cranial markers obtained in the metrograph to the measured and calculated CT slice coordinates.

The standard deviation in dY of 1.0mm, in table 3.7, is slightly greater than the accuracy normally expected from the GSH scanner. Upon further investigation, it was found that the GSH scanner is the bottom of the range scanner, and it's imaging quality, when compared to the other two CT scanners in the hospital, is noticeably poorer. When comparing CT surviews of patients' heads, where external cranial markers have been attached to the heads prior to CT scanning, the definition of the markers against the bone is not as good on the GSH scanner surviews, as on other CT scanner surviews. The lack of definition of the markers on the GSH surviews makes the placement of the GSH scanner's digitising cursor on the marker difficult. The poorer image quality on the GSH scanner, may also have been due to the GSH scanning parameters, which may not have been ideal for dry bone specimens. (The other two CT scanners in the hospital were not used for the research in this thesis, as they are continuously overloaded with routine work.)

## 3.8 CONCLUSION

As a result of the CT scanner's excellent imaging capabilities, it has become part of the standard equipment of any large hospital. The CT scanner's 3D measuring capabilities are also undisputed. The aim of this chapter was to show that CT surviews could be utilised to determine 3D CT "slice" coordinates of external cranial markers.

The accuracy of determining 3D coordinates of external markers from surviews, utilising the surview equation, is within the accuracy determined by the CT scanner's slice system of 1.5mm.

Before using this technique in earnest in the clinical environment, clinical tests should be carried out by scanning volunteers, to whose scalps external markers have been attached. Using the surview equation to determine the 3D coordinates of the external markers, the effect of living bone and tissue on the technique could be ascertained, and the accuracy of the method in the actual clinical environment determined.

# CHAPTER 4 A STEREOPHOTOGRAMMETRIC SYSTEM TO CATER FOR PATIENT MOVEMENT DURING A CT PROCEDURE

## 4.1 INTRODUCTION

With any stereotactic procedure three dimensional coordinates of points, external and internal to the human head, have to be determined using a CT scanner. To set the new stereotactic device - the Cape Pointer, several external markers and a point within the intracranial lesion have to be coordinated in the CT scanner (see figure 4.1). The CT scanner's capability of obtaining accurate three dimensional coordinate patient data is dependent on the patient remaining motionless throughout the CT scan procedure.

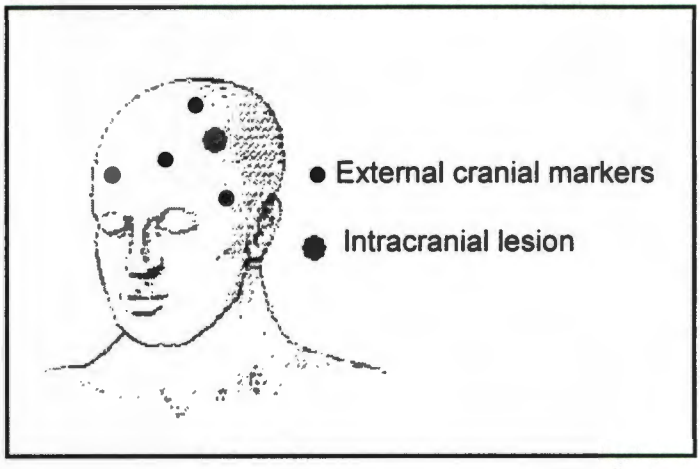


Figure 4.1: The external markers and the intracranial lesion that have to be coordinated by the CT scanner for the Cape Pointer procedure

The Cape Town neurosurgeons, who played a vital role in the design team and whose speciality is paediatric neurosurgery, felt that the Cape Pointer design should avoid the necessity of screwing the stereotactic device to the head, as is the case with frame-based stereotactic devices. Especially with the young patients in mind, the neuorsurgeons requested that the patient in no way be restrained during the CT scan, even though any movement by the patient would invalidate the CT data.

To allow a patient freedom of movement during the CT scan, and to still obtain valid CT data, any movement by the patient has to be compensated for, and this was achieved by utilising a stereophotogrammetric system (SPG system, figure 4.2), i.e. a three dimensional measuring system. A brief overview of the theory of stereophotogrammetry, and some of the algorithms used in this chapter, are described in Appendix C.

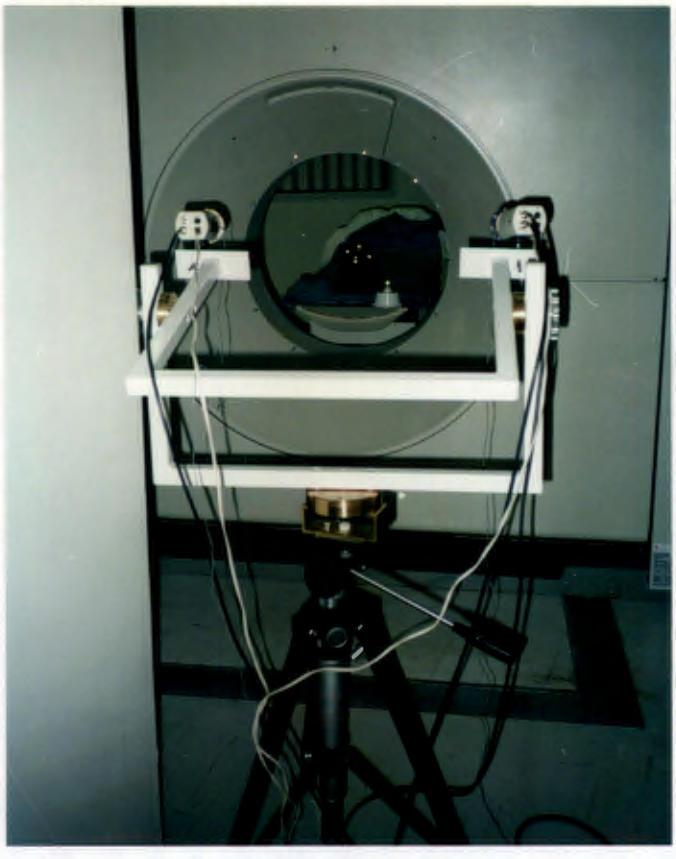

Figure 4.2: The stereophotogrammetric system in conjunction with the CT scan system

In simple laymen's terms, the SPG system records the position of the patient's head throughout the CT scan procedure. Once the procedure has been completed and the recorded image data has been processed, the position of the patient's head is determined in three dimensional space, whenever the CT scanner scanned a CT image. With this information, the movements made by the patient can be mathematically quantified and used to correct the CT data. The resultant CT data, required to set the stereotactic device, would thus appear to have been obtained from a motionless patient.

Figure 4.3: The phantom - a mould of a human head

In chapters four to six, the "patient" consisted of a phantom (figure 4.3), a plastic mould of a human head painted with matt black paint to reduce reflections. Patient movement was simulated by moving the phantom prior to any CT slice or surview being scanned.

## 4.2 THE SPG SYSTEM IN ACTION - AN OVERVIEW

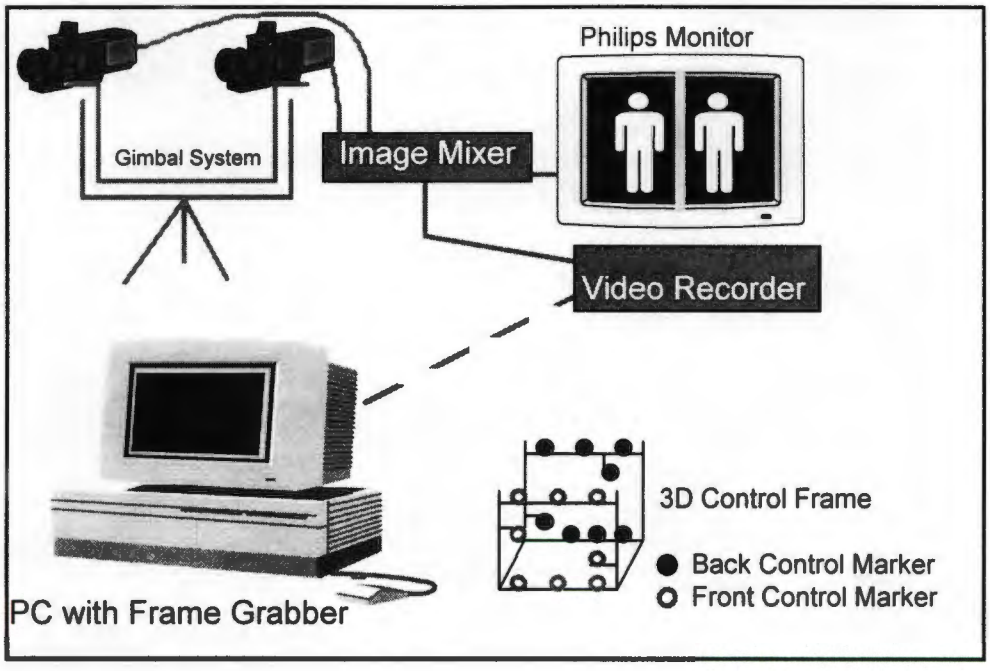


Figure 4.4: The SPG system at a glance

The equipment making up the SPG system (figure 4.4) consisted of the following :

1. two CCD monochrome cameras (Burle TC650EX Series Cameras)
2. two camera lenses (Computar 8.5mm 1:1.3)
3. a tripod and camera mounting in form of a gimbal system
4. an image mixer (Primebridge PVW1-Video Wiper)
5. a Sanyo video cassette recorder (VHR-D500SA)
6. a Philips monitor CM8833
7. infrared LEDs (light emitting diodes), to illuminate the control and patient, mounted around the camera lenses
8. a 3D control frame
9. a personal computer (PC)
10. an image frame grabber card (Matrox IP8 card) installed in the PC

All the equipment, with the exception of the PC, is taken into the CT scanner room and set up. Camera images, of the 3D control frame placed on the CT bed, are recorded on the video cassette recorder (VCR), and CT slices and surviews of the control frame are scanned by the CT scanner. By digitising the control markers on both the camera and CT images, and using various photogrammetric algorithms, the relationship between the SPG and CT system is determined. Due to all these calculations, the SPG system can now determine the 3D CT coordinates of any other markers which fall within the area occupied by the control frame. The control frame is removed and the phantom placed on the CT bed.

(All digitising and calculations are done after the CT procedure has been completed. The VCR is connected to the PC and all the necessary camera images are transferred and digitised. The digitised CT data is entered via the keyboard. The image transferral, digitising, data entry, and all the necessary calculations are done using the SPG systems software.).

For the SPG system to be able to monitor and quantify the phantom's position during a CT scan, four "tracking" markers are attached to the phantom's forehead, where they will be clearly visible to both the SPG cameras. (The four tracking markers are the four white markers on the black phantom head in figure 4.2). The cameras continually record the phantom throughout the CT scanning process. The 3D coordinates of the tracking markers are determined by the SPG system from the camera images, and used to define the phantom's initial position at the start of the CT scan, and at various stages throughout the scanning process. At these stages, the change from the initial position is determined using various algorithms, and used to correct the CT data obtained at that stage, thus mathematically removing any phantom movement from the CT data.

Once all the CT data has been corrected, that is the three dimensional coordinates of points, external and internal to the phantom head, have been corrected to eliminate any patient movement, the data can be used to set the stereotactic device.

### 4.2.1 SPG system equipment setup

All the equipment, with the exception of the PC, is taken into the room housing the CT scanner and set up. The PC is not used at this stage, as the whole CT scanning procedure is recorded on video tape. Only at a later stage is the VCR connected to the PC and the video tape analysed.

The SPG system's two CCD cameras are mounted on the gimbal system with normal camera mountings (see figure 4.5). The gimbal system, mounted on a sturdy tripod, is used to simplify the setting up of the cameras, as both cameras can thus be moved as one unit. The tripod, gimbal system, and cameras are set up at the head of the CT bed, i.e. behind the CT gantry.

Figure 4.5: The SPG cameras mounted on the gimbal system

Both cameras are connected to the image mixer, which synchronises the two cameras, and utilises half of each camera image to form a single mixed/stereoimage, which is displayed on the monitor and recorded on the video cassette recorder (VCR). As shown in figure 4.4, the cameras are set up so that the resultant stereoimage displays the patient/phantom twice on the Philips monitor, the left half of the screen shows the image from the left camera and the right half of the screen the image from the right camera.

The illumination is provided by infrared LED's mounted on two short hollow tubes that fit onto the two CCD camera lenses (in figure 4.5 the left camera's infrared LED tube is grey and the right camera's tube is white). Infrared light sources have been used as the CCD cameras are sensitive to infrared, and the illuminated retroreflective tape, used on the various markers,

are clearly visible on the stereoimages. The infrared light sources do not disturb the patient, as infrared light is below the human's visible range. (In human movement studies, very bright lights are used to illuminate the retroreflective body markers attached to healthy subjects. These lights would be unsuitable in the CT scanner, as they would shine directly into the patient's face when illuminating the four tracking markers.)

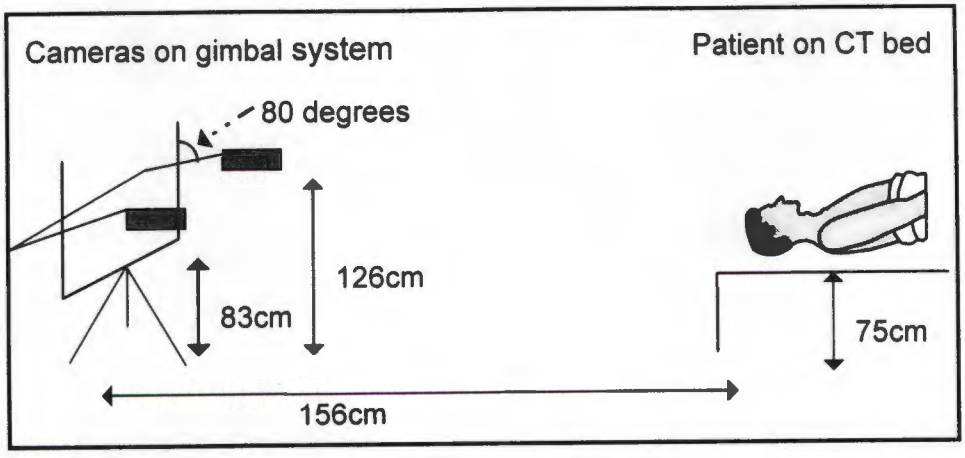


Figure 4.6: The dimensions of the SPG camera setup

Once all the equipment had been set up, the various dimensions of the setup were measured and are shown in figure 4.6. These dimensions are for a particular setup, and are fairly representative of other SPG setups.

## 4.3 THE CONTROL PROCEDURE

The control frame, i.e. a frame with control markers that have known 3D coordinates, is required by both the SPG system and the CT scan system to determine parameters. The 3D coordinates of the control markers were originally determined using a reflex metrograph (Scott, 1981), that has a measuring resolution of 0.1mm in all its three axes. The use of the control frame in the CT scan system has been explained in chapter 3.

The control frame for the SPG system is what the stars were to the earlier ship's captains; without the stars they were lost at sea, but as the stars positions in the sky were known, the ship's position at sea could be determined. By using a control frame that has control markers with known three dimensional coordinates, the cameras positions in relation to the markers can be determined. The determination of the cameras positions, with various other information is contained in the CCD camera parameters, which are calculated using the Direct Linear Transformation algorithm (the DLT algorithm, Abdel-Aziz et al, 1971; see

Appendix C). By a reversal of the procedure, using the parameters in the DLT algorithm, the 3D coordinates of any other marker can be determined, as long as that marker is visible to both cameras (see Appendix C).

As the SPG system has to determine what movement the patient is making and correct this in the CT scan system, the simplest solution was to make the SPG system coincident with the CT system. This was achieved by using a dual purpose control frame, i.e. one that could be used by both the SPG and the CT system.

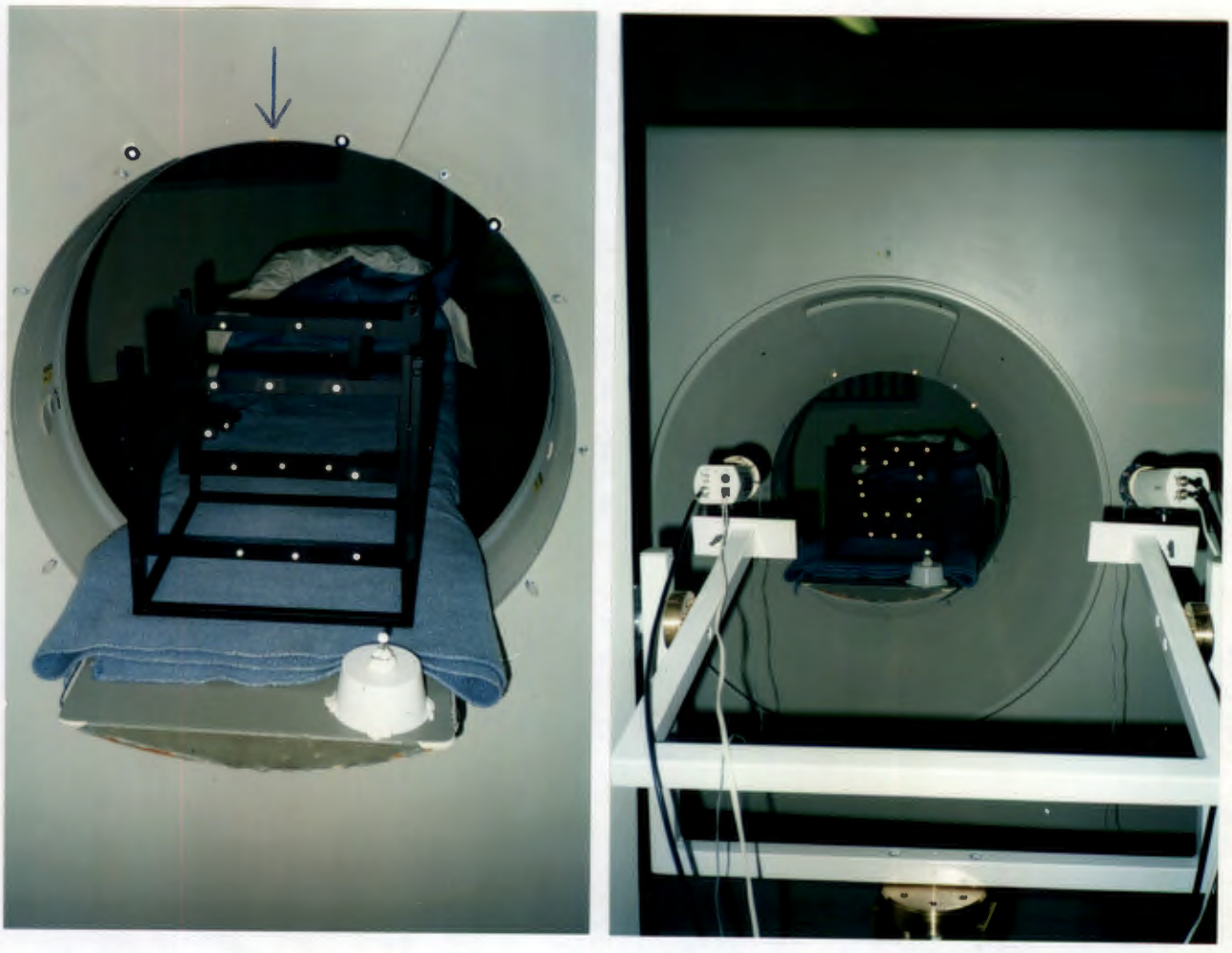

Figure 4.7: The dual control frame on the CT bed - left a close-up view, right - a more distant view including the cameras on the gimbal system

The control frame (see figure 4.7) is constructed from a metal skeleton and two flat plastic sheets. The metal skeleton gives the frame rigidity. The plastic sheets have been cut out so that, bar certain portions to which markers have been attached, only the outer edges remain. This reduces the area of the plastic sheets used to a minimum, making them as radio translucent as possible. The two plastic sheets are mounted on the metal frame so that they are parallel to each other. Eight retroreflective SPG control markers (see figure 4.8) are attached to each plastic sheet. Only four of the eight markers on each sheet contain radio-

opaque ball-bearings, and are therefore control markers for both the SPG and the CT system. This simplifies marker identification on the CT surviews, as all the markers containing ball-bearings are imaged on one single line on the surview.

Figure 4.8: All control markers have retroreflective discs at their centres (left); where a control marker is dual purpose, a radio-opaque ball-bearing lies below the retroreflective disc (right)

With the aid of the CT laser beam, the control is set up so that all eight markers on a plastic sheet are bisected by the beam. The CT laser "beam" actually consists of two laser beams at right angles to one another, both beams lying in the CT's imaging plane. The beams can be rotated in the imaging plane, so that any point in the plane can be illuminated by one of the laser beams. The CT "beam" is therefore used to ensure that the eight markers on the sheet lie in the CT imaging plane (the XY plane) and therefore image on a single slice. As the two plastic sheets are parallel, this also holds true for the second plastic sheet. Thus all eight dual purpose control markers are imaged on two CT slices.

An additional marker, dubbed a Z marker (white marker on white base in front of the control frame in figure 4.7) is attached to the head end of the CT bed. This Z marker is used to correct for the difference in the CT and SPG system, caused by the movement of the CT bed. Unlike a conventional coordinate system, such as the SPG system, where there are three static axes, the Z axis of the CT system is "created" by the movement of the CT bed. Although the bed moves, the control is "perceived" to be stationary by the CT system, as its position on the bed has not altered. However the control as "seen" by the SPG system appears to have moved along the SPG Z axis. By determining the Z marker's initial position at the start of the CT scan procedure, a Z correction can be determined for each new position the CT bed moves to. By applying this Z correction to the coordinates determined by the SPG system at that position, any discrepancy between the two systems is removed. The relationship between the SPG and CT system can be clarified by an example: a person is standing on earth, i.e. he is stationary; a person in a spaceship above earth is stationary in

themselves to be stationary, yet the CT system is moving due to the bed's movement, just as the earth is rotating. It is for this discrepancy for which the Z marker has been introduced.

As the CT bed moves through quite a wide Z range, it is necessary when setting up the CCD cameras that the full area, through which the control and the patient will move, will be covered by the cameras. The inner edge of the CT gantry opening must appear in the field of vision of both cameras (see figure 4.7 - left). In the upper part of the inner edge, a small light is attached (indicated by an arrow in figure 4.7 - left), which flashes when the CT X-ray beam is activate. This indicates that a surview or a slice is being scanned and that the patient's position needs to be determined at this point.

Also attached to the inner edge of the CT gantry opening are three retroreflective SPG markers, which serve as fiducial markers (see figure 4.7), and are of the same type as the control markers. The fiducial markers are used by the SPG system, in a two dimensional transformation, to correct for any image movement of the video image that may occur on image transfer from the VCR to the PC via the image frame grabber card (Adams et al, 1990, see Appendix F).

Prior to starting the VCR recording, the infrared illumination, and the zoom, focus and aperture of the CCD cameras are checked to ensure that all retroreflective markers, i.e. the Z marker, control and fiducial markers, are clearly visible to both cameras. The CT bed is then moved to the initial starting position. VCR recording is begun, and is continued until scanning of the patient has been completed.

An AP and LAT surview and two slices of the control frame are scanned. The area occupied by the control frame is marked, so that the patient's head can later be positioned in the same area.

## 4.4 CT PATIENT PROCEDURE AND SCANNING

Prior to placing the phantom on the CT bed, external cranial markers are attached to the phantom. To simulate the CT scanning process for the Cape Pointer, four external markers, of which one is an entry point marker, are used. An internal point, representing the centre of an intracranial lesion, is simulated by placing a ball-bearing within the phantom. The external markers are radio-opaque markers and are very similar to the dual purpose control markers, with the exception that the ball-bearings are not covered with retroreflective tape.

The four tracking markers are attached to the phantom's forehead, where they are clearly visible to both CCD cameras. The placement of the tracking markers should give a good geometrical "fix", that is the markers should be well distributed on the forehead. The tracking markers are of the same type as the dual control markers and therefore are "visible" to both the CT and SPG system. The reason for not using the four external markers as tracking markers, is that the external markers are not always visible to both cameras, especially if the external markers are placed on the lateral sides of the head.

An AP and LAT surview of the phantom are scanned. A single slice, through the ball-bearing simulating the lesion centre is also scanned. Where the CT procedure involves an actual patient, several slices would be scanned in the region containing the lesion, which would be selected by the neurosurgeon with the aid of the patient's initial diagnostic CT images.

## 4.5 CT DIGITISING

The CT scans of the control frame, i.e. the AP and LAT surviews and the two slices, are recalled onto the CT screen and all the control markers, imaged on the scans, are digitised. The AP and LAT surviews of the phantom are recalled and the four external markers, and the four tracking markers are digitised on both surviews. The lesion centre marker is digitised on the slice scanned through that marker. In the patient case, where several slices have been scanned through the area containing the lesion, the neurosurgeon will determine the lesion centre by viewing the various slices, and the selected point is digitised. (The point selected by the neurosurgeon is, for various pathological reasons, not necessarily the lesion centre).

As the digitised coordinates have to be recorded manually from the CT screen, great care has to be taken that the data is correctly "recorded". A transcription error, for example, in recording the slice coordinates of the lesion centre can be disastrous. A good practice to

adopt, is to double check everything, or have a second person record the same data, and do a cross check. (A South African land surveyor by law has to provide a check for every measurement he makes when surveying property, with the consequence that land disputes are rare.)

## 4.6 THE 3D CT SCAN AND SPG SOFTWARE PACKAGE AND ITS OPERATIONS

From this point onwards a whole series of steps have to be undertaken, all of them software related. All these steps are run from a single menu system (figure 4.9).

| THE SPG SYSTEM | | | |
|---|---|---|---|
| **CT INPUT** | **CAMERA CONTROL** | **CAMERA OBJECT** | **CALCULATIONS** |
| GSH Slices | Snap Control | Snap Object | Control Check |
| GSH APLAT | Dig. Left Control | Dig. Left Object | LAT rotation |
| GSH Lesion | Dig. Right Control | Dig. Right Object | APLAT to 3D |
| | Rotate Control | 3D Calculations | Lesion Pt. Rotation |
| | CCD parameters | | |
| | | | |

Figure 4.9: The menu of the SPG software package

All the menu options, relating to the processing of the video images, are dependent on the IP8 image processing card. The libraries that are provided with the card only cover a very small range of programming languages. Therefore all the software relating to the card is written in Turbo C version 2.1, and all other software is written in True Basic (all the software has been written by the author of this thesis, unless otherwise stated).

### 4.6.1 CT Input

The first section of the menu, "CT Input", deals with the CT data entry. For the "GSH Slices" option, only slice coordinates of the control markers are entered. For the "GSH APLAT" option, control and patient surview coordinates of control and external markers, are entered, and for the "GSH Lesion" option, the slice coordinates of the lesion centre are entered. Instructions, concerning the data entry, are specified by the software. All entered data is stored on the harddrive to be utilised at a later date.

### 4.6.2 Camera image transfer

The menu sections, "Camera Control" and "Camera Object", deal with the video images, their transfer from the VCR to the PC, their digitisation, and various calculations pertaining to the images.

The options "Snap Control" and "Snap Object" deal with the transfer of the video images to the PC. Both the VCR and the Philips monitor are connected to the PC via the IP8 frame grabber card; images from the VCR and any other image outputs from the IP8 are displayed on the Philips monitor. The image showing the control frame on the CT bed is transferred to the PC. The video image, that first shows the CT active light in operation with the phantom in the image field, indicates that the AP surview of the phantom is being scanned, and this image is also transferred to the PC. As the scanning period for surviews and slices is two seconds per scan, the video image at the start of each scanning period is used. Any patient/phantom movement during this two second period would be detected at the time of the scan due to the poor resultant CT image quality, and that particular slice or surview would be repeated.

In total the following video images are transferred to the hard drive:

1. Camera image of the control prior to the first scan
2. Camera image of patient's head at the start of the AP surview
3. Camera image of the patient's head at the start of the LAT surview
4. Camera image of the patient's head at the start of the lesion slice

The various locations of the images on the video tape are determined by utilising the time clocks on the VCR and on the CT scanner. Each CT image, be it surview or slice, is annotated with the CT's clock time. Therefore, once the image at the start of the AP surview has been located, it is a simple matter of locating the other images on the video tape, using the time intervals between the various scans.

An alternative option to streamline the use of the SPG system with the CT system, is to connect the cameras, via the image mixer, directly to the PC and immediately transfer the appropriate images to the PC.

### 4.6.3 Camera Control - Digitising and Calculation

The SPG digitising software, used to digitise the various markers, is mouse driven and utilises a centre of gravity algorithm to determine the marker centres to sub pixel accuracy (see Appendix D). No attempt, at this stage of the SPG software development, was made to automate the digitising of the markers. At a later date this is an area of the SPG system which will have to be amended, for the SPG system to become more streamlined. All the control markers are digitised on both the left and right part of the stereoimage (see figure 4.10), and the coordinates stored on the PC.

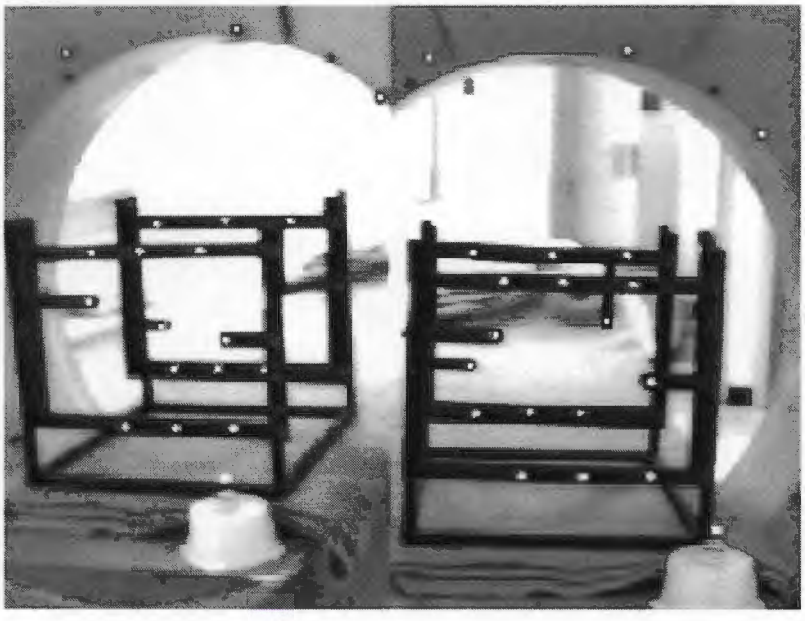

Figure 4.10: Stereoimage of the control frame

It has already been established that the SPG and CT systems are to be made coincident for ease of use. As the SPG system is defined by the 3D coordinates of the control markers, measured in the reflex metrograph, it is necessary to transform these 3D SPG coordinates into the CT system, with a three dimensional transformation utilising the Rodrigues matrix (Thompson, 1969, see Appendix E).

For the Rodrigues transformation, a minimum number of three points must be common to both systems in order to calculate the necessary parameters. Once the parameters have been calculated, any other points in the SPG system can be transformed into the CT system, as the relationship between the two systems is now known.

The common points in the SPG and CT system are the eight dual purpose control markers. The eight markers have 3D CT coordinates determined from the CT slices, i.e. in the CT system. The eight markers also have 3D coordinates measured in the reflex metrograph, which define the SPG system. Using the common points, the Rodrigues parameters are calculated and the relationship between the SPG and CT system established. Utilising the Rodrigues transformation, all the 3D SPG control coordinates are transformed into the CT system, i.e. all control markers now have 3D CT coordinates.

The Direct Linear Transformation (DLT, see Appendix C) utilises the 3D CT coordinates of the control markers and their 2D coordinates, digitised from the left and right parts of the stereoimages, to calculate the CCD camera parameters. As the CCD cameras remain undisturbed during the whole recording procedure, 3D CT coordinates can be calculated for any subsequent marker by backsubstitution into the DLT, provided that the marker is imaged on both the left and right portion of the stereoimage on the Philips monitor.

### 4.6.4 Camera Object - Digitising and Calculation

All video images, featuring the phantom, are referred to as object images, and are dealt with under the menu subheading "CAMERA OBJECT". As listed previously, these are the video images of the phantom head at the start of the AP surview, the LAT surview and the lesion slice.

Prior to dealing with the object images, the fiducial markers, that are used to correct for any movement of the video image due to the transfer process from the VCR and the PC, have to be digitised. The control video image is recalled, and the fiducial markers digitised on both

the left and right part of the stereoimage. This sets up the reference system for all subsequent video images. The Z marker is also digitised on the control video image to determine its reference position.

The fiducial markers, the Z marker and the four tracking markers are digitised on both the left and right part of the object stereoimages. Utilising the fiducial markers, any image movement is determined, and the 2D coordinates of the Z marker and the four tracking markers are corrected, thus mathematically eliminating any image movement. The DLT is used to calculate the 3D coordinates of the Z marker and the four tracking markers from their corrected 2D coordinates. This procedure is repeated for each object image.

Prior to writing the 3D coordinates to file, the Z coordinates are adjusted to correct for the Z differences between the SPG/CT system due to the CT bed movement. The Z marker should always have the same Z coordinate, as its position on the CT bed remains unchanged throughout the CT scan. However, due to the CT bed movement in respect to the SPG system, its Z coordinate is continually changing. All Z coordinates of markers on a particular object image have to be corrected by adding a constant, so that the Z coordinate of the Z marker on that object image is equal to the Z coordinate of the Z marker in its reference position. This procedure is repeated for each object image.

### 4.6.5 CT Control Calculations

As with the cameras, parameters have to be determined for the CT scanner. Using the slice and surview coordinates of the eight dual control markers, the h parameters for each particular surview are determined using the surview equation (see chapter 3.6).

### 4.6.6 LAT Rotation

It has been shown that 3D slice coordinates can be obtained from the CT AP and LAT surviews. The same technique is used in the SPG system to determine the 3D coordinates of the external markers, with the added complication that the phantom has moved between the AP and LAT surview. The reason for using this technique in the SPG system, is to reduce the number of scans and calculations that have to be performed to obtain the 3D coordinates of the external markers. As the AP surview is chosen as the phantom's initial position, only the LAT surview coordinates have to be corrected for the phantom movement; this correction is done using the LAT rotation software option.

The LAT rotation software utilises the four tracking markers (dual purpose markers), seen by both cameras and the CT scanner, to determine parameters required to adjust the marker coordinates of the external cranial markers on the LAT surview.

Equation 4.1, which determines the parameters a, b and c, is based on the parallax formulae. The 3D SPG coordinates, and 2D surview coordinates, of the four tracking markers at the time of the AP and LAT surviews, are used in equation 4.1 to solve for the parameters using a least squares adjustment. (The coordinate labelling of the CT slice system is shown in figure 3.6, and that of the CT surview system in figure 3.11.)

$$dY(i) = a + b*xap(i) + c*zlat(i) \qquad 4.1$$

where
- i : from 1 to 4 for the 4 tracking markers
- xap(i): x coordinate on AP surview
- zlat(i): Z coordinate on LAT surview
- dY(i) : dY(i)= YAP(i) - YLAT(i) 4.2
- YAP(i): Y coordinate in the SPG system at the time of AP surview
- YLAT(i): Y coordinate in the SPG system at the time of LAT surview

Now, utilising the parameters a, b and c, the x coordinates on the LAT surview have to be corrected, to mathematically remove any phantom movement. This is done using the following equation:

$$\text{corrected } xlat(i) = xlat(i) + a + b*xap(i) + c*zap(i) \qquad 4.3$$

This correction is applied to all the marker coordinates of the LAT surview, that is to the four tracking markers and the external markers required for the Cape Pointer. The reason for applying the correction to the four tracking markers as well, is that once their 3D coordinates have been calculated from the AP and corrected LAT surview data, these can be compared, and should be equal, to the 3D coordinates of the four tracking markers determined by the SPG system, at the time of the AP surview, i.e. the phantom's initial position. The comparison of the two sets of 3D coordinates provides a check, that no errors have crept into the system, where the four tacking markers are concerned.

Due to the manner in which the AP and LAT surview are scanned, if no movement had occurred, the Z surview coordinate of any point on the AP surview will be equal to the Z surview coordinate of that point on the LAT surview. So the Z coordinates of markers on the AP surview are adopted for the markers on the LAT surview. However, to obtain Z slice coordinates, a constant has to be added to the Z surview coordinates (see chapter 3.6). This constant is determined from the 4 tracking markers:

$$Zconstant = \left( \sum_{i=1}^{n} ( ZAP(i) - zap(i)) \right) \Big/ 4 \qquad 4.4$$

where:

ZAP(i): Z coordinate of tracking marker i in the SPG system at the time of the AP surview
zap(i): Z coordinate of tracking marker i on AP surview
n: total number of tracking markers, n=4.

The Z constant is applied to all the Z surview coordinates on the AP surview, to obtain Z slice coordinates. The surview coordinates, that is the xap, and corrected xlat coordinates, as well as the newly calculated Z slice coordinates are written to file. These are then used by the APLAT to 3D program, to calculate the 3D coordinates of the four tracking markers and the external markers.

### 4.6.7 APLAT to 3D - Converting surview coordinates into 3D CT coordinates

The AP and corrected LAT surview coordinates are transformed into X and Y slice coordinates, using the surview equation and the previously determined h parameters (chapter 3.6). As the Z slice coordinates have already been determined, all the external markers that were imaged on the AP and LAT surviews, i.e. the four tracking markers and the external cranial markers, now have 3D CT slice coordinates. These 3D CT coordinates have been determined at the time of the AP surview, i.e. at the phantom initial position, prior to any phantom movement occurring.

To ascertain that the four tracking markers have been identified correctly on the AP and LAT surviews, and that the calculations have been carried out correctly, the 3D CT coordinates of the four markers from the APLAT to 3D calculations are compared to the 3D CT coordinates of the four tracking markers obtained by the SPG system at the start of the AP surview, using the Rodrigues transformation. If the resulting precisions from the transformation are satisfactory, the results from the APLAT to 3D software are accepted. (An example of the resulting precision of this transformation is given in the system trial in chapter 6.)

### 4.6.8 Lesion Point Rotation

The only remaining step in the SPG system calculation, is to determine the 3D coordinates of the lesion centre, as if no phantom movement had occurred. The lesion point rotation routine does this by transforming the 3D CT coordinates of the lesion centre back into its initial phantom position.

The Rodrigues transformation is used to determine the transformation parameters from the two sets of 3D coordinates of the four tracking markers in the SPG system - the first set at the time the AP surview was scanned and the second set at the time the lesion slice was scanned. Once these parameters have been determined, they are used to transform the 3D lesion coordinates, thus mathematically removing any movements the patient may have made between the scan of the AP surview and the lesion slice.

The 3D CT coordinates of the external markers and the lesion centre, which are required to set the Cape Pointer, have now been corrected for any phantom movement.

## 4.7 CONCLUSION

The motivation for using the SPG system in combination with the CT system is to monitor any phantom movement, and to mathematically remove any movement, so that the resultant three dimensional CT coordinates for the external markers and the intracranial points are 'free' of any such movement. These three dimensional CT coordinates can now be used for such applications as stereotactic neurosurgery.

The accuracy that is achieved by this method is within the accuracy that would have been achieved using only the CT system with the phantom being restrained during the imaging procedure. This is verified in chapter 6, where the system trial, undertaken with the phantom and the Cape Pointer, is described.

Although the present format of the SPG system, is 'non invasive' where the patient is concerned, it is cumbersome to set up and takes up a fair amount of space in the already crowded CT scanner room. The effort that is required to run the system places an additional burden on the already very busy (overworked) staff.

The SPG system would have to have a more permanent setup in the CT scan room, so that when the SPG system is required, it would be available immediately. The SPG system would have to be streamlined, so that many of its functions occurred automatically, at the time the CT scanning procedure was in progress.

Although the SPG system in conjunction with the CT system fulfils the requirements of removing phantom/patient movement, in its present state it is too cumbersome to be used on a clinical basis, and the above suggestions will have to be implemented prior to the SPG system becoming a viable tool in the clinical environment.

## CHAPTER 5 THE CAPE POINTER IN CONJUNCTION WITH THE SPG SYSTEM

### 5.1 INTRODUCTION

The aim of any stereotactic device is to guide the neurosurgeon's instrument to a chosen point within the cranium, such as a lesion centre. To achieve this aim, an external environment has to be related to the internal environment within the cranium. With many stereotactic devices this external environment is established by a three dimensional coordinate system in the form of a stereotactic frame, which is attached to the skull. As both the frame and the lesion are imaged on the CT images, the spatial relationship between them can be determined, and the stereotactic device can be set to guide the neurosurgeon's instrument to the chosen destination.

Despite the elegant designs and efficient pointing facilities of frame-based stereotactic devices, many neurosurgeons have found these frames to be cumbersome, time consuming and uncomfortable for the patient, as the frame is anchored to the patient's skull using surgical screws or pins. In defence of these frame-based stereotactic devices, as mentioned in the literature review, many were designed in the late 1940's, prior to the invention of computed tomography (CT) and the computer, and all the settings had to be done using conventional X-rays and all calculations were done by hand. With the introduction of computers and the CT scanner, these devices were adapted to suite the new technology.

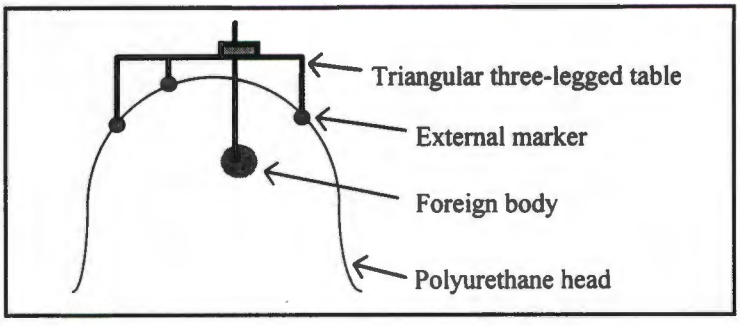


Figure 5.1: The forerunner of the Cape Pointer

An alternate method of establishing an external environment / external three dimensional coordinate system is by attaching radio-opaque markers directly onto the head, thus eliminating the necessity of a stereotactic frame. By determining the three dimensional coordinates of both the external markers and the lesion centre, in the same three dimensional coordinate system, the spatial relationship between the lesion and the external markers is established. This approach was used by Adams (1981), where the forerunner of

the Cape Pointer was used to find the 'foreign body' within a polyurethane model head (figure 5.1).

The device was somewhat similar to the present day Cape Pointer, with two exceptions - that the foreign body could only be reached along a single trajectory that was orthogonal to the device's table surface, and that all marker coordination was done using stereo x-rays and x-ray stereophotogrammetry.

It was not until the early 1990's that the seed planted by the forerunner of the Cape Pointer began to germinate and resulted in the design of the Cape Pointer - a very simple, easy to use, mechanical, frameless stereotactic device, that replicates the accuracy of its much more sophisticated counterparts. The design of the Cape Pointer has undergone a metamorphosis from its first design, by replacing the use of conventional x-rays with CT scanner technology, and by altering the design so that the chosen point within the cranium can be reached along a multitude of trajectories. The final design of the Cape Pointer is only approximately a quarter of the size of conventional frame-based stereotactic systems and only weighs approximately 150 grams.

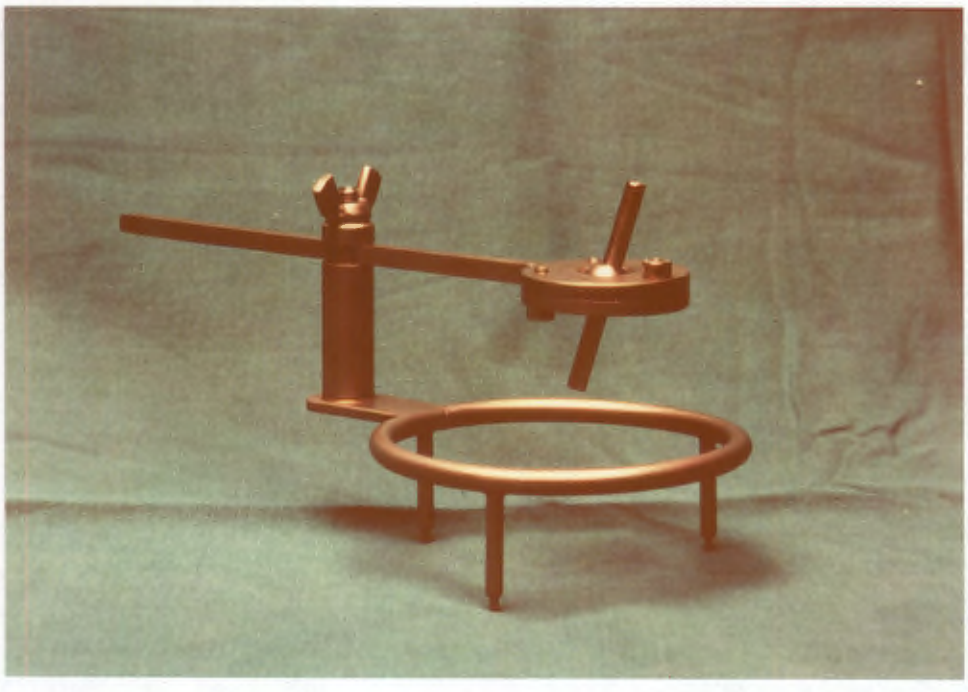

Figure 5.2: The Cape Pointer

The procedure to set the device is simple. The Cape Pointer (figure 5.2), as with its forerunner, has three legs, whose corresponding positions on the patient's head are marked with radio-opaque markers - these external markers establish the external environment. One additional external marker is attached to the head, to mark the point of entry into the cranium

- this entry point is selected by the neurosurgeon. By putting the patient through the CT scanning procedure, with the CT scanner operating in conjunction with the SPG system, three dimensional CT coordinates of the external markers and the lesion centre are determined from which any patient movement has mathematically been removed.

The three dimensional data is fed into a software package, which generates a setting diagram for the Cape Pointer. With the aid of the diagram, only simple mechanical rotations and translations have to be applied to the Cape Pointer to set the trajectory, which will guide the neurosurgeon's instrument to the lesion centre through the entry point. To ensure that, when the instrument is inserted into the cranium along the trajectory, the tip of the instrument comes to rest in the lesion centre and not above or below it, a depth clamp/stop is attached to the instrument at a certain distance from the tip of the instrument. This distance, determined by the software, is printed out on the setting diagram.

In theatre a burr hole is drilled at the site of the entry marker. The Cape Pointer is placed on the patient's head, i.e. the three legs are placed on their corresponding markers, and the neurosurgeon's instrument is guided down the preset trajectory until the stop prevents the instrument from being inserted any deeper into the cranium. The tip of the instrument is now coincident with the lesion centre.

The beauty of the Cape Pointer lies in the simplicity of its design and its ease of use. The power and ingenuity of the Cape Pointer lies in the three dimensional geometrical principles on which its design has been based, and that the three dimensional geometrical algorithms, that generate the Cape Pointer's setting diagram, remain hidden to the user in the software.

(The part of the software, that produces the setting diagram itself, was initially written by Adams, using some of the concepts and principals he had developed for the forerunner of the Cape Pointer (Adams, 1981) and using an idea put forward by Jaros (see chapter 1), which is outlined in the first paragraph of chapter 5.2, i.e. in the next paragraph.)

## 5.2 THE THREE DIMENSIONAL GEOMETRICAL PRINCIPLES OF THE CAPE POINTER

The Cape Pointer is a simple device based on three dimensional geometric principles. The fundamental principle behind the device is that any vector, in three dimensional space, can be defined by two points separated in space, and that this vector can be reconstructed by making use of two such points, each located on one of two parallel planes at a known distance apart.

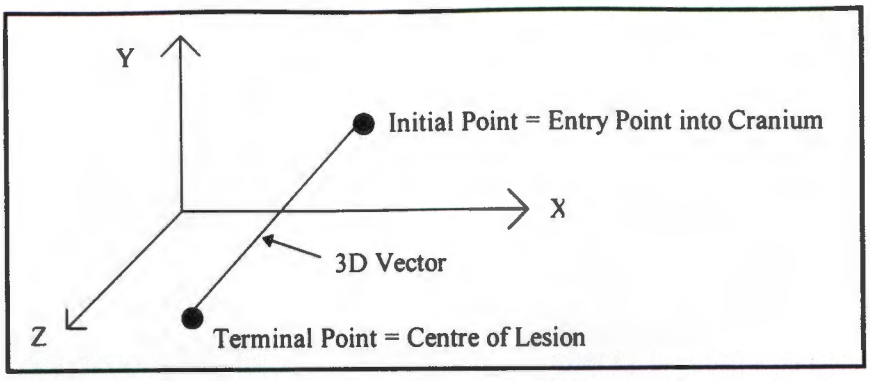


Figure 5.3 A vector in space

A vector, that has an initial and terminal point, has both direction and magnitude (length). In a stereotactic procedure, such as a lesion biopsy, the vector's initial point is the entry point into the cranium, and the terminal point is the centre of the lesion (see figure 5.3). If the path to be followed by the neurosurgeon's instrument, such as a biopsy needle, is coincident with this vector, the centre of the lesion can be reached and a tissue sample can be removed for pathological examination.

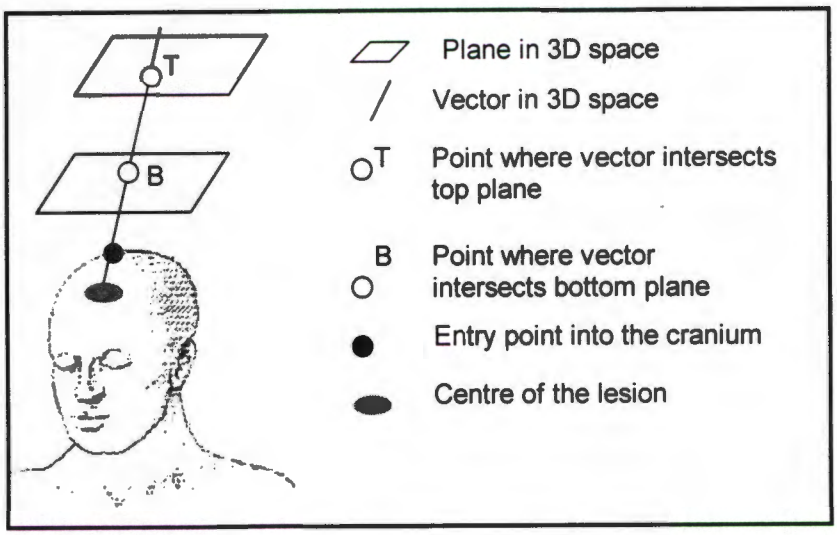


Figure 5.4: A vector in 3D space can be reconstructed using two parallel planes

The vector can be defined by using the two parallel planes, as shown in figure 5.4. The vector, defined by the lesion centre and entry point, is extended upward above the cranium to intersect the bottom plane at point B and the top plane at point T. If the positions of the two parallel planes in relation to the cranium, and therefore to the entry point and lesion centre, can be determined, and points T and B calculated, then the vector to reach the lesion can be reconstructed.

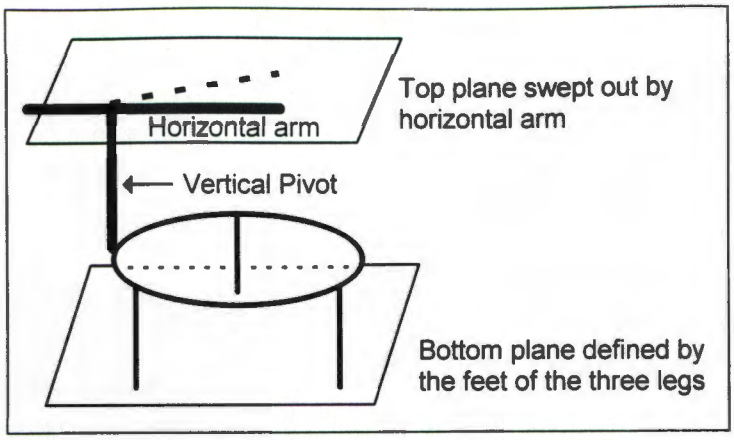


Figure 5.5: The two parallel planes of the Cape Pointer

The Cape Pointer (figure 5.5) does this with admirable simplicity. Making use of the fact that any three points in 3D space define a plane, the Cape Pointer is constructed with three legs. The "feet" of the three legs define the bottom plane. The three legs are attached to a ring (for easier handling by the neurosurgeon), to which a vertical pivot is mounted. Attached to the pivot is a moveable horizontal arm (see figure 5.5 & 5.6), that sweeps out a plane that is parallel to the bottom plane and thus forms the "top plane". The horizontal arm has been constructed at a known distance above the bottom plane, and therefore the distance between the two planes is known.

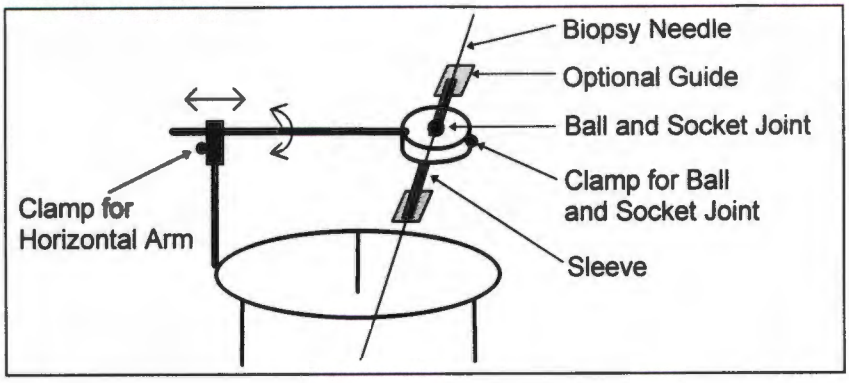


Figure 5.6: The Cape Pointer components

A ball and socket joint is attached to the end of the horizontal arm (see figure 5.6) and the centre of the ball lies in the top plane. A hollow sleeve passes through the centre of the ball, and the inner tube dimensions of the sleeve are wide enough to allow a biopsy needle to be inserted into the sleeve. Various adapters/optional guides can be attached to either end of the sleeve to narrow the dimension of the sleeve and thus allow for a good fit for various narrower needles to be used. The horizontal arm and the ball and socket joint can be

securely locked in place once the Cape Pointer has been set, by tightening the clamps (figure 5.6) with an Allen key.

To establish the relationship between the two planes of the Cape Pointer and the cranium, and therefore to the lesion centre, the corresponding positions of the three legs are marked on the cranium with radio-opaque markers. These markers, as well as the entry marker and lesion centre, are coordinated in the CT/SPG system. Utilising these 3D CT coordinates, the Cape Pointer software calculates the vector between the entry point and lesion centre, determines the points where this vector will intersect the bottom and top plane of the Cape Pointer, and with this information produces the setting diagram. The setting diagram, in simple terms, is the projection of the three leg markers (1-3 in figure 5.7) and the top and bottom points (T and B respectively in figure 5.7, where the vector bisects the top and bottom plane), onto a plane/sheet of paper. The various mathematical algorithms to produce the setting diagram are explained in Appendix G.

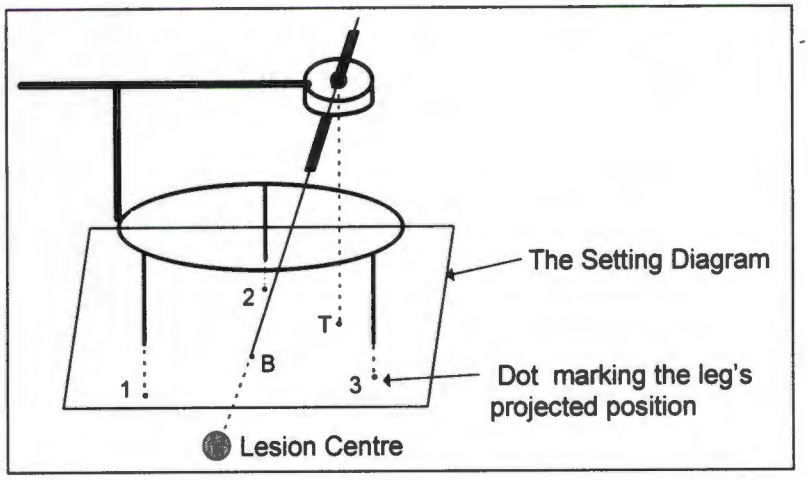


Figure 5.7: The projection of the three leg markers and the top and bottom point onto a sheet of paper - the setting diagram

With the aid of the setting diagram, the horizontal arm and ball and socket joint of the Cape Pointer are manipulated to set the trajectory which will guide the neurosurgeon's instrument to the lesion centre through the entry point. The setting of the Cape Pointer is a simple mechanical exercise, which is performed by the neurosurgeon in a few minutes.

## 5.3 PHANTOM PREPARATION AND CT SCANNING PROCEDURE

The relationship between the Cape Pointer and the phantom, is established by the contact points of the three legs on the phantom's head. The sites have to be marked with radio-opaque markers, which are of the same type as the SPG dual control markers without the retroreflective tape (a sample of the markers is shown in the previous chapter in figure 4.8).

First the entry point is marked by the neurosurgeon with the same type of marker used for the leg markers. Making use of a setting jig, a modified replica of the Cape Pointer consisting only of the ring and the three legs, the neurosurgeon positions the leg markers around the entry point. The leg markers should preferably surround the entry point (figure 5.8), to avoid mathematical extrapolation, which could degrade the accuracy of the Cape Pointer setting. The markers are attached with a special adhesive (approved for human use), to ensure they are not disturbed. Once the markers have been attached, the corresponding leg numbers are written onto each marker for identification purposes. The lesion centre is represented by a radio-opaque marker placed within the phantom.

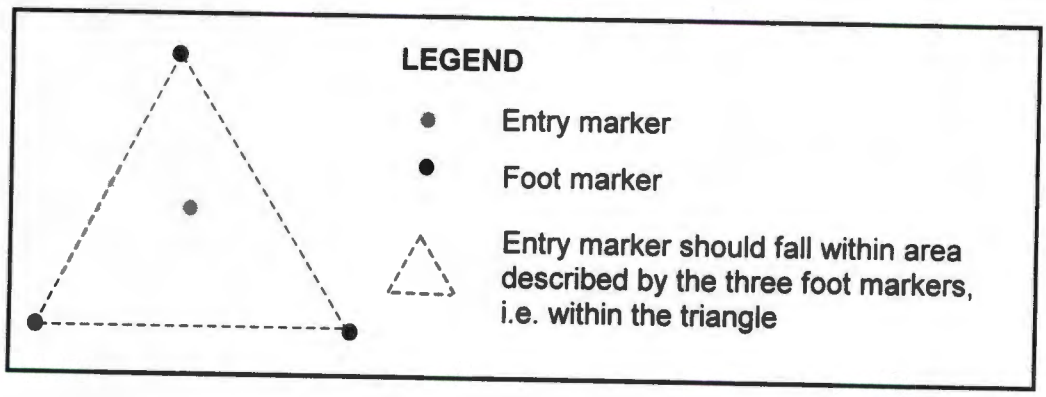


Figure 5.8: The configuration of the Cape Pointer's three foot markers and the entry point

Once the SPG system has been set up and the control procedure for the SPG system has been completed (chapter 4.2 & 4.3), the phantom is transferred to the CT bed. The bed is positioned at the start of the AP surview, ready for scanning to begin. The four SPG tracking markers are attached to the phantom's forehead, where they are clearly "visible" to both CCD cameras.

An AP and LAT surview are scanned. Several slices are scanned in the region containing the lesion. The patient movement is simulated by moving the phantom between the AP and LAT surview and between the slices.

Once all the scans have been completed, the various markers on the CT surviews and slices are digitised utilising the CT scanner software. The markers that have to be digitised are the control markers on the slices and surviews, the external markers on the surviews, and the lesion centre on the particular slice on which the lesion marker is imaged.

This completes the CT scanning procedure. To obtain "movement free" three dimensional CT coordinates of the external markers and the lesion centre, the video tape, in conjunction with the CT data, has to be processed by the SPG system.

## 5.4 AMENDING THE SPG SYSTEM TO SUIT THE CAPE POINTER

Only two additions are made to the SPG system, to enable it to be used for the Cape Pointer procedure. These additions are both software programs, that are added under the subheading "Calculations" in the software package. The two software programs are listed under the menu headings of "Checking" and "Setting diagram" in figure 5.9.

| THE CAPE POINTER IN CONJUNCTION WITH THE SPG SYSTEM | | | |
|---|---|---|---|
| CT INPUT | CAMERA CONTROL | CAMERA OBJECT | **CALCULATIONS** |
| GSH Slices | Snap Control | Snap Object | Control Check |
| GSH APLAT | Dig. Left Control | Dig. Left Object | LAT rotation |
| GSH Lesion | Dig. Right Control | Dig. Right Object | APLAT to 3D |
| | Rotate Control | 3D Calculations | Lesion Pt. Rotation |
| | B parameters | | **Checking** |
| | | | **Setting Diagram** |

Figure 5.9: The menu of the software package to set the Cape Pointer in conjunction with the SPG system

Utilising the software, the necessary video images of the control and phantom are transferred to the PC. The data pertaining to the control and phantom markers, which is digitised from the CT images, is entered into the PC. The software performs all the necessary calculations to obtain three dimensional CT coordinates of the leg markers, the entry marker and the lesion centre, from which any phantom movement has mathematically been removed (chapter 4.6).

It is at this stage of the calculations that the software program under the heading of "Checking" is run. This program's only function is to ascertain that the calculations have been carried out correctly, by comparing the three dimensional CT coordinates of the three leg markers, obtained by the CT/SPG system, to the three dimensional coordinates of the actual three legs, measured in the reflex microscope, using the Rodrigues transformation. (The reflex microscope, operating on similar principles as the reflex metrograph, is a three dimensional measuring instrument and has a measuring precision of +/- 4 micrometers in all three axes (Scott, 1981)).

If the resulting precisions are within the expected accuracy of the CT/SPG system, the various procedures are deemed to have been carried out correctly. Any large discrepancies in the precisions could be due to such problems as marker misidentification, incorrect data entry of the digitised data from the CT images etc. Before proceeding with the setting diagram, the various routines have to be checked to ascertain where the error occurred, and the routines affected by the error recalculated. Once the resulting precisions of the "Checking" routine are satisfactory, the setting diagram can be generated.

## 5.5 THE SETTING DIAGRAM

The last software section to be run, prior to setting the Cape Pointer, is that which produces the setting diagram (see figure 5.10a). With the information contained within the diagram, the Cape Pointer can easily be set by the neurosurgeon in a few minutes.

The setting diagram (figure 5.10a) consists of a header section, the first part of which states the patient's name - in this case the phantom's name is Thomas, which is the full name for TOM (Totally Obedient Moron). The "probe distance from the top" is the distance from the top of the sleeve on the Cape Pointer to the lesion centre (see figure 5.10b), and the "probe distance from the top with guide" is the distance from the top of the guide mounted on the sleeve to the lesion centre (described in chapter 5.2).

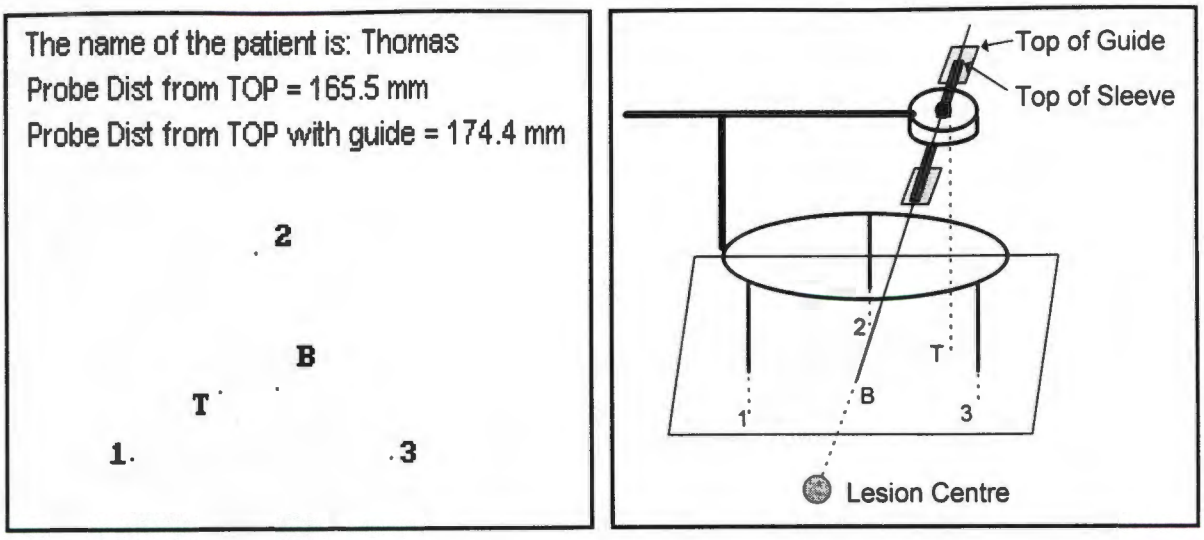


Figure 5.10: (a) The Setting Diagram for the Cape Pointer (on the left)
(b) The Cape Pointer on the Setting Diagram (on the right)

The remaining part of the setting diagram consists of the projections of the three leg markers (1, 2 & 3 in figure 5.10a), and the projections of the top and bottom points (T and B in figure 5.10a), where the vector passing through the entry point and lesion centre, intersects the top and bottom plane respectively.

The diagram in figure 5.10a is plotted on the screen. By setting the PC into graphics mode using the DOS command graphics.com, a hardcopy is obtained by using the "PrintScreen" key on the PC keyboard. Scaling parameters for the x and y plotting coordinates are used to ensure that the resultant hardcopy is true to scale. These scaling parameters are specific to the PC and printer model combination. (Should another printer be used inadvertently to produce the setting diagram, the legs of the Cape Pointer would not fit on their corresponding markers on the setting diagram, thus alerting the user that an error has occurred.)

## 5.6 SETTING THE CAPE POINTER

All the information to set the Cape Pointer ready for theatre is included in the setting diagram. The initial setting is done in the CT scan room, so that the final checks can be carried out, prior to taking the patient to theatre.

To set the Cape Pointer, it is placed on the diagram so that each leg is coincident with the corresponding dot marking its projected position. The legs of the Cape Pointer do not exactly correspond to the projected points, as the points are plotted from the three dimensional CT/SPG coordinates and thus are subject to the inaccuracies of the CT/SPG system. The Cape Pointer is placed on the diagram, so that the best optimum fit, between the actual legs and their projected positions, is obtained (see figure 5.11).

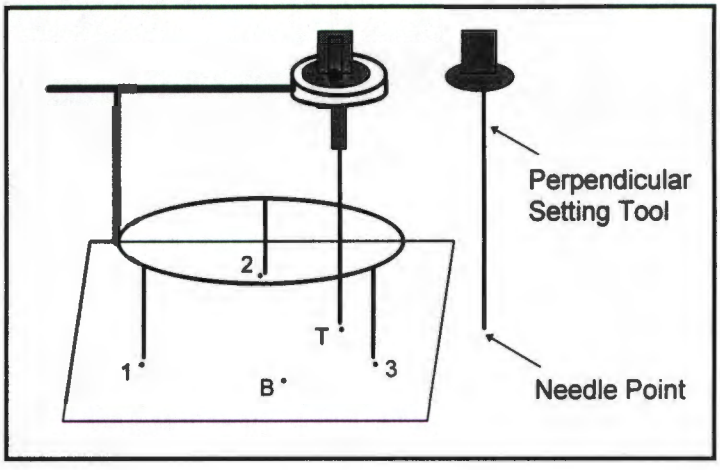


Figure 5.11: The Perpendicular Setting Tool for the Cape Pointer

The sleeve of the ball and socket joint has to be set perpendicular to the horizontal arm. A perpendicular setting tool has been designed (figure 5.11), which fits over the sleeve, and when it comes to rest on the portion of the horizontal arm holding the ball and socket joint, forces the sleeve to be perpendicular to the horizontal arm. The ball and socket joint clamp is tightened, thus locking the sleeve into the perpendicular position.

The horizontal arm is moved until the needle point of the perpendicular setting tool is coincident with the dot T on the setting diagram, and then horizontal arm clamp is locked. The centre of the ball and socket joint is now positioned at the point where the vector, defined by the entry point and lesion centre, cuts the top plane.

The perpendicular setting device is removed, the ball and socket joint clamp loosened, and a long pointer inserted down the sleeve. The ball in the socket is rotated until the tip of the pointer is pointing at dot B, and the ball and socket joint clamp tightened. The pointer is now coincident with the vector defined by the entry point and lesion centre. The final setting is to attach the depth clamp to the pointer, so that the distance from the pointer tip to the depth clamp is 165.5mm, i.e. the "Probe Dist from TOP" , as shown in figure 5.10a.

As a final check, the Cape Pointer is placed on the phantom's head, so that the three legs rest on their corresponding markers. The pointer is inserted down the sleeve and should come to rest on the entry marker. Any deviations greater than 2mm need to be examined to ensure that no unnecessary errors, such as incorrect data entries, are present.

From this and from the distance that the pointer still has to be inserted, which is determined from how much the depth clamp is protruding above the sleeve, the neurosurgeon ascertains whether he/she is satisfied with the general direction and depth of the pointer. This is a vital check, as it is impossible to ascertain whether the lesion centre coordinates have been correctly determined. For example, if an error is made when reading the digitised data off the CT screen, this error is undetectable by the software.

However with a phantom, this does not present a problem. A hole is drilled at the site of the entry marker, and the pointer is inserted into the phantom until it comes to rest "in the lesion centre". The tip of the pointer should come to rest in the very close proximity of the radio-opaque ball-bearing marking the lesion centre. The expected pointing accuracy is approximately 2mm, which is attained/verified in the system trial in chapter 6.

## 5.7 CONCLUSION

Using the Cape Pointer in conjunction with the SPG system fulfils the design criteria initially set by the neurosurgeons. The patient remains unrestrained during the CT procedure and any patient movement is mathematically removed from the resultant data. The data is used to set the simple, easy to use, mechanical frameless stereotactic device, and still replicates the accuracy of its much more sophisticated counterparts. This is verified in the system's trial in chapter 6.

The Cape Pointer on its own is a very simple device to use. In conjunction with the SPG system in its present state, the Cape Pointer loses many of its advantages and takes considerably more time, effort and manpower to operate, than is warranted for such a simple device.

As discussed in the conclusions on the SPG system (chapter 4.7), the SPG system would have to have a permanent setup in the CT scan room, and the whole SPG system streamlined, before the SPG system, in conjunction with the Cape Pointer, became a viable proposition in a very busy hospital environment.

Before using the SPG system, in conjunction with the Cape Pointer, in the clinical environment further tests would have to be carried out. A thorough error analysis would have to be undertaken to estimate what the expected errors are, what the standard deviations are and what outliers are to be expected from the system. Only once the neurosurgeon knows with what accuracy and reliability a system can be employed, can the neurosurgeon safely use that system in the clinical environment.

# CHAPTER 6 THE CT/ SPG SYSTEM TRIAL TO SET THE CAPE POINTER USING A PATIENT PHANTOM

## 6.1 THE SYSTEM TRIAL

A system trial, using the CT/SPG system to set the Cape Pointer, was carried out using the black phantom head. As the lesion was represented by a radio-opaque marker, the setting of the Cape Pointer could be verified at the end of the trial by placing it on the phantom and ascertaining whether the tip of the neurosurgical instrument did in fact coincide with the lesion marker (see figure 6.1).

Figure 6.1: The phantom head - a black face mask - and the Cape Pointer in place on the phantom

Prior to scanning the phantom, the control procedure (chapter 4.3) for the CT/SPG system had to be carried out. The control frame was recorded on video tape, and an AP and LAT surview of the control frame, as well as two slices through the two planes of the control frame were scanned. The control frame was then removed from the CT bed.

Prior to placing the phantom on the CT bed, an entry point was marked with a radio-opaque marker, and using the Cape Pointer's setting jig, the three leg markers were placed on the phantom, so that they surrounded the entry marker. The phantom was placed on the CT bed in the area previously occupied by the control frame. The four tracking markers, required by the SPG system to correct for any phantom movement, were attached to the phantom's forehead (figure 6.2), so that they were 'visible' to both SPG cameras.

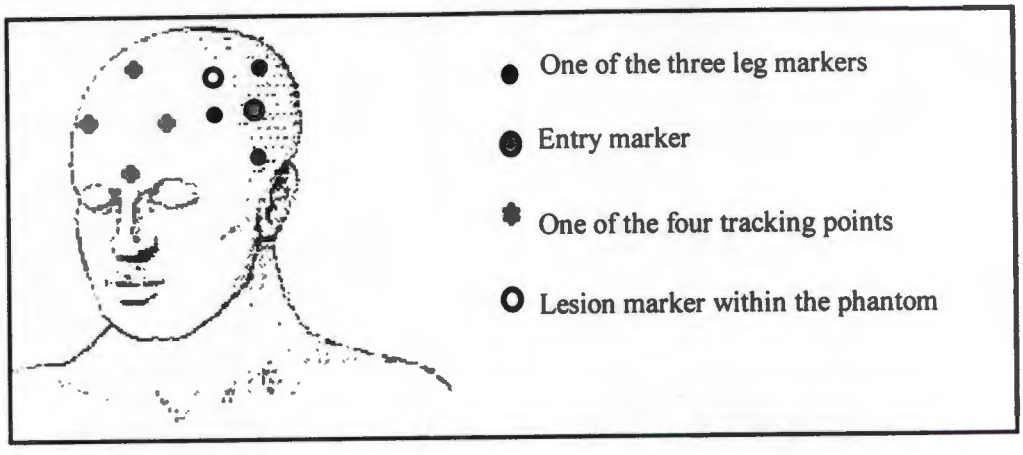


Figure 6.2: The nine phantom markers for the system trials

Video recording was again commenced, and only terminated once all the CT scans had been completed. An AP and LAT surview, and slices through all nine markers (figure 6.2), were scanned before any movement simulation was done, to obtain a set of "uncontaminated/motionless" data. The phantom head was then moved to simulate patient movement and a second, "contaminated", LAT surview was scanned. The phantom head was again moved to simulate patient movement and a second, "contaminated", slice was scanned through the lesion marker.

Data acquisition was begun by first digitising all the control and phantom markers on the surviews and slices. The CT data was entered into the PC using the CT input options of the CT/SPG software. The VCR was connected via the IP8 frame grabber card to the PC, and the necessary video images transferred and digitised (chapters 4.6.2 to 4.6.4).

The first step of the data reduction was the 3D transformation of the control frame. Using the Rodrigues transformation, the 3D coordinates of the 16 control markers, measured in the reflex metrograph, were transformed into the CT system. The resulting transformation precisions, for the 8 dual purpose control markers, common to both systems, are listed in table 6.1.

| Marker No. | dX (mm) | dY (mm) | dZ (mm) |
|---|---|---|---|
| 1 | +0.1 | +0.3 | -1.2 |
| 2 | +0.9 | +0.4 | -1.1 |
| 3 | -1.0 | +0.6 | +1.0 |
| 4 | -0.3 | +1.3 | +2.2 |
| 5 | +0.7 | -0.8 | -0.7 |
| 6 | -0.3 | -0.3 | -1.4 |
| 7 | +0.2 | -1.4 | +0.0 |
| 8 | -0.2 | -0.1 | +1.3 |
| | **Standard deviations for the 8 markers** | | |
| | 0.6 | 0.8 | 1.4 |

Table 6.1: Transformation precisions from the metrograph to the CT system

Once all 16 control marker coordinates had been transformed into the CT system, the DLT parameters for the SPG system could be calculated. The resulting SPG system precisions for all 16 control markers are shown in appendix C - table C.1, and their standard deviations are shown in table 6.2.

| Std. Dev. - dX (mm) | Std. Dev. - dY (mm) | Std. Dev. - dZ (mm) |
|---|---|---|
| 0.3 | 0.3 | 0.9 |

Table 6.2: Standard deviation for the SPG system precisions

Once the DLT parameters had been calculated, they were used to solve for the 3D coordinates of the four tracking markers (chapter 4.6.4) on the video images at the start of the AP surview, at the start of the "contaminated" LAT surview, and the "contaminated" lesion centre slice. Thereafter, the CT control calculations were carried out (chapter 4.6.5). The h parameters were calculated, using the slice and surview coordinates of the eight dual control markers, and the resulting CT control precisions are shown in table 6.3.

| dX (mm) | dY (mm) |
|---|---|
| 0.5 | -0.6 |
| -0.1 | -0.1 |
| 0.1 | 0.4 |
| -0.1 | -0.5 |
| -0.5 | 0.8 |
| -0.0 | -0.4 |
| -0.0 | 0.1 |
| 0.0 | 0.2 |
| **Std. Deviations for dX & dY** | |
| 0.3 | 0.5 |

Table 6.3: The CT control precisions

The LAT rotation software made use of the 3D SPG coordinates of the four tracking markers on the video images at the start of the AP and "contaminated" LAT surview, and the CT coordinates of the four tracking markers on the AP surview, to correct the "contaminated" LAT surview coordinates (chapter 4.6.6). As the Z coordinates of the AP surview are adopted for the LAT surview, only the x coordinates of the LAT surview are shown in table 6.4. In table 6.4, the uncontaminated LAT x coordinates have been digitised from the "uncontaminated" LAT surview, prior to any phantom movement, the contaminated LAT x coordinates have been digitised from the "contaminated" LAT surview after the phantom was moved, and the corrected LAT x coordinates are calculated by the LAT rotation software. Ideally the corrected LAT x coordinates and the uncontaminated LAT x coordinates should be the equal. The LAT rotation algorithms, applied to the LAT x coordinates of the eight external markers, resulted in a mean error of -0.4 and a standard deviation of 0.6.

| **Marker Description** | **Contaminated LAT x (mm)** | **Corrected LAT x (mm)** | **Uncontaminated LAT x (mm)** | **LAT dx (mm)** |
|---|---|---|---|---|
| Track. Marker 1 | -11 | -12.3 | -14 | -1.7 |
| Track. Marker 2 | -23 | -27.6 | -28 | -0.4 |
| Track. Marker 3 | -45 | -47.7 | -48 | -0.3 |
| Track. Marker 4 | -51 | -57.4 | -58 | -0.6 |
| Leg 1 | -81 | -86.4 | -87 | -0.6 |
| Leg 2 | -35 | -40.8 | -41 | -0.2 |
| Leg 3 | -85 | -93.5 | -93 | 0.5 |
| Entry Point | -64 | -71.0 | -71 | 0.0 |
| | | | **Mean LAT dx** | -0.4 |
| | | | **Std. Dev. LAT dx** | 0.6 |

Table 6.4: Undistorted, distorted and corrected LAT x coordinates

The APLAT to 3D software transformed the AP and corrected LAT surview coordinates into 3D CT coordinates (chapter 4.6.7). These calculated coordinates were compared to the digitised 3D CT coordinates obtained from the "uncontaminated" slices, prior to any movement occurring, and the results are listed in table 6.5.

| Marker Description | dX (mm) | dY (mm) | dZ (mm) |
|---|---|---|---|
| Track. Marker 1 | 0.0 | 0.6 | -1.2 |
| Track. Marker 2 | -0.4 | 0.4 | -1.9 |
| Track. Marker 3 | -0.1 | -1.1 | 0.3 |
| Track. Marker 4 | -0.2 | 0.4 | 0.0 |
| Leg 1 | 0.2 | 1.5 | -1.0 |
| Leg 2 | -0.6 | 0.3 | -0.9 |
| Leg 3 | 0.0 | 1.5 | -1.0 |
| Entry Point | 0.7 | 1.3 | -0.9 |
| **Mean** | 0.0 | 0.6 | -0.8 |
| **Std. Dev.** | 0.4 | 0.9 | 0.7 |

Table 6.5: Comparison of the calculated and digitised 3D CT coordinates of the external markers

The above comparison/check can not be performed in the clinical situation, due to the lack of such "uncontaminated" slices. Therefore, to ensure that the LAT rotation software and the APLAT to 3D software had been functioning correctly, the 3D coordinates of the four tracking markers, determined from the video images, were compared to the 3D coordinates of the four tracking markers calculated by the APLAT to 3D software using the Rodrigues transformation (see chapter 4.6.7). The results of the comparison are listed in table 6.6.

| Marker Description | dX (mm) | dY (mm) | dZ (mm) |
|---|---|---|---|
| Track. Marker 1 | +0.2 | -0.2 | +0.2 |
| Track. Marker 2 | -1.3 | +0.1 | +0.0 |
| Track. Marker 3 | +1.9 | +0.2 | +0.0 |
| Track. Marker 4 | -0.9 | -0.1 | -0.2 |
| | **Standard deviations** | | |
| | 1.4 | 0.2 | 0.2 |

Table 6.6: Comparison of the 3D coordinates of the four tracking markers calculated by the software, and determined from the video images

The 3D slice coordinates of the lesion marker, obtained after the phantom had been moved, had to be transformed using the Lesion point rotation software (chapter 4.6.8), to remove any phantom movement. The resultant/calculated 3D coordinates of the lesion marker were compared to the digitised 3D CT coordinates obtained from the "uncontaminated" slice through the lesion marker, prior to any movement occurring, and the results are listed in table 6.7.

| | dX (mm) | dY (mm) | dZ (mm) |
|---|---|---|---|
| **Lesion Marker** | +0.2 | +0.4 | +1.3 |

Table 6.7: Comparison of the calculated and digitised 3D CT coordinates of the lesion marker

To ensure that the three leg markers had been correctly identified throughout the trial, their 3D coordinates, calculated by the APLAT to 3D software, were compared to their 3D coordinates, measured in the reflex microscope, using the Rodrigues transformation. From the resulting precisions in table 6.8, the accuracy with which the three leg markers had been coordinated could be ascertained, and the overall system accuracy estimated.

| Marker Description | dX (mm) | dY (mm) | dZ (mm) |
|---|---|---|---|
| Leg 1 | 0.0 | 1.3 | 0.3 |
| Leg 2 | -0.2 | -2.1 | -1.1 |
| Leg 3 | 0.1 | 0.8 | 0.8 |
| | **Standard Deviations** | | |
| | 0.2 | 1.8 | 1.0 |

Table 6.8: Comparison of the 3D coordinates of the 3 leg markers determined in the CT/SPG system, and in the reflex microscope

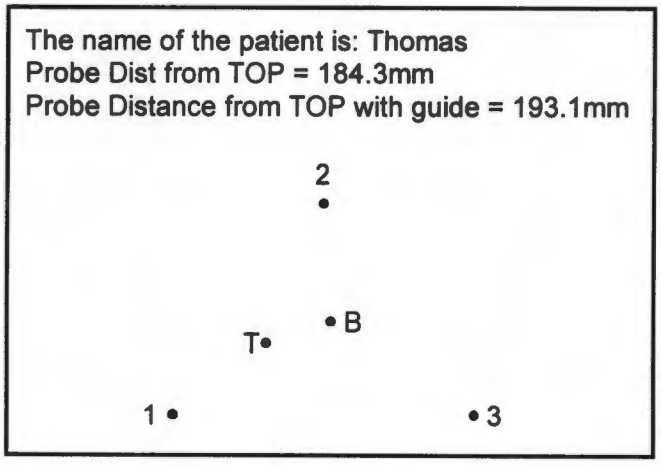


Figure 6.3: The setting diagram for the system trial

The last stage of the trial was to print out the setting diagram and set the Cape Pointer. Once the Cape Pointer had been set, and the clamp set at a distance of 184.3mm from the pointer tip (see figure 6.3), the Cape Pointer was placed on the phantom (see figure 6.1), so that each leg rested on its respective marker. The pointer was inserted through the hole, made at the site of the entry point, until the clamp prevented the pointer from being inserted any further. In this system trial, the pointer's direction was approximately 1mm off course and the pointer extended past the lesion marker by approximately 2mm.

## 6.2 CONCLUSION

The design criteria for the Cape Pointer was that it should be a simple, easy to use, mechanical, frameless stereotactic device, that replicated the accuracy of its much more sophisticated counterparts.

The measuring accuracy of 1.5mm for the CT scanner, sets a limitation on the accuracy that can be expected from the CT/SPG system. This is borne out by the various results listed in table 6.1, and tables 6.3 to 6.8.

The comparison between the calculated and digitised 3D coordinates of the lesion marker in table 6.7, show that the CT/SPG system can accurately determine the 3D coordinates of the lesion marker, even though the phantom movement had to be catered for. The same is true for the 3D coordinates of the three leg markers determined by the CT/SPG system, when compared against their 3D coordinates determined in the reflex microscope (table 6.8). The results, from these comparisons, give a good indication of the accuracy of the Cape Pointer, when used in conjunction with the CT/SPG system, and, when taking into account the accuracy limitation of the CT scanner, are very satisfactory.

The ultimate test for the Cape Pointer is how well the objective is achieved, i.e. how close the pointer tip is to the lesion centre marker. The system trial shows that the Cape Pointer when used in conjunction with the CT/SPG system, has an accuracy rate of approximately 2mm, which considering that the measuring accuracy of the CT scanner is approximately 1.5mm, is excellent for such a simple device.

Although the CT/SPG system, when used conjunction with the Cape Pointer, mathematically eliminates any phantom movement, and achieves the necessary accuracy, it is cumbersome, complicated and labour intensive. In the provincial hospitals, where staff shortages are always a problem, it was felt that unless the neurosurgeons could direct all the

necessary operational steps themselves, the Cape Pointer would never develop beyond the research phase, or become a viable tool in the operating theatre. Therefore the decision was made to test the Cape Pointer as a stand alone device, without the SPG system, and thus streamline the whole procedure.

# CHAPTER 7 THE CAPE POINTER AS A STAND ALONE STEREOTACTIC DEVICE

## 7.1 INTRODUCTION

Once the decision was made to use the Cape Pointer as a device in its own right, without the SPG system, the Cape Pointer system had to be developed and thoroughly tested before using it in the clinical environment.

The existing software, pertaining to the Cape Pointer, had to be amended and loaded onto dedicated hardware, thus forming a complete system that could be used for the clinical trials. Prior to starting the clinical trials, system trials had to be undertaken to ensure that everything was working satisfactorily, and to determine the accuracy of the system.

Various procedures for using the Cape Pointer in the CT scan room and the operating theatre had to be developed. As the SPG system would no longer monitor patient movement, procedures had to be developed to ensure that the patient would remain still throughout the CT scan procedure, while still keeping patient comfort as a high priority. Having placed the three leg markers and entry marker on the patient's head, the CT slice system is utilised to determine the 3D CT coordinates of the markers and lesion centre. Using the 3D CT coordinates, the software generates the setting diagram and the Cape Pointer is set ready for theatre. In theatre, once the Cape Pointer has been placed on the patient's head with its legs resting on their corresponding markers, the surgical instrument is inserted down the sleeve of the Cape Pointer to the preset depth. The instrument's tip is now coincident with the lesion centre and the surgical procedure can be completed.

Once the clinical trials began, and practical experience in using the Cape Pointer was gained, so the various procedures were altered and improved. A phantom, to help the neurosurgeon visualise the position of the lesion in relation to the Cape Pointer, was built and proved to be such an excellent device for setting the Cape Pointer, that it now supersedes the setting diagram, which in later patient trials was only used for checking the setting of the phantom.

The Cape Pointer system, with its software run on dedicated hardware, with CT and theatre procedures developed during system trials and clinical trials, which now include over 40 successful patient procedures, has proved to be an efficient, yet simple stereotactic device.

## 7.2 THE SOFTWARE AND HARDWARE FOR THE CAPE POINTER SYSTEM

The Cape Pointer software package was created by utilising only a small part of the CT/SPG software. As the SPG system was not used to monitor patient movement, the bulk of the CT/SPG software could be discarded, and the only program to be retained was the program to actually generate the setting diagram.

This setting diagram program utilises the 3D coordinates of the three leg markers, the entry marker and the lesion centre, from which all patient movement had been removed (see Appendix G), to produce the setting diagram. As no patient movement would occur during the CT scanning procedure, the program could be adopted in its entirety. One small section was added to the start of the setting diagram program, to ascertain the accuracy with which the leg markers' 3D coordinates had been determined by the CT scanner, by comparing them to the 3D coordinates of the leg markers measured in the reflex microscope, using the Rodrigues transformation.

A small data entry program was written, so that the 3D coordinates of the leg markers and lesion centre could be entered, and written to a text file that would be utilised by the setting diagram program.

The Cape Pointer system was developed further by adding a mouse driven menu to run the various software options. The mouse driven menu was written in Turbo C, whereas the setting diagram program, and other programs added at a later date, were all written in True Basic.

To make the Cape Pointer system as portable as possible, so that it could easily be moved between the CT scan room and the operating theatre, dedicated hardware was purchased (figure 7.1). The hardware consisted of a laptop computer (Compaq Contura / Aero 4/25) and portable printer (Canon Bubble Jet printer BJ-10SX), both equipped with rechargeable Nicad batteries.

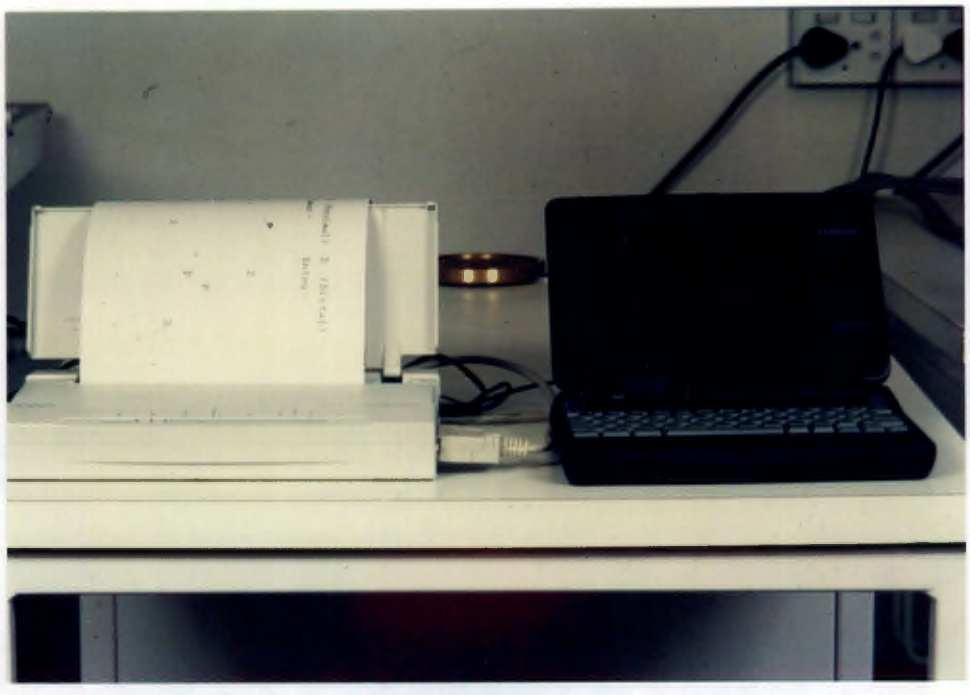

Figure 7.1 The printer and laptop

The Compaq laptop is supplied with DOS and Windows already installed. The autoexec.bat file on the laptop was amended, so that the last command in the file runs a small start-up routine for the Cape Pointer. This routine simply enquires whether the user wants to run the Cape Pointer software, and if the answer is affirmative, the DOS command - graphics.com is run setting the laptop into graphics mode, prior to running the Cape Pointer menu program.

These start-up routines were added, so that inexperienced computer users would not have to be embroiled in the actual workings of the computer, but would be guided directly to the Cape Pointer menu. The start-up routine also ensures that the software is run from the true DOS environment, and not simply shelled out of Windows to DOS. The software has to be run from the true DOS environment, as the printing of the setting diagram with the Print Screen key does not operate from the Windows environment.

Initially the Cape Pointer software only consisted of the data entry and the setting diagram program. At a later date, as clinical trials progressed and the Cape Pointer system was improved, three further software options were added, and these will be described later in the chapter.

## 7.3 PHANTOM TRIALS

Before starting any clinical trials, it was necessary to ascertain that everything was operating correctly. Various trials were run on various phantoms to ascertain that the Cape Pointer system was functional and to ascertain the accuracy of the system.

The first trials were carried out with the black phantom head used for the CT/SPG system trials. The three leg markers, corresponding to the positions of the three legs of the Cape Pointer, and the entry marker were attached to the outer surface of the phantom, so that the three leg markers surrounded the entry marker. The lesion centre was represented by the radio-opaque marker within the phantom. The phantom was placed on the CT bed and secured, so that no movement could occur during the CT scanning procedure. CT slices were scanned through the three leg markers and the entry marker. The data was digitised from the slices, using the CT scanner's digitiser, and entered into the Cape Pointer software using the data entry program. The setting diagram was generated and the Cape Pointer set with the aid of the diagram.

The Cape Pointer was placed on the phantom, and a long needle pointer was inserted down the sleeve of the Cape Pointer to the required depth. The accuracy with which the Cape Pointer can locate the lesion marker is determined by the difference in the positions of the pointer tip and the lesion marker. From repeated phantom trials, the pointer tip placement accuracy was in the range of 2mm.

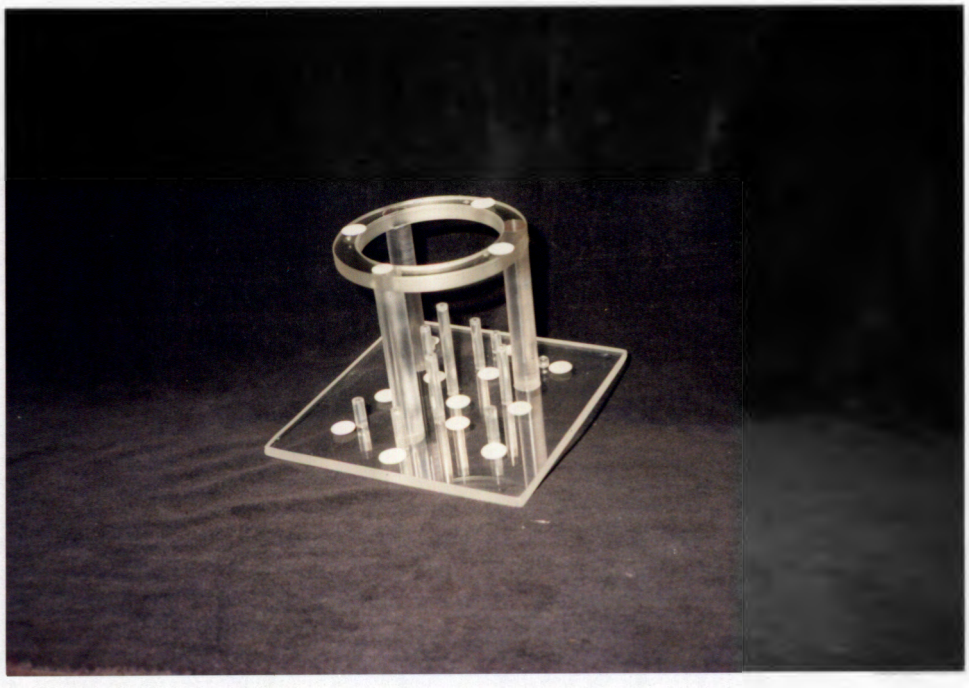

Figure 7.2: The ring phantom

At a later stage, a more formal trial was set up, to ascertain the mean accuracy of the Cape Pointer system, and the deviations that could be expected from this mean. For this purpose a new phantom was designed, so that the three leg markers and the various lesion markers could easily be measured in the reflex microscope. The ring phantom (figure 7.2), has three leg markers embedded in the upper ring, and 12 lesion markers mounted at various heights above the bottom plane. The leg and lesion markers all consist of 2mm diameter steel ball-bearings.

As the reflex microscope is a very accurate measuring instrument (measuring precision of +/- 4 micrometers in all three axes), the 3D coordinates of the three leg markers and 12 lesion markers, measured in the reflex microscope, are considered "error free". The first test was to ascertain how accurately the lesion markers could be determined by the CT scan system. Using the three leg markers as the common points between the CT scan system and reflex microscope system, the 3D CT coordinates of the 12 lesion markers were transformed into the reflex microscope system, using the Rodrigues transformation. The transformations precision for the three leg markers are listed in table 7.1.

| **Leg Marker No.** | **Difference in X (mm)** | **Difference in Y (mm)** | **Difference in Z (mm)** | **Vector difference (mm)** |
|---|---|---|---|---|
| 1 | -0.7 | -0.0 | -0.3 | 0.7 |
| 2 | +0.2 | +0.0 | +0.3 | 0.4 |
| 3 | +0.5 | +0.0 | +0.0 | 0.5 |
| | | | | **Mean vector diff.**= 0.5 |
| **Standard Deviations** | | | | |
| | 0.6 | 0.0 | 0.3 | 0.2 |

Table 7.1: Precisions for the Rodrigues transformation using the three leg markers

The 3D CT coordinates of the 12 lesion markers, transformed into the reflex microscope system, were compared to their corresponding 3D coordinates measured in the reflex microscope. The differences between the two sets of coordinates are listed in table 7.2.

| Lesion Marker No. | Difference in X (mm) | Difference in Y (mm) | Difference in Z (mm) | Vector difference (mm) |
|---|---|---|---|---|
| 1 | -1.5 | -1.4 | -0.8 | 2.2 |
| 2 | -0.1 | -0.3 | -1.1 | 1.1 |
| 3 | +0.1 | -0.7 | -1.2 | 1.4 |
| 4 | -0.4 | -0.9 | -0.6 | 1.2 |
| 5 | +0.1 | -1.3 | -0.7 | 1.5 |
| 6 | +0.1 | -1.0 | -0.5 | 1.1 |
| 7 | +0.1 | -0.9 | -0.4 | 1.0 |
| 8 | -0.2 | -0.9 | -0.6 | 1.1 |
| 9 | -0.7 | -1.6 | -0.6 | 1.9 |
| 10 | -1.1 | -0.2 | -0.2 | 1.1 |
| 11 | +0.0 | +0.2 | -1.1 | 1.1 |
| 12 | -0.3 | -1.6 | -0.7 | 1.8 |
| **Mean Values** | | | | |
| | -0.3 | -0.9 | -0.7 | 1.4 |
| **Standard Deviations** | | | | |
| | 0.5 | 0.6 | 0.3 | 0.4 |

Table 7.2: Differences for the 12 lesion markers

The values in table 7.2 show how well the GSH scanner can determine the 3D coordinates of the lesion markers, and present the minimum accuracy that can be achieved when the GSH scanner is used in conjunction with a device such as the Cape Pointer. The values in table 7.2 obviously do not take into account the inaccuracies that arise from setting the Cape Pointer on the setting diagram. Setting diagrams were therefore produced for 11 lesion markers, using a theoretical entry point midway between the three legs markers. (Due to the design of the ring phantom, the 12th lesion marker was not accessible to the Cape Pointer.) The Cape Pointer was set on each setting diagram, and thereafter placed on the phantom, with the three legs corresponding to the three markers. The pointer was inserted down the sleeve to the predetermined depth for that particular lesion. The pointer's tip position was "recorded" by making an indentation in soft putty, placed on the ring phantom. Once this procedure had been repeated for the 11 lesion markers, the 3D coordinates of the lesion markers and their corresponding putty indentations were measured in the reflex microscope, and the 3D coordinate differences are listed in table 7.3. The vector differences are the actual distances between the lesion marker and the corresponding putty indentation.

| Lesion Marker No. | Difference in X (mm) | Difference in Y (mm) | Difference in Z (mm) | Vector difference (mm) |
|---|---|---|---|---|
| 1 | +0.8 | -0.2 | -1.7 | 1.9 |
| 2 | -0.7 | +0.2 | -1.6 | 1.7 |
| 3 | -0.4 | +0.7 | -0.8 | 1.2 |
| 4 | -0.9 | +0.7 | -0.6 | 1.3 |
| 5 | -0.8 | -1.7 | -0.3 | 1.9 |
| 6 | +1.2 | -1.2 | -0.5 | 1.7 |
| 7 | -0.2 | -0.8 | -1.0 | 1.4 |
| 8 | +0.1 | -2.2 | -1.8 | 2.8 |
| 9 | -0.6 | -1.3 | -1.3 | 2.0 |
| 10 | -0.4 | -1.5 | -0.0 | 1.6 |
| 11 | -0.6 | +0.3 | -2.3 | 2.3 |
| **Mean Values** | | | | |
| | -0.2 | -0.6 | -1.1 | 1.8 |
| **Standard Deviations** | | | | |
| | 0.7 | 1.1 | 1.5 | 0.3 |

Table 7.3: Differences in the positions of the actual lesion marker and the pointer's tip, as indicated by the Cape Pointer set on the setting diagram

From table 7.3, although the mean values for the differences in X, Y and Z alter only slightly in comparison to those in table 7.2, the standard deviations are considerably larger, and the overall accuracy decreases from a mean of 1.3 and a standard deviation of 0.4, to a mean of 1.8mm with a standard deviation of 0.3mm.

Therefore, taking everything into account, the Cape Pointer will place the surgical instrument tip within approximately 2.0mm of the lesion marker. These accuracies are determined for the Cape Pointer, used in conjunction with a CT scanner that has an approximate measuring resolution of 1.5mm. (The accuracy of determining the lesion marker's position within 2.0mm, does not take into account any skin movement. Both during the CT scan and surgical procedure involving a patient, the effect of skin movement is reduced to an absolute minimum, by ensuring that the scalp lies smoothly on the cranium in its most natural position.)

With the Cape Pointer system thoroughly tested, and the accuracy with which the lesion centre can be pinpointed by the Cape Pointer, the system was ready for the patient trials.

## 7.4 PATIENT PREPARATION PRIOR TO THE CT SCAN

Prior to CT scanning, the external markers have to be attached to the patient's head. The neurosurgeon, with the aid of the patient's initial CT scans indicating the presence of a lesion, selects an optimal site for the entry point. The criteria used to select this site are determined by the actual location of the lesion within the cranium, the avoidance of any critical structures such as vascular brain areas, sylvian fissure and ventricles, on the vector defined by the entry point and the lesion centre, and a stable fit of the Cape Pointer's three legs on the cranium.

Once the entry site has been selected, the entry marker has to be attached to the scalp. As hair proves quite a problem for secure marker attachment, the hair surrounding the entry site is shaved, so that both the entry marker and leg markers are attached to cleanly shaved scalp. Since shaving, if done too far in advance of the actual operation, raises the risk of infection, the CT scanning procedure occurs just prior to the patient going to theatre.

Various adhesives for the marker attachment to the scalp were tested. The adhesive had to be approved for medical use, and be strong enough to ensure that the markers could not easily be detached from the scalp. The medical adhesive that was found to be very effective, was Dow Corning Medical Adhesive B, produced in France by Dow Corning. It was a non-allergenic, pressure sensitive, silicone based adhesive for external use, which was used, for example, for attaching maxilla-facial prosthetic devices. Markers, attached with this adhesive, were very firmly attached to the scalp. Unfortunately this particular adhesive is no longer manufactured. As this particular adhesive had proved so effective, another maxilla-facial adhesive was tested, and was subsequently used for a short period, until the whole marker attachment procedure was completely revised. The adhesive used was Cosmesil, a pressure sensitive adhesive PSA-1, produced by Principality Medical LTD in the United Kingdom.

Both adhesives could easily be removed with alcohol or with medical adhesive remover wipes, such as the product Convacare Adhesive Remover Wipe, manufactured for ConvaTec by Bristol-Myers Squibb in the United States of America. Prior to using any of these adhesives or adhesive remover wipes on a patient, the author tested the adhesives and the remover wipes on herself and found them to be very effective and "patient friendly".

(Other marker attachments were explored, such as attaching the markers to various types of head gear attached to the head with straps, ear plugs etc. The reason for testing all these marker attachment techniques was to try and reduce the area to be shaved to an absolute minimum, so that the shaved area, after the surgical procedure, would hardly be noticeable. Unfortunately none of the attachment methods tested were satisfactory, as it was impossible to secure the head gear to the head, so that the head gear did not move. Therefore these types of marker attachment were discarded as impractical.)

After the neurosurgeon has attached the entry marker to the scalp, the setting jig (see chapter 5.3) is used to position the three leg markers, so that they surround the entry marker. Care has to be taken to ensure that each leg marker is attached to scalp covering the cranium, and not to skin overlying such soft tissue structures as the neck, to ensure a stable fit of the Cape Pointer on the cranium. The type of marker used for the entry and leg markers is shown in figure 7.3.

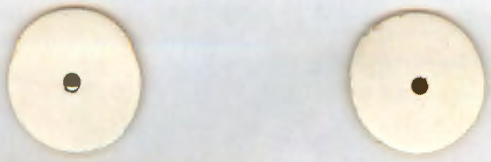

Figure 7.3: An example of the marker, with and without ball-bearing

All leg markers are labelled by the neurosurgeon with their respective numbers to aid identification during the CT scan and surgical procedure, and an ink mark is made on the scalp through the central hole of the marker (see figure 7.3). The ink mark serves as an additional reference, should the marker become detached. A 2mm ball-bearing is then placed in the central hole of each marker, thus making the centre of the marker radio-opaque (see figure 7.3).

The patient preparation occurs either in the ward, or in the CT scanning rooms. Once all the markers have been attached, the patient is then moved onto the CT bed for scanning to commence.

## 7.5 CT SCAN PROCEDURE

An important precursor to a successful CT scanning procedure, is the manner in which the patient is positioned on the CT bed. The more comfortable and secure the patient's position is, prior to scanning, the less likely it will be that the patient moves during a scan.

The patient is positioned in approximately the same position as he would be placed on the operating table, to reduce any errors due to scalp movement. The patient is asked to make himself as comfortable as possible, and the patient's head is comfortably supported by a head support. Various cushioning/padding is also used to reduce any head movements. When positioning the patient's head in the head support, care is taken that the scalp does not "bunch up", but lies smoothly over the cranium. As a final safeguard, a few strips of tape are used to hold the patient's head in position.

The patient is requested to lie as still as possible. Should the patient appear restless, or move during the scanning, thus necessitating a repeat scan, one of the medical staff, wearing a lead apron for radiation protection, accompanies the patient in the CT scan room. The presence of the medical person has a calming effect on the patient, and the patient can be reminded at intervals during the scan to remain still. From the various patient trials, this definitely has a beneficial influence on the patient, to an extent where it has become a matter of course that the patient is accompanied during the scan.

Just prior to CT scanning commencing, IV (intra-venous) radiological contrast, if required, is administered to the patient, to improve visualisation of the lesion on the resultant CT scan slices.

CT scanning is commenced by scanning an AP or LAT surview of the patient. The area containing the lesion is identified by the neurosurgeon on the surview, and 5mm thick slices are scanned in this area. The neurosurgeon selects the most appropriate slice for the destination point, for example the slice showing the lesion centre, and this particular slice is rescanned with a slice thickness of 2mm to allow for a more accurate position fix of the lesion centre.

The lesion centre is digitised using the CT scanner system and the 3D CT coordinates are manually recorded from the CT screen, and entered on the patient's CT form (figure 7.4).

**PATIENT FORM FOR CT SCAN DATA TO SET CAPE POINTER**

| Patient's Label / Information | |
|---|---|

| | |
|---|---|
| CT scan file name | |
| CT scan date | |
| CT scan proforma (e.g. supine) | |
| PC file name (less than 5 characters) | |

| | X | Y | Z/Bed | Scan No. | Slice Width |
|---|---|---|---|---|---|
| Lesion 1 | | | | | |
| Lesion 2 | | | | | |
| Entry | | | | | |
| Leg 1 | | | | | |
| Leg 2 | | | | | |
| Leg 3 | | | | | |

| Data logger's name | |
|---|---|

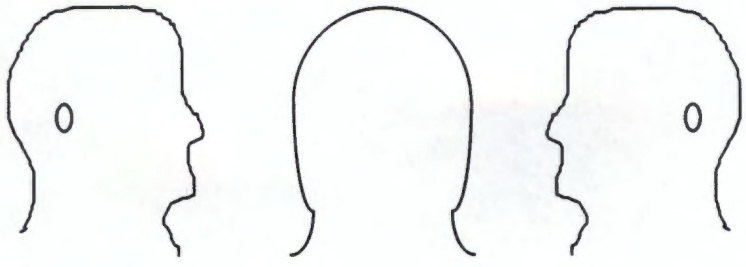

| | X | Y | Z/Bed |
|---|---|---|---|
| **Phantom Setting** | | | |

Figure 7.4: The patient's CT form

The patient's CT form is designed to ensure that all the relevant information is recorded. Most of the items on the form are self explanatory. The CT scan proforma is dependent on the how the patient is lying on the CT bed; for example if the patient is lying face up, i.e. in the supine position, the CT proforma is set to supine. There is space on the form to target two destination points (lesion 1 & 2 in figure 7.4), should an additional destination point be required by the neurosurgeon. Besides the X, Y and Z (CT bed position) coordinates for the lesion, entry and external markers, the slice number and slice width are also recorded. The slice number is required when that particular slice needs to be recalled at a later date, and the recording of the slice width serves as a important reminder to set (or check) the slice thickness to 2mm. The CT data should preferably be recorded by two different data loggers, and the data recorded on the two CT forms cross checked to ensure that no recording errors

have occurred. The three diagrams of the head are for sketching the positions of the markers on the head, and serve as a rough record of the marker placement on the cranium.

Positioning of the CT bed for scanning a slice through an external marker, is dependent on the CT scanner hardware. The GSH scanner has a low-powered laser mounted in the CT scanner gantry to indicate the plane in which a slice is scanned - the medical personnel manually move the CT bed so that the laser beam bisects the marker. This method of positioning the CT bed is faster and more accurate than utilising the GSH scanner's surview for planning the slice positions. Some CT scanners do not have a laser for slice positioning, and the slice planning has to be done using the surview, the CT bed is then automatically moved to each position, where a slice is to be scanned.

Scanning is always done in a specific order, first leg markers 1 to 3, and then the entry marker. Each marker is digitised and recorded on the CT form, as soon as the slice through that marker has been scanned. The slice through leg marker 1 is rescanned, and its 3D coordinates compared to those from the first scan of that marker. Any discrepancies in the two sets of 3D coordinates indicate that the patient has moved, and therefore the CT scanning procedure has to be repeated. The slice containing the destination point is rescanned, and the previously chosen destination point is 'targeted' with the CT cursor. The position of the CT cursor in relation to the lesion is compared to the previous slice of the destination point, to ensure that no movement occurred during the period between scanning the destination point and the external markers. The duration of a successful scan is less than 15 minutes. Once scanning has been completed, the patient, although he is free to move, is asked to remain on the CT bed.

The CT data is run through the Cape Pointer software to generate the Cape Pointer setting diagram. To minimise incorrect data entry, the data entry software gives the user the option of entering the data twice, and the two data sets are cross checked to ensure that both sets are identical. The 3D CT coordinates of the leg markers are compared to their corresponding 3D coordinates measured in the reflex microscope, using the Rodrigues transformation. The transformation precisions indicate the accuracy with which the leg markers have been coordinated, and any gross discrepancies indicate that markers have either been incorrectly identified, or that data has been incorrectly entered into the software. If the transformation precisions are satisfactory, the setting diagram is printed, and the Cape Pointer set.

The Cape Pointer is placed with its legs on their corresponding markers on the patient's head. The pointer is inserted down the sleeve of the Cape Pointer, until the tip of the pointer touches the scalp. The tip of the pointer should be coincident with the entry marker, if this is

not the case, an error has occurred. The pointer also indicates the lesion's position within the cranium, due to the direction the pointer is pointing in, and the distance the pointer still has to be inserted before the depth stop prevents the pointer being inserted any deeper into the cranium. This serves as a final check for the neurosurgeon. Should the neurosurgeon feel that the pointer is pointing to an illogical position within the cranium, the data entry of the destination point's 3D coordinates should be checked. If this error check reveals no errors, the actual digitising and recording of the 3D coordinates of the destination point must be checked. If this check reveals no errors, the whole procedure should be thoroughly rechecked. In the interest of patient safety, the patient should not leave the CT scan room until the neurosurgeon is satisfied with the setting of the Cape Pointer, even if this requires rescanning of the patient.

Before leaving the CT room, the Cape Pointer is placed on a mounting block. This prevents the Cape Pointer from falling over and allows the medical staff to take the Cape Pointer for autoclaving without actually touching it and thus inadvertently altering any of its settings. The mounting block consists of a 2cm thick plastic block, in which three holes, corresponding to the three legs of the Cape Pointer, have been drilled. Once the Cape Pointer has been placed on the block, with the three legs resting in their respective holes, the Cape Pointer is secure. The material of the block is made of high density polyethylene and is unaffected by the autoclaving.

Both the patient and the Cape Pointer, with its components and computer peripherals, are taken to the theatre suite, the patient to the Pre-op room, and the Cape Pointer and its components for sterilisation.

## 7.6 THE CAPE POINTER PROCEDURE IN THEATRE

The sterilisation of the Cape Pointer and its components has to be done prior to the surgical procedure. It is important that all components are autoclaved, as a missed component can cause up to a 15 minute delay during the surgical procedure, while the forgotten component is sterilised in the autoclave.

The various components that have to be sterilised prior to the surgical procedure are:

- the Cape Pointer and its mounting block
- the Allen key for loosening and tightening clamps on the Cape Pointer
- the perpendicular setting tool
- the long pointer and the depth stop
- the stainless steel ruler for setting the distance on the pointer and on neurosurgical instruments
- the optional guides for altering the diameter of the sleeve of the Cape Pointer allowing for different thicknesses of biopsy and aspiration needles
- the various biopsy and aspiration needles required by the neurosurgeon

Figure 7.5: Using the Cape Pointer setting jig to ensure that the leg markers have remained undisturbed

Once the patient has arrived in theatre, it is vital to check that the markers are still in position on the head. This is done using the Cape Pointer setting jig to confirm that the three leg markers still correspond to the actual positions of the three leg markers (see figure 7.5).

General anaesthesia is administered to the patient, if indicated. Alternatively, the procedure may be performed with sedation and local anaesthesia. Intravenous Decadron and a stat dose of Cefazolin i.m. is administered. Unless there is a specific indication, prophylactic anti-convulsants are not necessary.

In theatre the ball-bearings are removed from the external markers. The small mark, made on the scalp at the centre of each marker (see right marker in figure 7.3), ensures that, if a marker comes adrift during prepping, its position is still discernible. As the entry marker has to be removed prior to making a scalp incision, the entry marker is removed at this point, prior to the scalp being prepped (medical terminology for preparing an area prior to surgery, i.e. sterilising the skin etc.).

The scalp is prepped with a Chlorlexidine/Alcohol solution. A local anaesthetic and vaso-constrictor are infiltrated into the region of the incision. Steritape ("sterile clingfilm") is placed over the whole area to reduce skin movement. The three markers are thus sealed between the steritape and the scalp, thus preventing any infection arising from the markers.

The patient is then draped, and the neurosurgeon dons a sterile gown and gloves. The setting diagram is used to check that the setting of the Cape Pointer has not altered. As the setting diagram is unsterile, it has to be covered by steritape. An unsterile theatre staff member carefully places the setting diagram on a trolley, whose surface has been covered by sterile drapes, making sure that he/she does not make any contact with the trolley surface. The neurosurgeon uses a large sheet of steritape to cover the setting diagram and the trolley surface, without touching the unsterile setting diagram. The whole of the trolley surface is now sterile, and the Cape Pointer can be placed on the setting diagram, to ascertain that the setting has not been altered (see figure 7.6). If the setting has been altered, the Cape Pointer is simply reset using the setting diagram.

Figure 7.6: The setting of the sterile Cape Pointer being checked on the setting diagram covered by steritape.

Due to skin movement after the scalp incisions, tacks were introduced at a very early stage in the patient trials. These tacks are very similar to ordinary drawing pins, with the exception that they are made from stainless steel, the head of the pin has a concave surface and the pins are of varying lengths. The concave surface allows the tip of the Cape Pointer leg to rest securely within the hollow of the tack head, and also prevents the special bit, used for hammering in the tacks, from slipping off the tack. The different length tack pins cater for the varying thicknesses of scalp and cranium from patient to patient, as an adult, for example, has a much thicker scalp and cranium than a small child. In figure 7.7, a tack is being attached through the centre of the external marker, using a surgical hammer and the special bit, both made of stainless steel. The hammer, special bit and the pins are autoclaved with the rest of the Cape Pointer equipment prior to surgery.

Figure 7.7 Attaching the surgical tacks to the patient's head

The scalp incision is preferably made so that it lies in the central area between the three markers and runs through the entry point mark made on the scalp. A small self-retaining retractor (shown subsequently in figure 7.15) is placed in the incision, for easy access to the cranium for the burr hole to be drilled. As the entry point mark has been "destroyed" by the scalp incision, the set Cape Pointer is used to indicate where the trajectory, between the entry point and lesion centre, intersects the cranium. The Cape Pointer is placed on the patient's head, the legs resting on their corresponding leg markers, and the long needle pointer is inserted down the sleeve until it touches the cranium. If the angle of the pointer trajectory to the cranium is close to the perpendicular, the burr hole is drilled at the point indicated by the pointer tip. If the trajectory is fairly acute, the burr hole is offset from that point in the direction of the lesion, to ensure that the final opening into the cranial cavity lies on the trajectory (see figure 7.8).

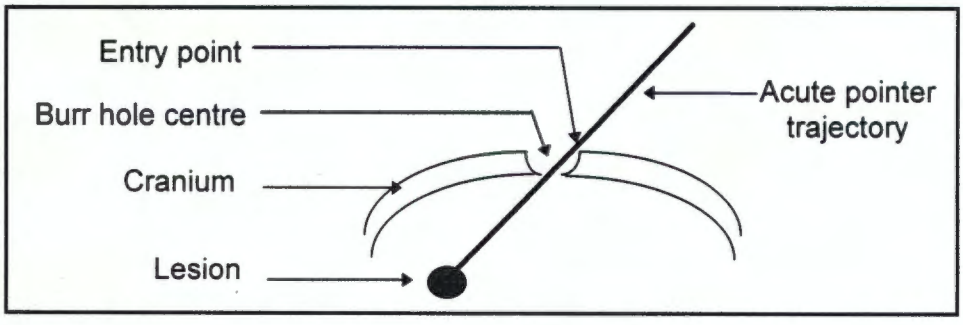


Figure 7.8: Offsetting the burr hole in the direction of the lesion

Once the burr hole has been made, the dura is incised (the dura is the tough outer tissue layer encasing the brain and spinal column). With the aid of the stainless steel ruler, the depth stop is attached to the surgical instrument at the distance specified on the setting diagram. When doing an aspiration, the distance is measured from the tip of the surgical instrument / aspirator. When doing a biopsy, the distance is not measured from the tip of the biopsy needle, but from the centre of the section to contain the biopsied tissue (see figure 7.9). This ensures that the centre of the section to be removed is coincident with the point selected by the neurosurgeon.

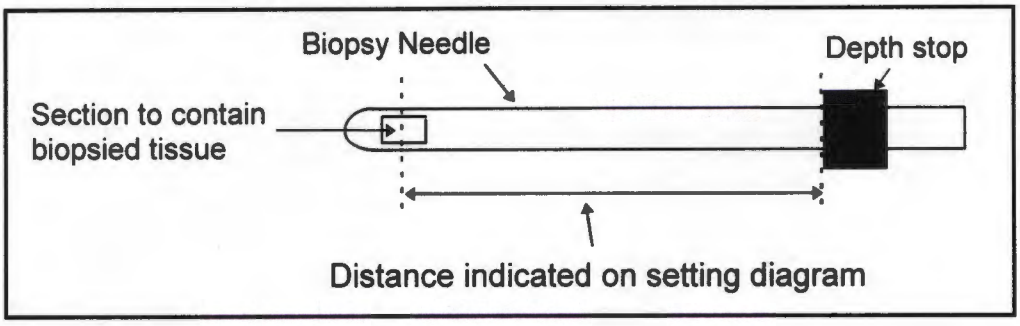


Figure 7.9: Setting the depth stop on a biopsy cannula/needle

The Cape Pointer is placed back on the patient's head, and the surgical instrument inserted down the sleeve to the point where the depth stop prevents the instrument from being inserted any deeper into the cranium. The tip of the surgical instrument is now at the destination point targeted on/in the lesion, and surgical procedure, such as a biopsy, can be performed.

Once the surgical procedure has been completed, the wound is irrigated with saline, haemostasis is established and the scalp closed with interrupted nylon sutures. For post-operative care, the patient should be observed in ICU for at least six hours post-operatively. A follow-up CT scan may be obtained, should this be required.

## 7.7 CHANGES / IMPROVEMENTS IN THE PROCEDURE

### 7.7.1 Overcoming the problems of changing 3D coordinate systems in the CT scanner

One of the problems which became apparent very early on during the patient trials, was that the various scanning protocols on the GSH (Groote Schuur Hospital) CT scanner, had varying coordinate systems. If a patient was scanned in the supine position (face up), the X axis increased from left to right, and when scanned in the prone position the X axis decreased from left to right. Due to medical procedures and ethics, it is not advisable to scan a prone patient with the supine protocol, to ensure that the coordinate system is always the same.

Therefore a fixed 3D coordinate system could not be adopted for the GSH CT scanner. The problem was further exacerbated in that other CT scanners, used in the patient trials, have a variety of different 3D coordinate systems. Therefore the Cape Pointer software had to be amended to ensure that, no matter what coordinate system was used, the results would always be the same.

The amendments made to the setting diagram software are explained in appendix H. A phantom trial was used to test the amended software. The 3D CT coordinate data of the three legs, the entry and lesion point, was utilised in different coordinate formats to ensure that the amended software always yielded the same results and setting diagram. The variations of the 3D coordinate system included the interchanging of the three axes in all possible variations, and changing the signs of the various axes (for example variations from the original data of x,y,z included -x,y,-z, ; y,z,x; -y,z,-x)

### 7.7.2 Allowing for additional entry points without repeating the CT scanning

Since the entry point had to be selected and marked prior to CT scanning, the neurosurgeon was severely restricted if the entry point proved to be unsuitable during surgery. Therefore an additional program was included in the Cape Pointer software to allow a new entry point to be selected, and its 3D coordinates determined, without repeating the CT scan. As the portable Laptop and printer are taken into theatre, it is a simple matter to select a new entry point and generate the new setting diagram in theatre.

The procedure to select a new entry point, and obtain the necessary information for the software to calculate its 3D CT coordinates, is a very simple procedure in keeping with the

rest of the Cape Pointer system. The only restriction is that the new entry point must lie on a trajectory within the mechanical range of the Cape Pointer.

The Cape Pointer is set perpendicular, using the perpendicular setting tool, prior to placing it on the patient's head, so that the Cape Pointer legs rest on their corresponding markers. The long pointer is inserted down the sleeve of the Cape Pointer. The horizontal arm clamp is loosened and the Cape Pointer arm moved until the pointer tip is coincident with the newly selected entry point. The clamp is then tightened. The depth clamp is clamped onto the long pointer, at the point where the pointer exits the top of the Cape Pointer's sleeve, so that the distance from the top of the sleeve to the new entry point can be determined. This is simply done by measuring the distance from the pointer tip to the depth clamp.

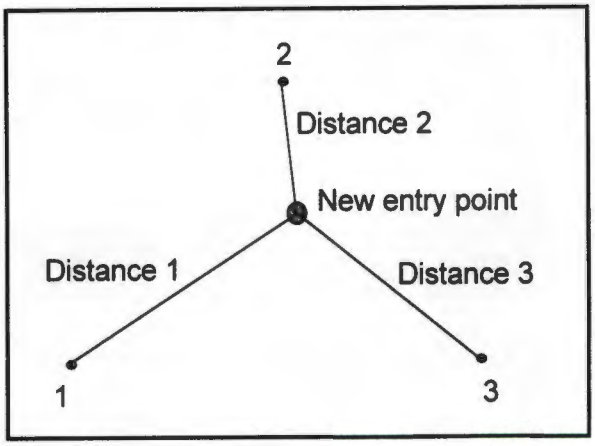


Figure 7.10 : Measuring the distances from the various legs to the projected new entry point on the setting diagram

The Cape Pointer is then placed on the setting diagram, so that each leg rests on its corresponding mark. The pointer, still inserted down the sleeve of the Cape Pointer, is used to make a mark on the setting diagram at the point where the pointer tip touches the diagram. This is the projection of the new entry point onto the setting diagram. The distances from the projected new entry point to each leg point is measured on the setting diagram using a stainless steel ruler (see figure 7.10). With the distances determined from the setting diagram, and the distance measured from the top of the sleeve to the new entry point, the software calculates a new entry point, using various algorithms (see Appendix J). Once the new entry point has been calculated, the new setting diagram can be printed out and the Cape Pointer reset.

### 7.7.3 The Fieggen phantom - An alternative setting procedure

The Fieggen phantom (figure 7.11) was designed and built at the request of the neurosurgeon (after whom it is also named), to aid him in visualising the lesion in relation to the Cape Pointer. Only once the phantom was built, was the realisation made that it could be used to set the Cape Pointer. Setting the Cape Pointer with the phantom is such a simple procedure, that the phantom has superseded the setting diagram. The setting diagram is still retained in the Cape Pointer software package, and can be used to check that the phantom has been set correctly.

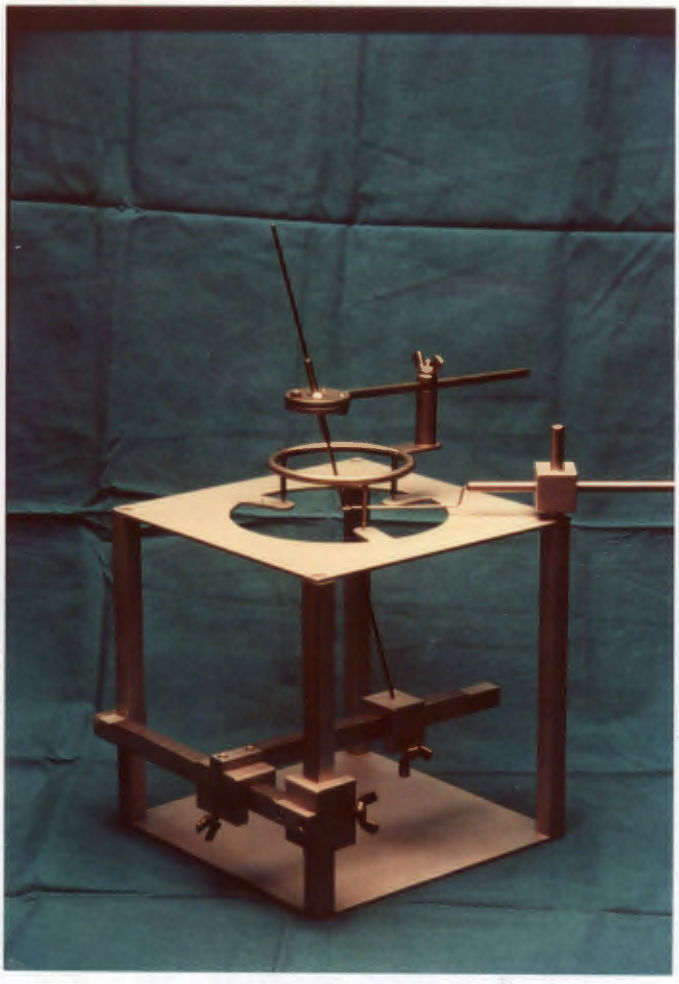

Figure 7.11: The Fieggen phantom

In simple terms the phantom is a mechanical 3D coordinate system, in which a phantom marker represents the actual lesion, and the phantom marker, via X, Y and Z translations can be moved to any position within the phantom's frame. In the upper surface of the phantom's top plate, three grooves have been cut, in which the three legs of the Cape Pointer rest securely. The only criteria for cutting the grooves is that they coincide with the three legs of the Cape Pointer, and that a theoretical line drawn between the grooves for leg 1 and leg 3 is parallel to the X axis of the phantom. Because of these criteria, the setting

diagram coordinate system can be adopted for the Fieggen phantom, that is the 3D coordinates of the three legs are leg 1 = (0,0,0), leg 2 = (cos A * Dist 1, sin A * Dist 1,0) and leg 3 = (Dist 3,0,0), (see figure G.2 in Appendix G).

The X, Y and Z scales, that are attached to the upper surfaces of the two horizontal bars and to one of the upright bars respectively (see figure 7.11), have arbitrary zero position placements. To make the origin of the X, Y and Z scales coincident with the origin of the setting diagram coordinate system, phantom correction factors have to be determined. This calibration is carried out in the reflex metrograph.

The phantom is placed in the metrograph, and the phantom marker set at various positions within the phantom's range. At each new marker position, the X, Y and Z phantom scales are read, and the three leg grooves and the groove representing the centre of the phantom marker are measured in the metrograph system. Utilising the Rodrigues transformation, and the 3D coordinates of the three legs in the setting diagram and metrograph system, the 3D metrograph coordinates of the phantom marker are transformed into the setting diagram system. The resultant X, Y and Z setting diagram coordinates for the phantom marker are compared to the readings from the X, Y and Z scales - the differences in X, Y and Z coordinates are the phantom corrections to be applied to the X, Y and Z scales. This procedure is repeated for each phantom marker position within the phantom's range and mean phantom corrections, for the X, Y and Z coordinates, are computed.

To utilise the Fieggen phantom to set the Cape Pointer, prior to use in theatre, the 3D CT coordinates of the three leg markers and the lesion centre are transformed into the setting diagram coordinate system using part of the setting diagram software. The X, Y and Z phantom corrections are applied to the 3D setting diagram coordinates of the lesion centre, and the resultant X, Y and Z values (phantom marker coordinates) are used to position the phantom marker within the Fieggen phantom. The phantom marker is clamped in position, and the Fieggen phantom can now be utilised to set the Cape Pointer (see figure 7.11). The Cape Pointer is simply placed on the Fieggen phantom, so that the three legs rest in their respective grooves. With all the Cape Pointer clamps loosened, the long pointer needle is inserted down the sleeve, and the needle moved until the pointer tip rests in the phantom marker. A whole range of approaches/trajectories are possible by moving the Cape Pointer's horizontal arm and ball and socket joint. Once the tip rests in the phantom marker groove, the Cape Pointer clamps are tightened and the Cape Pointer is set.

From the neurosurgeon's aspect, he simply enters the CT data into the software, and utilises the phantom marker coordinates, calculated by the software, to set the phantom marker on

the Fieggen phantom. The Cape Pointer is then set using the Fieggen phantom, and is ready for theatre. The Fieggen phantom, along with the Cape Pointer and other accessories, is sterilised in the autoclave. For this reason the Fieggen phantom is made of materials that can withstand autoclaving, and consists of stainless steel, anodised aluminium, and high density polyethylene.

In theatre, just prior to using the Cape Pointer, the Cape Pointer setting is checked using the Fieggen phantom. The pointer needle is inserted down the sleeve until its tip rests in the phantom marker groove. The clamp is attached to the pointer at the top of the sleeve. The distance from the pointer tip to the clamp is the distance that has to be set on the surgical instrument. Alternately, the surgical instrument can be inserted into the sleeve of the Cape Pointer and the clamp attached directly to the instrument. The surgical procedure can now be performed.

#### 7.7.3.1 The accuracy of setting the Cape Pointer with the Fieggen phantom

The ring phantom (figure 7.2) was used to ascertain how accurately the Cape Pointer could be set using the Fieggen phantom. 3D Phantom lesion coordinates were calculated for the 11 lesion markers on the ring phantom, using the CT scan data of the ring phantom. The phantom marker was set on each of the 3D phantom lesion coordinates. At each new setting, the Cape Pointer was placed on the Fieggen phantom, and the long needle pointer used to set the Cape Pointer, so that the pointer tip coincided with the centre of the phantom marker. The depth clamp was attached to the pointer, where it entered the top of the sleeve of the Cape Pointer, to set the distance that the pointer needed to be inserted down the sleeve.

The Cape Pointer was then placed on the ring phantom, with the three legs corresponding to the three markers. The pointer was inserted down the sleeve, until the depth clamp prevented it from being inserted any further. The pointer tip position was "recorded" by making an impression in soft putty, placed on the ring phantom. Once this procedure had been repeated for all 11 markers, the 3D coordinates of the lesion markers and their corresponding putty indentations were measured in the reflex microscope. The comparison of 3D coordinates of the actual markers and the corresponding putty indentations are listed in table 7.4. The vector differences are the actual distances between the lesion markers and their corresponding putty indentations.

| Marker No. | Difference in X (mm) | Difference in Y (mm) | Difference in Z (mm) | Vector difference (mm) |
|---|---|---|---|---|
| 1 | -0.6 | +0.4 | -1.4 | 1.6 |
| 2 | +1.0 | +0.0 | -1.6 | 1.8 |
| 3 | +0.9 | -0.2 | -1.8 | 2.1 |
| 4 | +0.7 | +0.5 | -0.7 | 1.1 |
| 5 | +1.0 | -0.1 | -1.5 | 1.8 |
| 6 | +1.5 | +0.2 | -1.0 | 1.8 |
| 7 | +1.0 | +0.5 | -1.3 | 1.7 |
| 8 | +0.9 | +0.9 | -1.3 | 1.8 |
| 9 | +0.7 | -0.7 | -2.3 | 2.5 |
| 10 | +0.4 | -1.4 | -0.9 | 1.7 |
| 11 | +1.6 | +0.4 | -2.0 | 2.6 |
| **Mean Values** | | | | |
| | +0.8 | +0.1 | -1.4 | 1.9 |
| **Standard Deviations** | | | | |
| | 0.6 | 0.1 | 0.4 | 0.6 |

Table 7.4: Accuracy evaluation of setting the Cape Pointer with the Fieggen phantom

From table 7.4, the mean vector difference/error for reaching a lesion marker is 1.9mm, with a standard deviation of 0.6mm, with the greatest vector error of 2.6mm.

Galloway et al (1991) did an independent accuracy assessment on four commonly used stereotactic systems - the Leksell , the BRW, the CRW and the Kelly-Goerss systems. The aim was to determine the application performance, that is the ability of the stereotactic device to accurately find a point in space, whereas most manufacturers only supply the mechanical accuracy of their stereotactic devices. This is due to the fact that the mechanical accuracy is the best accuracy that the device can achieve, and application accuracy is dependent on imaging medium factors, which are beyond the control of the manufactures.

The assessment of the four stereotactic systems was also done with a phantom, which contained radio-opaque markers scattered over the phantom's whole area. Each trial was run following the same protocol that would be used, if the phantom was a patient. The quoted accuracies from Galloway et al only include the images taken at a slice thickness of 1mm, as this is very similar to the tests run on the Cape Pointer. The other trials conducted by Galloway et al included imaging at a slice thickness of 1mm, with the CT gantry canted, and imaging at slice thicknesses of 4 and 8mm. The values in table 7.5 are quoted from the table in Galloway et al, and the mean error given in table 7.5 is the vector between the actual point and the point located by the stereotactic system.

| For CT slice thickness of 1mm | BRW (mm) | CRW (mm) | Kelly-Goerss (mm) | Leksell (mm) |
|---|---|---|---|---|
| Mean error | 1.9 | 1.8 | 1.0 | 1.7 |
| Std. Dev. | 1.0 | 1.1 | 0.6 | 1.0 |
| Maximum error value | 5.0 | 4.9 | 3.1 | 4.5 |
| 95% confidence interval | 4.8 | 5.1 | 2.7 | 4.6 |

Table 7.5: The performances of four stereotactic systems, using 1mm CT slice thicknesses (from Galloway et al, 1991)

As can be seen from table 7.5, the mean error of 1.9mm and a standard deviation of 0.6mm for the Cape Pointer, agrees well with other much more sophisticated stereotactic devices. The reason for including the maximum value and the 95% confidence interval from Galloway et al, is that for their independent assessment Galloway et al made 7681 independent measurements. It is therefore conceivable that if one were to make a similar assessment of the Cape Pointer, that the maximum values could also be in the range of those listed in table 7.5.

#### 7.7.3.2 Transferring selected entry points to the Fieggen phantom

When using the Fieggen phantom to set the Cape Pointer, an entry point no longer has to be selected prior to CT scanning. An entry point, selected in theatre, can be transferred to the Fieggen phantom, using the Cape Pointer and the Fieggen phantom's entry point simulation device (see figure 7.12).

The entry point simulation device consists of a metal arm ending in a small metal loop, simulating the entry point. The metal arm is attached via a metal block to a vertical pin, which in turn is attached to the upper plane of the Fieggen phantom. By loosening the clamp on the metal block, the arm can be raised and lowered, swivelled about the vertical pin, and the metal arm extended or protracted. The simulated entry point can thus be moved to any feasible entry point in the range of the Cape Pointer. To be able to reach an entry point below the plane of the Cape Pointer's three legs, for example the opening of the burr hole into the cranial cavity (i.e. just above the dura lining the brain), the metal arm has been bent, to allow the simulated entry point to be lowered below the top plane of the Fieggen phantom.

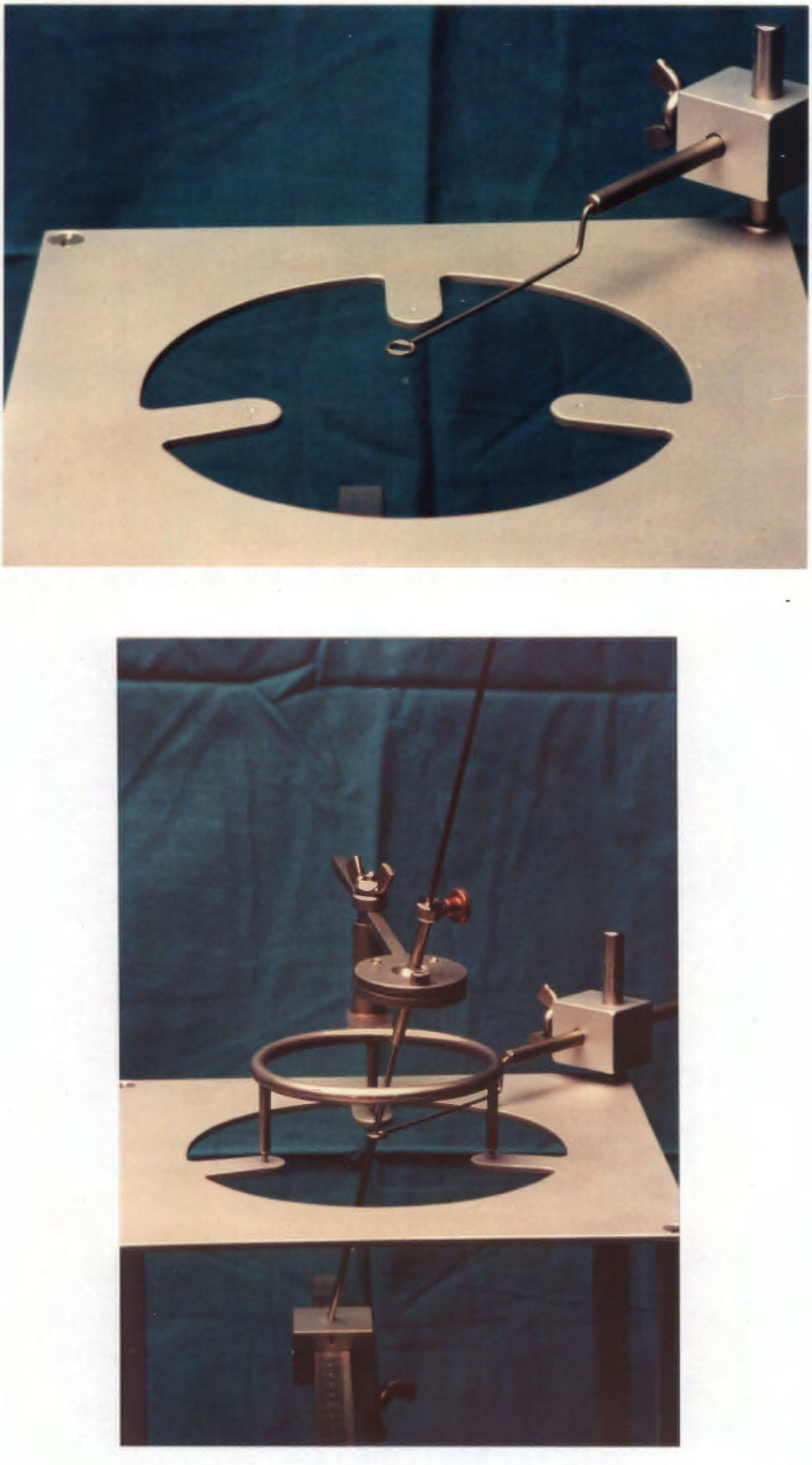

Figure 7.12: a - the entry point simulation device on the Fieggen phantom
b - using the device to set the Cape Pointer on the Fieggen phantom

To set the simulated entry point, the Cape Pointer is placed on the patient's head, with its three legs resting on its corresponding markers. The ball and socket joint is loosened and the long needle pointer, inserted into the Cape Pointer's sleeve, moved until the pointer tip rests on the entry point. The clamp of the ball and socket joint is tightened and the depth clamp attached to the needle pointer, where the needle exits the sleeve. The Cape Pointer, without removing the needle pointer, is placed on the Fieggen phantom and the simulated entry point moved until the tip of the pointer lies within the centre of the loop.

All the clamps on the Cape Pointer can now be loosened and the needle pointer positioned, so that it passes through the entry point loop and its tip comes to rest in the phantom marker groove. Once the clamps have been tightened, the Cape Pointer is set and ready for the surgical procedure.

### 7.7.4 An alternative method of attaching the external markers to the scalp

Skin movement remained problematic even though the tacks had been introduced, as these only solved the skin movement problems in theatre. Some skin movement may however occur during the CT scanning phase. To overcome this problem a more secure attachment of markers had to be developed, which would ensure that markers would remain in place from the CT scanning procedure until the operation had been completed.

Figure 7.13: The Taylor halo attached to the patient's cranium

For this purpose, one of the neurosurgeons suggested placing the markers in a single unit and attaching this to the patient's head. The lightweight, 10 cm diameter polycarbonate halo (see figure 7.13), containing the three markers (radio-opaque ball-bearings) corresponding to the positions of the three legs of the Cape Pointer, has been named after the neurosurgeon. The advantages of using the Taylor halo are that the relationship between the three markers in the halo is always constant, and that the halo does not move relative to the patient's head.

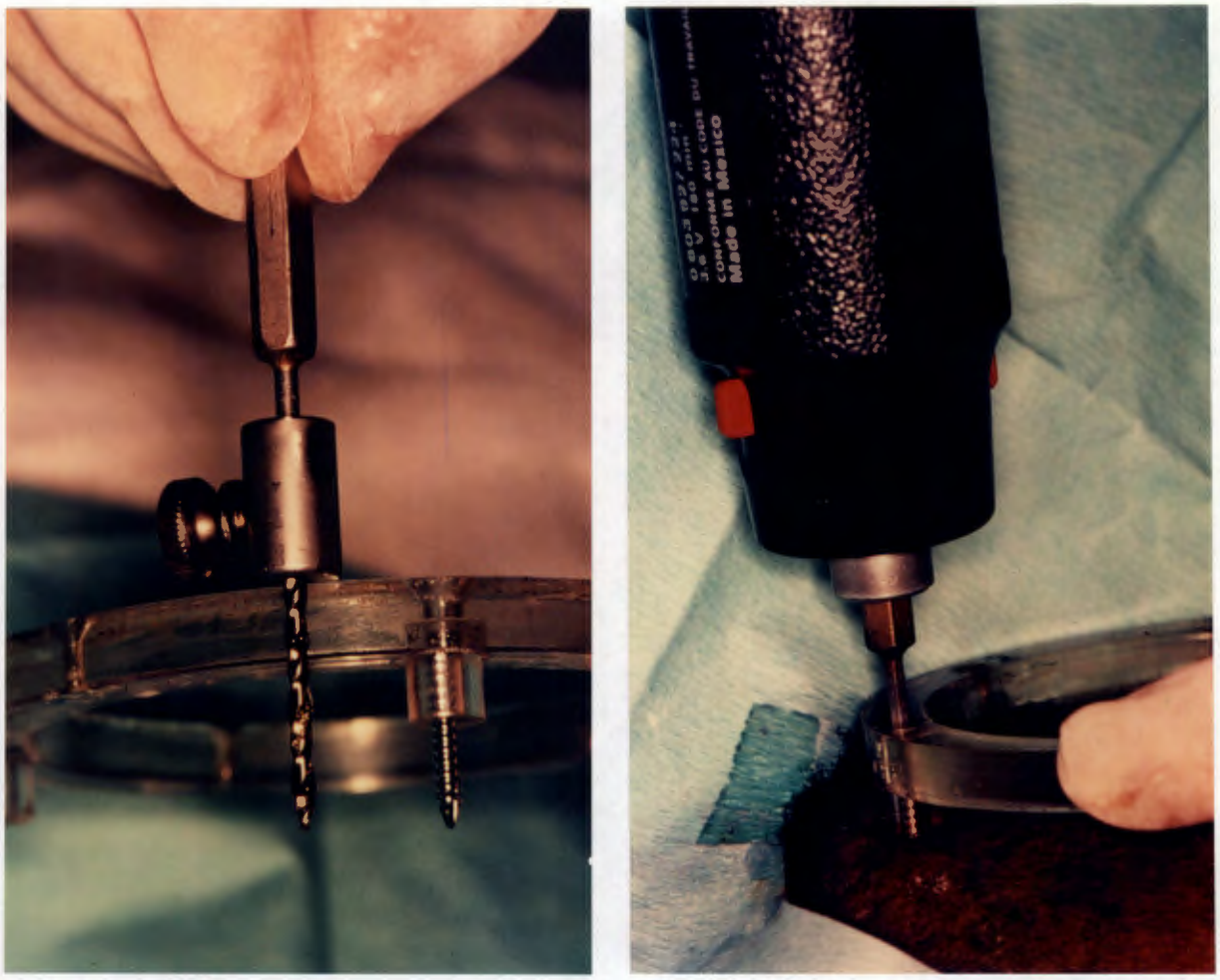


Figure 7.14: a - The stainless steel adapters and b - the battery operated screw driver for the Taylor halo attachment

Initially, the halo was attached to the patient's cranium, with two small self-tapping surgical screws, under local anaesthetic (see figure 7.14a). The screws were screwed into the cranium with a battery operated screw driver (see figure 7.14b). Special stainless steel adapters ensured that the screws did not penetrate the cranial cavity, but only penetrated the cranium just far enough to ensure that the halo was secure. The halo is now more commonly attached to the scalp by 4 x 2/0 silk sutures, which is a far easier procedure for both attachment and removal of the halo.

To be able to utilise the Cape Pointer with MRI at a later date, only the Taylor halo has to be adapted, as it is the only part of the Cape Pointer system to be used during the imaging procedure. By replacing the ball-bearing markers in the halo with a mixture of jopamidol and copper sulphate in a ratio of 1:1, the external markers would be visible to both CT and MRI (Alesch, 1994). If the halo is to be attached to the patient's head with screws, they should consist of material, such as titanium, which will cause no artefacts on the MRI images.

In theatre the whole scalp area, including the halo, is covered with steritape prior to any surgical procedure, to ensure sterile conditions. When using the halo, the scalp incision is preferably made in the centre of the halo (the scalp incision line is marked by a big black cross on the patient's scalp, see figure 7.13). Once the incision is made and the retractor placed, the burr hole can be made and the dura incised (see figure 7.15).

Figure 7.15: The self-retaining retractor allows easy access to the burr hole in the cranium

The Cape Pointer is placed on the halo, with the three legs resting on their corresponding markers. The location of the dural incision is translated to the Fieggen phantom, using the Cape Pointer and the Fieggen phantom's entry point simulation device. With the Cape Pointer still placed on the Fieggen phantom, the correct trajectory to the phantom marker is set - i.e. the long needle pointer is passed through the simulated entry point until its tip rests in the phantom marker groove. The pointer is replaced with the surgical instrument, and the depth clamp attached to the instrument at the top of the Cape Pointer's sleeve.

The Cape Pointer is replaced on the Taylor halo, ensuring that the legs are placed on their corresponding markers. The surgical instrument is inserted down the Cape Pointer's sleeve until the depth clamp prevents the instrument form being inserted any deeper into the cranium. The surgical procedure can now be completed (figure 7.16).

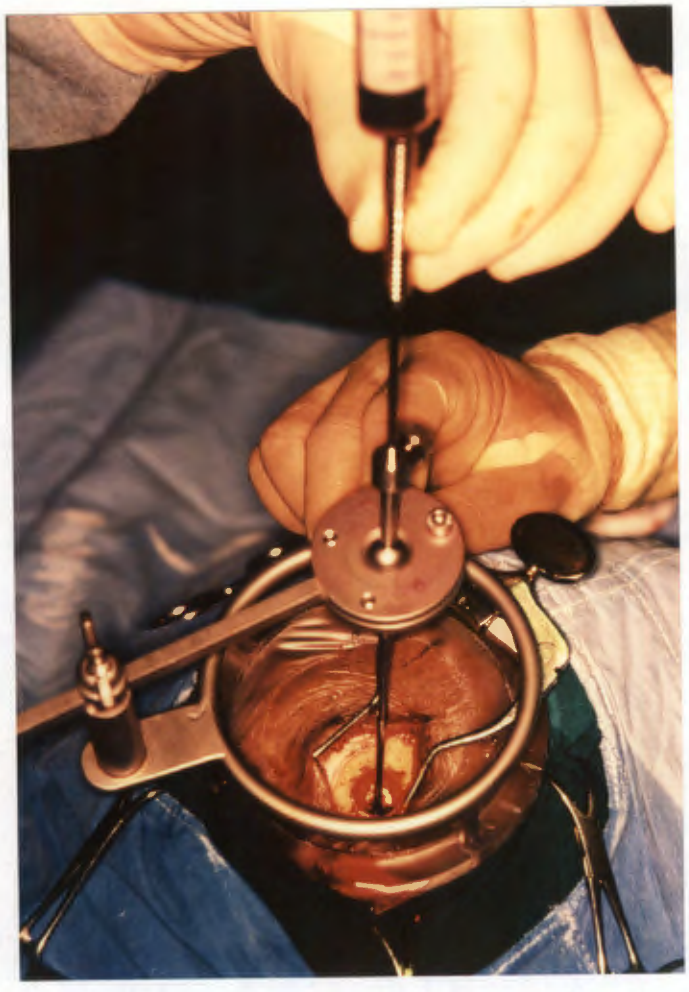

Figure 7.16: An abscess aspiration, with the Cape Pointer positioned on the Taylor halo

The Cape Pointer, in its present format, is well suited for carrying out biopsies of intracranial lesions, the evacuation of fluids from cysts, abscesses, and hematomas, and for some functional stereotactic procedures. Even though the Cape Pointer can be used to indicate the position of the intracranial lesion prior to an open craniotomy, the area within the Taylor halo is far to small for the surgical procedure required. It has been suggested that a Taylor halo consisting of two sections be used. By attaching the two small screws in one section of the Taylor halo, the other section of the Taylor halo could simply be removed. The only criteria would be that the removed section could be exactly replaced when the Cape Pointer was needed to guide the surgical instrument. This procedure would give the neurosurgeon the required space to perform the open craniotomy.

## 7.8 PATIENT PROCEDURES PERFORMED TO DATE

From June 1994 to November 1996, 40 patient procedures have been performed successfully. The oldest patient was 70 years old, and the youngest a 3 month old infant. The only complication, arising from the procedures, was a local wound sepsis in one patient, who had a brain abscess stereotactically aspirated. A summary of the procedures is listed in table 7.6.

| | |
|---|---|
| **BIOPSY** | |
| Glioma | 12 |
| Metastasis | 11 |
| Inflammatory | 3 |
| Non-diagnostic | 4 |
| **Aspiration** | |
| Abscess | 5 |
| Tumour cyst | 1 |
| **Catheter Insertion** | |
| Craniopharyngioma | 2 |
| Quadrigeminal plate cyst | 2 |

Table 7.6: Patient procedures completed thus far

Of the 30 biopsies performed, the most frequent diagnoses have been gliomas followed by metastases. Gliomas (glia=glue, oma=tumour) are neoplasms derived from various types of cells that support the neurons of the brain. A neoplasm, according to the Stedman's Medical Dictionary (Stedman, 1982) is defined as: "new growth; tumour; an abnormal tissue that grows by cellular proliferation more rapidly than normal and continues to grow after the stimuli that initiated the new growth cease. Neoplasms show partial or complete lack of structural organisation and functional coordination with the normal tissue and usually form a distinct mass of tissue which may be either benign or malignant". Metastasis is when disease moves from one point of the body to another. This often occurs in cancer, where the cranial neoplasm is a secondary tumour, and cancer cells have been carried via the blood vessels or the lymphatics to the cranium from the primary tumour, located in a remote body part.

Specific inflammatory diseases were diagnosed in 3 of the biopsy cases. For example, in one patient the inflammation was due to an infection knows as actinomycosis, which arises from bacteraemia, the transient presence of bacteria or other micro-organisms in the blood (Stedman, 1982). Four of the earlier biopsy cases yielded abnormal tissue, but no diagnosis of the tissue could be made on histological examination by the pathologist.

For two of the biopsy cases, silastic catheters were placed in position within the cranium. A catheter is a small sterile rubber tube, normally meant for the passage of fluid. The one end, with the aid of the catheter needle, was placed at the centre of the lesion, while the other end was cut off just below the level of the burr hole. At the subsequent craniotomy, the catheter was followed from the site of the burr hole to the small subcortical lesion, which was then excised. This is of particular value when the lesion is small and therefore not visible on the surface of the brain. The catheter, after it has been followed to the tumour, is discarded.

Six aspirations were performed, five for abscesses and one for a tumour cyst. An abscess, as described by Stedman's Medical Dictionary (Stedman, 1982), "is a circumscribed collection of pus appearing in acute or chronic, localised infection, and associated with tissue destruction and, frequently, swelling". The pus is removed from the abscess with an aspiration needle and syringe, as can be seen in figure 7.16. A cyst is an abnormal sac, with a membranous lining, which is filled with fluid, gas or semisolid material. The same procedure for removing the pus from the abscess is followed for removing the fluid from the cyst.

Four permanent catheter insertions were performed, two for craniopharyngioma and two for quadrigeminal plate cysts, as was the case for the 3 month old infant. A craniopharyngioma is a neoplasm, which is usually cystic and develops from the nests of epithelium derived from Rathke's pouch, which is the rudiment of the anterior lobe of the hypophysis (Stedman, 1982). A quadrigeminal plate cyst is a cyst found in the region of the pineal body, and is most probably the encystment of the quadrigeminal plate cistern; encystment being the condition of becoming encapsulated by a membranous bag (Till, 1975). These cysts, when they become enlarged, compress the 3rd ventricle or aqueduct, and due to the enlargement of the cerebrospinal fluid pathways, increase intracranial pressure and give rise to hydrocephalus. The catheters were placed either for brachytherapy or shunting purposes.

For brachytherapy, the one end of the catheter is inserted into the centre of the lesion, while the other end is cut off just above the burr hole. A reservoir, a small chamber covered by a silicone rubber membrane, is attached to the end of the catheter above the burr hole. The reservoir is covered by the scalp after the procedure and can remain there indefinitely. At any stage after the procedure, chemotherapeutic drugs can be injected through the scalp into the reservoir, from where they filter down the catheter directly into the lesion, i.e. directly treating the lesion and minimising damage to the surrounding tissue.

For the shunting procedures, the one end of the catheter is placed within the cyst. The other catheter end is cut off just above the burr hole and a small L tube attached. A second catheter is attached to the other end of the L tube, and fed beneath the skin from the scalp to the skin overlying the abdominal area. From here the catheter is surgically inserted into the peritoneal cavity, a membranous sac which lines the abdominal cavity and covers most of the viscera contained therein. The catheter normally remains in place for the duration of the patient's life, diverting the excess fluid from the brain to the abdominal area, where it can be reabsorbed by the body.

## 7.9 CONCLUSIONS

The development of the Cape Pointer would never have progressed from the drawing board, without the support of the neurosurgeons, whose enthusiasm and design input was present from the very start of the project to its completion. The result is a simple system that can be used by a single neurosurgeon, with the assistance of a CT radiographer and a scrub nurse.

Although one frequently reads about submillimetre mechanical accuracy, it is the application accuracy by which a stereotactic system should be evaluated. The mean error of 1.9mm and standard deviation of 0.6mm for the Cape Pointer, compare well with those of widely-used stereotactic frame-based systems (Galloway et al, 1991).

The Cape Pointer, in conjunction with the Fieggen phantom and Taylor halo, is a simple, yet effective and accurate stereotactic system. The Taylor halo, in comparison to other external reference systems/frames is very light and the procedure for attaching it to the scalp is far less invasive, and patient discomfort is minimal.

Only 4 points have to be coordinated in the CT scanner - the three markers corresponding to the Cape Pointer legs, and the point selected on/in the lesion. The CT procedure therefore is short and takes approximately 10 - 15 minutes. No understanding of the software is required - at the software prompts the 3D coordinates are simply entered into the software and the setting diagram, as well as the coordinates for setting the phantom marker on the Fieggen phantom, are produced. If necessary the setting of the Fieggen phantom can be checked, using the Cape Pointer that has been set on the setting diagram.

An entry point does not have to be selected prior to CT scanning, and any entry point, within the mechanical range of the Cape Pointer and the Fieggen phantom, can be selected at any time prior to the actual surgery. As it is a simple procedure for the neurosurgeon to reset the

Cape Pointer for additional lesion points using the Fieggen phantom, additional lesion points can be coordinated during the CT procedure and its phantom marker coordinates calculated - ready for setting on the Fieggen phantom in theatre.

From the 40 patient procedures so far completed, it has been shown that the surgical procedures have been accomplished safely and effectively. One of the neurosurgeon's comments sums up the Cape Pointer's qualities in a nutshell, "It is so easy to use, that even a neurosurgeon can use it".

# CHAPTER 8 A REVIEW OF INTERACTIVE IMAGE-GUIDED NEUROSURGICAL SYSTEMS

## 8.1 INTRODUCTION

Once the Cape Pointer had been designed, the neurosurgeons from Groote Schuur Hospital asked about the possibility of designing a system, that could aid them during an open craniotomy to accurately identify points within the cranium on the CT slices of the patient. The removal of an intracranial lesion, which is visible on the CT slices, would be simplified, if the exact position at which the neurosurgeon was working could be identified on the appropriate CT slice. This would aid the neurosurgeon in removing the whole of the lesion, which is essential in cases where the lesion is carcinogenic.

A number of very sophisticated interactive image-guided neurosurgical systems are already available commercially. The reason for designing a local system, instead of purchasing one of the commercial systems, is a matter of cost. Due to the changes that are occurring in South Africa, money available to the Ministry of Health is mainly channelled into primary health care. Therefore, funding for new neurosurgical equipment, for example, is in extremely short supply, and the poor foreign exchange rate has made the purchase of commercial products from overseas a very expensive business. Therefore, the only way to obtain such a neurosurgical system is to design one locally. The other reason for designing a local system, is to produce a relatively inexpensive system with "off the shelf" components; should the system prove to be successful, it could be adapted for use in other neurosurgical units in South African hospitals.

The simplest, and cheapest, solution for designing the neurosurgical aid system (NSA system) requested by the neurosurgeons, was to make use of equipment that was already available. Therefore, the SPG system equipment was re-utilised for the NSA system, that is making use of the CCD cameras, the image mixer, the Philips monitor and the PC with the IP8 image frame grabber card. Before embarking on the design of the new system, an investigation was carried out into the literature covering existing interactive image-guided neurosurgical systems.

The most comprehensive literature on this subject is a textbook published by the American Association of Neurological Surgeons called "Interactive Image-Guided Neurosurgery" (Maciunas, 1993). Another good source of information is the Journal of Stereotactic and Functional Neurosurgery, published by the World Society of Stereotactic and Functional Neurosurgery. From these and other sources it became clear that the literature covering

image-guided neurosurgery was fairly large and that numerous different types of neurosurgical systems had been designed from approximately 1990 onwards. The neurosurgical systems all have a common goal of assisting the neurosurgeon in reaching specific point within the brain, by making use of CT images of the patient's brain for example. By attaching external markers either directly to the patient's head or via a stereotactic frame, the 3D relationship between the external markers and the scanned images can be established. By using a 3D measuring system in theatre, the external markers can be coordinated. Using a variety of different 3D transformations, the geometrical relationship between the theatre and imaging system is established. Thereafter, any intracranial point that is 'marked' by the neurosurgeon and coordinated by the 3D measuring system can be identified and displayed on softcopies of the scanned images nearly instantaneously, using computer systems with image processing capabilities. At any given point in time during the surgical procedure, the neurosurgeon now knows exactly where he is working within the patient's brain. With minimal disturbance to the brain the neurosurgeon can now, for example, remove a lesion that may be indistinguishable from normal brain tissue when seen with the naked eye, but will show up clearly on CT and MRI (magnetic resonance images).

## 8.2 THE COMPONENTS OF TYPICAL NEUROSURGICAL SYSTEMS

The different neurosurgical systems have a variety of different components, that distinguish one system from another. Some of these components are:

1. The type of images that are used: these are CT, MRI, angiography etc.; some systems use both CT and MRI for example, as CT gives better geometrical/3D results and MRI produce superior images of the brain.

2. The type of computer hardware used ranges from PCs to Sun workstations.

3. The level of image processing capabilities - this ranges from registering the intracranial point on the scanned image, to a comprehensive 3D model of the patient's head and brain built up from the scanned images, where the 3D model can be viewed from any conceivable angle and from any viewpoint, even a viewpoint that falls within the brain itself. Some very sophisticated systems display the outline of the lesion into the line of sight of the neurosurgeon in the operating microscope used in open craniotomies.

4. The manner of attaching the external markers to the patient - either directly to the scalp or via some type of structure attached to the head, such as a stereotactic frame.

5. The software - some software options in the different systems include planning procedures prior to the operation, navigational assistance during the surgical procedure, i.e. assisting the neurosurgeon in following the optimal route to the lesion, etc.

6. The type of 3D measuring system used to determine the 3D coordinates of external markers and intracranial points. What all 3D measuring systems have in common, is that some sort of pointer has to be employed, so that the neurosurgeon can point to (mark) the intracranial point he wishes to identify on the scanned images.

The 3D measuring system is critical to interactive image-guided neurosurgical systems, as without it the relationship between the scanned images and the patient's head can not be established. Also, the accuracy of the neurosurgical system is not only dependent on the measuring accuracy of the imaging system employed (for example, CT images), but also on

the accuracy of the 3D measuring system. Therefore the type of 3D measuring system, employed by the neurosurgical system, has been used to structure the literature review for the NSA system. The computing hardware, and image processing hard and software, are at a fairly basic level in the NSA system at present, and do not pretend to compete with their much more sophisticated counterparts; the author however feels that the NSA system delivers value for the time and money spent on it. The NSA system only makes use of CT images, as that is all that is readily available at the GSH hospital. As the NSA system will most probably be used in conjunction with the Cape Pointer, the external marker attachments used for the Cape Pointer are also used for the NSA system.

## 8.3 TYPICAL 3D MEASURING SYSTEMS USED IN NEUROSURGICAL SYSTEMS

The 3D measuring systems, used in neurosurgical systems, can be classified into two broad groups - those systems that require a mechanical link between the pointer and the neurosurgical system, and those that don't. The mechanically linked systems usually consist of jointed robotic arms, where angle detectors, located in the joints, are used to determine the 3D position of the arm's tip in space. Two such systems are the PUMA 200 industrial robot-based system (Westinghouse Electric, Pittsburgh, PA, United States of America (USA)) and the ISG viewing wand (ISG Technologies, Toronto, Canada) (Drake et al, 1993). Although these mechanical systems produce the necessary accuracy (standard deviations in position of +/- 0.7mm for both the PUMA and ISG system, and observed position errors of less than 2mm (Drake et al, 1993)), they are very bulky to use and, due to the sophisticated robotics hardware, are also very expensive.

The non-linked 3D measuring systems are much more common, and either utilise magnetic, sonic or optical emissions to coordinate points in 3D space. Magnetic 3D measuring systems impose a magnetic field over the working area, i.e. the area to be occupied by the patient's head. The 3D position of a probe tip is determined by the fact that the probe can detect gradients in the magnetic field. The advantage of such a system is that the magnetic field penetrates the body, and therefore no clear line of sound or sight is required, as is the case for the sonic and optical 3D measuring systems. The magnetic field digitiser, described by Manwaring (1993) has been shown to be accurate to within 2mm of the exact location. The drawback to such systems is that they require a precise magnetic field, and ferromagnetic substances and noise impinge adversely on the magnetic field (Bucholz et al, 1993). These systems are seldom used in neurosurgical systems, due to the problems experienced with them.

The sonic and optical systems both have some drawbacks. A clear line of sound is required between the emitters and microphones for the sonic systems, and a clear line of sight is required between the light-sources and the camera array. In sonic systems the speed of sound is used to determine the distances between emitter and microphones, and in optical systems angles between light-source and cameras' optical sensors are determined; the distances and angles in the sonic and optical systems respectively are utilised to determine the 3D position of the emitter/light source in space.

As the pointer tip is invariably hidden within the patient's cranium in both sonic and optical systems, a minimum of two emitters/light-sources have to be attached to the pointer shaft/handle (see figure 8.1). As the 3D measuring system can determine the position of the

emitters/light-sources, and the geometrical relationship between the emitters/light-sources and the pointer tip is known, the position of the tip can be calculated. When using only two emitters/light sources, the emitters/light sources and the pointer tip all have to lie on a straight line, and three dimensional vector geometry is employed to determine the position of the tip from the positions of the two emitters/light-sources.

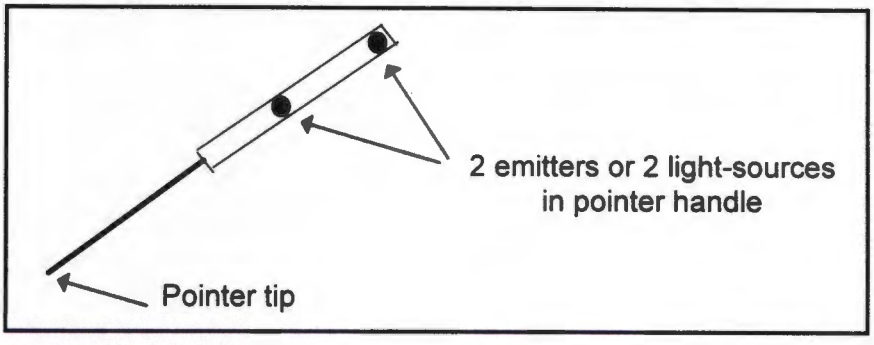


Figure 8.1: Positioning of 2 emitters/light-sources on a pointer

Other drawbacks of the sonic systems are that the speed of sound is effected by temperature gradients, and that emitter sounds, that have bounced off walls and other smooth surfaces, may be measured, both resulting in incorrect distances being calculated (Bucholz et al, 1993). The first problem can be overcome by measuring a known distance, just prior to the surgical procedure, to determine correction factors for temperature gradients; the second problem can be overcome by slowing the firing rate of the emitters (Bucholz et al, 1993). Three examples of sonic systems are listed below:

1. The sonic 3D measuring system, designed by Horstmann et al (1994), makes use of a ranging panel with built in ultrasound emitters, fastened to a head-holder ring during surgery and an ultrasound receiving unit in the pointer handle. The accuracy vector in space was 0.9mm with a standard deviation of 0.6mm (hereafter using the nomenclature of 0.9mm+/-0.6mm), determined by measuring 2312 points on an accurate measuring device. Only laboratory testing was done; no testing was done on points where their 3D coordinates were obtained from CT slices. Comments on the technical paper, made by R.D. Bucholz of ST. Louis, Missouri, were to caution about the pit falls in sonic systems, i.e. temperature gradients to be found in theatre, echoes, and also the ability of the costly emitters in the pointer handle to withstand sterilisation.

2. The sonic 3D measuring system (Model GP8-3D), utilised by Barnett et al (1993a), and manufactured by Science Accessories Corp., Connecticut, USA, utilises ultrasonic pulses produced by two emitters on the pointer. These pulses are detected by an array of four microphones, each microphone is placed at a corner of a square frame, which is mounted at an oblique angle above the operating table. The measurement accuracy of this 3D measuring system is 1.1mm+/-1.0mm, determined from 24 distances measured within a cube of 1000cm$^3$. In five patients, an external marker, that was not used for the 3D transformation procedure, was measured and compared to the CT coordinates obtained from 1mm thick CT slices. The mean linear error was 1.5mm+/-0.7mm. Another paper by Barnett et al (1993b) describes 48 patient procedures using the system.

3. The sonic digitising microscope, described by Roberts et al (1993), also makes use of the same sonic digitiser as Barnett et al (1993a, 1993b), that is the Model GP8-3D by Science Accessories Corp., to position and orientate the operating microscope. The digitiser was tested on its own, prior to use with the microscope, and vector errors of 1.2mm+/-0.4mm were obtained from measuring various test points inscribed on plexiglas phantoms. After the phantoms had been scanned using 1.5mm thick CT slices, vector errors in locating a point on the phantom were 2.0mm+/-0.5mm.

   Various images can be superimposed on the surgical field through the microscope - quoting from Roberts et al (1993) "Prior to making an incision, the surgeon may view the scalp through the microscope and see a contour representing the outline of an object of interest deep to the focal plane (such as that of a tumour) in the correct location, orientation, and scale." The error in locating a point on a phantom on which the microscope was focused, was 1.7mm+/-0.9mm when compared to the CT coordinates obtained from 1.5mm thick CT slices. During clinical use, the error in determining the position of a test point in 17 patient cases was 3.4mm+/-1.8mm when compared to the CT coordinates.

It was interesting to note, that Roberts et al (1993) like many other authors, found that the goal of 1mm accuracy - historically cited as the accuracy that is supposedly obtainable for conventional frame-based systems, was unrealistic. That this accuracy is unrealistic, has been confirmed by Galloway et al (1991), who made an independent assessment of four

well-known stereotactic frame-based systems - the BRW, CRW, Kelly-Goerss and Leksell systems.

Before embarking on the literature concerned with the optical 3D measuring systems, the systems that make use of conventional stereotactic frames to obtain the necessary 3D information, have to be described. Two examples of such systems are listed here:

1. The first system is described by Gildenberg et al (1994), where the authors make use of the CRW stereotactic frame. An endoscope is externally mounted on the CRW arc. As the position and angular setting of the arc are known, the endoscope images can accurately be related to the computer-generated image obtained from CT, MRI or angiography images.

2. The second system, is described by Nuttin et al (1994), where the authors make use of a BRW stereotactic frame. This is a fairly simple system, in that the BRW frame provides both the 3D measuring system, and the external markers/fiducial marks, which establishes the relationship between the scanned images and the patient's head. Any intracranial point that is targeted by the BRW measuring system, can be identified on the softcopies of the scanned images using the fiducial marks appearing on the scanned images.

The optical 3D measuring systems seem to be the most popular, having fewer drawbacks and better stability than other 3D measuring systems (Bucholz et al, 1993). In optical digitisers a camera array is used to detect light from either active or passive light-sources. Passive light-sources consist of retroreflective markers, that will reflect visible or infrared light; active light-sources consist of a light emitting diodes (LEDs), that will emit either visible or infrared light, usually over an angle of 120 degrees. Infrared light is frequently used, because the ambient light entering the camera array can be controlled better (Bucholz et al, 1993).

Two types of CCD cameras are utilised in optical 3D measuring systems:

i) a conventional CCD camera, which is often used for surveillance purposes, and which produces conventional video images, due to its two dimensional CCD array.

ii) a CCD camera, with a one dimensional CCD array and a cylindrical lens; the cylindrical lens focuses the light from an LED onto a single element of the array

Using a minimum of two conventional CCD cameras, and employing such photogrammetric techniques as the Direct Linear Transformation (see Appendix C), the 3D coordinates of a point in space can be determined. No restriction is placed on the number of points that can be coordinated at any given instant. If points are to be coordinated automatically or semi-automatically, the more points there are, the more sophisticated the image processing software and hardware have to be.

For the one dimensional array CCD cameras, a minimum of 3 CCD cameras are required. These are usually mounted on a horizontal bar, with two of the one dimensional arrays placed parallel to the bar, and the third one dimensional array perpendicular to the bar (figure 8.2). In very simplistic terms, the system measures horizontal and vertical angles and thus can determine the 3D coordinates of an LED.

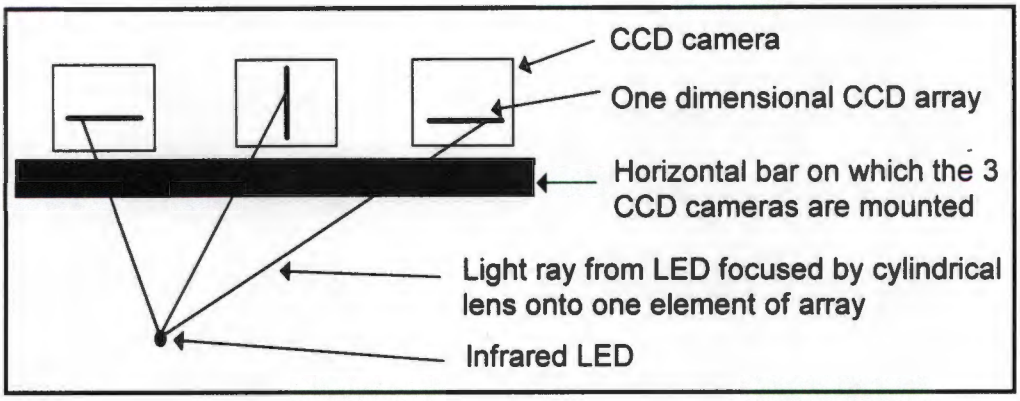


Figure 8.2: 3D measuring system using three, one dimensional array, CCD cameras

When using one dimensional array CCD cameras, the points to be coordinated are normally infrared LEDs, and only one LED can be coordinated at any given instant in time. Various optical and electronic filters are utilised, so that only light in a specific range of the infrared band is processed. In this way light from other unwanted sources is simply discarded. As the CCD array is one dimensional, it is impossible for the software to distinguish between 2 LEDs, which are triggered simultaneously. Therefore LEDs are triggered in a sequential fashion, and the number of LEDs that can be utilised by the system, depends on the scanning rate of the system. The two LEDs on the pointer can therefore never both be coordinated at the same instant in time, but the scanning rates of most of these systems is so high that 2 LEDs are coordinated almost simultaneously. The major advantage that the one dimensional array CCD cameras have over conventional CCD cameras, is that the bulk, if not all, of the processing occurs in a "black box" system and 3D coordinates of the LEDs are produced at very high speeds. With conventional CCD cameras, a fair amount of the processing is done by the software and therefore may take more time to process, than is the

case with one dimensional array CCD camera systems. With conventional systems, where several points are coordinated at the same time, the system operator may have to intervene to sort out various problems. The one-dimensional array CCD camera systems, compared to the conventional CCD camera systems, are more commonly used in neurosurgical applications.

Two examples of systems utilising one dimensional array CCD cameras are:

1. The optical digitiser, produced by Pixsys Inc. (Bucholz et al, 1993), consists of 3 CCD cameras, each camera having a 1x4000 linear CCD array. The 3 CCD cameras are mounted on a 1m long aluminium horizontal bar in such a way that the one dimensional arrays in the two outer CCD cameras are perpendicular to the bar and the array of the central CCD camera is parallel to the bar. Like many other 3D measuring systems, the aluminium bar with the 3 CCD cameras is placed above the operating table, in this case suspended from the overhead lights at a distance of 1.5m from the patient's head. Two LEDs, each with a unique intra-emitter spacing (the measuring system localising at 100Hz), are placed on the pointer. The accuracy of the system was not affected by the laboratory or the operating theatre environment. The accuracy of the measuring system was tested by moving the pointer throughout a volume equal to that of a human head. Error displacements of over 200 points were shown graphically in two XY planes, one at Z=0mm and one at Z=50mm and vector displacements in the two XY planes ranged from approximately -1.5mm to approximately 1.8mm. The mean localisation error is stated as 0.9mm and no standard deviation is listed (Bucholz et al, 1993). (From the literature it is impossible to determine what the range of displacement in the Z axis was; if the Z axis was the axis that was perpendicular to the bar on which the cameras were mounted, displacements would have been greater than those shown graphically on the XY plane, due to the geometrical configuration of the system.)

2. A very similar 3D measuring system (Optotrak 3-D Bar, Northern Digital, Waterloo, Canada), utilising 3 CCD cameras with 1x2048 linear CCD arrays and cylindrical lenses, is described by Zamorano et al (1994). A strober unit can connect up to 256 miniature infrared LEDs, and the system's pre-processors, connected directly to the cameras, scan at a very high rate of 3500 Hz. A 24 LED adapter is attached to the pointer, to enable the system to determine the pointer's tip in space. The accuracy, that is stated for locating the spatial position of an LED marker in an operating volume of 1x1m at a distance of 2m, is 0.1mm,

with a resolution better than 0.01mm. No mention is made of how this accuracy was obtained, and whether it was determined by the authors or is quoted from manufacturers specifications. The authors state that the accuracy of the infrared system is due to the high scanning rate of 3500Hz. (From looking at the diagrammatic presentation of the 3 cameras employed, the distances between the 2 outer cameras on the horizontal bar is well below 1m. From the geometrical configuration of the measuring system, and the accuracies achieved by Bucholz et al (1993) using a very similar system, makes the author question the accuracy stated by Zamorano et al (1994).)

Beside the NSA system, only two other neurosurgical 3D measuring systems utilising conventional CCD cameras, could be found in the literature. Matthew et al (1994) utilises two high-resolution cameras, rigidly attached to a robotic arm pedestal, to position and orientate the probe held by a robotic end effector. The cameras are positioned in such a manner as to view a reference assembly incorporated with the CRW stereotactic frame. The position of the probe, to which reference points have been attached, is determined independently by the robotic arm joint transducers and the cameras. No accuracies are quoted for the system.

The other system, utilising conventional CCD cameras, is described by Heilbrun et al (1992; 1993). This 3D measuring system bears the closest resemblance to the NSA system, which is described in chapter 9 of this thesis. Therefore this system will be described in slightly more detail than the other systems.

In the one article by Heilbrun et al (1992), a machine vision technique, using two video cameras, is being developed to determine the 3D coordinates of a point. The two video cameras are attached to a base about 1m apart, and the base is suspended approximately 2m above the surgical workspace. The cameras are linked to a computer equipped with dual frame grabbers and image processing capabilities. A video localizer, similar to the control frame used by the SPG system in that it consists of control markers with known 3D coordinates, is used to calibrate the 3D Cartesian coordinate system of the surgical workspace (Heilbrun et al, 1993). The video localizer, depicted in Heilbrun et al (1993), occupies only approximately a quarter of the volume of a patient's head. In photogrammetry, control markers should surround the space that one is likely to work in, or else 3D coordinate data will have to be extrapolated instead of interpolated, thus possibly introducing unnecessary errors.

Mechanical accuracy tests of the machine vision system have been carried out. 3D coordinates of the video localizer markers were determined by both the machine vision system and the BRW stereotactic frame. Heilbrun et al (1993) stated "The averaged independent measurement error was less than 1mm for each coordinate for the BRW phantom, and less than 1.5mm for each vector using the machine vision system. Thus the mechanical accuracy of the system is within the application accuracy of the stereotactic system." Heilbrun however goes on to state that "the application accuracy is more dependent on the scan slice thickness than the mechanical accuracy of the machine vision system".

What Heilbrun did not take into account, is that the application accuracy is not only dependent on the scan slice thickness; it is also dependent on the accuracy of determining the position of the pointer's tip from the positions of the two light-sources placed on the pointer handle (from Heilbrun's illustrations and photographs (Heilbrun et al, 1993), the light-sources appear to be reflective spherical markers). To ascertain the application errors of the machine vision system, the system needs to be tested using both the scanned images and the pointer.

Heilbrun et al (1993) also states that at the time of writing the article, the process was static in that the pointer markers had to be marked and digitised on the two video images by the operator. For a more dynamic process faster computer workstations and automatic pattern recognition algorithms were required, and that this was to be implemented.

## 8.4 CONCLUSIONS

To obtain a better overview of the non-linked 3D measuring systems, the various systems and their accuracies have been summarised very briefly.

SUMMARY OF NON-LINKED 3D MEASURING SYSTEMS:

Magnetic field digitiser

1. Manwaring (1993)
   - vector accuracy within 2mm of exact location

Sonic 3D measuring systems:

1. Horstman et al (1994)
   - vector accuracy is 0.9mm+/-0.6mm for the 3D measuring system
2. Barnett et al (1993a, 1993b) - (GP8-3D by Science Accessories Corp.)
   - vector accuracy is 1.1mm+/-1.0mm for the 3D measuring system
   - vector accuracy is 1.5mm+/-0.7mm, when using 1mm thick CT slices in clinical trials
3. Roberts et al (1993) - (GP8-3D by Science Accessories Corp.)
   - vector accuracy is 1.2mm+/-0.4mm for the 3D measuring system
   - vector accuracy is 2.0mm+/-0.5mm, when using 1.5mm thick CT slices

Stereotactic frame systems (application accuracies are quoted from Galloway et al (1991)):

1. Gildenberg et al (1994)
   - vector accuracy for CRW frame is 1.8mm+/-1.1mm, when using 1mm thick CT slices
2. Nuttin et al (1994)
   - vector accuracy for BRW frame is 1.9mm+/-1.0mm, when using 1mm thick CT slices

Optical measuring system, utilising 3 one dimensional array CCD cameras:

1. Bucholz et al (1993)
   - mean vector error of 0.9mm; no standard deviation is quoted
   - vector displacements in XY plane range from -1.5 to 1.8mm for 100 observations. No comment is made about errors in the Z axis.
2. Zamorano et al (1994)
   - accuracy claimed is questioned by the author of this literature review

Optical measuring system, utilising 2 two dimensional array CCD cameras:

1. Heilbrun et al (1993)
   - vector error is less than 1.5mm (This is the mechanical accuracy for the machine vision system, and does not include pointer use, nor any inaccuracies that may arise from using CT slices.)

It is important to note what is being claimed for each particular system. In some systems, only the accuracy of the system to locate a point in space is listed; in others the effect of the pointer is included in the system's accuracy; application accuracy refers to testing the system using both the pointer and the scanned images. In some systems only the mean errors are listed - the reader is left in the dark about how any single measurement may deviate from the mean.

From the summary, most of the 3D measuring systems can locate a point in space (when utilising a pointer), with an accuracy of approximately 1mm and a standard deviation ranging from 0.4mm to 1mm. Application accuracies for the sonic systems and the stereotactic frame-based systems range from 1.5mm+/-0.7mm to 1.9mm+/-1mm for 1mm thick CT slices, and 2mm+/-0.5mm for 1.5mm thick CT slices.

The type of system used is often dependent on personal preference. The conventional CCD camera systems are not as popular as the one dimensional array CCD cameras, as they are mainly software driven and may require intervention by the operator. However, the equipment for the NSA system was already available and, as shown in chapter 9, the conventional CCD cameras do form the basis of a viable 3D neurosurgical measuring system.

# CHAPTER 9 DEVELOPING AN INTERACTIVE IMAGE-GUIDED NEUROSURGICAL AID FOR THE CT SCANNER AT GROOTE SCHUUR HOSPITAL

## 9.1 INTRODUCTION

The neurosurgical aid (NSA) system, designed at the request of the neurosurgeons at Groote Schuur Hospital (GSH), is an interactive image guided neurosurgical system designed specifically to operate with the GSH scanner. The whole purpose of the NSA system is to identify the exact intracranial point, at which the neurosurgeon is working, on the appropriate CT slice and do this in theatre at the time the surgery is being performed.

To be able to identify an intracranial point on the appropriate CT slice, the relationship between the theatre and CT coordinate system has to be established. For this purpose, as with the SPG system and the Cape Pointer, external markers are attached to the patient's head prior to the CT procedure. CT slices are scanned at regular intervals across the cranial region that will be affected by the open craniotomy, and also through the external markers, so that their 3D CT coordinates can be determined. The CT images are transferred to a PC equipped with an image frame grabber card, which is used to display the CT images in theatre. In theatre, two CCD cameras are used to determine the 3D coordinates of the external markers in the theatre coordinate system. As 3D CT coordinates have already been determined for the external markers, the relationship between the theatre and CT systems can be determined. Therefore any other point that is coordinated in the theatre system, can also be coordinated in the CT system. Once 3D CT coordinates have been obtained for that point, it is a simple matter to identify that point on the relevant CT slice.

## 9.2 OVERVIEW OF THE NEUROSURGICAL AID SYSTEM

As the NSA system would most probably be used in conjunction with the Cape Pointer, the Taylor halo, with its three markers corresponding to the Cape Pointer's three legs, is attached to the patient's head. One or two additional markers should also be attached to the scalp to improve the accuracy of the external 3D coordinate system.

The Cape Pointer can be used to insert a catheter into the cranium to mark the route to the lesion centre. A burr hole is made at a selected entry point, and the catheter placed so that its one end is at the lesion centre and the other end is cut off directly above the dura within the cranial cavity. The procedure is then completed, by closing the incision over the burr

hole. The open craniotomy is begun by making the necessary scalp incisions and removing a whole segment of the cranium. The one end of the catheter is now visible just above the dura and can be followed down to the lesion. The reason for using the catheter as a route marker, is that, due to the destruction of the external coordinate system, the Cape Pointer can no longer be used to guide the neurosurgeon to the lesion. (The external coordinate system is destroyed, as the external markers have to be removed to allow the neurosurgeon to perform the open craniotomy.) The procedure of using a catheter as a route marker has already successfully been employed in an open craniotomy.

The CT procedure, to coordinate the external markers, is conducted in the same manner as that for the stand alone Cape Pointer. CT slices are scanned through all the external markers. CT slices are also scanned at regular intervals through the region of the brain that will be affected by the open craniotomy. In addition an AP and Lateral surview, as well as any other CT slices required by the neurosurgeons for the open craniotomy, are scanned.

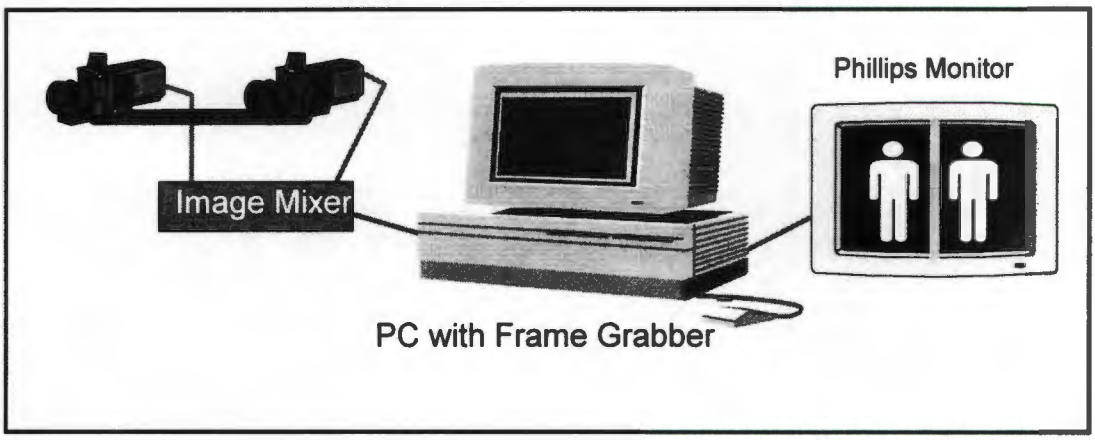


Figure 9.1: The neurosurgical aid system (NSA system)

The NSA equipment (figure 9.1) consists of the following :

1. two CCD monochrome cameras (Burle TC650EX Series Cameras)
2. two camera lenses (TV Zoom Lens 12.5-75mm F1.8)
3. an image mixer (Primebridge PVW1-Video Wiper)
4. a Philips monitor CM8833
5. a 3D control frame (not shown in figure 9.1)
6. a personal computer (PC)
7. an image frame grabber card (Matrox IP8 card) installed in the PC

Once the CT procedure is complete, the patient is taken back to the ward to await the surgical procedure. The CT images of the patient are transferred to the NSA PC. The NSA system is controlled via a software package run on the PC, and the NSA menu is displayed in figure 9.2. All the software has been written by the author using Turbo C 2.0 and True Basic.

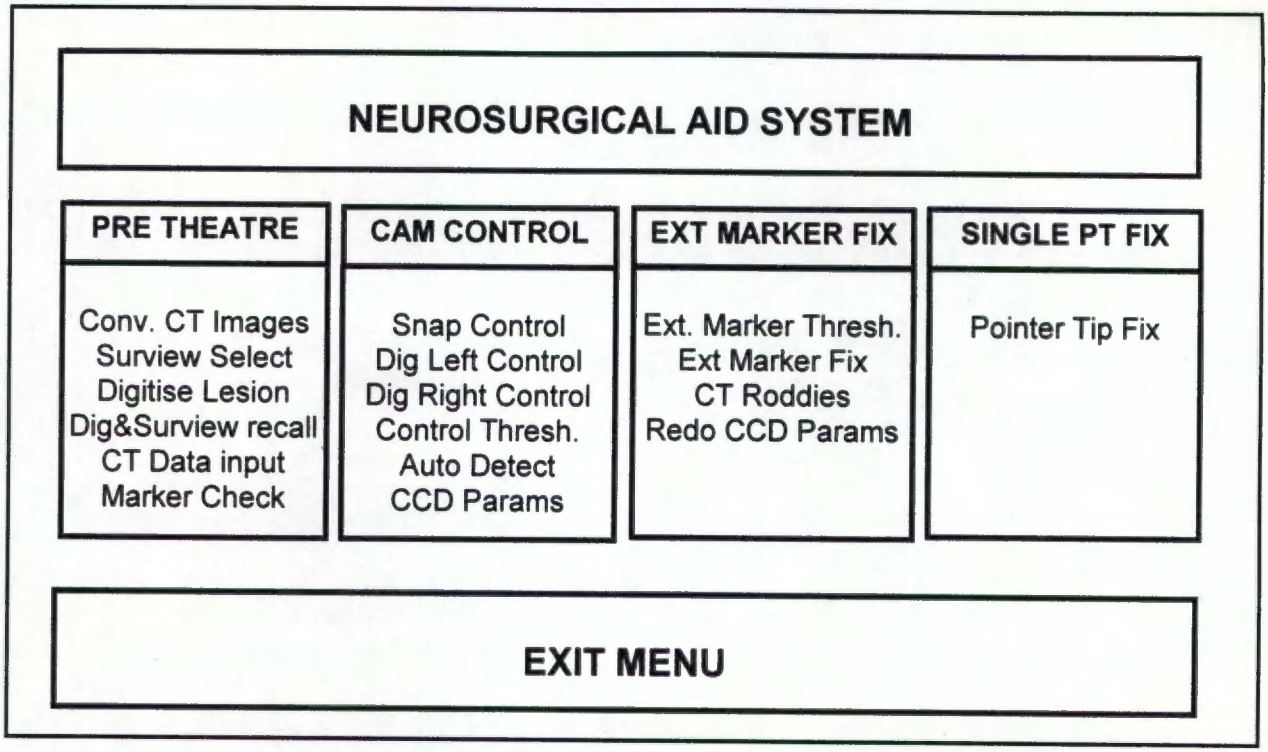


Figure 9.2: The NSA menu

When first accessing the NSA software, the user is prompted to enter the patient's PC name, using five letters or less. The PC file name is stored as a global variable, and therefore only has to be entered once when using the NSA system. Throughout this chapter the patient will be referred to as Mrs. R Smith - a fictitious name. The PC file name entered for Mrs. Smith is SMITH.

In the pre-theatre section of the NSA menu (see figure 9.2), the CT images are converted into an appropriate format for the IP8 image frame grabber card. The CT surviews are selected for display, and the outline of the patient's head and the outline of the lesion are digitised on the various CT slices. The 3D CT coordinates for the external markers, digitised and manually recorded from the CT screen, are entered into the NSA software. The coordinate data entry is checked by recalling the relevant CT slices and annotating the external marker's coordinate position with a cursor. If the marker coordinates have been entered correctly, the cursor and marker should coincide.

As can be seen in figure 9.3, the cursor, placed on the digitised CT coordinates of marker 5 on slice 12, does coincide with the marker.

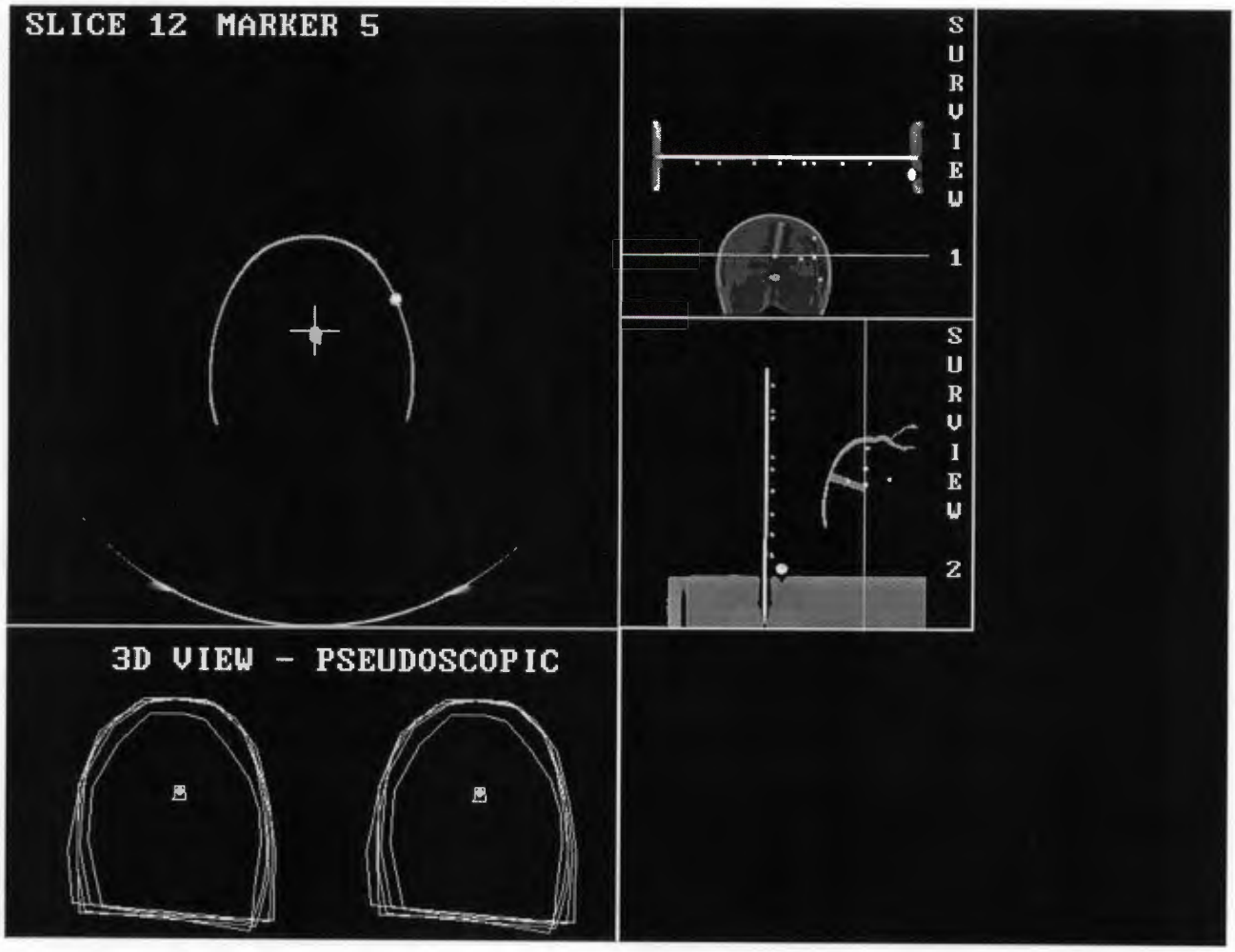


Figure 9.3: Philips screen showing CT slice through the ball-bearing representing the lesion centre

Figure 9.3 is the standard CT output from the IP8 card on the Philips monitor. The screen size consists of 1024x768 pixels (1024 on the horizontal screen axis, 768 on the vertical screen axis). The top left area is for displaying CT slices, occupying a pixel area of 512x512. To the right of the CT slice area, the CT surviews are displayed, one below the other, each surview occupying a pixel area of 256x256. Below the CT slice area, a pseudoscopic view of the digitised outline of the patient's head is displayed. By using the cross-eyed viewing method (Adams, 1974), the outline of the patient's head can be perceived in 3D.

Once these preliminary procedures have been completed, the NSA system can be set up in theatre. The CCD cameras are set up in such a way that the area, that will be occupied by the patient's head is "seen" by both cameras. The control frame is placed in this area and an image of the control frame captured. The control markers are coordinated, and the CCD camera parameters calculated using the DLT (appendix C). The control frame is removed and the patient's head positioned in that area.

A pointing device is used to coordinate external markers and points within the cranium, as often these points are out of sight of the cameras. The pointer consists of a long needle, with a point at one end. Attached to the opposite end are three pointer markers, whose geometrical relationship to the pointer tip is known. By capturing an image of the pointer pointing at a certain point, the 3D coordinates of the three pointer markers can be calculated. As the relationship between the pointer markers and the pointer tip is known, the 3D coordinates of the tip can be determined, even though the tip may not be visible to the cameras.

The pointer is used to obtain 3D coordinates for all the external markers in the theatre system. As the external markers have already been coordinated in the CT system, the theatre system can be transformed into the CT system using the Rodrigues transformation. Thereafter, any point that is coordinated using the pointer is automatically coordinated in the CT system, and can be identified on the relevant CT slice.

## 9.3 THE PRE-THEATRE PROCEDURES

### 9.3.1 Converting the CT Images

The CT scanner, operating on a UNIX based system, and the Matrox IP8 frame grabber card, running on a DOS based PC, have different image protocols. To display the CT images on the Philips monitor via the IP8 card, various procedures have to be completed to download and convert the CT image data.

The CT image data protocol for the GSH scanner is not available to the public. With the assistance of a Masters student in the Department of Electrical Engineering at the University of Cape Town (UCT), Alan Bub, who had been using the CT data for another application to run on a Sun system (UNIX based system), some of the CT protocol became more transparent. All the CT images of a patient are stored in a single large file, which is

downloaded onto an 8mm metal digital data cartridge (112 meters in length and capable of storing 2.3 Gigabytes). Using an external Exebyte drive at UCT's Information Technology Service, the file is read from the tape onto the UNIX system at UCT, and from there is moved onto the NSA PC's harddrive using UCT's network connections. This is definitely not an on-line procedure, as 3 kilometre's of Cape Town's busiest highways separate the NSA system and UCT's Information Technology Services. Therefore, depending on how often the NSA system is used in future, an Exebyte drive should be purchased for the NSA PC, and the CT files downloaded directly from the tape onto the PC.

The CT file consists of a header segment of 8.192 Kilobytes (K), followed by the CT images. Each CT image, be it a slice or a surview, consists of 532.992 K, of which the first 8.704 K is the image information segment pertaining to that image. The other 524.288 K are the grey level values making up a 512 by 512 image, each grey value requiring 2 bytes for storage. After n number of images, a small data chunk of variable length remains (usually 5K to 10K), which is discarded. (The information in this paragraph was supplied by Alan Bub.)

As UNIX and DOS have different ways of storing 2 byte data chunks, a C program was written to decode the Hounsfield grey values into a DOS compatible format (decoding procedure explained in Appendix K). The reason why the CT scanner requires 2 bytes to store a grey value, is that Hounsfield grey values range from -1024 to 3072. The IP8 grey values range from 0 to 255, and only require 1 byte per grey level value. The 4096 Hounsfield grey range therefore has to be condensed into the 256 IP8 grey range. At a glance this seems impractical, but makes more sense when taking into account that the human eye can only resolve approximately 40 distinct shades of grey (Castleman, 1979).

It would have been simple to compress the range from 4096 to 256 in a linear manner, i.e. multiply each CT grey level by approximately 0.06. This however would not be optimal, as a large part of the 4096 range is not of any significance. Hounsfield values greater than 1200 appear white and are normally bone or objects such as the stainless steel ball-bearings used for markers. Therefore all Hounsfield values greater or equal to 1200 are allocated an IP8 value of 255, i.e. white. Below the Hounsfield value of -1000 everything is black, and is usually filled with air. After examining various CT files, it was found that no image resolution was lost if Hounsfield values below -800 were given the IP8 value of 0, i.e. black.

The most crucial Hounsfield values range from -100 to 180, which encompass the bulk of the intracranial tissue, and therefore are allocated a large portion of the 256 IP8 grey range. The remainder of the 4096 Hounsfield range are then distributed in the remainder of the 256 IP8 range. The Hounsfield to IP8 range distribution is shown in table 9.1. The main reason for this distribution is to obtain an image that is visually as close as possible to the hardcopies of the CT slices.

| Hounsfield Range = -1024 to 3072 | IP8 Range = 0 to 255 |
|---|---|
| -1024 to -800 | 0 |
| -799 to -101 | 1 to 8 |
| -100 to 180 | 9 to 224 |
| 181 to 1199 | 225 to 254 |
| 1200 to 3072 | 255 |

Table 9.1: The compression of the Hounsfield range into the IP8 range for CT slices

The Hounsfield compression in table 9.1, worked well for CT slices, but did not prove optimal for CT surviews. Since CT surviews do not show up any intracranial tissue detail, a different Hounsfield to IP8 grey range compression is employed, and this is shown in Table 9.2. The IP8 grey values from 1 to 29 have intentionally not been mapped, to lighten the whole image and give a better perception of the actual cranium.

| Hounsfield Range = -1024 to 3072 | IP8 Range = 0 to 255 |
|---|---|
| -1024 to -601 | 0 |
| -600 to 1199 | 30 to 254 |
| 1200 to 3072 | 255 |

Table 9.2: The compression of the Hounsfield range into the IP8 range for CT surviews

The other difference between the processing of slices and surviews, is the resultant size of the images. To display both a CT slice and two CT surviews on the Philips screen, the surviews have to be compressed to half their size, that is from 512x512 to 256x256. This is simply done by discarding every second grey value from one line, and discarding every second line. This approach is suitable, as the CT surviews are only utilised for indicating to the neurosurgeon where on the cranium the CT slices were scanned.

Once it had been ascertained that the CT images could successfully be converted to the IP8 format, the CT header segment and individual image information segments had to be examined. The header segment is discarded, as each image information segment, preceding a CT image, contains all the necessary information for that image. The

information, extracted from each image information segment, is written to a text file and given the patient's PC file name, e.g. SMITH.TXT. A section of that file is listed here:

```
058
01 31-Jan-96  726.87      R SMITH     000 HALF -256 ADULT BRAIN 240 1516    4
02 31-Jan-96  727.00      R SMITH     090 HALF -256 ADULT BRAIN 240 1516    4
05 31-Jan-96  670.00      R SMITH     000 HALF -256 ADULT BRAIN 240 1516 1024
07 31-Jan-96  666.00      R SMITH     000 HALF -256 ADULT BRAIN 240 1516 1024
```

The first line of the text file (058 from the example) is the total number of CT images in the CT file. Each line thereafter contains the information from one image information segment. The second line of the above example is used to illustrate the various items:

| | |
|---|---|
| 01 | Number of the CT image scanned, which also appears on the hardcopy of the CT image. Numbers may be missing, as is the case in the example of the text file above. These images were not required for the NSA system, and therefore were not written to the CT file by the CT system. |
| 31-Jan-96 | Date on which CT scan took place |
| 726.87 | Table position / Z coordinate at which either the CT surview scan began, or the CT slice was scanned. |
| R Smith | Patient name. From the second image information segment read, every reading of the patient's name is checked against the patient's name obtained from the first image information segment, to ensure that all the images were scanned of the same patient. |
| 000 | Gantry angle setting. It is only of interest, when the image is a CT surview, as this angle indicates what type of surview has been scanned, for example 000 indicates a Lateral surview, and 090 an AP surview. |
| HALF | Indicates whether the image was scanned as a 256x256 image, i.e. half the size of the normal 512x512 image, and then enlarged to fill the 512x512 image space. If an image is scanned as a 512x512 image, it is labelled as FULL. |
| -256 | Index - indicates how much of the image space is occupied by the surview. This particular surview was scanned on HALF protocol, i.e. scanned as a 256x256 image; the index of -256 indicates that all of the 256x256 block was filled with the surview image. Another example, two CT surviews scanned on FULL with an index of -350, is shown in figure 9.4. |

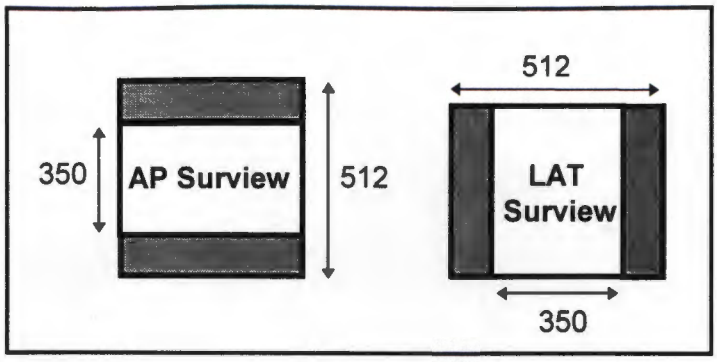


Figure 9.4: Showing how the index effects the CT surviews

ADULT BRAIN Type of protocol used for the CT procedure. Using the brain protocol, only half the scanning field is utilised, whereas the pelvic protocol utilises the whole of the scanning field.

240 Size of the scan, if the scan is done on HALF it is 240, if the scans is done on FULL it is 480. (This information is not utilised by the software.)

1516 Patient's study number. As with the patient name, it is compared to the study number of the other images to ensure that all images originate from the same patient study. This is also the number under which the CT scanner stores the images on its harddrive.

4 Number indicates whether a CT image is a slice or a surview, a 4 indicates a surview, and a 1024 indicates a slice.

When dealing with any CT file, the C program first ascertains how many images are contained in the CT file, the header segment is then discarded, and a loop entered which is run until all the images are processed. The necessary information is extracted from each image information segment and written to the text file, e.g. SMITH.TXT. The image data for each image is decoded either as a slice or surview, depending on the information in the image information segment. Each image is written to a separate file, with the file name consisting of the patient's name and the number of the image, e.g. image 10 is stored as SMITH10.IMG. To decode a CT file containing 50 images takes approximately 5 minutes.

### 9.3.2 Surview Select

On the standard output from the IP8 card to the Philips monitor, a CT slice as well as two surviews are displayed. The plane in which the CT slice was scanned is displayed on the surviews with horizontal line on the AP surview and a vertical line on the LAT surview (see figure 9.3). This assists the neurosurgeon in visualising the CT slice in relation to the patient's cranium. For the NSA software to display the CT surviews on the Philips screen, the CT surviews first have to be selected.

For this purpose the text file SMITH.TXT is recalled, and the image information for the various images is inspected. The last entry in a line indicates whether that particular image referred to in that line, is a surview or slice, i.e. coded with a '4' or '1024' respectively. Each image, that is identified as a surview, is displayed. This procedure is continued, until all surviews have been displayed. The user, now having viewed all the surviews, is prompted to select one or two surviews. If only two surviews were scanned, that is the AP and LAT surview, both should be selected and displayed.

The information, that is required for the selected surviews, is extracted from the text file SMITH.TXT and written to the text file SMITHS.TXT, where the S appended to the patient's name indicates the surview text file. The following lines are stored in the surview file SMITHS.TXT

```
002
01 726.87 000 -256 HALF
02 727.00 090 -256 HALF
```

A subroutine, named RECALS, uses the information in the surview text file to recall the selected surviews when needed.

### 9.3.3 Digitising the Lesion

To display the pointer tip in relation to the lesion during an open craniotomy, the outline of the cranium and the lesion are digitised on those CT slices on which the lesion is imaged, and a pseudogram produced from the digitised coordinates. A pseudogram of the outlines of the black face mask, and the outline of the ball-bearing representing the lesion centre, are displayed in figure 9.3. By viewing the pseudogram with the cross-eyed axis method (Adams, 1974), the viewer perceives three dimensional outlines of the black face mask and the lesion centre.

For digitising lesion and cranial outlines, the SPG digitising software (chapter 4.6.3) was adapted to display, and save, CT coordinates by converting the X and Y IP8 pixel coordinates into X and Y CT coordinates, using correction factors determined from various CT procedures (see Appendix L). As no specific markers are coordinated when digitising the outlines, and sub pixel accuracy is not required, the centre of gravity algorithm was disabled for this particular digitising procedure.

The user is prompted to digitise the outline of the cranium, and then recall the same slice before digitising the outline of the lesion, so that the cranium and lesion outlines are stored as separate data groups. When drawing the pseudogram, each separate data group is treated as a separate closed figure, i.e. the first point digitised in a group is joined to the last point digitised in that group. The digitising procedure is repeated for each slice on which the lesion appears, and all the digitised data is written to the pseudogram text file SMITHP.TXT, where the P appended to the patient's name indicates the pseudogram text file. The data for each digitised point consists of the X and Y CT coordinates digitised on the slice, and the Z coordinate at which that particular slice was scanned.

Once digitising has been completed, the subroutine PSEUDO utilises the pseudogram text file to draw the pseudogram. The cranium and lesion outline are drawn twice, each one from a slightly different perspective, creating the left and right images of the pseudogram. By viewing the left image with the right eye and the right image with the left eye the outlines of the cranium and lesion will be perceived as a three dimensional model - this is known as the cross-eyed axis method or pseudoscopic viewing. By drawing the pointer tip on both the left and right pseudogram images, the 3D relationship between the lesion and the pointer tip can be perceived. The reason for using a pseudogram is that with a little practice the pseudogram can be viewed with the naked eye, and the only restriction on the distances between the left and right images of the pseudogram is the extent to which the viewer can cross his eyes (Adams, 1974). (In the case of a stereogram, the left image is viewed with the

left eye and the right image with the right eye, and the distance between the left and right image has to be approximately equal to the viewer's eye base, i.e. approximately 60 to 65 mm.)

To draw the left and right images of the pseudogram, the centre of gravity for all the data in the pseudogram text file is calculated, and all the data points reduced to that centre of gravity. From these coordinates the x and y image coordinates for the left and right images are calculated, using the parallax equations ((Karara, 1989), (Slama, 1980)):

$$xl = X_{CT} * F / (H - Z_{CT}) \qquad 9.1$$

$$yl = Y_{CT} * F / (H - Z_{CT}) = yr \qquad 9.2$$

$$xr = xl + F * B / (H - Z_{CT}) \qquad 9.3$$

where:

| | |
|---|---|
| $X_{CT}$, $Y_{CT}$, $Z_{CT}$ | 3D CT coordinates of a point digitised on the CT slice |
| xl, yl | Image coordinates of that point, on the left image of the pseudogram |
| xr,yr | Image coordinates of that point on the right image of the pseudogram |
| F = 150 | Focal length of the "pseudo camera" |
| B = 65 | Base length between the two exposures for the left and right image |
| H = 3000 | Height of the camera above the object imaged in the pseudogram |

(The values for F, B and H have been selected to represent a human observer, with an eye base of 65mm, 3m away from the object and with a focal length of 150mm.)

Once all the pseudogram image coordinates have been calculated, the minimum and maximum values for xl, yl, and xr are determined and scaling and translation factors calculated. These factors are applied to all pseudogram image coordinates, so that the resultant pseudogram fits in the window provided for the pseudogram.

When a pointer tip's 3D CT coordinates have been determined, it is a simple matter to calculate the pseudogram image coordinates for the pointer tip, using equations 9.1 to 9.3, and draw the pointer tip on the left and right image of the pseudogram. The neurosurgeon is thus able to visualise the position of the pointer tip in relation to the lesion in three dimensions.

### 9.3.4 Recalling the digitised lesion and surviews

To be able to refresh the screen at any stage, the NSA menu option Dig&Surv Recall runs a subroutine called FIRST, which runs the subroutines RECALS and PSEUDO, after ascertaining that the surview and pseudogram text files SMITHS.TXT and SMITHP.TXT exist. The subroutine FIRST is also run as a part of the start-up routine of the NSA software, so that if the two text files have already been created, the surviews and pseudogram pertaining to that patient are automatically recalled.

### 9.3.5 CT data input

The CT data input program is written in True Basic, and allows the user to enter the 3D CT coordinates of the external markers. External marker coordinates are entered in ascending order, i.e. marker 1, 2 3 etc. The text file that is created to store the CT data is called SMITHCT.TXT, i.e. CT appended to the patient's name, and contains the number of external markers, as well as their X, Y and Z coordinates, as is shown in the following example:

004
001 0073.00 -005.00 0833.00
002 0045.00 0047.00 0800.00
003 0063.00 -008.00 0764.00
004 0064.00 0013.00 0796.00

The CT text file is crucial to the NSA system, as it is later used to transform the theatre coordinate system into CT coordinate system .

### 9.3.6 Marker Check

As the CT text file is crucial for transforming the theatre system into the CT system, it is vital that the data in the file has been entered correctly. Although the user is prompted to check the CT coordinates at the time of the data entry, mistakes can still be overlooked. The subroutine MRK4 provides an additional independent check to ensure that the CT coordinates have been entered correctly into the CT text file.

The subroutine MRK4 reads in the data from the CT file, i.e. the X, Y and Z CT coordinates of all external markers. To recall the CT slice, on which an external marker was digitised, the patient data file is searched for the Z coordinate of that external marker. The CT image number pertaining to that Z coordinate, is used to call up the CT slice on the Philips monitor. A digitising cursor is placed on the CT slice at the X, Y coordinates of the external marker; for this purpose the CT X and Y coordinates have to be converted into IP8 X and Y coordinates using the correction factors determined in Appendix L. The cursor position should correspond to the image position of the external marker on the CT slice. Any abnormal deviations indicate that the external marker coordinates have been incorrectly entered. As CT digitisation is only accurate to approximately 1.5mm, there may be small discrepancies in the location of the cursor in relation to the marker.

At the same time that cursor is drawn on the CT slice, the AP and LAT surviews are marked with a horizontal and vertical line respectively to indicate the position of the CT slice, and the position of the external marker is superimposed on the pseudogram (see figure 9.3). The subroutine PSEUDODOT simply uses the parallax formulas (equations 9.1 - 9.3) to calculate the position of the marker in both the left and right image of the pseudogram, and draws solid white dots at those positions.

To determine the position of the CT slice on the AP and LAT surview, no scaling has to take place - however the Z coordinate and index of the CT surview, and the Z coordinate of the CT slice, have to be taken into account. The procedure for marking the CT slice position on the CT surviews is best illustrated using an example of two surviews and a slice, whose image information is listed below:

| | | | | |
|---|---|---|---|---|
| 01 | 31-Jan-96 | 800.80 | R SMITH | 090 FULL -350 ADULT BRAIN 240 1516 4 |
| 02 | 31-Jan-96 | 800.80 | R SMITH | 000 FULL -350 ADULT BRAIN 240 1516 4 |
| 03 | 31-Jan-96 | 604.70 | R SMITH | 000 FULL -350 ADULT BRAIN 240 1516 1024 |

Images 01 and 02 are AP and LAT surviews respectively. For both surviews scanning was commenced at a Z coordinate of 800.8, both surviews were scanned on FULL and with an index of -350. Image 03 is a slice scanned at the Z coordinate of 604.7 (scanned in the plane of the patient's eyes, as illustrated with a dashed line in figure 9.5).

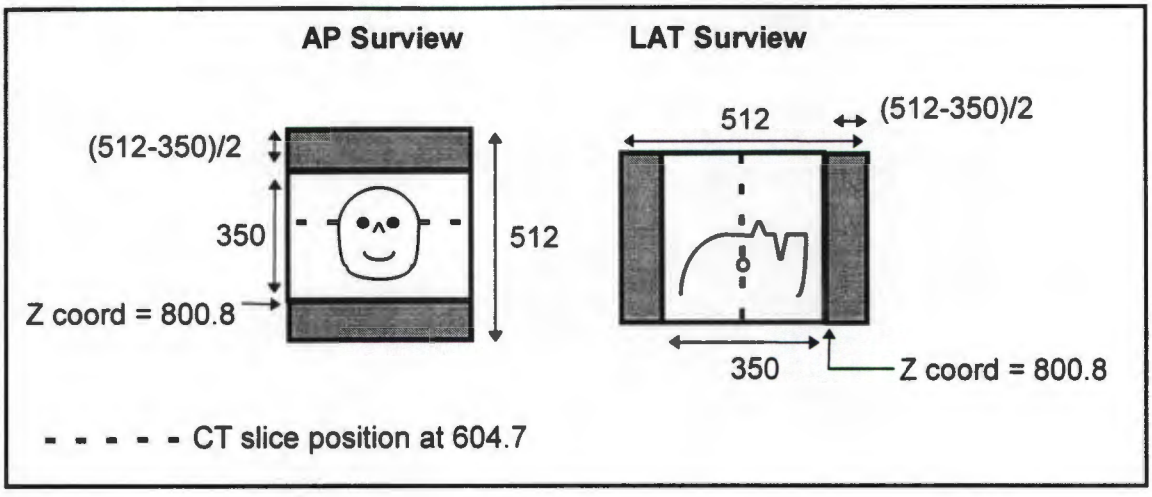


Figure 9.5: Indicating the CT slice position on the AP and LAT surview

Three other factors also have to be considered, that surviews are scanned on either FULL or HALF protocol, that surviews have been condensed into a 256x256 image by the NSA software, and the actual positions that the CT surviews occupy on the IP8 screen (see figure 9.6).

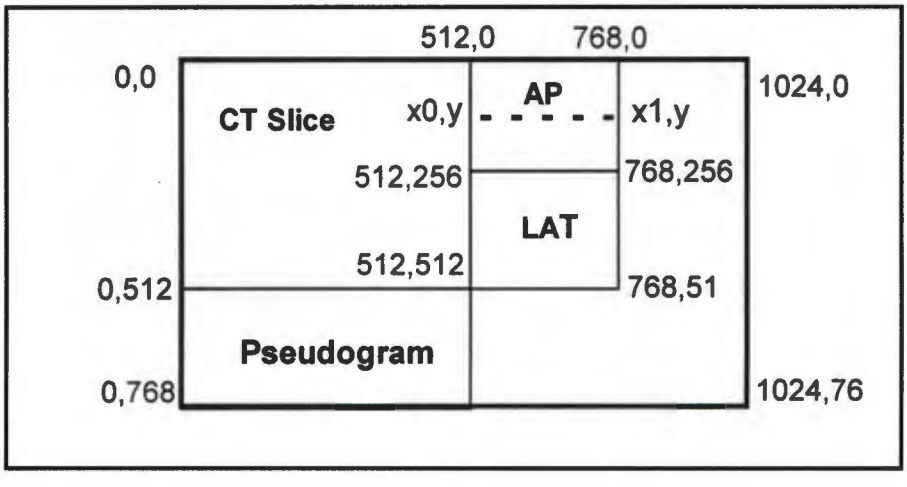


Figure 9.6: The relative positions of the surviews on the IP8 screen

The position of the CT slice on the AP surview, when the AP surview occupies the upper surview position on the IP8 screen, is shown in figure 9.6 by a dashed line from (x0, y) to (x1, y), and is simply calculated as follows:

$$y = \frac{\frac{256.0 * SIZE - abs(INDEX)}{2.0} + Z_{Slice} - Z_{Surview} - INDEX}{2.0} \qquad 9.4$$

where:

| | | |
|---|---|---|
| SIZE | = 1.0 | if the protocol is HALF |
| SIZE | = 2.0 | if the protocol is FULL |
| INDEX | = -350.0 | |
| $Z_{Slice}$ | = 604.7 | |
| $Z_{Surview}$ | = 800.8 | |

and where:

| | |
|---|---|
| x0 | = 512 |
| x1 | = 768 |

The calculations are very similar for the LAT surview, and provision is also made should the AP and LAT surviews be swapped, i.e. the AP fall below the LAT surview on the IP8 screen. Once the marker check for all the external markers has been completed satisfactorily, the NSA system is ready to be used in theatre during the open craniotomy.

## 9.4 CALIBRATING THE CCD CAMERAS IN THE OPERATING THEATRE

To set up the 3D theatre coordinate system, the CCD cameras of the NSA system have to be setup, and calibrated using the control frame and the direct linear transformation algorithm. The 3D coordinate system of the control frame will thus be "adopted" as the theatre coordinate system, and any other point falling within the area of the control can thus be coordinated in the theatre system.

The two CCD cameras, equipped with zoom lenses, are set up on a heavy metal base with a base length of 160cm, using ball and socket camera mountings. The control frame is set up in the area that is later to be occupied by the patient's head (ring phantom, see figure 7.2), at a distance of 2 meters from the cameras. The cameras are connected to the IP8 card in the PC via the image mixer. The camera setup distances were decided upon after examining the operating theatre, but may have to be altered once theatre trials begin in earnest.

The control frame is very similar to the control frame shown in figure 4.7, with the exception that the whole control is made of metal and consists of 22 retroreflective markers, 13 markers spread over the back plane and 9 over the front plane. Bright lights are used to illuminate the control markers. For the clinical trials, the retroreflective markers will be replaced with infrared LED's, and the zoom lenses fitted with infrared filters. The use of an infrared filter and infrared lights has already proven very satisfactory in another project, which only required a single camera. Unfortunately, at the time of running the laboratory trials, additional infrared filters had been ordered for the other camera, but had not yet been obtained.

The stereo image of the control frame has to be captured, using the Snap Control option on the NSA menu. The operator of the system has the option of choosing Live video or Memory video. Memory video is for recalling images stored on the harddrive, and Live video is used if the control frame image has not yet been captured. Once Live video has been selected, the images from the two CCD cameras are displayed on the Philips screen as a stereo image (see chapter 4.2.1). It is at this stage, that the cameras are adjusted, so that the control frame is displayed on both the left and the right part of the stereo image. The adjustments include repositioning of the cameras, using the ball and socket mounts, and setting the zoom, aperture and focus on the zoom lenses. Once the cameras have been set, the settings remain unaltered throughout the procedure. The stereo image of the control frame is captured and stored on the harddrive under the name of SMITHc.TGA (the c denoting the control image for the patient SMITH).

The control markers can be digitised manually using the options of Dig Left Control and Dig Right Control on the NSA menu, but normally are "digitised" using semi-automatic marker detection. Using the menu option Control Threshold, the threshold value for the stereo image of the control frame is set. Depending on the camera settings, the control markers usually have grey values greater than 220, i.e. the markers appear white. Once the threshold value has been set, all grey values below 220 are set to zero, i.e. black. Beside the threshold value, the exact position of the boundary between the left and right part of the stereo image has to be set. This is achieved by moving a vertical line drawn on the stereo image with the keyboard arrow keys, until the vertical line is coincident with the boundary between the left and right parts of the stereo image. Once this has been done the software treats the two parts of the stereo image as separate units

Using the menu option Auto Detect, the left part of the stereo image is searched for pixel values above the threshold value. Pixel values, above the threshold value, that are found in a proximity of 12 pixels to other pixel values, above the threshold value, are discarded, as these pixels both fall on the same marker. The marker detection is semi-automatic in that the software can detect all the white control markers, but the software user has to "label" the control markers, for example that the fifth marker detected is control marker 8. Once all the markers have been labelled, a centre of gravity algorithm (Appendix D) is applied to each marker, determining the marker centre to sub pixel accuracy. The 2D IP8 screen coordinates are saved in a text file. The same procedure is repeated for the right part of the stereo image.

Once all the control marker coordinates have been "digitised", the menu option CCD Params calculates the CCD camera parameters using the DLT (Appendix C) and the 3D coordinates of the control markers. (The control markers' 3D coordinates were measured in the reflex metrograph (Scott, 1981)). The resulting precisions, determined by the DLT for the 22 control markers, were standard deviations of 0.3mm, 0.3mm and 0.4mm for X, Y and Z respectively.

Once the CCD camera parameters have been determined, the control frame is removed, and the patient's head is placed in the area previously occupied by the control frame. Should the control procedure need to be rerun at some later stage, for example if the neurosurgeon wants to satisfy himself that the operator has set everything up correctly, the control image can simply be recalled from the harddrive and the procedure rerun.

The patient's head has to be immobilised throughout the open craniotomy, to allow the neurosurgeon to do the very delicate surgery. For this purpose, a Mayfield clamp is attached to the operating table. The patient's head is placed within the Mayfield clamp, and the clamps then applied to the patient's head, effectively immobilising the patient's head. This also ensures that the theatre system/CT system, that will be established in relation to the patient's head, is not destroyed by any movement of the patient's head during the open craniotomy. Once the patient's head has been immobilised, the NSA procedures can be continued.

## 9.5 EXTERNAL MARKER ROUTINE

To be able to transform the theatre system into the CT system, common points in both systems need to be coordinated. The external markers, common to both systems, have already been coordinated in the CT system. The external marker routine is used to coordinate the external markers in the theatre system and to transform the theatre system into the CT system. Thereafter, any other point coordinated in the theatre - on or in the patient's cranium - is automatically coordinated in the CT system, and can therefore be identified on the relevant CT slice.

Figure 9.7: The NSA pointer

To be able to coordinate the external markers, and any intracranial point, a pointer is utilised (see figure 9.7). Such pointers are not uncommon in interactive image-guided neurosurgery, and the pointer used by Heilbrun et al (1993) consisted of a long straight pointer, to which two spherical markers had been attached, so that the pointer passed through the centre of each marker. With the sonic digitiser systems, these markers are replaced with emitters (Bucholz et al, 1993).

The reason for using a pointer, is that points within the cranium are not visible to the measuring devices, in the case of the NSA system the intracranial points are not visible to the two cameras. To coordinate a specific intracranial point, the pointer tip is placed on that point. The three retroreflective markers attached to the other end of the pointer (see figure 9.7), and which are visible to the 2 cameras, are coordinated by the NSA system. As the relationship between the pointer's three markers and the pointer's tip is known, the position of the tip is calculated and thus the 3D coordinates of the intracranial point are determined.

The pointer, shown in figure 9.7, is only used in the laboratory trials. Both the type of marker, and the configuration of the markers, will have to be altered before it can be used in theatre. The retroreflective markers will have to be replaced by infrared LEDs, either battery operated or connected to some external power source. This may seem more cumbersome, but is quite common in an operating theatre, where a standard piece of equipment such as the bipolar coagulator, used to cauterise small blood vessels, is also connected to an external power source. The marker configuration will have to be altered, so that the markers can only be viewed from one direction. The pointer in figure 9.7 can be rotated by 180 degrees without the cameras losing sight of the markers, and this was also the intention of the design. Unfortunately, the Rodrigues transformation, used to determine the position of the pointer tip from the positions of the three pointer markers, arrives at an incorrect result when the pointer is rotated by 180 degrees, due to the left and right handed system problem. This problem will be solved when the retroreflective markers are replaced with infrared LEDs, as the LEDs emit an infrared beam, which does not extend much more than 30 degrees from the beam's main axis, and therefore can only be viewed from "one" direction.

The marker configuration would also have to be changed, so that the plane through the three markers, is not orthogonal to the actual pointer. If one marker obscures another, due to the manner in which the pointer is positioned, the system would not be able to identify the individual markers. In figure 9.8 the present and future pointer configurations are displayed.

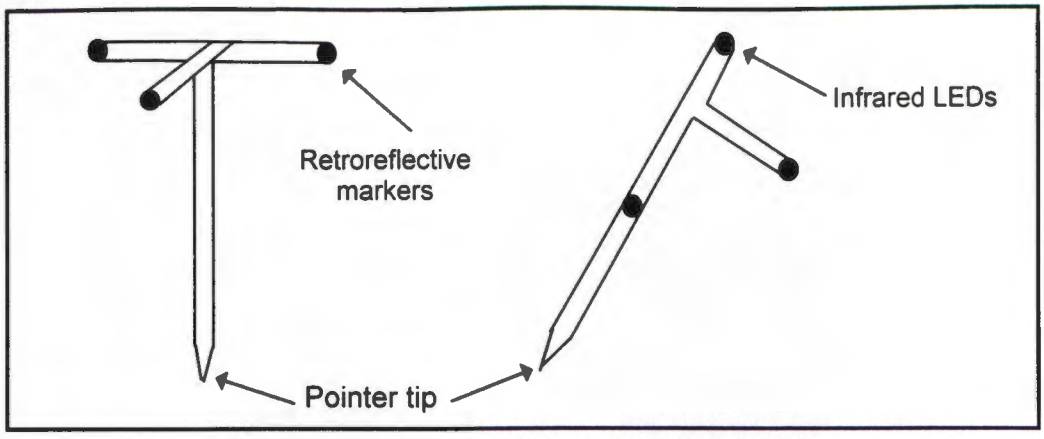


Figure 9.8 The present and future NSA pointer design

One criteria applies to both the present and future configuration of the pointer markers - the distances between the markers must not be equidistant, as the different distances between the markers are used to identify the individual markers. The three pointer markers and the pointer tip are coordinated in the reflex metrograph (Scott, 1981), the distances between the markers calculated and the data written into the software.

The procedure for coordinating the external markers using the NSA system, begins with setting the threshold value. For this purpose the pointer is simply held so that the pointer markers are "visible" to both cameras. This image is captured and thresholded in the same manner as the image of the control frame was thresholded. The threshold value is set so that preferably only the pointer markers remain white against the black background. Other white spots, remaining in the field, are not too problematic, as they are "weeded" out at a later stage by the software. As with the control frame image, the boundary between the left and right part of the stereo image needs to be identified. (The position of this boundary will be identical to the one on the control frame image, as the cameras are not disturbed once the control procedure has been completed. The reason for repeating this procedure is that the thresholding and the boundary setting is done in the same subroutine, and this subroutine is used for both the control image and the external marker image routine.)

Once the threshold and boundary value have been set, the External Marker Fix routine is run to coordinate the external markers. The external markers have to be fixed in the order in which their 3D CT coordinates were entered into the PC, that is in ascending order. The user is prompted to enter the number of the first external marker. Once this has been done the software calls a subroutine called MARKER, passing the external marker number to the subroutine. This subroutine is responsible for determining the 3D coordinates of the pointer tip.

The subroutine MARKER begins by prompting the operator whether Live or Memory video is to be used. If the Ext Marker Fix routine has not yet been run, the operator selects the Live video option, so that the images being picked up by the cameras are displayed on the Philips monitor. The pointer tip is placed on the first external marker to be coordinated, and the image is captured and saved using the patient's name and the external marker umber, for example marker 1 is saved as SMITH1o.tga (the o indicating an object image, rather than a control image). The reason for including an option of Live or Memory video at the start of the subroutine MARKER, is that if the Ext Marker Fix needs to be rerun at a later stage, if only to obtain a printout of the calculations for the records, the saved images are used.

The IP8 card is switched to Memory Video and the captured image displayed on the Philips monitor. The automatic target detection is employed to find any markers appearing in both the left and right part of the stereo image. The centre of gravity algorithm is used to determine the centre of each marker to sub pixel accuracy.

To be able to calculate the 3D pointer marker coordinates, the pointer markers appearing in the left part of the stereo image have to be matched to their corresponding pointer markers appearing in the right part of the stereo image. This is done mathematically using the DLT equations (equations C.3 to C.6 in Appendix C). As stated in Appendix C, the four equations, C.3 to C.6, are normally used to determine the 3D coordinates of a marker. However the 3D coordinates of a marker can be calculated using only three of the equations, either using equations C.3, C.4 and C.5 together, or using equations C.3, C.5 and C.6 together. Both combinations will yield very similar 3D coordinates, and will also be very similar to the 3D coordinates calculated using all four equations. This is used by the External Marker Fix routine to correctly match the marker on the left part of the stereo image to its corresponding marker on the right part of the stereo image.

Using equation C.3, C.4 and C.5, a marker on the left image is matched to every marker on the right image of the stereo image, and their 3D coordinates calculated. The same procedure is repeated using equations C.3, C.5 and C.6. The two sets of 3D coordinates are compared, and if any of the 3D coordinates agree within 1mm in X and Z and 5mm in Y, that particular marker combination from the left and right image is recalculated using all four equations C.3 to C.6, thus obtaining 3D coordinates for that marker combination. It may occur that more than one marker on the right could be matched to the marker on the left, if the markers on the right fall on the same epipolar line (Karara, 1989). Any additional and incorrectly calculated 3D coordinates for the markers are "weeded" out by the software, using the known distance between the pointer markers.

The pointer markers then have to be labelled, using the known distances between the markers. For example, if the distances from one unlabelled marker to two other unlabelled markers are within 2mm of the known distances a and b in figure 9.9, then that one unlabelled marker is marker 1 in figure 9.9. This procedure is repeated until all the markers are labelled.

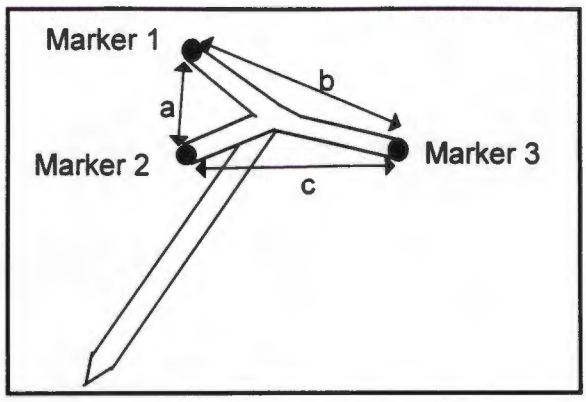


Figure 9.9: The known distances between the pointer markers

Using the 3D coordinates of the pointer markers in the theatre system, and in the reflex metrograph system, transformation parameters between the two systems are calculated using the Rodrigues transformation, and the 3D coordinates of the pointer tip are transformed from the reflex metrograph system to the theatre system. The resultant 3D coordinates of the pointer tip are also the 3D coordinates of the external marker.

As a check to ensure that all pointer markers have been identified correctly, the resulting precisions arising from the Rodrigues transformation between the theatre and metrograph system, are printed on screen. Should a marker have been identified incorrectly, the resultant precisions will be large. Before using the system in clinical trials, this procedure should be automated - if the precisions are not satisfactory, the pointer marker fix should automatically be repeated.

Another check has also been incorporated, in that the DLT equations are used "in reverse" to calculate the left and right 2D image coordinates from the 3D coordinates calculated for the pointer markers. Using these 2D image coordinates, the positions of the pointer markers are annotated and labelled on the left and right parts of the stereo image. These annotated positions should coincide with the pointer markers on the image. With the new pointer design, the user will also be able to check that, not only have the markers been correctly detected, but also correctly labelled, as the configuration of the new pointer allows the user to distinguish between individual markers.

The subroutine MARKER to detect, coordinate and label all the pointer markers, and to determine the 3D coordinates of the pointer tip, works extremely well. From the time the image of the pointer is captured to the time the pointer tip has been calculated takes less than 2 seconds. The only situation the subroutine MARKER cannot handle, is when the pointer markers are too close or overlapping. With the revised marker configuration of the new pointer, this problem should no longer occur. If the routine is not successfully executed, due to overlapping markers, the user is informed of this by the software, and the fix for that particular external marker is simply repeated. With the present pointer this problem was usually avoided by simply watching the Live Video output of the pointer on the Philips monitor and rotating the pointer until all three markers could clearly be seen, before capturing and saving the stereo image of pointer.

The External Marker Fix routine repeats the procedure for coordinating external markers until all external markers have been coordinated in the theatre system and the 3D coordinates of the external markers are written to a file for use by the NSA menu option CT Roddies. CT Roddies carries out the procedure of transforming the theatre system into the CT system. The 3D coordinates of the external markers in the CT and theatre system are used in the Rodrigues transformation to determine the transformation parameters between the two systems. Using these transformation parameters, the 3D coordinates of the control markers (which were measured in the reflex metrograph and determine the theatre coordinate system) are transformed into the CT system.

Using the menu option Redo CCD Params, the CCD camera parameters are recalculated, using the new 3D coordinates of the control markers in the CT system. The result of this procedure is, that any point that falls within the area previously occupied by the control frame, and is "visible" to both cameras, can be coordinated in the CT coordinate system. In other words, the theatre system and the CT system are now coincident.

## 9.6 SINGLE POINT FIXATION WITHIN THE CRANIUM

Once the theatre and CT systems are coincident, the neurosurgeon can proceed with the open craniotomy procedure. When the neurosurgeon wishes to identify a specific point within the cranium on the CT slices, the NSA menu option Pointer Tip Fix is employed.

The Pointer Tip Fix routine also makes use of the subroutine MARKER, and when calling the subroutine, passes a zero to it. The operator of the NSA system selects the LIVE image option, and once the neurosurgeon has placed the pointer tip on a specific intracranial point, the stereo image of the pointer is captured and saved as SMITH0o.TGA. (The zero passed to the subroutine MARKER is appended to the patient's name, and indicates an image that has been captured in the Pointer Tip Fix routine.) The subroutine then detects, coordinates and labels the pointer markers and determines the 3D coordinates of the pointer tip, which are also the 3D coordinates of the intracranial point. As the theatre and CT system are now coincident, the 3D coordinates of the intracranial point are 3D CT coordinates.

The next stage of the Pointer Tip Fix routine is to refresh the Philips screen by clearing the camera images off the screen, and displaying the CT surviews and pseudogram using the subroutine FIRST (see chapter 9.3.4). The CT slice nearest to the intracranial point has to be determined and displayed on the Philips screen. The position of the intracranial point has to be marked on the pseudogram and on CT slice, and the position of the CT slice marked on the CT surviews.

To be able to determine the CT slice nearest to the intracranial point, the patient data text file, i.e. SMITH.TXT, is scanned for all the CT slice numbers and their corresponding Z coordinates. The CT slice, with the Z coordinate closest to the Z coordinate of intracranial point, is selected. If CT slices, with 2mm slice thicknesses, were scanned at intervals of 5mm through the region of the brain effected by the open craniotomy, the closest CT slice to the intracranial point would, at maximum, be 2.5mm off from the most desirable slice position to display that intracranial point. (In the area of the lesion, CT slices are normally scanned at 2mm intervals.)

Once the CT slice has been selected, it is displayed on the Philips screen, and the CT slice number is displayed in the upper left corner of the CT slice. Using the correction factors determined in Appendix L, the CT X and Y coordinates of the intracranial point are converted into IP8 X and Y coordinates. A cursor is drawn at the IP8 X and Y coordinates to mark the position of the intracranial point on the CT slice. The subroutine PSEUDODOT draws the intracranial point on the left and right image of the pseudogram, so that the 3D relationship

between the intracranial point and the lesion and cranial outlines of the patient can be ascertained. The position of the CT slice is marked on both the AP and LAT surviews.

The neurosurgeon can now see the position of the intracranial point on the CT slice, and see where the CT slice was scanned in relation to the patient's head on the CT surviews. Once the neurosurgeon has extracted the necessary information from the marked position of the intracranial point on the CT slice, the operator quits the SINGLE POINT FIX subroutine. The NSA menu is displayed on the PC screen, the Philips screen is cleared and the subroutine FIRST displays the pseudogram and the CT surviews on the Philips screen.

Should for some reason, prior to the next SINGLE POINT FIX, the neurosurgeon wish to re-examine the last intracranial point, the SINGLE POINT FIX routine is run, this time selecting the Memory video option. The subroutine MARKER recalls the image SMITH0o.TGA and simply reruns the whole procedure, until the intracranial point is marked on the relevant CT slice. Only the last intracranial point can be re-examined, as the routine saves the images under the same file name, thus continually overwriting the image file SMITH0o.TGA.

From the neurosurgeon's point of view, the procedure is very simple. He simply places the pointer tip on the intracranial point he wishes to see on the CT slice. Once the operator has captured the image, which takes a fraction of a second, the pointer can be moved, while the software performs the calculations. The calculations and the marking of the intracranial point on the relevant CT slice and pseudogram, and the marking of the CT slice on the CT surviews, take approximately 2 seconds (and this on a 1992 486 PC running at 33MHz).

## 9.7 PHANTOM TRIALS FOR THE ACCURACY DETERMINATION OF THE NSA SYSTEM

To establish the accuracy of the NSA system, the ring phantom (figure 7.2) was once again employed. As described in chapter 7.3, the ring phantom has three leg markers embedded in the upper ring and 12 lesion markers mounted at various heights above the bottom plane (all markers consist of 2mm ball-bearings). The markers were all measured in the reflex microscope and compared to the CT scan coordinates - see table 7.1 & 7.2 of chapter 7.3.

The CT procedure for the ring phantom included scanning an AP and LAT surview and CT slices through the three leg markers and the 12 lesion markers. The CT software was used to digitise all the markers on the CT slices.

The first phantom trial, using only the three external markers, did not yield as good a result as expected. A fourth "external marker" was made on the ring phantom, by drawing a single dot on the upper ring, and the four markers were measured in the reflex microscope. By using the three external markers, common to both the CT and reflex microscope system, 3D CT coordinate values were calculated for the fourth "external marker" using the Rodrigues transformation. The standard deviations for the Rodrigues transformation precisions in X, Y and Z were 0.4mm, 0.0mm and 0.2mm respectively. In the other three phantom trials, the sixth lesion marker was used as an external marker. As the phantom was only scanned once in the CT scanner, all four trials made use of the same CT images and CT data.

The file, containing all the CT images, was transferred to the PC using the procedures described in chapter 9.3.1. The CT images were extracted from the file and converted into IP8 compatible format, using the menu option Conv. CT Images. The Surview Select menu option was run to select the AP and LAT surview images, and the Digitise Lesion option run to digitise the "lesion". In the ring phantom case, on four of the CT slices the outer area of the phantom was digitised to simulate digitising the outline of the patient's head, and small squares were digitised around the outer edges of the lesion markers. This was only done for four slices, as in a clinical situation a lesion would not span more than four or five CT slices. Also, if too much information is digitised, the 3D image can not be visualised, as the pseudogram just becomes a mass of indistinguishable lines. The Dig & Surview recall menu option draws the pseudogram and places the surviews on the Philips screen.

The CT data input menu option is used to enter the 3D CT coordinate data of the external markers into the software, and the menu option Marker check is run to check that the external marker coordinates have been entered correctly.

Once all these procedures have been completed, the NSA system is ready to be used in theatre. In the phantom trials the cameras are set up on a sturdy base in the laboratory. The baselength is 1.6m and the distance to the operating table is 2.0m. These distances may have to be changed once testing begins in theatre. An ordinary table is used to model the theatre bed, and the control frame is placed on the table. Once the cameras have been adjusted, the stereo image of the control frame is captured. Once the threshold values for the control image have been set, the automatic target detection is employed to coordinate all the control markers. The menu option CCD Params is used to calculate the CCD camera parameters. The precisions for the control markers are shown in table 9.3.

| No. of the Control Marker | dX (mm) | dY (mm) | dZ (mm) | Vector differences (mm) |
|---|---|---|---|---|
| 1 | 0.0 | -0.1 | 0.4 | 0.4 |
| 2 | -0.2 | 0.1 | 0.7 | 0.7 |
| 3 | -0.2 | -0.2 | 0.2 | 0.3 |
| 4 | -0.1 | -0.4 | 0.3 | 0.5 |
| 5 | 0.0 | 0.1 | -0.3 | 0.3 |
| 6 | 0.2 | -0.1 | 0.2 | 0.3 |
| 7 | 0.2 | 0.2 | -0.7 | 0.8 |
| 8 | 0.0 | 0.0 | -0.5 | 0.5 |
| 9 | 0.0 | -0.1 | -0.3 | 0.3 |
| 10 | 0.0 | -0.2 | -0.2 | 0.3 |
| 11 | 0.3 | -0.1 | 0.6 | 0.7 |
| 12 | 0.5 | 0.6 | 0.9 | 1.2 |
| 13 | 0.2 | 0.1 | 1.0 | 1.0 |
| 14 | 0.4 | 0.3 | 0.2 | 0.5 |
| 15 | 0.3 | 0.2 | 0.4 | 0.5 |
| 16 | -0.1 | 0.2 | 0.3 | 0.4 |
| 17 | 0.3 | -0.3 | 0.4 | 0.6 |
| 18 | 0.2 | -0.1 | -0.1 | 0.2 |
| 19 | 0.7 | -0.5 | 0.0 | 0.9 |
| 20 | -0.3 | 0.2 | -0.2 | 0.4 |
| 21 | -0.1 | 0.0 | 0.2 | 0.2 |
| 22 | -0.7 | -0.1 | 0.4 | 0.8 |
| Std. Dev. | 0.3 | 0.2 | 0.4 | 0.3 |

Table 9.3: The precisions for the control frame markers

To transform the theatre system into the CT system, the four external markers have to be coordinated in the theatre system using the External Marker Routine. The pointer is pointed at each external marker in turn and the camera stereo image captured. In figure 9.10, the pointer tip is in contact with one of the external markers on the Taylor halo.

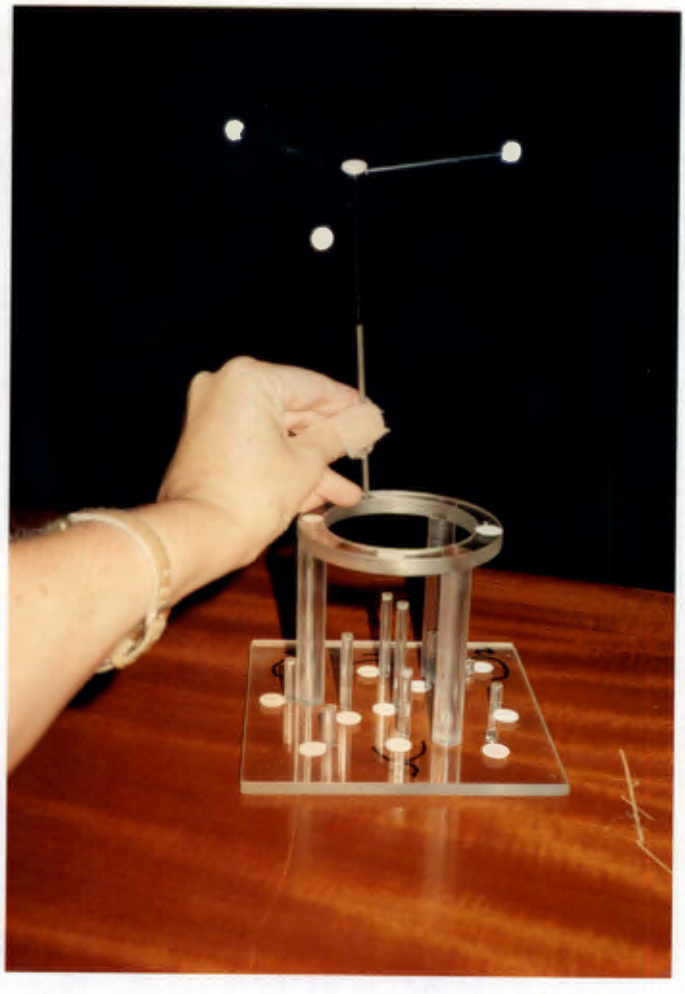

Figure 9.10: The pointer tip in contact with an external marker on the Taylor halo

For each external marker, the subroutine MARKER detects, coordinates and labels the pointer markers on that image. The subroutine MARKER then determines the 3D coordinates of the pointer tip, using the Rodrigues transformation and the 3D coordinates of the pointer markers in the theatre and reflex metrograph system. The resulting transformation precisions (arising from transforming the 3D coordinates of the three pointer markers from the reflex metrograph system to the theatre system) and their standard deviations are listed for each external marker fix in tables 9.4.

| Transf. precisions & Std. Dev. for fixing external marker 1 | | | |
|---|---|---|---|
| No. of pointer marker | dX (mm) | dY (mm) | dZ (mm) |
| 1 | 0.4 | -0.2 | 0.2 |
| 2 | 0.0 | 0.4 | -0.7 |
| 3 | -0.4 | -0.2 | 0.4 |
| Std. Dev. | 0.4 | 0.3 | 0.6 |

| Transf. precisions & Std. Dev. for fixing external marker 2 | | | |
|---|---|---|---|
| No. of pointer marker | dX (mm) | dY (mm) | dZ (mm) |
| 1 | 0.0 | -0.2 | 0.3 |
| 2 | 0.1 | 0.4 | -0.5 |
| 3 | -0.1 | -0.1 | 0.2 |
| Std. Dev. | 0.1 | 0.3 | 0.4 |

| Transf. precisions & Std. Dev. for fixing external marker 3 | | | |
|---|---|---|---|
| No. of pointer marker | dX (mm) | dY (mm) | dZ (mm) |
| 1 | 0.1 | -0.1 | 0.2 |
| 2 | 0.0 | 0.3 | -0.4 |
| 3 | -0.1 | -0.2 | 0.2 |
| Std. Dev. | 0.1 | 0.3 | 0.3 |

| Transf. precisions & Std. Dev. for fixing external marker 4 | | | |
|---|---|---|---|
| No. of pointer marker | dX (mm) | dY (mm) | dZ (mm) |
| 1 | 0.4 | -0.2 | 0.1 |
| 2 | 0.0 | 0.3 | -0.4 |
| 3 | -0.4 | -0.2 | 0.3 |
| Std. Dev. | 0.4 | 0.3 | 0.4 |

Table 9.4: Transformation precisions and standard deviations for fixing external markers

Once all the external markers have been coordinated in the theatre system, the Rodrigues transformation uses the 3D coordinates of the external markers in the theatre and CT system to calculate the transformation parameters between the two systems. The Rodrigues transformation precisions are listed in table 9.5.

| No. of external marker | dX (mm) | dY (mm) | dZ (mm) |
|---|---|---|---|
| 1 | -0.1 | 0.0 | 0.6 |
| 2 | 0.4 | 0.0 | -0.3 |
| 3 | -0.3 | 0.0 | -0.1 |
| 4 | 0.0 | 0.0 | -0.2 |
| Std. Dev. | 0.3 | 0.0 | 0.4 |

Table 9.5: Transformation precisions between the theatre and CT system, using the four external markers

The transformation parameters are used to transform the control markers from the theatre system to the CT system. The CCD camera parameters are recalculated, using the new control marker coordinates. The resulting precisions are very similar to those listed in table 9.3. The standard deviations of the precisions in X, Y and Z are 0.3mm, 0.2mm and 0.4mm respectively.

All lesion markers were treated as intracranial points to be fixed. Once the image of the pointer pointing at the lesion marker was captured, the 3D coordinates were calculated using the subroutine MARKER. The differences in the 3D coordinates of the lesion markers obtained by the NSA system and those measured in the CT scanner, are listed in table 9.6.

| No. of lesion marker | dX (mm) | dY (mm) | dZ (mm) | Vector differences (mm) |
|---|---|---|---|---|
| 1 | -0.7 | -0.8 | 2.0 | 2.3 |
| 2 | 1.1 | -1.7 | 1.9 | 2.8 |
| 3 | 0.6 | -1.4 | 2.4 | 2.8 |
| 4 | -0.3 | -0.8 | 1.5 | 1.7 |
| 5 | -0.8 | -0.5 | 1.5 | 1.8 |
| 6 | -1.5 | -1.0 | 2.0 | 2.7 |
| 7 | 0.2 | -0.9 | 1.1 | 1.4 |
| 8 | 0.0 | -1.0 | 1.1 | 1.5 |
| 9 | 0.5 | -0.3 | 1.4 | 1.5 |
| 10 | -0.4 | -0.9 | 1.5 | 1.8 |
| 11 | -1.7 | -1.5 | 1.9 | 2.9 |
| 12 | -0.3 | -2.8 | 1.2 | 3.1 |
| Mean | -0.3 | -1.1 | 1.6 | 2.2 |
| Std. Dev. | 0.8 | 0.7 | 0.4 | 0.6 |

Table 9.6: Comparing 3D coordinates of the lesion markers obtained in the NSA system and the CT scanner

Once the 3D coordinates of an intracranial point (lesion marker) had been determined, the CT slice closest to the intracranial point was determined and its position marked on the slice; the position of the CT slice was marked on the CT surviews; and the position of the intracranial point was marked on the pseudogram (see figure 9.11).

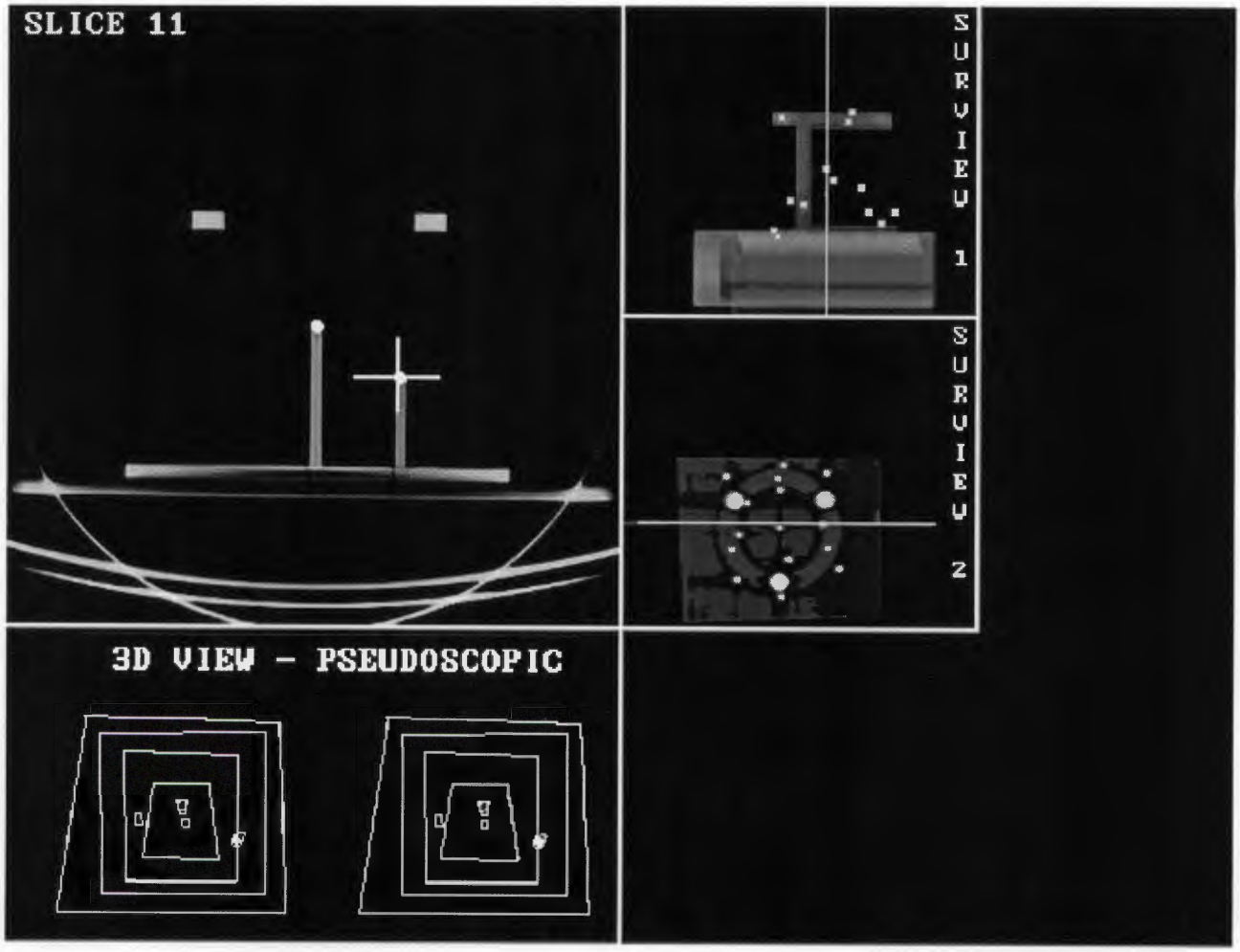


Figure 9.11: The Philips screen showing the ring phantom displayed on the CT slice, CT surviews and pseudogram

In table 9.7, abbreviated results of all the four phantom trials are listed. Trial 1 is the phantom trial that has just been described, i.e. using a dot drawn on the Taylor halo as the fourth external marker, and has been included in table 9.7 for ease of comparison. Trial 2 to 4 are the phantom trials, where the fourth external marker is represented by the sixth lesion marker. Not all the information from trial 1 is listed in table 9.7, as the precisions and standard deviations for the control markers varied very little from trial to trial. Only the standard deviations are listed to simplify the comparison of one phantom trial with another, with the exception of the comparison of the 3D lesion coordinates in the NSA and CT system, where both the mean and standard deviation are given.

| | TRIAL 1 | | | TRIAL 2 | | | TRIAL 3 | | | TRIAL 4 | | |
|---|---|---|---|---|---|---|---|---|---|---|---|---|
| | dX | dY | dZ | dX | dY | dZ | dX | dY | dZ | dX | dY | dZ |
| Standard Deviations (unless otherwise stated) for: | All values are in millimetres | | | | | | | | | | | |
| Transf. precisions for fixing Marker 1 | 0.4 | 0.3 | 0.6 | 0.6 | 0.2 | 0.3 | 0.4 | 0.3 | 0.6 | 0.5 | 0.3 | 0.4 |
| Transf. precisions for fixing Marker 2 | 0.1 | 0.3 | 0.4 | 0.4 | 0.3 | 0.5 | 0.1 | 0.3 | 0.4 | 0.4 | 0.3 | 0.4 |
| Transf. precisions for fixing Marker 3 | 0.1 | 0.3 | 0.3 | 0.1 | 0.2 | 0.3 | 0.1 | 0.3 | 0.3 | 0.2 | 0.2 | 0.3 |
| Transf. precisions for fixing Marker 4 | 0.4 | 0.3 | 0.4 | 0.5 | 0.2 | 0.2 | 0.3 | 0.2 | 0.6 | 0.6 | 0.2 | 0.2 |
| Transf. precisions between theatre & CT system using 4 external markers | 0.3 | 0.0 | 0.4 | 0.9 | 1.0 | 0.6 | 0.2 | 0.6 | 0.8 | 0.5 | 0.7 | 0.8 |
| **Mean differences -** comparing the 3D lesion coordinates in the NSA & CT system | -0.3 | -1.1 | 1.6 | -0.6 | -0.9 | 1.1 | -0.5 | -1.0 | 0.0 | 0.3 | -1.3 | 0.9 |
| Comparing of 3D lesion coordinates in NSA & CT system | 0.8 | 0.7 | 0.4 | 0.9 | 0.4 | 0.7 | 1.1 | 1.1 | 0.5 | 1.2 | 0.5 | 0.7 |

Table 9.7: Standard deviations, and one set of meaned values, obtained from the four phantom trials

Taking all 48 comparisons of the 3D lesion marker coordinates in the NSA and CT system, the mean differences between the two systems are 0.0mm, -1.1mm, 0.9mm for dX, dY and dZ respectively. The standard deviations of the differences for all 48 observations are 1.1mm, 0.7mm and 0.8mm for dX, dY and dZ respectively. The mean vector error for all 48 observations is 1.9mm, with a standard deviation of 0.7mm (not listed in table 9.7).

The coordinate comparisons, from comparing the 3D lesion coordinates in the NSA & CT system, that yielded coordinate differences greater than 2mm were:

- the Z coordinate difference of marker 10 for trial 4 was 2.1mm,
  the X coordinate difference of marker 11 for trial 3 was -2.1mm - neither of the two differences is excessively large

- the Y coordinate differences for lesion marker 12, which ranged from -2.8, -1.5, -3.7, and -2.5 for trials 1, 2, 3, and 4 respectively, indicates a systematic error, which could be due to an incorrect digitisation of marker 12 at the CT scanner stage.

- the Z coordinate difference for marker 3 in trial 1 was 2.4mm,
  the X coordinate difference for marker 3 in trial 4 was 3.3mm - examining the dX, dY and dZ coordinate differences for marker 3 for the four trials showed the errors to be random.

## 9.8 DISCUSSION

The mean vector difference and standard deviation, calculated from the precisions for the control frame markers (table 9.3), were 0.5mm and 0.3mm respectively. The NSA 3D measuring system can therefore coordinate a point in space with vector errors of less than 1mm. The mean vector error and standard deviation for the NSA system to coordinate an intracranial point, when using both the CT images and the pointer, is 1.9mm+/-0.7mm.

The accuracy of the NSA system is similar to the accuracies obtained for the sonic and stereotactic frame systems, especially when taking into account that all the CT images, used by the NSA system, were scanned with 2mm CT slice thicknesses. (Application accuracies (vector differences) for sonic and stereotactic frame systems ranged from 1.5mm+/-0.7mm to 1.9mm+/-1mm for 1mm thick CT slices, and 2mm+/-0.5mm for 1.5mm thick CT slices - see chapter 8.4).

There seems to be a definite shift in both the Y and Z coordinates axes between the two systems, as indicated by a mean Y difference of -1.1mm and a mean Z coordinate difference of 0.9mm. Only one Y coordinate difference was greater than 0mm, with a value of 0.3mm and 42 of the Z coordinate differences were greater than 0mm. The problem may be due to the fact that the four phantom trials undertaken in this chapter all obtained their CT images and CT data from a single CT scanning session of the phantom, and the error may be inherent in that particular CT procedure. Whatever the cause, the problem will have to be solved in future phantom trials, by rescanning the phantom for each individual trial. Once further phantom trials have been carried out, it may be necessary to apply correction factors to all the NSA Y and Z coordinates. The phantom trials will also have to be carried out, using the new pointer design with the infrared LED markers and the new marker configuration, to ascertain what effect this will have on the accuracy of the NSA system.

The neurosurgeon has to be aware of the limitations of the NSA system, to be able to use it effectively. Beside being aware that any intracranial point fixed by the NSA system may be in error by approximately 2.5mm, the neurosurgeon must also be aware that the intracranial point is displayed on the nearest CT slice, even though it may not fall on that CT slice. Therefore the difference between the Z coordinate of the intracranial point and the CT slice, should be displayed on the Philips screen. This will give the neurosurgeon the necessary perspective of the Z coordinate difference between the CT slice displayed and the intracranial point.

Beside adding the Z difference to the Philips screen, the name of the patient and the date of the CT scan procedure should be displayed. This will ensure that the correct patient images are used, and if more than one CT procedure has been done of the patient, that the correct CT procedure is displayed. As the bottom right corner of the Philips screen is blank, when CT images are displayed (see figure 9.11), there is ample space to display the above data.

Although a minimum of three external markers is all that is required to set up the NSA system, much better results were achieved using four markers. To further improve the accuracy of the NSA system, and to reduce some of the outliers, it may be advisable to even use five external markers. Beside the three external markers in the Taylor halo, two others external markers should be placed on the patient's scalp, so that they provide a good geometrical fix. Beside providing for a better geometrical fix, the additional markers allow for an overdetermined solution.

Once the open craniotomy is begun, the external marker configuration is usually destroyed, as the markers have to be removed prior to opening the cranium. The patient's head is kept immobile throughout the surgical procedure, by clamping the patient's head in the Mayfield clamp. If at some stage during the procedure, the neurosurgeon has to move the patient's head, the theatre/CT system is destroyed. As the external markers are no longer in place, it is impossible to reconstruct the CT coordinate system. This problem can be overcome if a series of markers are placed on the Mayfield clamp, as the Mayfield clamp, the patient's head and the operating table move as one rigid body. These Mayfield markers have to be coordinated in the theatre/CT system using the pointer, and this procedure has to be carried out after the external marker fix routine and prior to the open craniotomy. Using the 3D CT coordinates of the Mayfield markers, the theatre/CT system can be reconstructed at any stage and the surgical procedure continued. This is an option that should be included in the NSA system before starting theatre trials.

The pseudogram is the weakest part of the NSA system, and definitely needs some revision, if not a completely different approach. Not all the neurosurgeons can see pseudoscopically, and the pseudograms are very primitive at present and the depth visualisation is not too good. It may be necessary to investigate the use of 3D glasses, to give the neurosurgeons a good three dimensional perspective.

## 9.9 CONCLUSIONS

The NSA system has the potential of fulfilling the neurosurgeon's request of identifying points within the cranium on CT slices of the patient during an open craniotomy, with very little expense to the neurosurgeon, if existing equipment is to be used.

If the neurosurgeon requires a dedicated system, the cost of the hardware is not exorbitant. The NSA system still needs to undergo some vigorous testing and some adjustments to improve its usability and accuracy. The accuracy already achieved by the system makes it extremely feasible that the necessary accuracy, for using the NSA system in the clinical environment, will be achieved.

At present, the NSA system is what its name implies, a neurosurgical aid system. Once the 3D presentation of the lesion, in relation to the patient's cranium, has been improved, it is not too great a step to upgrade the NSA system to a full neuronavigational system. The planning of the surgical route to the lesion would be done prior to the operation, and this route would be represented on the 3D display of the lesion, in relation to the patient's cranium. By simply following the route on the 3D display, the neurosurgeon would reach the lesion with minimal disturbance to the brain. As the exact position at which the neurosurgeon is working can be identified on both the 3D display and on the CT slices, the whole of the lesion can successfully be removed.

## CHAPTER 10 CONCLUSIONS

The aim of this thesis has been to develop a simple stereotactic device, which is accurate, cost-effective, easy to use and patient friendly, and which neurosurgeons in African/Third World countries could utilise to perform stereotactic procedures, without the necessity of being stereotactic specialists. This aim has been achieved in the final design of the Cape Pointer - a very simple/ basic, yet elegant, solution to the stereotactic problem.

To use the Cape Pointer, the neurosurgeon simply attaches the light-weight Taylor halo to the patient's head, using either two small self-tapping screws or silk sutures, so that the Taylor halo surrounds the area in which the entry point will be placed. The patient is made comfortable on the CT bed, with his/her head resting in the head support, and asked to keep as still as possible during the procedure. The CT scanner is used to coordinate the three radio-opaque markers, embedded in the Taylor halo, and the intracranial point selected by the neurosurgeon. The first marker is re-scanned to verify that the patient has not moved during the CT scanning procedure. The coordinates are typed into a PC containing the Cape Pointer software, and the software, once having carried out all the necessary checks, prints out the three translations, which are set on the Fieggen phantom. The Cape Pointer is placed on the phantom with all its clamps loosened. A long pointer is inserted into the Cape Pointer's sleeve and manoeuvred until its tip is coincident with the phantom marker. The clamps are tightened and the distance from the phantom marker to the top of sleeve is determined by attaching the depth stop to the pointer where it exits the Cape Pointer sleeve. This effectively completes setting the Cape Pointer and it is ready for theatre.

Due to the design of the Cape Pointer and the Fieggen phantom, any trajectory to any number of intracranial points can be utilised, so long as they are in the mechanical range of the Cape Pointer and the Fieggen phantom. The only criteria is that the various intracranial points are digitised on the CT slices, and the translations that need to be set for that intracranial point are calculated. No entry point has to be marked on the patient's head prior to scanning, and setting the Cape Pointer for a specific entry point is a simple mechanical exercise using the entry point simulation device. The setting of the Cape Pointer can easily be altered in theatre using the Fieggen phantom, as the phantom is sterilised along with all the other surgical instrumentation required in theatre. The Cape Pointer can be utilised with any CT scanner, as the software will determine the correct translations (and setting diagram), irrespective of the type of coordinate system employed by the CT scanner.

The Cape Pointer is extremely easy to use, and the neurosurgeons, in conjunction with the radiotherapists running the GSH scanner, perform all the aspects of the stereotactic procedure. An important aspect of the Cape Pointer, and for that matter any medical device, is to ensure that all the checking routines have been carried out, and that where necessary they have been counter-checked by a second person; for example, the radiotherapist counter-checking the transfer of coordinates from the CT scanner to the PC, and the theatre sister counter-checking the translations set on the Fieggen phantom, when the phantom is reset in theatre.

When comparing the Cape Pointer to other well known stereotactic devices, it is approximately only a quarter of the size of most of its counterparts and only weighs 150grams. It does not require a frame to be bolted to the patient's head, nor a fiducial localising system to determine the geometrical relationship between the CT scanner and the stereotactic frame. In contrast to the frame-based systems, where six to nine fiducial marks have to be coordinated on each slice, only four points need to be coordinated for the setting of the Cape Pointer - the three external markers and the intracranial point. In comparison to other stereotactic devices, the Cape Pointer does not have a single micrometer, vernier, graduated circle or axis. The only three graduated axes are on the Fieggen phantom for setting the three translations calculated by the Cape Pointer software, thus making the setting of the Cape Pointer and Fieggen phantom a simple exercise, compared to some of the other stereotactic frames.

Having reviewed other stereotactic devices, the Cape Pointer is definitely the most simple, yet is achieving the accuracies of its much more sophisticated counterparts. From Galloway et al (1991) the mean vector errors and standard deviations determined for four well known frame-based stereotactic devices using 1mm slice thicknesses, ranged from 1.0mm+/- 0.6mm to 1.9mm+/-1.0mm, with maximum values ranging from 3 to 5mm. The accuracy of setting the Cape Pointer with the Fieggen phantom is 1.9mm +/- 0.6mm (table 7.4), and with the setting diagram 1.8mm +/- 0.3mm (table 7.3). Even taking into account that the mean vector errors and standard deviations for the Cape Pointer have been determined from small sample groups, and therefore may alter slightly for larger sample groups, such as used by Galloway et al (1991), it has been shown that the Cape Pointer is achieving comparable accuracies.

The accuracies of the Cape Pointer are dependent on the patient remaining still during a CT scan. The light-weight Taylor halo, temporarily attached with two small screws or sutures and therefore causing minimal inconvenience to the patient, can not be used to constrain the patient, as is the case with the frame-based stereotactic systems. Every precaution is

taken to ensure that the patient does not move during the CT procedure, and if any movement occurs, the scanning procedure is repeated. As the whole scanning procedure takes less than 15 minutes, this does not present too much of a problem. However, it may be advisable to investigate some manner of gently restraining the patient during the CT procedure, without the necessity of indirectly bolting the patient's head to the CT bed utilising a stereotactic frame.

The SPG system was designed to allow the patient freedom of movement during the CT procedure and nevertheless determine 3D coordinates of the external markers and intracranial points from which all patient movement had mathematically been removed. The SPG system achieves this objective by making the SPG and CT coordinate system coincident. Any movement made by the patient is quantified by the SPG system, and applied to the CT system, thus obtaining corrected CT coordinates, from which any patient movement has mathematically been removed. To assist in this process, the SPG system utilises the surview equation (chapter 3). Instead of scanning slices through the Cape Pointer's external markers and the SPG's four tracking markers, one AP and LAT surview are scanned, and utilising the surview equation, the 3D CT coordinates of the external markers and tracking markers are determined. As the LAT surview is scanned after the patient/phantom has moved, the LAT surview has to be corrected for patient movement, prior to determining the 3D CT coordinates from the AP and corrected LAT surview. The resultant 3D coordinates of the Cape Pointer markers and the SPG tracking markers were compared to their 3D CT coordinates, digitised prior to any movement taking place. This resulted in mean errors and standard deviations of 0.0mm+/-0.4mm, 0.6mm+/-0.9mm and -0.8mm+/-0.7mm in X, Y, and Z respectively (table 6.5), i.e. a vector error of 1mm+/-1.2mm. The lesion centre marker 3D CT coordinates were corrected for any phantom movement, and then compared to the 3D CT coordinates digitised prior to any phantom movement taking place. The differences in X, Y, and Z were .2mm, 0.4mm and 1.3mm respectively (table 6.7) - a vector error of 1.4mm. The Cape Pointer, set with the aid of the setting diagram produced from the corrected 3D CT coordinates, resulted in the pointer being approximately 1mm off course and extended past the lesion centre marker by 2mm. The above results, not only verify that the survey equation can be utilised to determine 3D CT coordinates from CT surviews with good accuracy, but also show that the SPG system is capable of mathematically removing patient movement from CT data, so that the Cape Pointer can still be set within the accuracy expected from frame-based stereotactic systems.

Although the SPG system has achieved its aims admirably with an intracranial point "hit rate" of approximately 2mm, it proved too time consuming and unwieldy in its present format. It was felt that unless the neurosurgeons could direct all the operational steps themselves, the

Cape Pointer would never progress past the research phase, and so the SPG system was set aside, and the Cape Pointer developed as a stand alone stereotactic device. To make the SPG system a viable option for correcting patient movement during a CT procedure, it would have to be set up on a permanent basis in the CT room, and streamlined to operate semi-automatically and in near real time. The Cape Pointer, without the SPG system, is an accurate stereotactic device, and as it has been designed to assist African/Third World neurosurgeons, it would be counter productive to combine it with the SPG system, as this would increase both the cost and expertise required. This does not invalidate the SPG system and its concept may be used in other CT or stereotactic applications.

Some alterations could still be made to the Cape Pointer and the Fieggen phantom to widen its range of applications. The Cape Pointer is presently only used with CT scanners. However, as the only part of the Cape Pointer that "interacts" with the imaging system is the Taylor halo and the three markers embedded in the Taylor halo, it is a fairly simple matter to make the Taylor halo compatible with MRI by simply altering the type of marker used in the Taylor halo. At present the designs of the Cape Pointer and Taylor halo do not lend themselves for performing open craniotomies, as the area within the halo is far to small for the surgical procedure required. It has been suggested that a Taylor halo consisting of two sections be used. By attaching the two small screws in one section of the Taylor halo, the other section of the Taylor halo could simply be removed. The only criteria would be that the removed section could be exactly replaced when the Cape Pointer was needed to guide the surgical instrument. This procedure would give the neurosurgeon the required space to perform the open craniotomy.

To assist the neurosurgeons in performing an open craniotomy, the Cape Pointer is used to insert a catheter through a burr hole into the cranium to mark the route to the lesion centre. During the craniotomy, the neurosurgeon simply follows the catheter down through the tissues of the brain to the lesion. The NSA system has been developed to further assist the neurosurgeons at Groote Schuur Hospital with open craniotomies. This system, in near real time, identifies the exact intracranial point at which the neurosurgeon is working on the appropriate CT slice.

The CT images are transferred to the NSA PC and converted, so that they can be displayed on the additional monitor when required. With the aid of the two NSA CCD cameras, the external markers, attached to the patient's head prior to CT scanning, are coordinated in the theatre coordinate system. This system is transformed into the CT coordinate system, utilising the external markers. As the tissues of the brain within the cranium are not visible to the two cameras, a long pointer is used to point to various intracranial points. The three

markers, attached to the pointer in a known configuration, are used to coordinate the pointer tip in the theatre system, and therefore also in the CT system. The intracranial point in contact with the pointer tip, is identified on the relevant CT slice, which is displayed on the additional monitor and the intracranial point identified with a flashing cursor. The cycle of fixing the pointer tip within the cranial cavity is repeated when necessary, with a single point fix taking approximately 2 seconds. By continually fixing intracranial points and identifying them on the relevant CT slices, the neurosurgeon is assisted in reaching his destination and removing all of the lesion.

A phantom, with four external and twelve lesion markers, was utilised to test the accuracy of the NSA system. Four trials resulted in a mean vector error and standard deviation of 1.9mm+/-0.7mm for the lesion marker determination, utilising 2mm CT slice thicknesses. The accuracy of the NSA system is within that obtained by sonic and stereotactic frame systems, which range from 1.5mm+/-0.7mm to 1.9mm+/-1mm for 1mm CT slice thicknesses and 2mm+/-0.5mm for 1.5mm CT slice thicknesses. Although the NSA system is achieving the required accuracy, and in near real time, the graphical 3D aspect of the NSA software needs to be improved and further developed. The whole NSA system still needs further adaptation and vigorous testing before being used outside the research environment.

The three systems developed in this thesis, the NSA system, the SPG system and the Cape Pointer, have all achieved the necessary accuracy to be used in various aspects of stereotactic work. Although the SPG system may never be used in conjunction with the Cape Pointer, it may be used as a viable tool for other applications. The NSA system still has to undergo further development to assess how successful it will be in the clinical environment.

The stand alone Cape Pointer has proven itself as a clinical tool in the neurosurgical environment, and represents a simple, yet elegant, solution to the complex stereotactic problem, and may yet come to represent a viable option for the neurosurgeons seeking a cost-effective way of adding a stereotactic string to their surgical bow.

## REFERENCES


Abdel-Aziz, Y.I., Karara, H.M., 1971. Direct Linear Transformation from Comparator Coordinates into Object Space Coordinates. Symposium Close-Range Photogrammetry, American Society of Photogrammetry, Falls Church, Virginia, United States of America: 1-18.

Adams, L.P., Gutschow, B., Tregidga, A., Klein, M., 1990. Near real time studies of regional body surface motion. Close Range Photogrammetry meets machine vision. A Gruen / EP Baltsavias - Editors. PROC SPIE 1395:762-767.

Adams, L.P., 1981. X-ray stereophotogrammetry locating the precise three-dimensional position of image points. Med. and Biol. Eng. and Comput., 19:569-576.

Adams, L.P., 1974. Stereoscopic viewing of image pairs with the naked eyes. Photogrammetric Record, 8(44):229-230 (Abstract).

Alesch, F., 1994. A simple technique for making a stereotactic localiser both CT and MRI compatible. Technical Note. Acta Neurochirurgica, 127:118-120.

Ambrose, J., 1973. Computerised transverse axial scanning (tomography): Part2. Clinical application. British Journal of Radiography, 46, 1023-1047.

Barnett, G.H, Kormos, D.W., Steiner, C.P., Weisenberger, J., 1993a. Intraoperative localization using an armless, frameless stereotactci wand. Technical note. J Neurosurg 78:510-514.

Barnett, G.H, Kormos, D.W., Steiner, C.P., Weisenberger, J., 1993b. Use of a frameless, armless stereotactic wand for brain tumour localization with two-dimensional and three-dimensional neuroimaging. Neurosurgery, Vol 33, No.4:674-678.

Bucholz, R.D., Smith, K.R., 1993. A comparison of sonic digitizers versus light emitting diode-based localization. Pgs 179-200 of Maciunas, R.J.(Editor), 1993. Interactive Image-Guided Neurosurgery. Published by the American Association of Neurological Surgeons, United States of America.

Carol, M., 1986. European Patent 0 207 452. Method and apparatus for performing stereotactic surgery.

Carol, M., 1985. A true "advanced imaging assisted" skull mounted stereotactic system. Appl Neurophysiol 48:69-72.

Castleman, K.R., 1979. Digital Image Processing. Publishers: Prentice-Hall, INC, Englewood Cliffs, New Jersey, United States of America.

Cromwell, L., Weibell, F.J., Pfeiffer, E.A, 1973. Biomedical Instrumentation and measurements, Second Edition. Publishers: Prentice-Hall, INC, Englewood Cliffs, New Jersey, United States of America.

Ditmar C, 1873. Über die Lage des sogenannten Gefässzentrums in der Medulla Oblongata. Ber Saechs Ges Wiss Leipzig (Math Phys) 25:449-469.

Drake, J.M., Prudencio, J., Holowka, S., 1993. A comparison of a PUMA Robotic System and the ISG Viewing Wand for neurosurgery. Pgs 121-133 of Maciunas, R.J.(Editor), 1993. Interactive Image-Guided Neurosurgery. Published by the American Association of Neurological Surgeons, United States of America.

Galloway, R.L., Maciunas, R.J., Latimer,J.W., 1991. The accuracies of four stereotactic frame systems: an independent assessment. Biomedical Instrumentaion & Technology; 25:457-460.

Gildenberg, P.L., Ledoux, R., Cosman, E., Labuz, J., 1994. The Exoscope - A frame-based video/graphics system for intraoperative guidance of surgical resection. Stereotactic Funct Neurosurg, 63:23-25.

Gouda, K.I., Freidberg, S.R, Larsen, C.R., Baker, R.A., Silverman, M.L., 1983. Modification of the Gouda frame to allow stereotactic biopsy of the brain using the GE 8800 computed tomographic scanner. Neurosurgery 13:176-181.

Graham, J.D., Warrington, A.P., Gill, S.S, Brada, M., 1983. A non-invasive, relocatable stereotactic frame for fractionated radiotherapy and multiple imaging. Technical Note. Radiotherapy and Oncology: 1991, Vol 21, Part 1:60-62.

Guthrie, B.L., Adler J.R., 1992. Computer-assisted preoperative planning, interactive surgery, and frameless stereotaxy [Review]. Clinical Neurosurgery. 38:112-131.

Gütschow, B.A., 1990. A near real time photogrammetric PC based system to study the regional body surface motions of human beings during respiration. Master of Science in Engineering Thesis, University of Cape Town, South Africa.

Hansen, A., 1988. Learn C now. Published by: Microsoft Press, A Division of Microsoft Corporation, Redmond, Washington, United States of America.

Heilbrun, M.P., Koehler, S., McDonald, P., Peters, W., Sieminov, V., Wiker, C., 1993. Implementation of a machine vision method for stereotactic localization and guidance. Pgs 169-177 of Maciunas, R.J.(Editor), 1993. Interactive Image-Guided Neurosurgery. Published by the American Association of Neurological Surgeons, United States of America.

Heilbrun, M.P., McDonald, P., Wiker, C., Koehler, S., Peters, W., 1992. Stereotactic localization and guidance using a machine vision technique. Stereotact Funct Neurosurg, 58:94-98.

Heilbrun, M.P., 1988. Stereotactic Neurosurgery. Volume 2: Concepts in Neurosurgery. Editor M.P.Heilbrun, Published by Williams and Wilkins, Baltimore, United States of America.

Heilbrun, M.P., Roberts, T.S, Apuzzo, M.L.J., Wells, T.H., Sabshin, J.K., 1983. Preliminary experience with Brown-Roberts-Wells (BRW) computerized tomography stereotaxic guidance system. J Neurosurg 59:217-222.

Horner, N.B., Potts, D.G., 1984. A comparison of CT-Stereotaxic Brain Biopsy Techniques. A special review article. Invest Radiol 1984;19:367-373.

Horstmann, G.A., Reinhardt, H.F, 1994. Ranging accuracy test of the sonic microstereometric system. Neurosurgery, Vol 34, No 4: 754-755.

Hounsfield, G.N., 1973. Computerized transverse axial scanning (tomography): Part 1. Description of the system. British Journal of Radiology, 46:1016-1022.

Kandel, E.I., Schavinsky, U.V., 1972. Stereotaxic apparatus and operations in Russia in the 19th century. J Neurosurg 37:407-411.

Karara, H.M., 1989. Non-topographic photogrammetry, 2nd edition. Published by American Society for Photogrammetry and Remote Sensing, Falls Church, Virginia, United States of America.

Kelly, P.J., 1991. Tumour Stereotaxis. Published by W.B. Saunders Company, Philadelphia, United States of America.

Kitchen, N.D., Lemieux, L., Thomas, D.G.T., 1993. Accuracy in frame-based and frameless stereotaxy. Stereotact Funct Neurosurg 1993; 61:195-206.

Levin, C.J., Hough, J., Adams, L.P., Boonzaier, D., Ruther, H., Wynchank, S., 1993. Determining the locations of intracerebral lesions for proton therapy. Phys. Med. Biol., 38:1393-1401.

Maciunas, R.J.(Editor), 1993. Interactive Image-Guided Neurosurgery. Published by the American Association of Neurological Surgeons, United States of America.

Manwaring, K.H., 1993. Intraoperative Microendoscopy. Pgs 217-232 of Maciunas, R.J.(Editor), 1993. Interactive Image-Guided Neurosurgery. Published by the American Association of Neurological Surgeons, United States of America.

Matthew, J., Krishnan, S.M., Mital, D.P., Pillay, P.K., 1994. A new approach for controlling a surgical assistant robot in brain surgery using stereo cameras. Abstract OS02-1.3 of the proceedings of the World Congress on Medical Physics and Biomedical Engineering, Rio de Janeiro, Brazil.

Mcglone, J.C., Mikhail, E.M., Padres Jr., F.C., 1989. Analytical Data-Reduction Schemes in Non-Topographic Photogrammetry. Non-Topographic Photogrammetry, 2nd edition, edited by H.M. Karara, American Society of Photogrammetry, Falls Church, Virginia, United States of America, 1989; ch 4, pg:37-57.

Mikhail, E.M., Mcglone, J.C., Paderes Jr., F.C., 1989. Introduction to metrology concepts. Non-Topographic Photogrammetry, 2nd edition, edited by H.M. Karara, American Society of Photogrammetry, Falls Church, Virginia, United States of America, 1989; ch 2, pg:7-14.

Nuttin, B., Knauth, M., Gybels, J., Verbeeck, R., Vandermeulen, D., Michiels, J., Suetens, P., Marchal, G., 1994. How does the stereotactic workstation help the neurosurgeon? Stereotactic Funct Neurosurg, 63:17-22.

Patil, A.A., 1984. Computed tomography plane of the target approach in computed tomographic stereotaxis. Neurosurgery 15:410-414.

Pell, M.F., Thomas, D.G.T., 1991. The initail experience with the Cosman-Roberts-Wells stereotactic system. British Journal of Neurosurgery (1991) 5, 123-128.

Roberts, D.W., Friets, E.M., Strohbehn, J.W., Nakajima, T., 1993. The sonic digitizing microscope. Pgs 105-111 of Maciunas, R.J.(Editor), 1993. Interactive Image-Guided Neurosurgery. Published by the American Association of Neurological Surgeons, United States of America.

Rubenstein, M., Rüther, H., 1991. Comparison of Target Centring algorithms in Near Real Time Photogrammetry. Proceedings First Australian Photogrammetric Conference, Newcastle, Australia.

Schildt, H., 1987. C The Complete Reference. Publishers: Osborn McGraw-Hill, Berkeley, California, United States of America.

Scott, P.J., 1981. The reflex plotters: measurement without photographs. Photogrammetric Record Vol.X:435-446.

Slama, C.C., 1980. Manual of Photogrammetry, Fourth Edition. Published by the American Society of Photogrammetry, Falls Church, Virginia, United States of America: Two-dimensional projective transformation, p.729-731.

Spiegel, M.R., 1968. Mathematical Handbook of formuals and tables.Schaum's outline series. Published by McGraw-Hill Book Company, New York, United States of America.

Spiegel, E.A., Wycis, H.T., Marks, M., Lee, A.StJ., 1947. Stereotaxic apparatus for operations on the human brain. Science 106:349-350.

Stedman, LT, 1982. Illustrated Stedman's Medical Dictionary, 24th Edition. Reprinted 1983. Published by Williams & Wilkins, Baltimore, United States of America.

Swokowski, E.W., 1983. Calculus with analytical geometry, Third Edition. PWS Publishers, Boston Massachusetts, United States of America, pg 436-442.

Thompson, E.H., 1969. An introduction to the algebra of matrices with some applications. Adam Hilger, London, England. p.142.

Till, K., 1975. Paediatric Neurosurgery. Published by Blackwell Scientific Publications Ltd., Oxford, England.

Weatherall, D.J., Ledingham, J.G.G, Warrell, D.A., (Eds), 1985. Oxford Textbook of Medicine, Volume 2. Published by Oxford University Press, Oxford, England.

Williams, P.L., Warwick, R., (Eds.), 1980. Gray's Atlas of Anatomy, 36th edition, 1980. Published by Churchill Livingstone, Medical Devision of Longman Group Limited, London, England.

Zamorano, L.J., Nolte, L., Kadi, A.M., Jiang, Z., 1994. Interactive Intraoperative localization using an infrared-based system. Stereotact Funct Neurosurg, 63:84-88.

## APPENDIX A: THE HUMAN ANATOMICAL REFERENCE SYSTEM

The following three pages have been copied from Gray's Atlas of Anatomy (Williams et al, 1980), as both the diagrammatic and verbal description of the anatomical nomenclature/ human anatomical 'coordinate system' is very clear.

# INTRODUCTION

To perform an 'anatomy' was to make a 'dissection'; the two words are no longer synonymous. *Dissection* has remained a technique; *Anatomy* has become a field of study—a corpus of observations, still dependent upon technique, but capable of rational correlation among themselves and with other biological studies. Most narrowly, anatomy may be the investigation of biological structure—in plants or animals—with no other motive than description of form. Even so, such *topographical anatomy* has not remained insulated from technological progress; the usefulness of direct visual dissection persists, but its relatively crude results have become incalculably augmented by the advent of light microscopy, micro-dissection, electron microscopy, histochemistry, radiology, autoradiography, and many other techniques. The application of these, with ever-growing modifications and extensions, has revealed great new fields of discovery. Some, such as *histology* and *cytology*, the study of tissues and cells, are true extensions of the parent discipline; others—*electron microscopy*, *histochemistry* and *autoradiography*—are merely techniques capable of providing particular types of data.

The theme of growth and differentiation, both in individual development or *ontogeny* and in that of the species or kind—*phylogeny*—has led to the particular studies of *embryology*, *comparative anatomy* and *morphology*. Embryology, the study of individual development, also embraces problems of gametogenesis, fertilization and embryonic nutrition, and in the investigation of these in relation to mankind, *comparative embryology* has proved invaluable.

Studies of growth, whether upon the epochal time-scale of evolution or the rapid cycles of ontogeny, emphasize the mutability of structures; and the dynamic nature of all *living* structures entails an inescapable relation between form and function. It is, of course, possible to consider form in isolation, an exercise of most limited value, though the data of pure description may have particular applications. Such *applied anatomy* is usually concerned with human structural observations which are useful in medicine, especially in surgical technique, but also in clinical diagnosis. Descriptive anatomy, however, has a far more extensive application in relation to function. Few biological structures can be regarded as functionless, and no biological function is known to occur outside living fabric, which includes, it must be noted, everything from the whole creature to its molecular structure. In human considerations of nature it is possible to divorce structure from function (though not the reverse); but few structuralists are disinterested in function. The mere fact that topography can be described upon a *regional* or *systematic* basis necessarily entails functional considerations, for while the former is of particular vocational interest in medicine, *systematic anatomy* is based upon recognition of function. The *locomotor system* embraces structures directly concerned with movement—skeletal elements, articulations and ligaments, and muscles, the study of which may be formalized as *osteology*, *arthrology* and *myology*. Similarly, *neurology*, which treats of the nervous sytem, including its sensory organs, and *angiology*, the study of cardiovascular arrangements of organs and tissues, are correlated as much by function as by structure. It is equally clear that the *respiratory*, *alimentary*, *urogenital* and *endocrine systems* (though often grouped under the unilluminating anatomical term *splanchnology*), are clearly functional as well as anatomical fields of study.

All such 'systems' are investigated at macroscopic, histological, cytological, ultrastructural and biochemical levels. Furthermore, experimentation upon structures—classically illustrated by early work on the circulation, reflex behaviour and endocrine influences—has formed the vanguard of anatomical research, with increasing momentum in this century. *Experimental anatomy*, *experimental cytology* and *experimental embryology*, have contributed greatly to the advancement of knowledge in the field of human anatomy. Throughout the following sections, where relevant, numerous allusions will be made to the results of such experimental studies.

*Descriptive anatomy* obviously demands an internationally acceptable repertoire of names for structures, and there is also a need for an agreed convention upon terms for their spatial relationships (*see* accompanying figure). For this purpose the human body is assumed to be in its usual bipedal or erect position with the arms pendent and eyes and hands facing forwards. This position is open to certain objections; for example, the arms are rotated laterally at the shoulder joints and the forearms are fully supinated and are thus not in their usual position of rest (*see* p. 350). Moreover, comparisons of human anatomy with that of other animals, which are mostly quadrupedal in habit, are confronted with some difficulties. Nevertheless, the erect 'anatomical position' does provide an unambiguous system of correlation for man. In this posture the *median plane* divides the body vertically into right and left halves which are approximately symmetrical, apart from certain visceral details. The superficial contours of this plane form *anterior* and *posterior median lines* on the surface of the body. The median plane is also frequently called the *sagittal plane* (after the cranial suture of that name), but this term is also sometimes applied to any vertical plane parallel to the median, and hence the latter may be termed *paramedian* or *parasagittal planes*. To avoid confusion and to maintain simplicity, it is perhaps best to reserve the term *median* for the single *median plane* defined above, and to regard all other planes parallel to this as *sagittal*. Vertical planes at right angles to the median plane are usually described as *coronal planes*, after the coronal suture (p. 298). To complete the three-dimensional reference grid, *horizontal planes* are those which traverse the body at right angles to both the median and coronal planes.

The adjectives *anterior* and *posterior* are applied to the front or back surfaces of the body, including the limbs. Synonyms for these are *ventral* and *dorsal*, which, since they can be applied equally to quadrupeds, are sometimes preferable. All these terms are in fact used more extensively to specify the aspects or surfaces of individual structures *within* the body, and often to denote their relative positions. Thus—the heart is posterior (or dorsal) to the sternum, the posterior surface of which is close to the anterior (or ventral) aspect of the heart. Similarly, *superior* (or *cranial*) and *inferior* (or *caudal*) are adjectives qualifying the positions of structures in the vertical sense. Of the two venae cavae one is

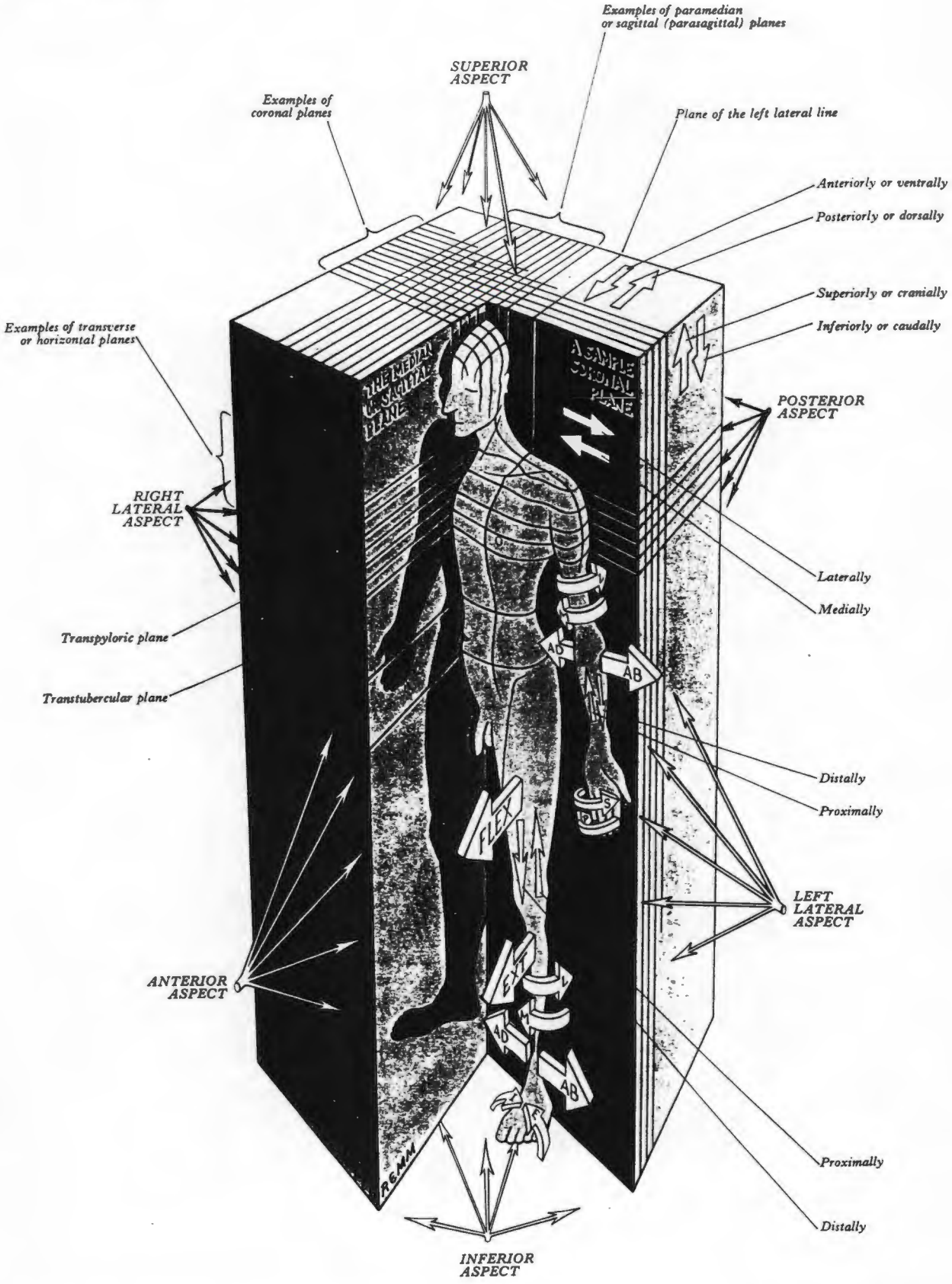


The terminology widely used in descriptive anatomy is illustrated in the figure above. The abbreviations on the solid arrows: AD—adduction, AB—abduction, FLEX—flexion (of the thigh at the hip joint), EXT—extension (of the leg at the knee joint), M and L—medial and lateral rotation, P and S—pronation and supination, I and E—inversion and eversion.

*superior, cranial* (headward) with respect to the other which is *inferior, caudal* (tailward) in position. (Incidentally, the *superior* and *inferior* venae cavae are *anterior* and *posterior* in the quadruped, but the terms cranial and caudal, which obviate this confusion, have not been adopted in this instance in mankind.) In describing structures within the cranium, the term *cranial* is obviously unsatisfactory. Particularly in describing positional terms to cerebral structures it is more appropriate to employ the term *rostral*, which indicates that a particular entity is nearer the *rostrum* (beak or nose). Thus, the cerebrum is *rostral* to the cerebellum, which is *caudal* to the former. To define the relation of structures to the median plane the terms *medial* and *lateral* are employed: the heart is *medial* to the lungs, which are *lateral* to it, and so on.

Any number of oblique planes can be imagined, and likewise the spatial relations of structures are not always so orthogonally simple as anterior, posterior, superior, medial, and so forth. Combined terms are therefore sometimes used for intermediate positional arrangements, such as anterolateral (ventrolateral), postero-inferior (dorsocaudal), etc., and these are self-explanatory. In the limbs certain variant terms are current—and since these do not involve reference to the 'anatomical position', they have some value in obviating confusion. Thus, structures which are superior, and hence nearer the limb root, are dubbed *proximal*; those relatively inferior in position are clearly more *distal*. Anterior and posterior aspects or regions may be described respectively as *flexor* or *extensor* in upper limbs, but the terms do not correspond in the lower limbs, which have undergone a contrasting form of morphological rotation (pp. 150, 350), such that the primitively extensor or dorsal aspect is now anterior. In the forearm, the terms *radial* and *ulnar* are occasional synonyms for lateral and medial, as are *fibular* (peroneal) and *tibial* in the lower limb. *Palmar* and *plantar* are variants for the flexor surface of the hand and foot. Finally, *superficial* and *deep* specify distance from the surface of the body; the somewhat similar terms, *external* and *internal*, are usually applied to the walls of hollow structures such as the head, thorax and abdomen and various viscera, including vessels and ducts.

It will be noted that throughout the text, the units of linear measurement are those of the Système Internationale (S.I.). These include the *micrometre* (micron, $\mu$m) $1\ \mu m = 1 \times 10^{-6}$ metre; $1000\mu m = 1$ mm), and the *nanometre* (nm) $1nm = 1 \times 10^{-9}$ metre; 1000 nm = 1 $\mu$m). Accordingly the use of Ångstrom unit (Å $= 1 \times 10^{-10}$ metre; 10Å = 1 nm) has been discontinued.

We have, in the main, continued the policy of adherence to *Nomina Anatomica* (3rd ed., by G. A. G. Mitchell, Excerpta Medica Foundation, 1968). Familiar variants and some eponyms have also been included where deemed advisable. We have also attempted to follow the proposed *Nomina Histologica* and *Nomina Embryologica*, prepared by the subcommittee of the International Anatomical Nomenclature Committee and presented to the Eleventh International Congress of Anatomists held in Leningrad in August 1970, at a plenary session at which these two drafts were approved. Unfortunately, both contain many common terms at variance with each other, important omissions, and some terms which have aroused belated dissatisfaction. Moreover, some ultrastructural details were overlooked, often obliging us to follow current practice, itself confused by synonyms and vernacular jargon. Therefore, we have regarded the recommendations of *Nomina Histologica* and *Nomina Embryologica* as less obligatory than *Nomina Anatomica*, which has been exposed to much more critical revision. Nevertheless, the latter does not meet all contingencies, especially in the central nervous system; it also still retains some intrinsically unsatisfactory terms. Notwithstanding, we have continued to adhere to most of these, though we have preferred not to handicap a whole section with the title of 'Syndesmology', for which 'Arthrology' has priority in time and in clarity of communication. We have also disregarded official disapproval of the hyphen, employing it frequently, though not perhaps consistently, to separate vowels likely to be compounded as diphthongs. (Since these remarks were written a 4th Edition of *Nomina Anatomica* (Ed. Roger Warwick, 1977) has appeared from the same publisher, and some of the difficulties referred to have been resolved. We have also had the advantage of consulting revisional proposals for a 5th Edition, which will be published shortly after the Twelfth International Congress of Anatomists, which is to take place in Mexico in 1980. The 4th Edition contains *Nomina Histologica* and *Nomina Embriologica*, which have therefore now been available for assessment for three years. It is to be hoped that active workers, especially in the fields of Cytology and Histology, will collaborate adequately with the I.A.N.C. to elaborate acceptable compromises between the jargon of the former and the sometimes impractical Latinity of the latter.) Even in Europe and the Americas, most university students, however, fall short of even 'a little Latin and no Greek', and this takes no account of the large numbers of schools outside these continents. Consequently, it must be assumed that a large majority of undergraduates and younger postgraduates find words of Greek and Latin derivation unfamiliar, and that this difficulty will increase in the future. Even the Latinist may find *bulbourethral* bothersome; *ou* is a diphthong not only in English but in other European languages; similarly, *sacro-iliac* aids in both pronunciation and understanding. The diaeresis is often frowned upon these days: but while *cooperate* perhaps no longer requires hyphen or diaeresis, *spermatozoön* and oöcyte are awkward words. We believe that an increasing number of readers need this help if unfamiliar words are to be pronounced with confidence, to the betterment of international communication. Officially, all anatomical terms are expressed entirely in Latin; but there is little objection to translating *flexor digitorum superficialis* into 'the superficial flexor of the digits', and this kind of vernacularization is practised in many countries, especially in Europe. Human anatomy, however, is a worldwide science, and the Latin terms are recognizable everywhere. A little effort with the first few pages of an elementary Latin grammar will quickly unveil the mysteries of masculine and feminine plurals, genitives and so on—a small personal concession to international understanding, in a world which must surely welcome unequivocal terms, even if based on a 'dead' language—perhaps all the more acceptable because no longer a contender in petty national rivalries.

## APPENDIX B : THE TWO DIMENSIONAL PROJECTIVE TRANSFORMATION ALGORITHM APPROACH TO THE SURVIEW EQUATION

### B.1 INTRODUCTION

Under the section headed "The Two Dimensional Projective Transformation" (Slama, 1980) the following is stated: "Positions of points on a plane can be related to their corresponding projected positions on another plane". The resultant linear fractional transformation is :

$$X' = \frac{a_{11}X + a_{12}Y + a_{13}}{a_{31}X + a_{32}Y + a_{33}} \qquad Y' = \frac{a_{21}X + a_{22}Y + a_{23}}{a_{31}X + a_{32}Y + a_{33}} \qquad \text{B.1}$$

These equations are normally used for the transformation between photograph and map coordinates systems, i.e. where the XY plane of the photograph is projected onto the XY plane of the map. The CT surview case is somewhat different, as each XY plane that the X-ray beam irradiates, is projected onto a single line (see figure B.1). By scanning a series of XY planes in the 3D space, the surview is compiled.

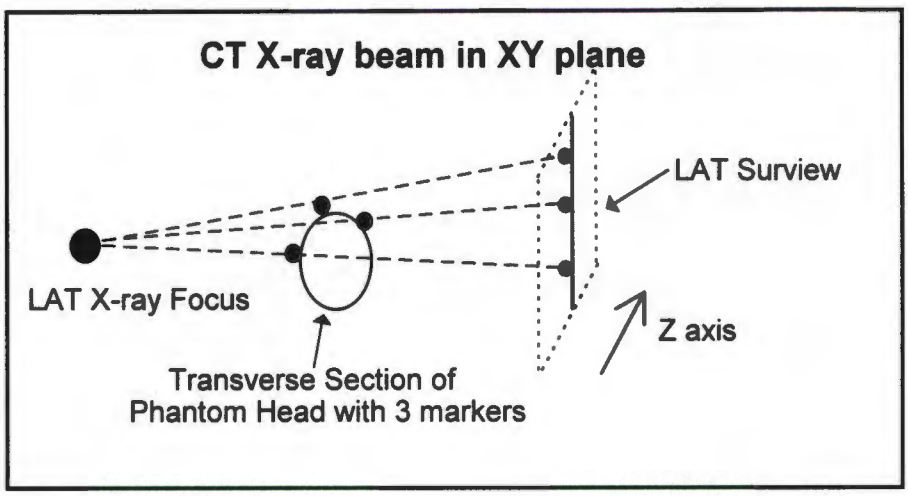


Figure B.1: The CT X-ray beam in the XY plane

Therefore the resultant fractional linear transformation equations cannot be used in their usual format and a new equation, a surview equation has been derived from them, along similar lines used by Adams (1981) when developing equations to determine 3D coordinates from conventional X-rays.

## B. 2 DEVELOPING THE CT SURVIEW EQUATION

$$\begin{pmatrix} X' \\ Y' \end{pmatrix} = A \begin{pmatrix} X \\ Y \end{pmatrix} \qquad \text{B.2}$$

A linear transformation, equations B.2, of homogenous coordinates in space is known as a projective transformation, when the matrix A is non-singular. In terms of non-homogenous coordinates it takes the form of equations B.3, i.e. the equations for a two dimensional projective transformation (Slama, 1980), where $a_{ij}$ is a typical element of A in equation B.2. The two dimensional projective transformation relates the points on one plane to their corresponding projected positions on another plane.

$$X' = \frac{a_{11}X + a_{12}Y + a_{13}}{a_{31}X + a_{32}Y + a_{33}} \qquad Y' = \frac{a_{21}X + a_{22}Y + a_{23}}{a_{31}X + a_{32}Y + a_{33}} \qquad \text{B.3}$$

The CT scan surview however introduces a singular transformation (figure B.2). The space lines containing the space points A1, A2 and An are all mapped onto only one line, the CT surview imaging line (In other words the CT imaging plane, i.e. the XY, plane is mapped onto a single line on the CT surview). This relationship, described by the transformation equations B.3, cannot be uniquely inverted for to every picture point there corresponds an infinity of space points; that is the image point a on the CT surview image line in figure B.2 could correspond to A1, A2, An etc.

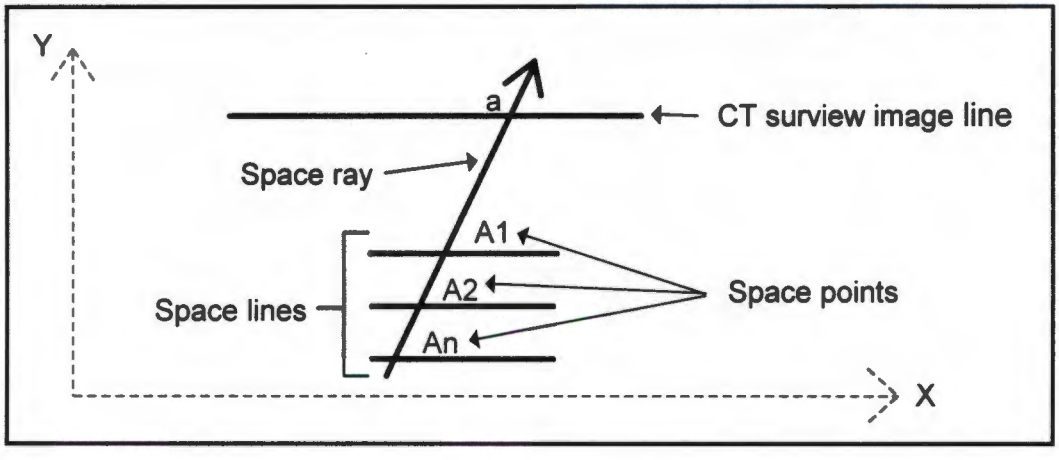


Figure B.2: Illustration of the singular transformation

In figure B.3 consider the one-dimensional space - i.e. the line E. Line E represents one of the imaging lines of a surview. On line E, P has a coordinate x in one dimension. One can interpret X, Y as rectangular coordinates in two dimensional space, i.e. X, Y in the CT scan slice system, and in this space one can choose a line Y=k parallel to the X line as the line E. If one joins the point P on line E to the origin O by a straight line, then for points on this line X/Y are constant. If one lets Y=k=1 say, in general one can write:

$$\frac{X}{Y} = x \qquad \text{B.4}$$

Accordingly the introduction of homogeneous coordinates signifies the representation of the line E into a space pencil of rays with the origin O as centre, of which E is a section; i.e. the homogenous coordinates of a point are the space coordinates of the points of the projecting ray of that point.

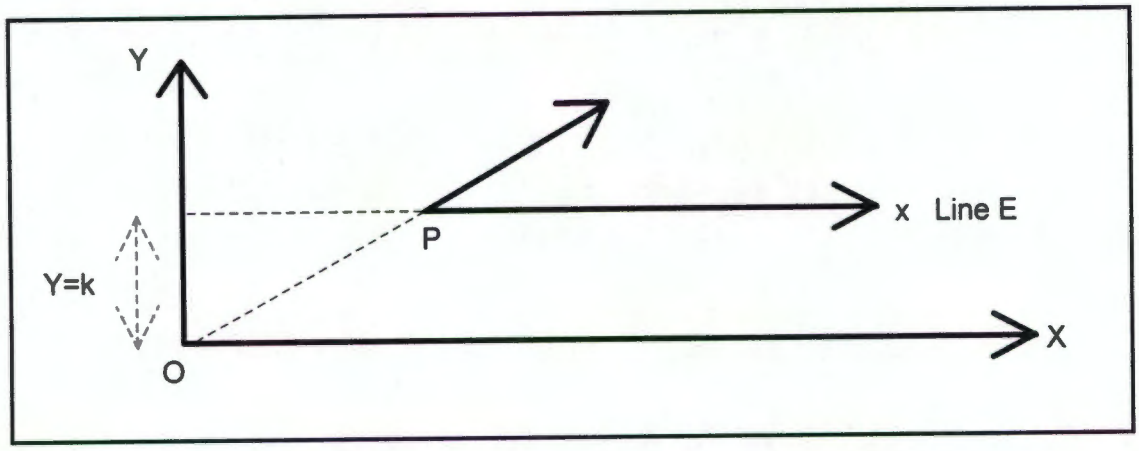


Figure B.3: Illustrating homogeneous coordinates

The equations B.3 are in terms of X', Y', but for the one-dimensional coordinates x, and using the homogenous coordinates, one can rewrite equations B.3:

$$x = \frac{X'}{Y'} = \frac{a_{11}X + a_{12}Y + a_{13}}{a_{31}X + a_{32}Y + a_{33}} * \frac{a_{31}X + a_{32}Y + a_{33}}{a_{21}X + a_{22}Y + a_{23}} = \frac{a_{11}X + a_{12}Y + a_{13}}{a_{21}X + a_{22}Y + a_{23}} \qquad \text{B.5}$$

The projectivity between planes is given by equation B.6, where all the $a_{ij}$ terms are divided by $a_{23}$ and new transformation parameters $h_{ij} = a_{ij} / a_{23}$ are introduced.

$$x = \frac{a_{11}X + a_{12}Y + a_{13}}{a_{21}X + a_{22}Y + a_{23}} = \frac{h_{11}X + h_{12}Y + h_{13}}{h_{21}X + h_{22}Y + 1} \qquad \text{B.6}$$

Rewriting equation B.6 and gathering terms:

$$x = h_{11}X + h_{12}Y + h_{13} - h_{21}xX - h_{22}xY \qquad \text{B.7}$$

## APPENDIX C: THE THEORY OF STEREOPHOTOGRAMMETRY AND THE DIRECT LINEAR TRANSFORMATION

In laymen's terms, stereophotogrammetry is the process of obtaining spatial data of an object from images taken of that object, where the images may be photographs, video images etc. Although the topic may seem unfamiliar, the same principles used in stereophotogrammetry apply to stereoscopic human vision, i.e. normal human sight (see figure C.1; stereoscopic - stereo from the Greek root meaning three dimensional, and scope - range of view).

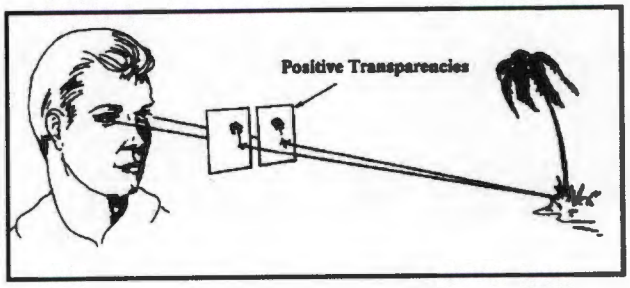


Figure C.1: Stereoscopic human vision
(from Mikhail et al, 1989)

The left and right eye see "two" slightly different images of the same object, which are combined by the brain so that we perceive one single image. The disparity in the images, seen by the left and right eye, creates depth perception (figure C.2). As the angle Øa is larger than the angle Øb, object a is perceived to be closer than object b.

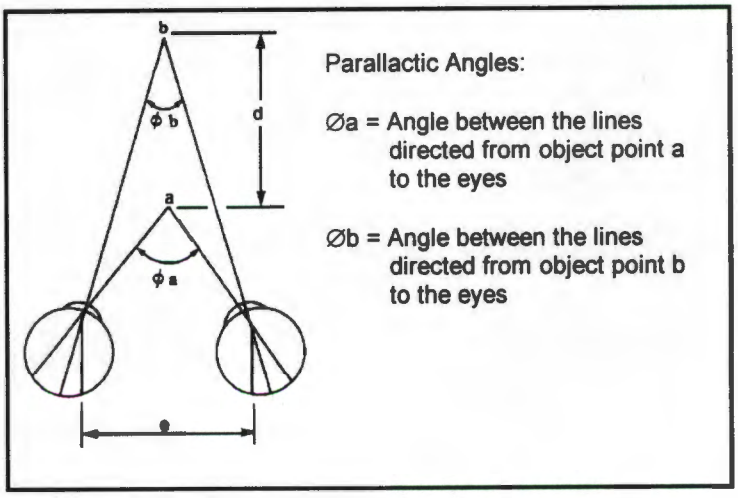


Figure C.2: Parallax allowing for depth perception
(from Mikhail et al, 1989)

Human vision requires both eyes in order to perceive depth. This also applies to stereophotogrammetry, where a minimum of two disparate/different images of an object are required to be able to determine the three dimensional shape of that object.

The Direct Linear Transformation (DLT), as first proposed by Abdel-Aziz and Karara (1971), determines the 3D object space coordinates directly from the 2D coordinates measured on the images of that object. (A more detailed description of the DLT in the use of medical applications can be found in Adams (1981) ). The main advantage of using this method is that it does not require a calibrated camera. The images can be produced using a good photographic or CCD camera, instead of a special photogrammetric camera.

The DLT equations, in their simplest form (Mcglone et al, 1989), are:

$$x = \frac{B_1X + B_2Y + B_3Z + B_4}{B_9X + B_{10}Y + B_{11}Z + 1} \qquad \text{C.1}$$

$$y = \frac{B_5X + B_6Y + B_7Z + B_8}{B_9X + B_{10}Y + B_{11}Z + 1} \qquad \text{C.2}$$

where: x, y - are the 2D image coordinates of a marker
X,Y,Z - are the 3D space coordinates of that marker
$B_1$ -$B_{11}$ - are the 11 parameters which describe the relationship between the 2D image and the 3D coordinate space/system

The 2D image and the 3D object space coordinate systems are shown in figure C.3.

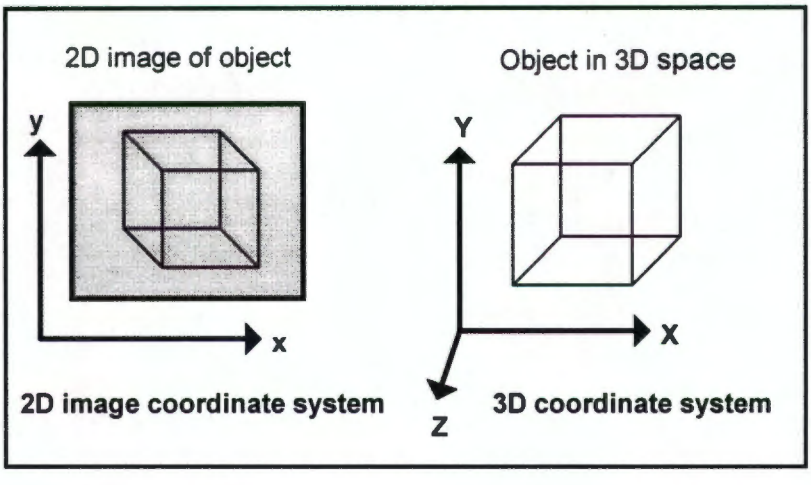


Figure C.3: The 2D image coordinate system and 3D object space coordinate system

To be able to utilise these equations, a minimum of six well distributed control markers, i.e. six markers with known 3D coordinates, have to be imaged on each image (see figure C.4).

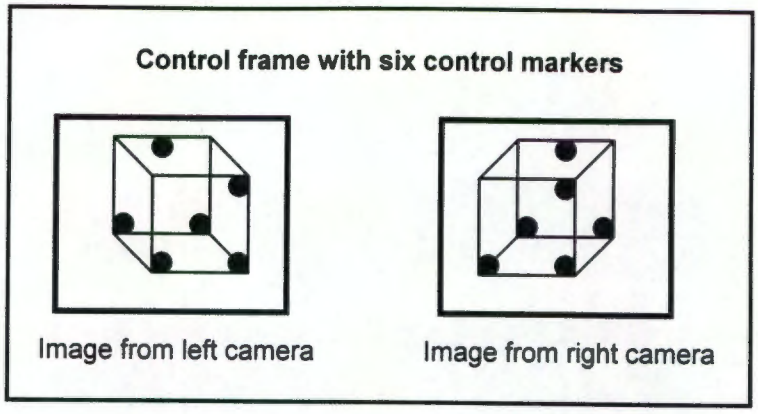


Figure C.4: Left and right camera images of a control frame

In a two CCD camera system, like the SPG system, a control frame with 16 control markers is set up, so that all the control markers image on the video images of both the left and right camera. The 3D coordinates of the 16 markers are known, as these were measured in the reflex metrograph (Scott, 1981), which has a measuring resolution of 0.1mm for each axis.

By measuring the coordinates ($x_L$, $y_L$) of the control markers on the left image, and knowing their 3D coordinates (X, Y, Z), the 11 $B_L$ parameters pertaining to the left camera can determined using equations C.1 and C.2, using a least squares adjustment. The same procedure is repeated for the right image, i.e. by measuring the coordinates ($x_R$, $y_R$) of the control markers on the right image, and knowing their 3D coordinates (X, Y, Z), the 11 $B_R$ parameters pertaining to the right camera can be solved.

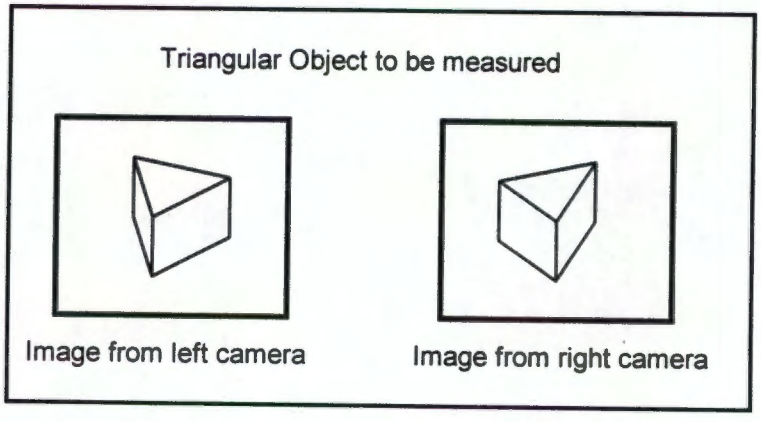


Figure C.5: Two disparate images of an object

Once B parameters have been calculated for each camera, and as long as the cameras remain undisturbed, the 3D coordinates of any point or object, that is imaged on both the left and right images, can be calculated. For example in the two disparate images of the triangular object in figure C.5, all the corners of the object are visible, and can be measured, on both images. Utilising the DLT equations, the 3D coordinates of all the corners can be calculated and therefore the three dimensional shape of the triangular object can be defined. The equations, to determine the 3D coordinates of a corner of the triangle, which has been measured on both the left and right image, are:

$$x_L = \frac{B_{L1}X + B_{L2}Y + B_{L3}Z + B_{L4}}{B_{L9}X + B_{L10}Y + B_{L11}Z + 1} \qquad \text{C.3}$$

$$y_L = \frac{B_{L5}X + B_{L6}Y + B_{L7}Z + B_{L8}}{B_{L9}X + B_{L10}Y + B_{L11}Z + 1} \qquad \text{C.4}$$

$$x_R = \frac{B_{R1}X + B_{R2}Y + B_{R3}Z + B_{R4}}{B_{R9}X + B_{R10}Y + B_{R11}Z + 1} \qquad \text{C.5}$$

$$y_R = \frac{B_{R5}X + B_{R6}Y + B_{R7}Z + B_{R8}}{B_{R9}X + B_{R10}Y + B_{R11}Z + 1} \qquad \text{C.6}$$

where:

$x_L$, $y_L$ - 2D image coordinates of the corner on the left image

$x_R$, $y_R$ - 2D image coordinates of the corner on the right image

$B_{L1}$-$B_{L11}$ - 11 B parameters pertaining to the left image

$B_{R1}$-$B_{R11}$ - 11 B parameters pertaining to the right image

X, Y, Z - 3D coordinates of the corner of the triangle.

The equations are solved by a least squares adjustment.

To determine what precision can be obtained when determining the 3D coordinates of any point using the SPG system, the sixteen control markers are treated like the corners of the triangle. Their 3D coordinates are calculated, using their 2D coordinates and the 11 B parameters from both the left and right image, in equations C.3 to C.6. The comparison between the calculated 3D coordinates of the control markers, and their known 3D coordinate values (as measured in the reflex metrograph), shows to what precision any other

point, that falls within the area occupied by the control frame, can be determined (see table C.1).

| dX (mm) | dY (mm) | dZ (mm) |
|---|---|---|
| +0.5 | -0.4 | -1.6 |
| +0.2 | -0.3 | -1.9 |
| +0.1 | -0.1 | -1.5 |
| +0.0 | +0.0 | +0.5 |
| +0.7 | -0.3 | -1.2 |
| +0.0 | -0.5 | -0.8 |
| +0.1 | -0.1 | -0.5 |
| +0.5 | -0.1 | -1.4 |
| +0.2 | +0.0 | -0.5 |
| -0.1 | +0.0 | +0.4 |
| -0.3 | +0.2 | +0.0 |
| -0.1 | +0.1 | +1.0 |
| +0.3 | -0.7 | -1.1 |
| +0.0 | -0.6 | -0.7 |
| +0.1 | -0.5 | -1.3 |
| **Std. Dev. - dX** | **Std. Dev. - dY** | **Std. Dev. - dZ** |
| 0.3 | 0.3 | 0.9 |

Table C.1: Precisions for the SPG system - comparison of 3D coordinates calculated by the SPG system and measured in the reflex metrograph

## APPENDIX D: THE CENTRE OF GRAVITY ALGORITHM

The IP8 Matrox card has only single pixel accuracy (pixel - a picture element of the image, see figure D.1). When the digitising cursor is placed on a marker to be digitised, the centre of that marker can only be determined to the nearest pixel. To improve the determination of the centre of that marker various algorithms can be employed to obtain subpixel accuracy when digitising. The SPG system makes use of the centre of gravity algorithm (Swokowski, 1983).

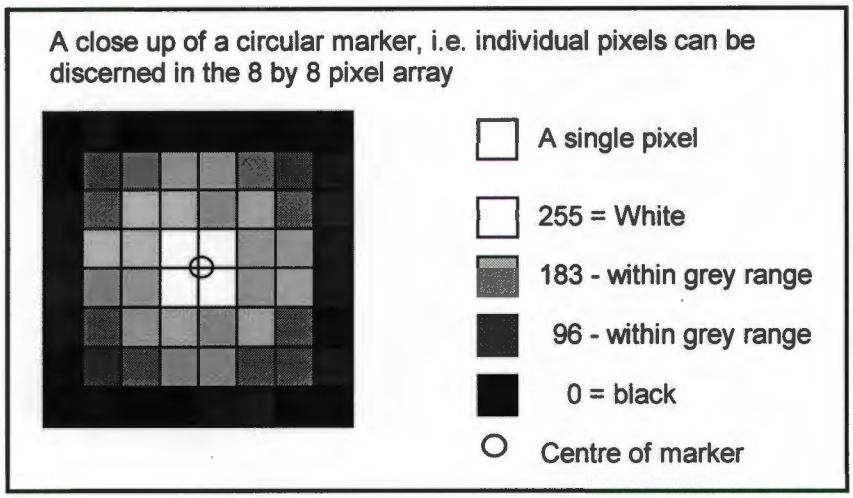


Figure D.1: A marker in pixel format

The video images, transferred to the IP8, are made up of a matrix of 768 * 576 pixels (i.e. 768 rows and 576 columns). The IP8, on transferring the video images, converts them into "black and white" images, where the grey values range from 0 to 255, 0 is black and 255 is white, with the various grey tones ranging between 0 and 255 (see figure D.1).

The centre of gravity algorithm determines the centre of the marker, i.e. M(xc, yc), by utilising the grey values of the pixels in a 15 by 15 pixel array, where the digitising cursor, placed at the approximate centre of the marker, lies in the centre of the 15 by 15 pixel array. The marker coordinates xc and yc are defined as:

$$m * xc = My \qquad \text{and} \qquad m * yc = Mx \qquad \text{D.1}$$

where m is defined as the total grey mass of the marker area:

$$m = \sum_{i=1}^{n} m_i \qquad \text{D.2}$$

$m_i$ is the grey value of the pixel i in the 15 by 15 pixel array and n is the total number of pixels in the array. Mx and My are the moments of the marker with respect to the x and y axis respectively and are:

$$Mx = \sum_{i=1}^{n} m_i y_i \qquad \text{D.3}$$

$$My = \sum_{i=1}^{n} m_i x_i \qquad \text{D.4}$$

and $x_i$ and $y_i$ are the coordinates of pixel i.

On average a retroreflective marker will span 8 or 9 pixels in length and breadth. The rest of the 15 by 15 array will be filled by the black outer circle surrounding the retroreflective marker. The pixel values of the "black" outer ring on the video image is not truly black due to the various lighting conditions. To minimise any adverse effect the "black" outer ring may have, the 15 by 15 array is searched and the highest grey value in the array determined. A threshold value for the array is determined by subtracting sixty from this value (This value was determined from various tests run on the markers). Any grey value in the array, that is less than the threshold value, is assigned a value of zero and therefore has no influence on the centre determination of that marker.

The centre of gravity algorithm is one of the algorithms that is successfully employed to determine the centre of markers to sub-pixel accuracy (Gütschow, 1990; Rubenstein et al, 1991).

## APPENDIX E: THREE DIMENSIONAL TRANSFORMATION USING THE RODRIGUES MATRIX

Transforming coordinates from one three dimensional system to another three dimensional system, where both systems have a common origin, the following algorithm is employed (Thompson, 1969):

$$\begin{pmatrix} x' \\ y' \\ z' \end{pmatrix} = R^T \begin{pmatrix} x \\ y \\ z \end{pmatrix} \qquad \text{E.1}$$

where: x, y, z - the three dimensional coordinates of a point in system A

x', y', z' - the three dimensional coordinates of a point In system B

$R^T$ - is the Rodrigues Matrix, and:

$$R = \frac{1}{\Delta}\begin{pmatrix} 1+\frac{1}{4}(\lambda^2-\mu^2-\nu^2) & -\nu+\frac{1}{2}\lambda\mu & -\mu+\frac{1}{2}\lambda\nu \\ \nu+\frac{1}{2}\mu\lambda & 1+\frac{1}{4}(-\lambda^2+\mu^2-\nu^2) & -\lambda+\frac{1}{2}\mu\nu \\ -\mu+\frac{1}{2}\nu\lambda & \lambda+\frac{1}{2}\nu\mu & 1+\frac{1}{4}(-\lambda^2-\mu^2+\nu^2) \end{pmatrix} \qquad \text{E.2}$$

and where:

$$\Delta = 1+\frac{1}{4}(\lambda^2+\mu^2+\nu^2) \qquad \text{E.3}$$

and $\lambda$, $\mu$ and $\nu$ bear some relation to rotations about the coordinates axes, and are known as the Rodrigues parameters.

The first step, when transforming from one 3D system to another, is to reduce both systems to a single common origin (x=0 ,y=0 ,z=0), using the points common to both systems. To be able to transform any other points from system A to B, the parameters $\lambda$, $\mu$ and $\nu$ have to be solved using a minimum of three common points. This is done, with equation E.1, rewritten in terms of $\lambda$, $\mu$ and $\nu$:

$$\begin{pmatrix} 0 & -(z+z') & (y+y') \\ (z+z') & 0 & -(x+x') \\ -(y+y') & (x+x') & 0 \end{pmatrix}\begin{pmatrix} \lambda \\ \mu \\ \nu \end{pmatrix} = 2*\begin{pmatrix} x'-x \\ y'-y \\ z'-z \end{pmatrix} \qquad \text{E.4}$$

If more than three common points are used, a least squares solution can be used to obtain the best solution for $\lambda$, $\mu$ and $\nu$.

Using equation E.2, the Rodrigues matrix can be calculated using $\lambda$, $\mu$ and $\nu$. Thereafter using equation E.1, any point in system A can be transformed to system B.

## APPENDIX F: TWO DIMENSIONAL TRANSFORMATION TO CORRECT FOR VIDEO IMAGE SHIFTS

Fiducial markers are used by the SPG system to correct for any movement of the video image that may occur on image transfer from the VCR to the PC, via the image frame grabber card. This image shift is caused by some process in the VCR, and is thought to be due to the way the VCR heads make contact with the actual video tape, when the Pause function is used. However the image shift occurs, it has to be mathematically corrected.

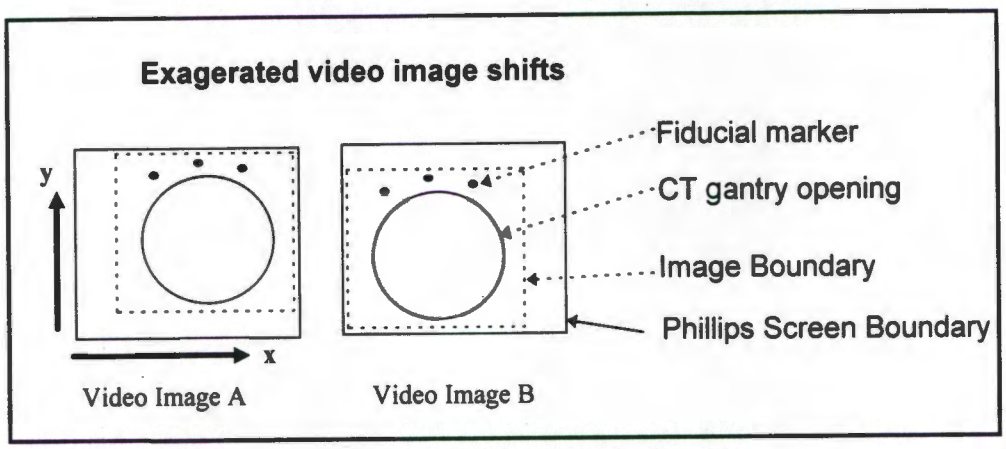


Figure F.1: Exaggerated video image shifts

In figure F.1, the CT gantry appears more towards the upper right corner in image A, and more to the left bottom corner in image B, as the image on the screen has moved. The image shift does not involve any distortions or scale changes of the image, merely a translation of the image on the IP8 screen and therefore on the IP8 image coordinate system. The coordinates of a stationary point, such as the fiducial marker, may therefore vary from image to image, due to the images shifting on the IP8 screen.

To correct these image shifts, the first image used by the SPG system, i.e. image A, is selected as the origin for subsequent images. Any subsequent image must be "shifted back" so that, were the two images overlaid, the fiducial markers would occupy the same positions in both images, thus removing any video image shift.

In reality, the subsequent image is not moved, but the two dimensional coordinates, obtained from that image, are mathematically corrected, to eliminate any image movement, using a two dimensional transformation (Slama, 1980). The two dimensional transformation equations are:

$$X = a^*x + b^*y + Cx_0 \qquad \text{F.1}$$

$$Y = -b^*x + a^*y + Cy_0 \qquad \text{F.2}$$

where: X,Y - coordinates of a marker in the coordinate system of the original image

x,y - coordinates of a marker in the coordinate system on a subsequent image i

$Cx_0, Cy_0$ - centre of gravity of the "original image"

$Cx_i, Cy_i$ - centre of gravity of the subsequent image I (I = 1 to n)

$$Cx_i = \frac{\sum_{j=1}^{m} x_j}{n} \qquad Cy_i = \frac{\sum_{j=1}^{m} y_j}{n} \qquad \text{F.3}$$

where $x_j$ and $y_j$ are the coordinates of the fiducial marker j on all video images and m is the total number of fiducial markers used

a,b $a = m^*\cos(\theta)$ $b = m^*\sin(\theta)$ F.4

where m is the scale change and $\theta$ is the rotation of the axes

The first step is to calculate the centre of gravity of the coordinate system of the "original image", i.e. $Cx_0$ and $Cy_0$, using the fiducial marker coordinates on that image in equation F.3. The original image in the SPG system is the video image of the control frame. The centre of gravity is also determined for all subsequent video images, i.e. $Cx_i$ and $Cy_i$ are determined for each subsequent image i using the fiducial marker coordinates on image i. Both the original image and the subsequent images are reduced to a single common origin (0,0), by subtracting $Cx_0$ and $Cy_0$ from the coordinates of all markers (including the fiducial marker coordinates) on the original image, and by subtracting $Cx_i$ and $Cy_i$ from the coordinates of all markers (including the fiducial marker coordinates) on the subsequent image i.

The fiducial marker coordinates, reduced to a single common origin, of both the original and subsequent image i, are then used in equations F.1 and F.2 to solve for the parameters a and b. Using only two fiducial markers results in a unique solution. Using three or more fiducial markers and a least squares solution, results in redundancies and a more accurate solution. Using a and b and the marker coordinates, reduced to a single common origin, in the subsequent image i, in equation F.1 and F.2, new marker coordinates are calculated in the coordinate system of the "original image", i.e. with all image shifts removed mathematically.

## APPENDIX G: THE SETTING DIAGRAM CALCULATIONS

Before describing the necessary calculations to generate the setting diagram in detail, a brief synopsis is given. Utilising the three dimensional coordinates of the three leg markers, the entry point and lesion centre, determined by the CT/SPG system, the software generates the setting diagram.

The first step in this procedure is to transform all marker coordinates, so that the three leg markers lie in a single horizontal plane, i.e. in the plane of the setting diagram. The vector, defined by the entry point and lesion centre, is used to calculate the points where the vector intersects the top and bottom plane. As the three leg markers have been transformed into the plane of the setting diagram, to produce the projections of the leg markers and the top and bottom markers on the setting diagram, their X and Y coordinates are simply plotted on screen and printed out to scale (see figure G.1).

The only remaining information to be calculated are the distances from the top of the sleeve to the lesion centre, and the top of the guide to the lesion centre. This information is printed out as part of the header of the setting diagram.

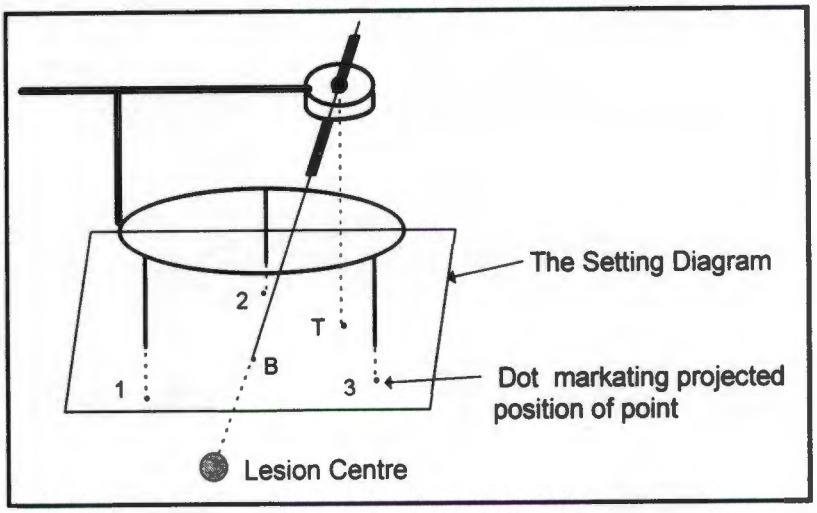


Figure G.1: The projection of the three leg markers and the top and bottom point onto a sheet of paper - the setting diagram

The first section of the setting diagram software transforms all marker coordinates, using the Rodrigues transformation (Appendix E), so that the three leg points lie in a single horizontal plane, i.e. in the plane of the page. The Rodrigues transformation requires that a minimum of three points are common to both the old and the new coordinate system. So coordinates for the three leg points have to be calculated in the new system, as shown in figure G.2.

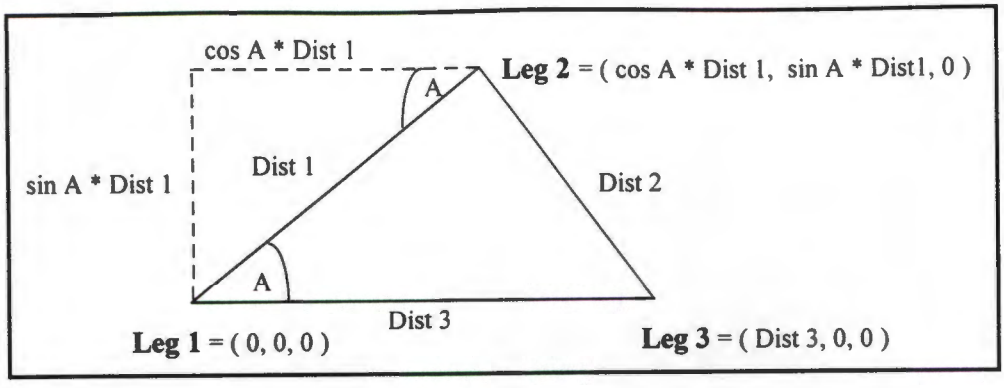


Figure G.2: Calculating the three leg points in the plane of the page

The three leg points in the new system are calculated using the distances between the three legs in the old system. The distance between leg 1 and leg 2, i.e. Dist 1 in figure G.2, is:

$$\text{Dist 1} = \sqrt{(xo_2 - xo_1)^2 + (yo_2 - yo_1)^2 + (zo_2 - zo_1)^2} \qquad \text{G.1}$$

where: $xo_1$ ,$yo_1$, $zo_1$ = 3D coordinates of leg 1 in the old system

$xo_2$, $yo_2$, $zo_2$ = 3D coordinates of leg 2 in the old system

(the 3D coordinates of the 3 leg points were measured in the reflex microscope)

Dist 2 between leg 2 and 3, and Dist 3 between leg 3 and 1, are calculated using equation G.1. Leg 1 in the new system is assigned the 3D coordinates of 0,0,0 (i.e. x=0, y=0, z=0). Leg 3 is assigned the values Dist 3, 0, 0. The angle A and Dist 1 are required to calculate the 3D coordinates of Leg 2 in the new system. The angle A is calculated using the standard cosine formulae:

$$\cos A = \frac{b^2 + c^2 - a^2}{2 * b * c} \qquad \text{G.2}$$

where: a = Dist 2, b = Dist 3, c = Dist 1

Using simple trigonometry, the 3D coordinates of Leg 2 are: cos A * Dist1, sin A * Dist1, 0. As all three leg points have been assigned a z coordinate of zero, they all lie within the same horizontal plane, the plane of the paper. Utilising the 3D coordinates of the three leg points in the old and new system, the Rodrigues transformation transforms the entry point and lesion centre into the new system.

The second part of the setting diagram software calculates the intersection point B, i.e. where the vector, defined by the entry point and lesion centre, intersects the bottom plane defined by the three legs. Point B is calculated using three equations to solve for the three unknowns, i.e. the X, Y, Z coordinates of point B. The three equations in matrix form are:

$$\begin{bmatrix} x_B \\ y_B \\ z_B \end{bmatrix} = \begin{bmatrix} a & b & c \\ y_4 - y_5 & x_5 - x_4 & 0 \\ z_4 - z_5 & 0 & x_5 - x_4 \end{bmatrix}^{-1} \begin{bmatrix} a * x_1 + b * y_1 + c * z_1 \\ x_5 * y_4 - y_5 * x_4 \\ x_5 * z_4 - z_5 * x_4 \end{bmatrix} \qquad \text{G.3}$$

In the above equations, and for the remaining equations in appendix G:

$x_1, y_1, z_1$ = 3D coordinates of leg 1
$x_2, y_2, z_2$ = 3D coordinates of leg 2
$x_3, y_3, z_3$ = 3D coordinates of leg 3
$x_4, y_4, z_4$ = 3D coordinates of entry point
$x_5, y_5, z_5$ = 3D coordinates of the lesion centre,
$x_B, y_B, z_B$ = 3D coordinates of the bottom point where the vector, defined by the entry point and lesion centre, intersects the bottom plane
$x_T, y_T, z_T$ = 3D coordinates of the top point where the vector, defined by the entry point and lesion centre, intersects the top plane

The first equation in G.3, is the equation of the plane (Spiegel, 1968), passing through the three leg points is:

$$\begin{vmatrix} x - x_1 & y - y_1 & z - z_1 \\ x_2 - x_1 & y_2 - y_1 & z_2 - z_1 \\ x_3 - x_1 & y_3 - y_1 & z_3 - z_1 \end{vmatrix} =$$

$$= \begin{vmatrix} y_2 - y_1 & z_2 - z_1 \\ y_3 - y_1 & z_3 - z_1 \end{vmatrix} (x - x_1) + \begin{vmatrix} z_2 - z_1 & x_2 - x_1 \\ z_3 - z_1 & x_3 - x_1 \end{vmatrix} (y - y_1) + \begin{vmatrix} x_2 - x_1 & y_2 - y_1 \\ x_3 - x_1 & y_3 - y_1 \end{vmatrix} (z - z_1) =$$

$$= a(x - x_1) + b(y - y_1) + c(z - z_1) = 0 \qquad \text{G.4}$$

where: $a = (y_2 - y_1) * (z_3 - z_1) - (y_3 - y_1) * (z_2 - z_1)$

$b = (z_2 - z_1) * (x_3 - x_1) - (z_3 - z_1) * (x_2 - x_1)$

$c = (x_2 - x_1) * (y_3 - y_1) - (x_3 - x_1) * (y_2 - y_1)$

Both a and b, for the horizontal plane containing the three leg points, are zero, as $z_3=z_2=z_1=0$.

Rewriting equation G.4, as it is used in matrix equation G.3:

$$a*x+b*y+c*z=a*x_1+b*y_1+c*z_1 \qquad \text{G.5}$$

which as a, b and z1 are all equal to zero is actually c * z = 0.

The second and third equations of G3, are derived from the equation for the vector joining two points (Spiegel, 1968). The equation for the line joining the entry point ($x_4$, $y_4$, $z_4$ ) and lesion centre ($x_5$, $y_5$, $z_5$) is:

$$\frac{x-x_5}{x_4-x_5}=\frac{y-y_5}{y_4-y_5}=\frac{z-z_5}{z_4-z_5} \qquad \text{G.6}$$

The second and third equation, derived from G.6, are:

$$(x-x_5)*(y_4-y_5)=(y-y_5)*(x_4-x_5) \qquad \text{G.7}$$

$$(x-x_5)*(z_4-z_5)=(z-z_5)*(x_4-x_5) \qquad \text{G.8}$$

Rewriting G.7 and G.8, as G.9 and G.10 respectively, as they are used in equation G.3:

$$(y_4-y_5)*x-(x_5-x_4)*y=x_5*y_4-y_5*x_4 \qquad \text{G.9}$$

$$(z_4-z_5)*x-(x_5-x_4)*z=x_5*z_4-z_5*x_4 \qquad \text{G.10}$$

The equations G.5, G.9 and G.10 are all equal for the point B where the vector, defined by G.9 and G.10, intersects the plane, defined by G.5. Therefore there are three equations (in matrix form in G.3) to solve for three unknowns, i.e. the x, y and z coordinates of point B.

The next step is to determine the point T, where the vector, defined by the entry point and lesion centre, intersects the top plane. With a small alteration the three equations, in the matrix format G.3, can be used to solve for the point T. As the second and third equations of

G.3, i.e. G.9 and G.10, derived from the vector equation defined by the entry point and lesion centre, remain unaltered, it is only the first equation of G.3, i.e. the equation G.5 defining the bottom plane, that has to be altered, so that the new equation defines the top plane. As the equation of the plane requires a minimum of three points to solve, the three leg points on the bottom plane are mapped onto the top plane, and the coordinates of the three leg points on the top plane simply are (0, 0, s) for leg 1, (cos A * Dist 1, sin A * Dist 1, s) for leg 2, and (Dist 3, 0, s) for leg 3, where s is the distance between the bottom and top plane. Thus the only change to the coordinates of the three leg points, from the bottom to the top plane, is a translation in the z coordinates by the value s, i.e. the distance between the two planes.

$$a*x+b*y+c*z=a*x_1+b*y_1+c*z_1 \qquad \text{G.5}$$

Rewriting equation G.5 above for the top plane, both a and b are zero, as the z coordinates of the three points of the top plane are equal, i.e. $z_{T1} = z_{T2} = z_{T3} = s$ (see equations for a and b in G.4), and thus the new equation for the top plane is:

$$c*z=c*z_{T1}=c*s \qquad \text{G.11}$$

As c is only calculated from the x and y coordinates of the three leg points (see equation G.4), and these do not alter from the bottom to the top plane, c of the bottom plane is equal to c of the top plane. Therefore, replacing equation G.5 with equation G.11, G.3 is rewritten to determine the three dimensional coordinates for the top point:

$$\begin{bmatrix} x_T \\ y_T \\ z_T \end{bmatrix} = \begin{bmatrix} 0 & 0 & c \\ y_4 - y_5 & x_5 - x_4 & 0 \\ z_4 - z_5 & 0 & x_5 - x_4 \end{bmatrix}^{-1} \begin{bmatrix} c*s \\ x_5*y_4 - y_5*x_4 \\ x_5*z_4 - z_5*x_4 \end{bmatrix} \qquad \text{G.12}$$

The remaining information that has to be calculated is the distance from the top of the sleeve to the lesion centre (see figure G.1). The distance from point T, i.e. the centre of the ball and socket joint, to the lesion centre is calculated using the distance formulae:

$$s1 = \text{Dist T to Lesion Centre} = \sqrt{(x_T - x_5)^2 + (y_T - y_5)^2 + (z_T - z_5)^2} \qquad \text{G.13}$$

The distance from point T to the top of the sleeve is known, as it is part of the manufacturing specifications for the Cape Pointer, and is equal to s2. Therefore the distance from the top of the sleeve to the lesion centre is:

$$\text{Dist Top of Sleeve to Lesion centre} = s1 + s2 \qquad \text{G.14}$$

If the guide is attached to the top of the sleeve, the guide itself adds on a distance s3 to the overall distance and the distance from the guide to the lesion centre is:

$$\text{Dist Guide to Lesion centre} = s1 + s2 + s3 \qquad \text{G.15}$$

Now all the necessary information has been calculated to produce the setting diagram. To obtain a printout of the setting diagram, the x, y coordinates of the three leg points and the top and bottom points are simply plotted on screen. By setting the PC into graphics mode, using the DOS command graphics.com, a hardcopy is obtained by using the "PrintScreen" key on the PC keyboard. Scaling parameters for the x and y plotting coordinates are used to ensure that the resultant hardcopy is true to scale. These scaling parameters are specific to the PC and printer model combination.

## APPENDIX H: AMENDING THE SETTING DIAGRAM SOFTWARE TO CATER FOR POSSIBLE VARIATIONS OF THE 3D CT COORDINATE SYSTEM

This appendix describes the amendments that were made to the setting diagram software to ensure that, no matter what coordinate system the CT data is in, the results from the software and the setting diagram are always correct. (In this appendix, the same annotation is used, as was used in appendix G.)

Using the Rodrigues transformation to transform the CT data of the three legs markers, the entry marker and lesion into the setting diagram system, the 3D coordinates of the three leg markers in the setting diagram system always remain the same no matter what the coordinate system is. That is leg 1 is (0,0,0), leg 2 is (cos A * Dist 1, sin A * Dist 1,0) and leg 3 is (Dist 3,0,0) (See figure G.2 in Appendix G). However, due to the various coordinate systems, the Z axis either increases positively out of, or increases positively into the setting diagram page, due to the problem of left handed and right handed systems. Therefore, although the coordinate values of the lesion and entry point are always the same, the sign of their Z coordinates vary.

The simple approach would have been to determine whether the Z coordinate of the lesion was positive or negative. The Z coordinate of the lesion in the setting diagram system must be negative, so that the lesion falls within the cranium, and does not float above the patient's head, which would be completely nonsensical. Therefore, if the Z coordinate of the lesion was positive, the Z coordinates of the three leg markers, the lesion and entry point in the setting diagram system would simply have to be multiplied by -1, to invert the Z axis.

However at the time of writing the software, the much simpler approach had been overlooked, and a slightly different solution is used for the problem. Quoting from appendix G:

> "As the equation of the plane requires a minimum of three points to solve, the three leg points on the bottom plane are mapped onto the top plane, and the coordinates of the three leg points on the top plane simply are (0, 0, s) for leg 1, (cos A * Dist 1, sin A * Dist 1, s) for leg 2, and (Dist 3, 0, s) for leg 3, where s is the distance between the bottom and top plane. Thus the only change to the coordinates of the three leg points, from the bottom to the top plane, is a translation in the z coordinates by the value s, i.e. the distance between the two planes."

That is the Z coordinates of the three leg points for the bottom plane are $z_{B1} = z_{B2} = z_{B3} = 0$, and when mapped onto the top plane are $z_{T1} = z_{T2} = z_{T3} = +s$, independent of the direction in which the Z axis is increasing.

If the Z axis is increasing positively out of the setting diagram page, i.e. the Z coordinate value of the lesion is negative, the bottom plane will fall between the lesion and the top plane; if the Z axis increases positively into the setting diagram page, i.e. the Z coordinate of the lesion is positive, the top plane will fall between the lesion and bottom plane (see figure H.1). To set the Cape Pointer for the second scenario is impossible, as the Cape Pointer would literally have to be upside down, as the top plane is defined by the plane swept out by the horizontal arm of the Cape Pointer and the bottom plane by the legs of the Cape Pointer (figure 5.5). For the Cape Pointer to be set correctly, the bottom plane must lie between the lesion and the top plane.

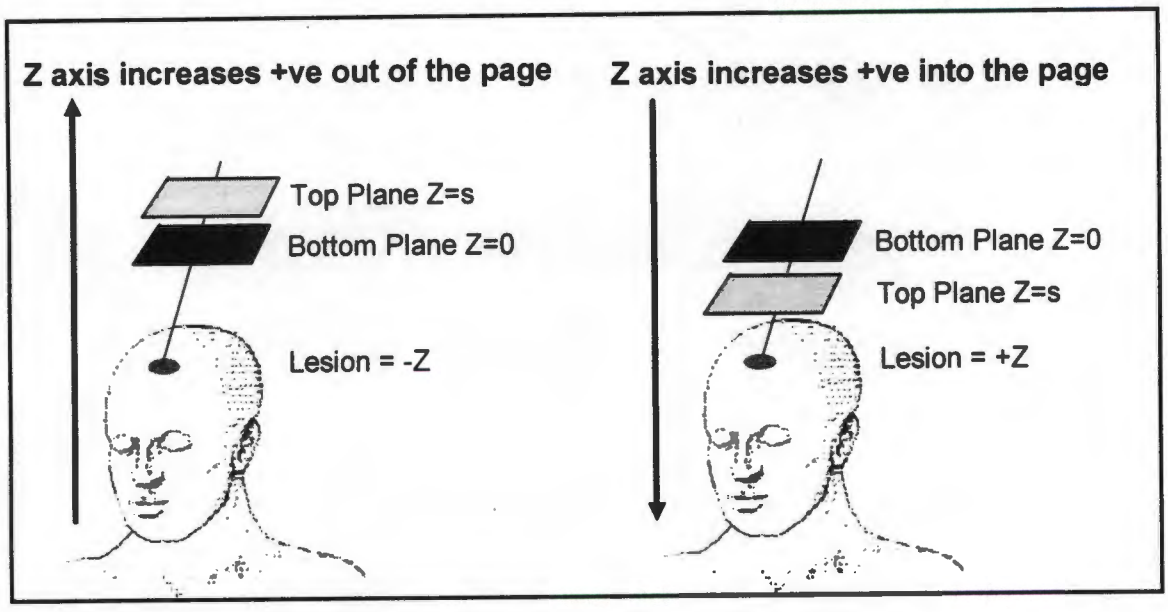


Figure H.1: The setting diagram coordinate system variations

For the right-hand diagram in figure H.1, where the Z axis increases positively into the setting diagram page, the Z coordinates of the three legs mapped onto the top plane should be made equal to $z_{T1} = z_{T2} = z_{T3} = -s$, thus ensuring that the bottom plane lies between the lesion and the top plane.

To determine whether the three leg points on the top plane should have Z coordinates equal to +s or -s, coordinates for leg 1 on "both top planes" are determined. The 3D coordinates of $leg1^{+s}$ are (0, 0,+s), and the 3D coordinates of $leg1^{-s}$ are (0, 0,-s). The distances from $leg1^{+s}$

and $leg1^{-s}$ to the lesion are calculated using equations H. 1 and H. 2, where the lesion coordinates are $x_5$, $y_5$, $z_5$.

$$\text{Dist Leg1}^{+s} \text{ to Lesion Centre} = \sqrt{(0-x_5)^2+(0-y_5)^2+(s-z_5)^2} \qquad \text{H.1}$$

$$\text{Dist Leg1}^{-s} \text{ to Lesion Centre} = \sqrt{(0-x_5)^2+(0-y_5)^2+(-s-z_5)^2} \qquad \text{H.2}$$

The greater of the two distances, calculated in equations H.1 and H.2, determines the correct top plane to be used, ensuring that the bottom plane falls between the top plane and the lesion.

By making these amendment to the calculations for the setting diagram in appendix G, the setting diagram and the information printed thereon, always remains the same and correct, no matter what 3D coordinate system is used.

## APPENDIX J: DETERMINING A NEW ENTRY POINT WITHOUT REPEATING THE CT SCAN

For the software to calculate a new entry point, the distances determined from the setting diagram (figure J.1), and the distance measured from the top of the Cape Pointer's sleeve to the new entry point, are required.

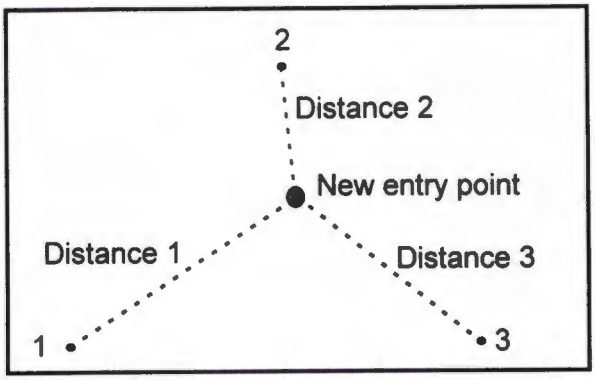


Figure J.1 : Measuring the distances from the three legs to the projected new entry point on the setting diagram

First the Z coordinate for the new entry point is calculated. The setting diagram plane is defined by the Cape Pointer's three legs, which all have been assigned a Z coordinate of zero (see diagram G.2, appendix G), and therefore any other points on the setting diagram plane also have Z coordinates equal to zero. The perpendicular distance from the setting diagram plane to the new entry point is therefore the Z coordinate for that entry point; this simply is the difference between the known perpendicular distance from the top of the sleeve to the setting diagram plane defined by the three legs, and the measured perpendicular distance from the top of the sleeve to the new entry point (figure J.2).

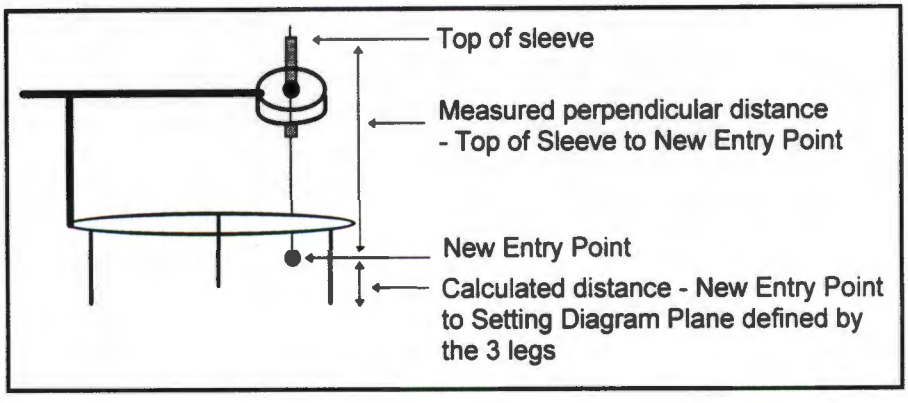


Figure J.2: Determining the Z coordinate of a new entry point

The next step is to determine the X and Y coordinates of the new entry point. The premise on which the calculations are based is that the calculated distances from the new entry point to the three leg markers must be equal to the distances measured on the setting diagram, that is:

$$[(ex - x_i)^2 + (ey - y_i)^2] - (Dist_i)^2 = 0 \qquad \text{J.1}$$

where:

| | |
|---|---|
| $Dist_i$ | = the measured distance from leg i to the new entry point |
| ex, ey | = the x and y coordinates of the new entry point |
| $x_i$, $y_i$ | = the x and y coordinates of leg i |
| $(ex - x_i)^2 + (ey - y_i)^2$ | = the square of the calculated distance between the new entry point and leg i. |

As there are three legs, three equations can be generated from equation J.1. If these equations are solved simultaneously in an iterative least squares method, with an approximation for the new entry point, the exact coordinates of the new entry point can be calculated.

As J.1 is non-linear, J.1 first has to be linearised, before use in the least squares approach. Linearising J.1, with respect to the 2 unknowns - ex and ey, results in the following equation:

$$[(ex - x_i)^2 + (ey - y_i)^2] - (Dist_i)^2 + 2*(ex - x_i)dx + 2*(ey - y_i)dy = 0 \qquad \text{J.2}$$

In the matrix format Ax=L, the three equations are:

$$\begin{bmatrix} 2*(ex - x_1) & 2*(ey - y_1) \\ 2*(ex - x_2) & 2*(ey - y_2) \\ 2*(ex - x_3) & 2*(ey - y_3) \end{bmatrix} * \begin{bmatrix} dx \\ dy \end{bmatrix} = \begin{bmatrix} (Dist_1)^2 - [(ex - x_1)^2 + (ey - y_1)^2] \\ (Dist_2)^2 - [(ex - x_2)^2 + (ey - y_2)^2] \\ (Dist_3)^2 - [(ex - x_3)^2 + (ey - y_3)^2] \end{bmatrix} \qquad \text{J.3}$$

The initial starting value for the new entry point is obtained from the point B of the previous setting diagram (see figure G.1, appendix G). Using the least squares solution $x=(A^TA)^{-1}A^TL$, dx and dy are solved for. A new approximate entry point is calculated, using equation J. 4.

ex=ex+dx

ey=ey+dy J.4

The procedure for calculating new dx and dy values and obtaining a better approximation for the new entry point is repeated, until dx and dy are both less than 0.001mm. This usually does not require more than four iterations. The final values for ex and ey are the X and Y coordinates of the new entry point. As the Z coordinate of the new entry point has already been calculated, the 3D coordinates of the new entry point have been determined, without repeating the CT scan.

## APPENDIX K: DECODING THE HOUNSFIELD NUMBERS FROM THE UNIX TO THE DOS SYSTEM FORMAT

Decoding the Hounsfield values correctly from the UNIX to the DOS system, the two bytes in the integer containing the Hounsfield number have to be swapped. This is due to the fact that in the UNIX system the least significant byte is on the left and the most significant byte is on the right, whereas the reverse is true in the DOS system. A C program was written to perform the decoding, as C supports bitwise operations.

The following C programming lines convert the Hounsfield number from the UNIX to the DOS system by swapping the 2 bytes:

| | |
|---|---|
| fread(&p1,2,1,fp); | This function reads in an integer p1, 2 bytes in length, 1 number only, from a file pointed to by the file pointer fp. p1 is read in as an integer (int), as C can only perform bitwise operations on character and integer data types (Schildt, 1987). |
| t1 = p1; | t1 is also an integer and is equal to p1. |
| t1 = t1 <<8; | The bits in t1 are shifted 8 bits to the left. As bits are shifted to the left, zeros are brought in on the right (Schildt, 1987). |
| p1= p1>>8; | The bits in p1 are shifted 8 bits to the right. As the data type is a signed int (a variable declared only as an int, is equivalent to a signed int), ones are brought in from the left if the sign bit (the left most bit) is one, and zeros are brought in from the left if the sign bit is zero (Hansen, 1988). (The sign bits in the Unix and DOS systems are labelled su and si respectively in table K.1 and K.2.) |
| p1= p1 & 255; | The bitwise AND (&) is applied to p1, to force all the 8 bits shifted in on the left to zero, without altering the 8 bits which have been shifted to the right. The AND operation causes any bit that is equal to zero in either operand. i.e. p1 or 255, to be set to zero. |
| t2 = p1\| t1; | The bitwise OR (\|), is the reverse of the AND operation, and causes any bit that is equal to one in either operand to be set to one. |

Two examples of these decoding operations are listed in table K.1 and table K.2, where su and si are the sign bits in Unix and DOS systems respectively. The example in K.1, the sign bit si is 0 and therefore zeros are brought in from the left, when p1>>8. In table K.2, the sign bit si is 1 and therefore ones are brought in from the left, when p1>>8. As can be seen p1 and t2 are identical, with the exception that the 2 bytes have been interchanged.

| | Least Significant Byte in Unix | | | | | | | | Most Significant Byte in Unix | | | | | | | |
|---|---|---|---|---|---|---|---|---|---|---|---|---|---|---|---|---|
| | | | | | | | | | su | | | | | | | |
| 2 bytes = 16bits | 16 | 15 | 14 | 13 | 12 | 11 | 10 | 9 | 8 | 7 | 6 | 5 | 4 | 3 | 2 | 1 |
| p1 read from file fp = 6396 | 0 | 0 | 0 | 1 | 1 | 0 | 0 | 0 | 1 | 1 | 1 | 1 | 1 | 1 | 0 | 0 |
| t1 = p1 | 0 | 0 | 0 | 1 | 1 | 0 | 0 | 0 | 1 | 1 | 1 | 1 | 1 | 1 | 0 | 0 |
| p1 = p1>>8 = 24 | 0 | 0 | 0 | 0 | 0 | 0 | 0 | 0 | 0 | 0 | 0 | 1 | 1 | 0 | 0 | 0 |
| 255 | 0 | 0 | 0 | 0 | 0 | 0 | 0 | 0 | 1 | 1 | 1 | 1 | 1 | 1 | 1 | 1 |
| p1 = p1&255 = 24 | 0 | 0 | 0 | 0 | 0 | 0 | 0 | 0 | 0 | 0 | 0 | 1 | 1 | 0 | 0 | 0 |
| t1 = t1<<8 = -1024 | 1 | 1 | 1 | 1 | 1 | 1 | 0 | 0 | 0 | 0 | 0 | 0 | 0 | 0 | 0 | 0 |
| t2 = p1\|t1 = -1000 | 1 | 1 | 1 | 1 | 1 | 1 | 0 | 0 | 0 | 0 | 0 | 1 | 1 | 0 | 0 | 0 |
| | si | | | | | | | | | | | | | | | |
| | Most Significant Byte in DOS | | | | | | | | Least Significant Byte in DOS | | | | | | | |

Table K.1: The first example of decoding a Hounsfield number

| | Least Significant Byte in Unix | | | | | | | | Most Significant Byte in Unix | | | | | | | |
|---|---|---|---|---|---|---|---|---|---|---|---|---|---|---|---|---|
| | | | | | | | | | su | | | | | | | |
| 2 bytes = 16bits | 16 | 15 | 14 | 13 | 12 | 11 | 10 | 9 | 8 | 7 | 6 | 5 | 4 | 3 | 2 | 1 |
| p1 read from file fp = -27395 | 1 | 0 | 0 | 1 | 0 | 1 | 0 | 0 | 1 | 1 | 1 | 1 | 1 | 1 | 0 | 1 |
| t1 = p1 | 1 | 0 | 0 | 1 | 0 | 1 | 0 | 0 | 1 | 1 | 1 | 1 | 1 | 1 | 0 | 1 |
| p1 = p1>>8 = -108 | 1 | 1 | 1 | 1 | 1 | 1 | 1 | 1 | 1 | 0 | 0 | 1 | 0 | 1 | 0 | 0 |
| 255 | 0 | 0 | 0 | 0 | 0 | 0 | 0 | 0 | 1 | 1 | 1 | 1 | 1 | 1 | 1 | 1 |
| p1 = p1&255 = 148 | 0 | 0 | 0 | 0 | 0 | 0 | 0 | 0 | 1 | 0 | 0 | 1 | 0 | 1 | 0 | 0 |
| t1 = t1<<8 = -768 | 1 | 1 | 1 | 1 | 1 | 1 | 0 | 1 | 0 | 0 | 0 | 0 | 0 | 0 | 0 | 0 |
| t2 = p1\|t1 = -620 | 1 | 1 | 1 | 1 | 1 | 1 | 0 | 1 | 1 | 0 | 0 | 1 | 0 | 1 | 0 | 0 |
| | si | | | | | | | | | | | | | | | |
| | Most Significant Byte in DOS | | | | | | | | Least Significant Byte in DOS | | | | | | | |

Table K.2: The second example of decoding a Hounsfield number

A simpler solution would have been to declare p1 and t1 as unsigned int. Unfortunately at the time of writing the program, this solution was overlooked. When shifting an unsigned int to the right (p1>>8), zeros are always brought in from the left. The operation p1=p1&255 could have been discarded, and t2 declared as a signed int, and the result of the OR operation forced into a signed int solution, with the following command: t2 = (signed int) (p1 | t1).

(Here again I must acknowledge Alan Bub's input, who came to my rescue with the solution p1=p1&255.)

## APPENDIX L: DETERMINING CORRECTION FACTORS TO CONVERT IP8 PIXEL COORDINATES TO CT COORDINATES

To be able to position a cursor on the CT slice in the IP8 system, and display the X and Y CT coordinates that the CT scanner would display for that image position, correction factors had to be determined and applied to the X and Y IP8 coordinates.

For this purpose three different CT files, which contained CT scans of three different phantoms, were used. From the CT scans of the phantoms, a total of 33 markers were digitised on both the CT scanner and on the IP8 frame grabber. The following two equations were used to determine the corrections to be made to the IP8 X and Y coordinates to obtain CT X and Y slice coordinates:

$$\left[\frac{X_{CT}}{size}\right] * mx + dx = X_{IP} \qquad \text{L.1}$$

$$\left[\frac{Y_{CT}}{size}\right] * my + dy = Y_{IP} \qquad \text{L.2}$$

| | | |
|---|---|---|
| where : | $X_{CT}$, $Y_{CT}$ | CT coordinates in millimetres |
| | $X_{IP}$, $Y_{IP}$ | IP8 coordinates in pixel values |
| | size | If the CT image is scanned on HALF, size = 1.0 |
| | | If the CT image is scanned on FULL, size = 2.0 |
| | mx, my, dx, dy | Parameters to be determined |

The parameters are determined using equations L.1 and L.2 in a least squares solution, and the 33 markers digitised in both systems. The resultant values for the parameters are:

mx = 2.142 dx =255.642 my = -2.148 dy =255.731

The reason why the sign for my is negative, is that the Y axis on the IP8 is reversed, i.e. it increases from the top downward, whereas the CT Y axis increase upwards.

These factors were verified, using the 21 markers of the patient R Smith. The mean differences in X and Y between the CT and the adjusted IP8 coordinates were -0.2 and 0.1 respectively, with a standard deviation of 0.4 for both X and Y, which is very satisfactory as the CT coordinates can only be read to the nearest whole number.